LEVEL (12)

RADC-TR-81-289
Final Technical Report
October 1981

AD A108910

ACOSS SIX (ACTIVE CONTROL OF SPACE STRUCTURES)

The Charles Stark Draper Laboratory, Inc.

DTIC
ELECTE
DEC 2 8 1981

H

ROME AIR DEVELOPMENT CENTER
Air Force Systems Command
Griffiss Air Force Base, New York 13441

81 12 28 0

This report has been reviewed by the RADC Public Affairs Office (PA) and is releasable to the National Technical Information Service (NTIS). At NTIS it will be releasable to the general public, including foreign nations.

RADC-TR-81-289 has been reviewed and is approved for publication.

APPROVED:

RICHARD W. CARMAN
Project Engineer

APPROVED:

FRANK J. REHM
Technical Director
Surveillance Division

FOR THE COMMANDER:

JOHN P. HUSS
Acting Chief, Plans Office

If your address has changed or if you wish to be removed from the RADC mailing list, or if the addressee is no longer employed by your organization, please notify RADC (OCSE) Griffiss AFB NY 13441. This will assist us in maintaining a current mailing list.

Do not return copies of this report unless contractual obligations or notices on a specific document requires that it be returned.

ACOSS SIX (ACTIVE CONTROL OF SPACE STRUCTURES)

R. R. Strunce   E. Fogel   G. J. Kissel
J. G. Lin   J. D. Turner   H. M. Chun
D. R. Hegg   R. K. Pearson   N. H. McClamroch

Approved for public release; distribution unlimited

UNCLASSIFIED

REPORT DOCUMENTATION PAGE		READ INSTRUCTIONS BEFORE COMPLETING FORM
1. REPORT NUMBER RADC-TR-81-289	2. GOVT ACCESSION NO. AD-A108 910	3. RECIPIENT'S CATALOG NUMBER
4. TITLE (and Subtitle) ACOSS SIX (ACTIVE CONTROL OF SPACE STRUCTURES)		5. TYPE OF REPORT & PERIOD COVERED Final Technical Report 14 Feb 80 - 15 Jul 81
		6. PERFORMING ORG. REPORT NUMBER R-1454
7. AUTHOR(s) R. R. Strunce E. Fogel G. J. Kissel J. G. Lin J. D. Turner H. M. Chun D. R. Hegg R. K. Pearson N. H. McClamroch		8. CONTRACT OR GRANT NUMBER(s) F30602-80-C-0096
9. PERFORMING ORGANIZATION NAME AND ADDRESS The Charles Stark Draper Laboratory, Inc. Cambridge MA 02139		10. PROGRAM ELEMENT, PROJECT, TASK AREA & WORK UNIT NUMBERS 62301E C6540106
11. CONTROLLING OFFICE NAME AND ADDRESS Defense Advanced Research Projects Agency 1400 Wilson Blvd Arlington VA 22209		12. REPORT DATE October 1981
		13. NUMBER OF PAGES 202
14. MONITORING AGENCY NAME & ADDRESS(if different from Controlling Office) Rome Air Development Center (OCSE) Griffiss AFB NY 13441		15. SECURITY CLASS. (of this report) UNCLASSIFIED
		15a. DECLASSIFICATION/DOWNGRADING SCHEDULE N/A

16. DISTRIBUTION STATEMENT (of this Report)

Approved for public release; distribution unlimited.

17. DISTRIBUTION STATEMENT (of the abstract entered in Block 20, if different from Report)

Same

18. SUPPLEMENTARY NOTES
RADC Project Engineer: Richard W. Carman (OCSE)

19. KEY WORDS (Continue on reverse side if necessary and identify by block number)

Output Feedback	Observation Spillover	Modal Spring
Structural Vibration Control	Stability	Large Angle Slew
Draper Model #2	Stabilizability	Maneuver
Control Spillover	Modal Dashpot	

20. ABSTRACT (Continue on reverse side if necessary and identify by block number)
This is The Charles Stark Draper Laboratory, Inc. Final Technical Report on its Active Control of Space Structures study. The research documented in this report addresses several major technical issues in vibration controller design methodologies that are of fundamental importance to control of large flexible space structures. Fundamentally important analytical and numerical results, as well as useful new insights, have been obtained on: optimality of fixed-form reduced-order compensators;

DD FORM 1473 EDITION OF 1 NOV 65 IS OBSOLETE
1 JAN 73

UNCLASSIFIED

full-order closed-loop stability and robustness with reduced-order
controllers; prevention of control and observation spillover; active
augmentation of damping, stiffness, and stability, stabilizability by
output feedback control; large-angle maneuver with simultaneous
vibration suppression; and possibilities for improving current controller
design methodologies.

ACKNOWLEDGEMENT

Accession For

NTIS CRA&I

DTIC TAB

Unannc

Justi

By

Distribution/

Availability Codes

Dist | Avail and/or Special

i

TABLE OF CONTENTS

PRECEDING PAGE BLANK

APPENDIX A

SECTION 1
SUMMARY

1.1 Introduction

Several spaceborne surveillance and weapon system concepts of interest to the USAF and DARPA have large flexible support structures and stringent line-of-sight (LOS) performance requirements. Severe environmental, onboard, and maneuver disturbances affect LOS performance to such a degree that current state-of-the-art disturbance accommodation techniques are not satisfactory for achieving the desired level of performance necessary to satisfy DARPA mission goals and objectives. The application of the current control theory and the state-of-the-art control techniques to such precision structures, however, has also been severely hampered by many fundamental technical problems not encountered before. Under the Active Control of Space Structures (ACOSS) program of the Defense Advanced Research Projects Agency (DARPA), The Charles Stark Draper Laboratory, Inc. has conducted a careful theoretical research on a broad selection of the major issues. Fundamentally important analytical and numerical results, as well as interesting new insights, have been obtained. Such results and insights will not only help improve the control theory and techniques for their applications to large flexible precision space structures but also help develop a unified generic structure-dynamics-control technology base for achieving DARPA mission goals and objectives for such spaceborne systems.

The research was performed from February 1980 through February 1981 under the ACOSS-6 Study. This document reports our new results beyond what have been documented earlier as an interim report [1].

1.2 Scope

Some major issues arise from the common practice of using only a reduced-order modal model in designing feedback control systems for a full-order model of a large flexible structure concerned. Some other major issues are related to active augmentation of damping and stiffness, stabilization by output feedback, vibration suppression during maneuvers, and possible improvement for controller design.

This report addresses the following major issues in various contexts.

Optimality of fixed-form reduced-order compensators: Section 2.

Full-order closed-loop stability with reduced-order controllers: Sections 3, 4.

Robustness of full-order closed-loop stability with reduced-order controllers: Sections 3, 4.

Effect of control and observation spillover: Sections 3, 4.

Techniques for preventing control and observation spillover: Section 5.

Active augmentation of damping and stiffness: Sections 3, 4, 6.

1-1

Output feedback stabilizability: Section 7.

Suppression of structural vibrations: Sections 3, 4, 6, 7, 8.

Large-angle maneuver combined with vibration suppression: Section 8.

Improvement possibilities for controller design: Sections 3, 4, 5, 6.

1.3   Highlights

Section 2. – Let the performance of a large flexible space structure under control be measured by a cost functional. For each n-mode approximate model, n = 1, 2, ..., design a fixed-form compensator that optimizes the cost functional for the approximate model. This design procedure is very practical but raises an important theoretical question. As the sequence of approximate models approach to a truth model of the structure, is the limiting compensator (if it exists) optimal for the truth model? Section 2 provides a positive answer and some sufficient conditions.

Section 3. – Velocity-sensor outputs can be fed back for augmentation of damping to large space structures and displacement-sensor outputs can for augmentation of stiffness. The design of feedback controllers for such distributed-parameter systems in practice must be based on only a relatively small number of modeled modes, however; usually the existence of spillover and the interaction with unmodeled modes are ignored. Due to the attendant control spillover and observation spillover, even stability of the closed-loop system with reduced-order feedback controllers may not be ensured, let alone the desired additional damping and stiffness.

Various useful conditions for ensuring closed-loop asymptotic stability have recently been established and are reported in Section 3. Such conditions and the insights thereby derived are useful as a guide to stability-ensuring designs of reduced-order feedback controllers. Large space systems considered are not limited to the class of large space structures, which are normally assumed to have only stable modes; possible presence of rigid modes and unstable modes are not excluded. Closed-loop stability conditions are also extended to the case of nonproportional damping. For the common class of large space structures having only stable elastic and rigid modes, specially useful simpler conditions for ensuring closed-loop asymptotic stability are also derived. In addition, conditions for robustness of closed-loop asymptotic stability to parameter variations and errors are obtained.

Section 4. – Since its conception by Canavin in 1978, the modal-dashpot design of vibration controllers has undergone significant advancement as a result of two initially separate research efforts at CSDL. The discouraging high-gain problem of Canavin with modal-dashpot design can now be alleviated by a bi-objective design optimization algorithm, which exploits the existent free parameters. The first part of Section 4 reports the development of such a bi-objective modal-dashpot optimizer (for adding the largest possible damping to primary modes while requiring the smallest possible feedback gains) and many interesting numerical results on closed-loop stability and robustness of modal-dashpot designs.

The presence of rigid-body modes was considered a difficult technical issue in stability analysis or modal analysis, and some unnecessary separate control was suggested to eliminate them. The second part of Section 4 shows that an integrated design of modal dashpots and "modal springs" will easily and practically resolve the problem with rigid modes. The attractive stability and robustness properties of modal-dashpot design have been expected intuitively from energy dissipativeness of passive member dampers and several numerical examples. Two simple but rigorous theorems on the full-order closed-loop asymptotic stability and robustness properties of both modal dashpots and modal springs are now established analytically here.

Section 5. - The techniques for preventing control spillover via proper synthesis of the influences of the existing actuators and via proper initial placement of the actuators are applied to two representative numerical models of large space structures (these techniques can be dualized for the prevention of observation spillover). The prevention of spillover to a significant number of nonprimary vibration modes is shown to be possible by proper synthesis of the influences of actuators existing on a structure. The synthesis procedure was programmed in FORTRAN, and demonstrated on Model 1 (the tetrahedral model) and Model 2. For Model 1, six actuators can be properly combined to form two synthetic actuators for independent control of four primary modes without any spillover to four secondary modes. For Model 2, synthesis of the 19 member actuators can prevent spillover to between 17 and 21 secondary modes, depending on the particular group of nonprimary modes selected as secondary modes; at least two independent synthetic actuators are available for control of the primary modes.

The synthesis program, because of its mathematical generality, is easily modified for studying the placement of actuators for prevention of spillover to all nonprimary modes. Spillover is found to be inevitable in Model 1 for each single actuator, be it placed at one node or between two nodes. For total prevention of spillover in Model 1, at least nine elementary actuators are required, each being placed to influence one degree of freedom but simultaneously controlled by a single input. This "superactuator" scheme when applied on Model 2 with 68 elementary actuators simultaneously controlled by as many as four independent inputs (i.e., four independent superactuators) can inhibit any control spillover therein.

Section 6. - There is usually inherent in the process of feedback controller design substantially more freedom of choice than is commonly exploited. This point is strongly emphasized again in Section 6 in the context of the problem of augmenting the damping and stiffness of second-order linear elastic systems by active feedback control. It is observed that considerable freedom of choice exists in specifying modal damping and stiffness matrices that lead to a particular set of closed-loop eigenvalues. In particular, a priori assumptions of symmetry or nonnegative definiteness for these specified matrices are unnecessary and without even physical motivation, since they are to be realized with active feedback control. In addition, once these specifications have been made, equations for the corresponding feedback gains may have multiple solutions. The extent of the design freedom available with this problem is not fully characterized. However, an example demonstrating how it can be used to advantage is given. As a practical matter, one may expect that such increased freedom of choice may facilitate the selection of a stabilizing controller.

1-3

Section 7. - The focus in Section 7 is on the general existence of
an output feedback gain matrix that stabilizes the closed-loop system. This
question has been discussed at some length in the literature, but no simple
algebraic characterization has been found. The technical approach taken is
based upon a comparison of the performance of output feedback with that of
optimal state feedback. This difference is expressed in terms of the output
of an open-loop-stable system operating under unity feedback. Sufficient con-
ditions for asymptotic stability of the output of the latter system are estab-
lished first. This result then leads directly to sufficient stability con-
ditions for the original plant operating under output feedback constraints.
Such conditions are similar to (but less restrictive than) those assumed in
the Kalman-Yakubovich-Popov lemma for an algebraic characterization of posi-
tive real matrices.

LIST OF REFERENCES

1.   Active Control of Space Structures Interim Report, CSDL Report
      No. R-1404, September 1980; also Rome Air Development Center
      Report No. RADC-TR-80-377, January 1981. (A097206)

SECTION 2

OPTIMAL FIXED-FORM COMPENSATORS
FOR LARGE SPACE STRUCTURES

2.1 Introduction

The basic problem considered here is that of designing physically simple controllers for highly flexible mechanical structures. This is an outgrowth of the stochastic output feedback compensator design problem considered in the interim report and is aimed at developing a systematic approach to the design of control systems subject to specific physically-motivated structure constraints. In addition, this design procedure provides quantitative information about the performance of the resulting control system performance as a by-product. Specifically, it is assumed that the dynamics of the flexible structure can be described by a system of time-invariant, linear partial differential equations. As a practical matter, however, these dynamics may be only approximately known in the form of a finite element model. It is important, therefore, that the design procedure developed here not rely on explicit knowledge of the distributed parameter "truth" model, but only on the approximate "design" model. In addition, the structure of the control system should fulfill certain practical requirements to insure that it is not prohibitively complex to implement. In particular, these implementation considerations will generally dictate the following structural constraints:

(2-1) a finite number of scalar observations serve as inputs to the control system.

(2-2) a finite number of scalar control signals are generated by the control system.

(2-3) the dynamics of the control system can be described by a finite dimensional linear state space model.

These conditions insure that the control system can be constructed from a finite quantity of standard electronic and electromechanical control hardware.

This design problem is formulated more precisely in the following sections. Specifically, Subsection 2.2 defines the distributed parameter models considered here for the dynamics of the undamped plant. To facilitate the discussion of the effects of inherent damping and external control on these dynamic models, Subsection 2.3 recasts the problem in terms of strongly continuous semigroups. Subsection 2.4 adds inherent damping to the problem and examines the extent to which the qualitative nature of the semigroup describing the plant dynamics is altered by various damping mechanisms. Proceeding along similar lines, Subsections 2.5 and 2.6 then examine the nature of the control problems arising from various restrictions on the types of sensors and actuators available for control. In particular, Subsection 2.5 demonstrates that, in general, optimal controllers for the distributed parameter plants considered here

are themselves distributed parameter systems and therefore do not meet the implementation constraints (2-1) to (2-3). Subsection 2.6 then defines a class of control laws that do meet these constraints and examines the consequences of requiring controllers to be of this class. In particular, the importance of including sufficient inherent damping in the dynamic model of the system is shown to arise from these restrictions.

The results presented in Subsections 2.2 through 2.6 are not new but are included here because they constitute a necessary background for the optimal fixed form compensator problem formulated in Subsection 2.7. This problem is a generalization of that considered in [1], considering a sequence of finite dimensional "design models" that converge to the distributed parameter "truth model" in the limit of infinite dimension. Optimal fixed form compensators meeting constraints (2-1) to (2-3) are then developed for each design model and the limit of this sequence is taken in an effort to arrive at a compensator design that is both optimal and implementable. Subsection 2.8 presents optimality results for this design approach and these constitute the principal contribution of this work. Specifically, sufficient conditions are developed for the optimality of this limiting compensator when it exists. Finally, Subsection 2.9 summarizes the principal advantages and disadvantages of this design procedure, identifies some important open questions raised by it and suggests several promising avenues for future investigation.

2.2   Undamped Flexible Structure Models

The flexible structures considered here will be linear, time-invariant distributed parameter systems whose open loop dynamics are described, in the absence of inherent damping, by the generalized wave equation considered in [2]. This model is very similar to those considered by other authors in their treatments of various aspects of the flexible structure control problem [3, 4, 5, 6, 7] and includes many popular specific flexible structure models as special cases. In particular, the dynamics of the systems considered here are described by the equation

$$\partial^2 x(z,t)/\partial t^2 + A_o x(z,t) = f(z,t) \qquad (2-4)$$

where $x(z,t)$ and $f(z,t)$ are elements of a Hilbert space H of functions defined on the bounded open spatial domain $\Omega \subset R^n$ and parameterized by the time variable $t \in [0,\infty)$. Here, A_o is a time-invariant, symmetric linear partial differential operator with domain D_o dense in H. It is further assumed that A_o is a positive definite operator [9]: there exists a positive constant a_o such that for all $x \in H$,

$$\langle A_o x, x \rangle \geq a_o ||x||^2 \qquad (2\text{-}5)$$

where $\langle \cdot, \cdot \rangle$ indicates the inner product on H and $||\cdot||$ represents the norm induced by that inner product. Finally, it is also assumed that A_o is an operator with compact resolvent [8,9]. That is, the resolvent operator $R(\lambda, A_o) = (A_o - \lambda I)^{-1}$ is required to be a compact operator [8,9,10] for some λ.

The notion of a compact operator and its properties will be discussed in detail in Subsection 2.6 in connection with compact linear feedback compensators. For the present, however, it is sufficient to note that the principal physical consequence of the requirement that A_o have compact resolvent is that the undamped flexible structure model Eq. (2-4) may be regarded as a countably infinite collection of discrete harmonic oscillators. It should be noted that this restriction is not difficult to meet in practice since a very broad class of partial differential operators can have compact resolvents. For example, any strongly elliptic partial differential operator has this property, i.e. any operator of the form [11]

$$A_o = - \sum_{j,k=1}^{m} \frac{\partial^j}{\partial_z^j} \left(a_{jk}(z) \frac{\partial^k}{\partial z^k} \right) + c(z) \qquad (2\text{-}6)$$

where m is a positive integer. Here, the functions $a_{jk}(z)$ satisfy the conditions that for some $c_o > 0$, all $\zeta \in C$ and almost all $z \in \Omega$,

$$\sum_{j,k=1}^{m} a_{jk}(z) \, \zeta_j \bar{\zeta}_k \geq c_o |\zeta|^2 \qquad (2\text{-}7)$$

where the overbar indicates complex conjugation. While this definition assumes the problem is set in R^1, it is not difficult to extend this class of operators to R^n [10]. The assumed boundedness of Ω, on the other hand, is an essential restriction. Specifically, if Ω is allowed to be unbounded, the operator A_o may have a continuous spectrum and will therefore not have a compact resolvent [11]. Consequently, while the notion of approximating a very large structure by one of infinite extent might seem like a reasonable approach on physical grounds, this would change

significantly the essential character of the problem and will not be considered here. It is also significant to note that for the second order case, $m = 1$, restrictions (2-6) and (2-7) reduce to the definition of a Sturm-Liouville operator. This class of operators pervades classical physics and is discussed extensively in [12].

In terms of specific distributed parameter models, Eq. (2-4) can be used to describe the motion of a variety of simple systems. For example, setting

$$A_o = -c^2 \partial^2 / \partial x^2 \tag{2-8}$$

and specifying appropriate boundary conditions, Eq. (2-4) describes the vibration of a uniform one-dimensional string, clamped at both ends. Similarly, setting

$$A_o = -\frac{1}{\mu(z)} \left\{ \frac{\partial}{\partial z} \left(f(z) \frac{\partial}{\partial z} \right) + \frac{\partial^2}{\partial z^2} \left(\alpha(z) \frac{\partial^2}{\partial z^2} \right) \right\} \tag{2-9}$$

Eq. (2-4) can describe the transverse vibration of a one-dimensional beam of nonuniform mass density $\mu(z)$ and flexural rigidity $\alpha(z)$ subject to a constant longitudinal tensile force $f(z)$ [13]. In two space dimensions, the vibrations of a thin rectangular plate may be described by setting [13]

$$A_o = -\left\{ c_1^2 \frac{\partial^2}{\partial z_1^2} + c_2^2 \frac{\partial^2}{\partial z_2^2} \right\} \tag{2-10}$$

while the vibrations of a thin circular plate may be described by setting [14]

$$A_o = -\frac{1}{r} \frac{\partial}{\partial r} \left(r \frac{\partial}{\partial r} \right) + \frac{1}{r^2} \frac{\partial^2}{\partial \phi^2} \tag{2-11}$$

where r and ϕ represent the radial and angular components of the vector $\underline{z} \in R^2$ expressed in cylindrical polar coordinates. Finally, it is also possible to consider more complex structural models like the Timoshenko beam [13] or more complex assemblies of simple structures like those just described within the framework of the model just described. One of the most common methods of combining such component structures into a dynamic

model, however, is to assume frictional coupling at the boundaries [5] which requires the introduction of a damping term into Eq. (2-4), a problem that will be considered in detail in subsection 2.4.

The assumption that A_o is a positive definite operator insures the oscillatory nature of the model (2-4), generalizing the scalar equation

$$\ddot{x}(t) + ax(t) = f(t) \tag{2-12}$$

describing the simple harmonic oscillator of frequency $a^{\frac{1}{2}}$, provided $a > 0$. This restriction on the flexible structure model does, however, exclude rigid body motions from the dynamics since these would correspond to zero eigenvalues of the operator A_o. As noted in [3], however, this is not a serious restriction since such dynamic modes may be considered independently of the rest of the plant which may then be described by model (2-4).

2.3   Semigroup Formulation

Returning to the scalar system (2-12), note that it may be cast in conventional state space form as

$$\dot{\underline{v}} = A\underline{v} + \underline{f} \tag{2-13}$$

by defining $\underline{v}$, $\underline{f}$ and A appropriately. There are, of course, an infinite number of possible ways of doing this, but two particularly popular choices are

$$\underline{v} = \begin{bmatrix} x(t) \\ \dot{x}(t) \end{bmatrix}, \; A = \begin{bmatrix} 0 & 1 \\ -a & 0 \end{bmatrix}, \; \underline{f} = \begin{bmatrix} 0 \\ f(t) \end{bmatrix} \tag{2-14}$$

and

$$\underline{v} = \begin{bmatrix} a^{\frac{1}{2}}x(t) \\ \dot{x}(t) \end{bmatrix}, \; A = \begin{bmatrix} 0 & a^{\frac{1}{2}} \\ -a^{\frac{1}{2}} & 0 \end{bmatrix}, \; \underline{f} = \begin{bmatrix} 0 \\ f(t) \end{bmatrix} \tag{2-15}$$

Similar expressions may be developed for the abstract model (2-4). In particular, in analogy with (2-14), we can define

$$\underline{v} = \begin{bmatrix} x(z,t) \\ \dfrac{\partial x(z,t)}{\partial t} \end{bmatrix}, \quad A = \begin{bmatrix} 0 & I \\ -A_o & 0 \end{bmatrix}, \quad \underline{f} = \begin{bmatrix} 0 \\ f(z,t) \end{bmatrix} \qquad (2\text{-}16)$$

reducing Eq. (2-4) to the form of Eq. (2-13). Also, since A_o is a positive definite operator, it is possible to define a unique square root $A_o^{1/2}$ [9, Theorem 3.351] such that $(A_o^{1/2})^2 = A_o$. This allows a description analogous to Eq. (2-15) by defining

$$\underline{v} = \begin{bmatrix} A_o^{1/2} x(z,t) \\ \dfrac{\partial x(z,t)}{\partial t} \end{bmatrix}, \quad A = \begin{bmatrix} 0 & A_o^{1/2} \\ -A_o^{1/2} & 0 \end{bmatrix}, \quad \underline{f} = \begin{bmatrix} 0 \\ f(z,t) \end{bmatrix} \qquad (2\text{-}17)$$

The first order model (2-13) obtained by defining $\underline{v}$, $\underline{f}$ and A as in either Eq. (2-16) or Eq. (2-17) is extremely useful in that it casts the dynamic model (2-4) in a form similar to that employed in finite dimensional linear systems theory. Many of the control results available for finite dimensional linear systems may be generalized to infinite dimensional problems set in this form by reformulating the problem in terms of semigroups.

In what follows, U, X and Y will denote Banach spaces, L(X,Y) is the space of bounded linear operators from X into Y and L(X) denotes L(X,X). A strongly continuous semigroup is defined [15] as a map T(t) from R+ into L(X) satisfying

$$T(t + s) = T(t)T(s) \qquad 0 \le s \le t \qquad (2\text{-}18)$$

$$T(0) = I \qquad (2\text{-}19)$$

$$||T(t)x_o - x_o|| \to 0 \quad \text{as } t \to 0\text{+ for all } x_o \in X \qquad (2\text{-}20)$$

Strongly continuous semigroups represent a generalization of the transition matrix arising from the state-space description of finite dimensional linear systems. That is, it is possible to describe the dynamics of many infinite dimensional systems by

$$x(t) = T(t)x_o + \int_o^t T(t-s)f(s)ds \qquad (2\text{-}21)$$

where $x(t)$ represents the state of the system at the time t, evolving from $x(0) = x_o$ under the influence of the driving function $f(t)$.

It is also possible to develop a differential description of the system dynamics represented by Eq. (2-21) by introducing the concept of the infinitesimal generator of the semigroup $T(t)$. This is defined [15] as

$$Ax = \lim_{t \to o^+} \frac{1}{t}(T(t) - I)x \qquad (2\text{-}22)$$

whenever this limit exists. The domain $D(A)$ of this operator is the set of $x \in X$ such that this limit exists. The state of the system described by Eq. (2-21) can then be cast in the form

$$\dot{x}(t) = Ax(t) + f(t), \quad x(0) = x_o \qquad (2\text{-}23)$$

provided $f(t)$ meets certain continuity or integrability conditions [15, Theorem 2.21 or Lemma 2.22].

In addition to this constraint on $f(t)$, the dynamic operator A must, of course, generate a strongly continuous semigroup $T(t)$ in order for the semigroup representation of the system and the control results that follow from it to be valid. Necessary and sufficient conditions for an operator to generate a strongly continuous semigroup are given by the Hille-Yosida Theorem [15]. These are very mild conditions to impose on physical systems, requiring only that the state of the system be sufficient to describe its future evolution and that this evolution be continuous in time and depend continuously on the initial state. Consequently, it is not surprising that systems described by Eq. (2-4) generate strongly continuous semigroups. In fact, it can be shown that such systems generate unitary groups [11, p. 466], a much stronger result.

If stricter constraints are placed on the operator A in Eq. (2-23), a particularly well-behaved class of infinite dimensional systems results. Specifically, if A is the infinitesimal generator of a strongly continuous semigroup $T(t)$ that satisfies the additional conditions [15]

(2-24)   T(t) can be analytically continued into the sector

$$S(\omega) = \{t \neq 0: |\arg t| < \omega\}$$

for some $\omega \in (0, \pi/2)$

(2-25)   for each $t \in S(\omega)$ and all $x \in X$,

$$\frac{d}{dt} T(t)x = AT(t) \text{ and } AT(t) \in L(X)$$

(2-26)   for any $0 < \zeta < \omega$ there is some $K > 0$ such that

$$||T(t)|| \leq K, \quad ||AT(t)|| \leq K/|t|$$

for all $t \in S(\omega-\zeta)$

then $T(t)$ is called a holomorphic (analytic) semigroup. Sufficient conditions for A to generate such a semigroup are

(2-27)   A is a closed, densely-defined linear operator on a Banach space X

(2-28)   the resolvent set for A is contained in the sector

$$S(\pi/2 + \omega) \text{ for some } \omega \in (0, \pi/2)$$

(2-29)   there exists $M > 0$, independent of λ such that

$$||R(\lambda,A)|| \leq M/|\lambda| \text{ for } \lambda \in S(\pi/2 + \omega).$$

Note that condition (2-27) is automatically satisfied by any operator A generating a strongly continuous semigroup [15, Theorem 2.9].

The most common class of systems generating holomorphic semigroups are finite dimensional linear systems whose associated semigroups are the transition matrices $\phi(t,t')$. In fact, systems generating holomorphic semigroups may be regarded as natural generalizations of the finite dimensional case. For example, condition (2-29) implies [3] that the frequency response of such systems is low-pass in nature, decaying at least as fast as $1/s$. On this basis, it is suggested in [3] that such systems may be effectively approximated by finite dimensional models, a result that is definitely not true for distributed parameter systems in general. In particular, this is not true for the undamped flexible structures described by Eq. (2-4).

The class of operators satisfying conditions (2-27) through
(2-29) is fairly broad, however. For example, if A is a bounded operator,
it generates the holomorphic semigroup defined by [9]

$$T(t) = \exp(At) \qquad (2-30)$$

The finite dimensional result follows directly from this since linear
operators between Hilbert spaces of finite dimension are bounded. Not
all operators generating holomorphic semigroups are bounded, however, as
illustrated by the fact that systems described by parabolic differential
equations usually generate holomorphic semigroups [15]. Finally, it is
important to note that the undamped flexible structure model of Eq. (2-4)
does not generate a holomorphic semigroup. The inclusion of damping in
the model can change its dynamic behavior radically, however, and it is
possible to have strong enough damping mechanisms to give rise to systems
that do generate holomorphic semigroups.

2.4   Damped Flexible Structures

Eq. (2-4) is an unrealistic model for the dynamics of a real
flexible structure because it describes a conservative system. Physically,
this corresponds to a structure that, once excited, vibrates forever
without loss of energy. Consequently, realistic dynamic models must
include a damping term to describe the loss mechanisms inherent in all
physical systems. Since it is the small magnitude of these losses that
motivates the control problem considered here, however, it is tempting
to neglect them altogether and deal with undamped models. Unfortunately,
as the following paragraphs illustrate, it is not the magnitude of these
losses that determines the nature of the control problem, but rather
the qualitative nature of the loss mechanisms.

To include these losses in the flexible structure model (2-4),
an additional term will be added, i.e.

$$\partial^2 x(z,t)/\partial t^2 + A_1 \partial x(z,t)/\partial t + A_0 x(z,t) = f(z,t) \qquad (2-31)$$

where A_1 is an operator with domain D_1 dense in H. It will further be
assumed that the operator A_1 is self-adjoint and non-negative so that

$$\langle A_1 v, v \rangle \geq 0 \quad \text{for all } v \in D_1 \qquad (2-32)$$

To see the significance of this, define the internal energy of the system
as [5]

2-9

$$E(t) = \{||\dot{x}(t)||^2 + ||A_o^{\frac{1}{2}}x(t)||^2\} \qquad (2-33)$$

and note that, in the absence of external forces,

$$dE(t)/dt = <\ddot{x}(t) + A_o x(t), \dot{x}(t)> \qquad (2-34)$$

$$= <-A_1 \dot{x}(t), \dot{x}(t)>$$

as easily shown by direct differentiation. Consequently, the non-negativity requirement on A_1 implies that the internal energy of the system decays monotonically to zero. More descriptively, it may be noted that these conditions imply that $-A_1$ is a dissipative operator [9].

As in the undamped case, this dynamic model may be cast in the form of Eq. (2-13) by defining either

$$\underline{v} = \begin{bmatrix} x(z,t) \\ \dfrac{\partial x(z,t)}{\partial t} \end{bmatrix}, \quad A = \begin{bmatrix} 0 & I \\ -A_o & -A_1 \end{bmatrix}, \quad \underline{f} = \begin{bmatrix} 0 \\ f(z,t) \end{bmatrix} \qquad (2-35)$$

or

$$\underline{v} = \begin{bmatrix} A_o^{\frac{1}{2}}x(z,t) \\ \dfrac{\partial x(z,t)}{\partial t} \end{bmatrix}, \quad A = \begin{bmatrix} 0 & A_o^{\frac{1}{2}} \\ -A_o^{\frac{1}{2}} & -A_1 \end{bmatrix}, \quad \underline{f} = \begin{bmatrix} 0 \\ f(z,t) \end{bmatrix} \qquad (2-36)$$

The question of whether the semigroup formalism may be applied to the damped system depends on the choice of A_1, as does the nature of the semigroup generated when the approach is applicable. To see this, let U denote either of the infinitesimal generators of the semigroup describing the undamped system defined in Eqs. (2-15) and (2-16) and define T as the perturbation of U due to the inclusion of damping in the system, i.e.

$$T = A - U = \begin{bmatrix} 0 & 0 \\ 0 & -A_1 \end{bmatrix} \qquad (2\text{-}37)$$

If A_1 is a bounded operator, then T is also a bounded operator and it is a standard result [9, 15] that U + T generates a strongly continuous semigroup if U does. If A_1 is an unbounded operator, however, the perturbed operator U + T may fail to generate a strongly continuous semigroup. Consequently, unbounded damping operators must be considered carefully.

Probably the most common unbounded damping operators are [3, 6, 16].

$$A_1 = 2\xi A_o^{\frac{1}{2}} \qquad (2\text{-}38)$$

and

$$A_1 = \gamma A_o \qquad (2\text{-}39)$$

which are used to describe hysteretic or structural damping in flexible structures. Both of these models are examined in [3] where it is shown that they do result in systems described by strongly continuous semigroups. The model defined by Eq. (2-38) is especially interesting since it is a generalization of the damped harmonic oscillator

$$\ddot{x}(t) + 2\xi\omega_o\dot{x}(t) + \omega_o^2 x(t) = f(t) \qquad (2\text{-}40)$$

from R^1 to the infinite dimensional Hilbert space H and may be viewed as an infinite collection of such oscillators. This model is investigated in detail in [3] where it is shown that it generates a holomorphic semigroup. In fact, the principal focus of that work is an investigation of the notion that all operators within a neighborhood of $2\xi A_o^{1/2}$ (relative to the uniform operator norm on H) generate holomorphic semigroups. While this is not established, several sufficient conditions for the damped system to generate a holomorphic semigroup are presented. For example, operators of the form

$$A_1 = 2\xi A_o^{1/2} + CA_o^{1/2} \qquad (2\text{-}41)$$

2-11

are considered where C is a bounded operator. Further, it is required that this operator be relatively bounded with respect to $A_o^{1/2}$ [9], i.e. that the domain D_1 of A_1 contain the domain $D_{1/2}$ of $A_o^{1/2}$ and that there exist non-negative constants a and b such that

$$||A_1 v|| \leq a||v|| + b||A_o^{1/2} v||, \quad v \in D_{1/2} \tag{2-42}$$

Under these conditions, it is shown that there exists a positive constant $m(\xi)$ such that if $||C|| \leq m(\xi)$, the damped system described by Eq. (7-31) generates a holomorphic semigroup.

The requirement that the damped system generate a holomorphic semigroup is too restrictive to include all cases of interest. For example, a structure with viscous damping is described by the damping operator

$$A_1 = \delta \tag{2-43}$$

for some positive constant δ. This is a very common damping model but it is not sufficient to yield a holomorphic semigroup. A weaker assumption that is satisfied by the viscous damping mechanism is that it be sufficient to endow the system with a uniform exponential decay rate [5]. That is, there should exist positive numbers K_o and K_1 such that

$$E(t) \leq K_o e^{-K_1 t} E(o) \tag{2-44}$$

Note that since E(t) is the norm of the state vector $\underline{v}(t)$ defined by Eq. (2-17), this is a statement that the system is exponentially stable [15] and is therefore a reasonable property to expect from physical systems of the type considered here.

A sufficient condition for the damping represented by A_1 to generate a uniform exponential decay rate is that A_1 be invertible. Such systems are referred to as strongly damped [5,17]. It should be noted that weakly damped systems can also exhibit uniform exponential decay rates [5]. Finally, it should also be noted that the requirement that the damped system exhibit a uniform decay rate is weaker than the requirement that it generate a holomorphic semigroup since the unbounded damping operators considered above lead to strongly damped systems.

2.5   Optimal Control of Flexible Structures

For control applications, it is necessary to include explicit sensor and actuator descriptions in the model describing the plant's dynamic behavior. As was the case with the inclusion of damping in the model, the assumptions made regarding these sensors and actuators will have a considerable impact on the resulting plant model. In particular, the sensors and actuators will, along with the specific control law assumed, determine the nature of the feedback operator that describes the perturbation of the open loop plant by the control system when the loop is closed.

Control inputs may enter the dynamic model of Eq. (2-31) in either of two ways. The most obvious approach is to control the system through the forcing term $f(z,t)$, i.e.

$$f(z,t) = Bu(z,t) \qquad (2-45)$$

where B is an operator mapping the space U of admissable controls into the Hilbert space H. This actuator model is general enough to include a very wide range of physical devices, including such unconventional control elements as the scanning actuators considered in [18]. Generally, however, the model is restricted to include actuators of the form

$$f(z,t) = B\underline{u}(t) \qquad (2-46)$$

where $B \in L(U,H)$ and $U = R^m$. Physically, this model corresponds to a collection of m distributed actuators B_i attached to the structure over fixed spatial regions, i.e.

$$B_i = \begin{cases} b_i(z) & z \in \Omega_i \\ \\ 0 & z \notin \Omega_i \end{cases} \qquad (2-47)$$

where Ω_i is a compact subset of $\overline{\Omega}$, the closure of the domain on which the structure is defined. It is important to note that this model does not include the case of point actuators for which each Ω_i consists of an isolated point z_i. To include this case, $b_i(z)$ must be taken as a Dirac delta distribution [19] which does not yield a bounded operator B [15]. Similarly, boundary control – the second control approach mentioned above – does not correspond to a bounded actuator model [15]. Here,

control forces are applied at the boundary $\partial\Omega$ of the structure and the effect in one dimensional systems is similar to that of a point actuator. In two or three dimensions, the situation becomes more complex.

Sensors are included in the system model in essentially the same way. Here, observations $y(z,t)$ are defined by

$$y(z,t) = C\underline{v}(t) \qquad (2\text{-}48)$$

where C is an operator mapping the Hilbert space V on which the model of Eq. (2-13) is defined into the space γ of observations. As before, this is a very general model, encompassing a wide variety of measurements, including both the case of complete state information for which C = I, the identity mapping from V into γ, and the more common case where

$\gamma = R^p$ and $C \in L(V,\gamma)$. Similarly, point observations and boundary observations may be included in the model, again resulting in unbounded mappings from V into γ.

Given the dynamic model (2-13) with actuator and sensor models of the form (2-45) and (2-48), respectively, the control problem is then to design a compensator mapping K between the space of observations γ and the space U of controls, i.e.

$$u(z,t) = Ky(z,t) \qquad (2\text{-}49)$$

This results in a closed loop system whose dynamics are described by the autonomous differential equation

$$\dot{\underline{v}}(t) = [A + BKC]\underline{v}(t), \quad \underline{v}(0) = \underline{v}_o \qquad (2\text{-}50)$$

provided the perturbed operator A + BKC generates a strongly continuous semigroup. If $B \in L(U,V)$, $K \in L(\gamma,U)$ and $C \in L(V,\gamma)$ then $F = BKC \in L(V,V)$ and, as in the case of bounded damping, A + F generates a strongly continuous semigroup. Similarly, as in the case of unbounded damping operators, if B, K or C are unbounded, then F may be unbounded and A + F may not generate a strongly continuous semigroup.

Consequently, there is some advantage in restricting consideration to bounded sensor, actuator and compensator models. This does, however, place some fairly significant constraints on the ability of the resulting feedback mapping F to alter the system's behavior. For example, if F is bounded and the open loop system operator A does not generate a holomorphic semigroup, then the closed loop operator A + F cannot generate a holomorphic

2-14

semigroup. This follows from the fact that holomorphic semigroups are stable under relatively bounded perturbations [9]. Hence, if $A + F$ generates a holomorphic semigroup and F is bounded, -F is relatively bounded with respect to $A + F$, implying A generates a holomorphic semigroup as well. On the other hand, it is not clear that physically motivated unbounded feedback operators are free of these constraints. For example, it is shown in [20] that boundary observations and controls will move the spectrum of the undamped wave equation uniformly into the left half plane. This is not enough, however, for the closed loop system to generate a holomorphic semigroup since the resolvent set of $A + F$ does not lie in a sector of the complex plane as required by condition (2-28).

Note that these results are quite different from the finite dimensional case for which the spectrum of the closed loop system could be modified arbitrarily if enough states were available for measurement [21]. The finite dimensional linear regulator makes use of this fact, modifying the system's dynamics to minimize a specified cost functional of the state and control trajectories. While this degree of control is not achievable in the infinite dimensional case, infinite dimensional versions of the linear regulator problem can be formulated and yield results that are similar in form to the better known finite dimensional results. For example, Curtain and Pritchard [15] consider both stochastic and deterministic formulations of the linear regulator with either finite or infinite time horizons. In the deterministic, finite time horizon case, the problem is to minimize a cost functional of the form

$$J(u, t_o, z_o) = \langle z(t_1), Gz(t_1) \rangle + \int_{t_o}^{t_1} \left\{ \langle z(s), Mz(s) \rangle + \langle u(s), Ru(s) \rangle \right\} ds$$

(2-51)

for the system described by

$$z(t) = T(t - t_o)z_o + \int_{t_o}^{t} T(t - s) Bu(s)ds \qquad (2-52)$$

Here, M, G and R are bounded operators as is the actuator influence operator B. In addition, R is assumed to satisfy

$$\langle Ru,u \rangle \geq \alpha ||u||^2 \qquad (2-53)$$

for some $\alpha > 0$ and all $u \in U$ and that the complete state $z(t)$ is observed. As in the finite dimensional case, the result is given by the control law

$$u(t) = -R^{-1}B*Q(t)z(t) \qquad (2\text{-}54)$$

where B* is the adjoint of the operator B, and the optimal cost is given by $\langle z_0, Q(t)z_0 \rangle$. Here, $Q(t)$ is the solution of the operator Riccati equation

$$\frac{d}{dt}\langle Q(t)h,k \rangle + \langle Q(t)h, Ak \rangle + \langle Ah, Q(t)k \rangle + \langle Mh, k \rangle = \langle Q(t)BR^{-1}B*Q(t)k, k \rangle$$

$$(2\text{-}55)$$

with $Q(t_1) = G$ and $h, k \in D(A)$, the domain of the infinitesimal generator A of the semigroup $T(t)$. Again as in the finite dimensional case, this reduces to a steady state Riccati equation as t_1 goes to infinity. These results can be extended to the case of boundary controls [15], although at the expense of additional constraints on the semigroup $T(t)$. Similarly, in the stochastic case [15], the optimal compensator is shown to separate into an infinite dimensional state estimator followed by the deterministic gain just described.

Finally, it is useful to conclude this chapter with a concrete example that illustrates the major issues just outlined. In [15], optimal control of the wave equation is considered, i.e.

$$\partial^2 x(t,z)/\partial t^2 - \partial^2 x(z,t)/\partial z^2 = u(z,t) \qquad (2\text{-}56)$$

subject to the boundary conditions

$$x(0,t) = x(1,t) = 0$$

$$x(z,0) = x_0(z), \ \dot{x}(z,0) = x_1(z) \qquad (2\text{-}57)$$

with the cost functional

$$J(u) = \int_0^1 \left[\left(\frac{\partial x(z,t_1)}{\partial z} \right)^2 + \dot{x}^2(z,t_1) \right] dz$$

$$+ \int_0^{t_1} \int_0^1 \left[\frac{1}{4} \dot{x}^2(z,t) + u^2(z,t) \right] dz dt \qquad (2\text{-}58)$$

This problem may be cast in the form of Eqs. (2-52) and (2-53) by defining

$$\underline{w}(t) = \begin{bmatrix} x(z,t) \\ \\ \dot{x}(z,t) \end{bmatrix} = T(t)\underline{w}_o + \int_0^t T(t-s)Bu(s)ds \qquad (2\text{-}59)$$

where

$$B = \begin{bmatrix} 0 \\ \\ I \end{bmatrix}, \quad \underline{w}_o = \begin{bmatrix} x_o(z) \\ \\ x_1(z) \end{bmatrix} \qquad (2\text{-}60)$$

Similarly, the cost may be expressed as

$$J(u) = \frac{1}{2} \langle \underline{w}(t_1), \underline{w}(t_1) \rangle_H + \int_0^{t_1} \left[\frac{1}{4} \langle M\underline{w}(t), \underline{w}(t) \rangle_H + \langle u(z,t), u(z,t) \rangle \right] dt$$

$$(2\text{-}61)$$

where $\langle \cdot, \cdot \rangle_H$ indicates the inner product

$$\langle \underline{w}_1, \underline{w}_2 \rangle_H = \langle x(z,t), x(z,t) \rangle + \langle \dot{x}(z,t), \dot{x}(z,t) \rangle \qquad (2\text{-}62)$$

with $\langle \cdot, \cdot \rangle$ including the usual inner product associated with $L_2[0,1]$. The bounded operator M is defined by

$$M = \begin{bmatrix} 0 & 0 \\ 0 & 1 \end{bmatrix} \qquad (2\text{-}63)$$

This particular problem can be solved analytically [15, p. 98] to yield the optimal control law

$$u(z,t) = \begin{bmatrix} 0 & 0 \\ 0 & -1 \end{bmatrix} \underline{w}(t) = -\dot{x}(z,t) \qquad (2\text{-}64)$$

Physically, this result says the best control law is achieved in this case by adding viscous damping to the system, providing it with a uniform exponential decay rate.

2.6   Compact Feedback Compensators

If X and Y are Hilbert spaces, a particularly interesting subspace of $L(X,Y)$ is the space $C(X,Y)$ of compact linear operators. A bounded linear operator $T : X \to Y$ is compact [23] if it maps bounded sets in X into subsets of compact sets in Y. These operators are in some sense natural generalizations of matrices into infinite dimensional Hilbert spaces since if $T \in L(X,Y)$ and either X or Y is a finite dimensional space, T is compact. Consequently, all mxn matrices are compact operators in $L(R^n, R^m)$. Further, it is true [8, 9, 23] that the adjoint of a compact operator is compact, as are products of compact operators with bounded operators. Finally, it is useful to note that $C(X,Y)$ is a closed subspace of $L(X,Y)$ [8, 9, 23] so that if $\{T_n\}$ is a sequence of compact operators and $||T_n - T|| \to 0$ as $n \to \infty$, the limit T is also a compact operator.

These operators are of interest here because the feedback mapping F arising from most realistic control schemes is compact. In particular, consider the open loop system described by

$$\dot{\underline{x}}(t) = A\underline{x}(t) + B\underline{u}(t)$$

$$\qquad (2\text{-}65)$$

$$\underline{y}(t) = C\underline{x}(t)$$

with $\underline{x}(t) \in H$ representing the state of the system, $\underline{u}(t) \in R^m$ representing the m scalar inputs available for control and $\underline{y}(t) \in R^p$ representing

2-18

the p scalar observations available from the sensors. Here, as long as
the operators B and C are bounded (i.e., pointwise and boundary controls
are excluded), it is clear that B and C are compact operators for any
finite m and p. Consequently, if constant output feedback control is
applied to the system, i.e.

$$\underline{u}(t) \quad = \quad M\underline{y}(t) \tag{2-66}$$

for some $M \in R^{mxp}$ it is also clear that the feedback operator $F = BMC$ is
compact.

Similarly, it is easy to show that dynamic compensators of the form

$$\underline{u}(t) \quad = \quad G\underline{z}(t) + M\underline{y}(t)$$

$$\dot{\underline{z}}(t) \quad = \quad F\underline{z}(t) + L\underline{y}(t) \tag{2-67}$$

where $\underline{z}(t) \in R^q$ for some finite q, can be described by compact feedback
operators. This is done by augmenting the state vector to

$$\underline{v}(t) = \begin{bmatrix} x(t) \\ \\ \underline{z}(t) \end{bmatrix} \tag{2-68}$$

defined on the Hilbert space $V = H + R^q$ with the inner product

$$\langle \underline{v}_1(t), \underline{v}_2(t) \rangle_V \quad = \quad \langle x_1(t), x_2(t) \rangle + \underline{z}_1'(t)\underline{z}_2(t) \tag{2-69}$$

The augmented system may then be described by the model

$$\dot{\underline{v}}(t) \quad = \quad [\overline{A} + \overline{BKC}]\underline{v}(t) \tag{2-70}$$

2-19

$$\overline{A} = \begin{bmatrix} A & 0 \\ 0 & 0 \end{bmatrix} \qquad \overline{B} = \begin{bmatrix} B & 0 \\ 0 & I \end{bmatrix}$$

$$\overline{C} = \begin{bmatrix} C & 0 \\ 0 & I \end{bmatrix} \qquad \overline{K} = \begin{bmatrix} M & G \\ L & F \end{bmatrix} \tag{2-71}$$

Note that if A generates the strongly continuous semigroup $T(t)$, the operator $\overline{A}$ generates the strongly continuous semigroup

$$\overline{T}(t) = \begin{bmatrix} T(t) & 0 \\ 0 & I \end{bmatrix} \tag{2-72}$$

Further, if $T(t)$ is a holomorphic semigroup, it is easy to see that $\overline{T}(t)$ is also a holomorphic semigroup. This augmented model is not exponentially stable, however, since $\underline{z}(t) = \underline{z}(0)$ for all $t > 0$, although this problem can be remedied if desired by replacing $\overline{A}$ and $\overline{K}$ with

$$\tilde{A} = \begin{bmatrix} A & 0 \\ 0 & -F_o \end{bmatrix} \qquad \tilde{K} = \begin{bmatrix} M & G \\ L & F+F_o \end{bmatrix} \tag{2-73}$$

where F_o is any arbitrary positive definite qxq matrix. This augmented system is described by the strongly continuous semigroup

$$T(t) = \begin{bmatrix} T(t) & 0 \\ 0 & e^{-F_o t} \end{bmatrix} \tag{2-74}$$

2-20

which is asymptotically stable if T(t) is. The dynamics of the closed loop system are described by

$$\dot{\underline{v}}(t) \; = \; [\overline{A} + \overline{F}]\underline{v}(t)$$

(2-75)

$$(\text{or } \dot{\underline{v}}(t) \; = \; [\tilde{A} + \tilde{F}]\underline{v}(t))$$

where $\overline{F} = \overline{BKC}$ (or $\tilde{F} = \overline{BKC}$) is the augmented feedback operator. This operator is clearly compact since $\overline{B}$, $\overline{C}$ and $\overline{K}$ (or $\tilde{K}$) are all compact as before.

Since all compact operators are bounded, it is clear that the control limitations outlined in Subsection 2.5 for bounded feedback operators apply to the compact case as well. Unfortunately, there are more severe control limitations on compact feedback operators than on arbitrary bounded operators, as noted in [22]. Specifically, it is shown in [22] that if the semigroup T(t) with infinitesimal generator A describes a conservative system (i.e., E(t) = E(0) for all t > 0 in Eq. (2-33)), then the system described by the semigroup S(t) with infinitesimal generator A + F cannot exhibit a uniform exponential decay rate if F is a compact operator. Further, even if the system is strongly stable (i.e., if E(t) → 0 as t → ∞ for all initial states $\underline{v}_o$) but does not

possess a uniform exponential decay rate, compact feedback cannot provide it with one. These results arise from the fact that compact perturbations of an operator with compact resolvent preserve the asymptotic behavior of the spectrum [24]. Thus, if the poles of the open loop system lie on, or asymptotically approach, the real axis of the complex plane, compact feedback will not alter this fact. Russel illustrates a specific example of this limitation in [20] where he shows that the closed loop poles λ_j of a controlled wave equation must each lie in neighborhoods of radius r_j of their open loop counterparts where $\{r_j\}$ is an ℓ_2 sequence. Consequently, while it is possible to construct compensators to place any finite subset of the closed loop eigenvalues at will, any features of the system that depend on the asymptotic behavior of its spectrum will remain unchanged by compact feedback.

Finally, note that while the compactness of B, C and K resulting from restrictions (2-1) to (2-3) insures the compactness of the feedback map F, the converse is not true. For example, the optimal linear regulator problem considered by Gibson [5, 22] results in compact feedback operator that is no easier to implement than those considered in Subsection 2.5. Specifically, C = I in this problem, which is bounded but not compact, while B is a compact operator. Consequently, the optimal state feedback map $F = -BR^{-1}B^*Q$ is compact and cannot impart a uniform

2-21

exponential decay rate to the undamped plant, as noted in [5, 22]. In contrast, in the optimal linear regulator problem considered in [15], the operators B and R are both bounded but not compact. Thus, this compensator can and does impart a uniform exponential decay rate to the undamped plant.

2.7   Optimal Compact Feedback Compensators

Since compact feedback cannot improve the performance of flexible structures arbitrarily, the question of how much improvement _is_ possible naturally arises. In particular, given a flexible structure model, a specific set of compensator constraints and a performance index, the basic question is how much the performance index can be improved relative to its open loop value.

The most common approach to this problem has been to develop a finite dimensional plant model P_n for the structure that approximates the true dynamics described by the distributed parameter model P. This reduces the problem to the finite dimensional one of designing the best compensator K_n* subject to the constraints, allowing the use of standard control approaches. This fact represents the greatest advantage of this approach and explains its great popularity. The most difficult aspect of this design procedure is that of determining a reasonable approximating model P_n. In particular, to achieve reasonable fidelity in approximating P, it is desirable to make P_n complex enough to capture all of the important details of the structure's dynamics, while for control purposes it is desirable to keep P_n as simple as possible to reduce the difficulty of designing K_n*. In practice, the usual approach is to start with a finite element model P_n that is large enough (several hundred states or more) to approximate P reasonably well and then employ any one of several model reduction approaches [25, 26, 27] to obtain a simpler model P_n' to be used as a basis for designing K_n*.

A second, less popular approach is that employed in [13]. Here, the distributed parameter control problem defined by the plant model P is first solved to obtain the optimal full-state feedback control law F* as described in the last chapter. Then, this control law is approximated subject to the implementation constraints (2-11) to (2-3) to obtain a finite dimensional compensator $\hat{K}$. This approach is less popular than the first one described because it requires the distributed parameter plant model to be known, which is not always the case. Also, distributed parameter control problems are generally harder to solve than finite dimensional ones.

Both of these approaches suffer from the ad-hoc nature of the approximations involved. In particular, it is not clear that either of these design approaches will yield the best compensator K* subject to

2-22

the implementation constraints imposed on the problem. Further, even
though it may be true that a "good" approximation will result in a
compensator whose performance is close to the optimal performance,
these design methods do not yield any quantitative information on this
difference. In fact, as noted in [28], a poor choice of approximate
plant model P_n (or P_n' if the model reduction approach is employed) can
result in closed loop instability when the compensator K_n^* is applied to
the distributed parameter plant P. An approach that avoids these
difficulties is that described in [5]. Here, the dynamics of the struc-
ture are described by a sequence $\{P_n\}$ of approximate models that con-
verge to the distributed parameter plant P as $n \to \infty$. Then, the optimal
full-state feedback controller F_n^* is determined for each plant model
P_n. Under the conditions described in [5], the sequence of compensators
$\{F_n^*\}$ converges to the optimal full-state feedback compensator F* as
$n \to \infty$. While this limit does not meet the implementation constraints
(2-1) to (2-3), this approach does provide a systematic way of approx-
imating it since the performance of the distributed parameter plant
with the control law F_N^* approaches that of the optimal control law F*

for sufficiently large N and insures the stability of the closed loop
system. Also, as a practical matter, this means that if a sufficiently
accurate finite element model of the structure is available, the dis-
tributed parameter dynamical model P need not be known.

Unfortunately, this last approach does have two distinct dis-
advantages. First, even though the control law F_N^* satisfies conditions
(2-1) to (2-3) for any finite N, it becomes progressively harder to
implement as N increases. Thus, if the sequence $\{P_n\}$ converges slowly,
the compensator resulting from this design procedure may be very complex.
On the other hand, simpler compensators may exist that will yield
acceptable performance. The second principal disadvantage of this
approach is that it cannot be used to design compensators meeting struc-
tural constraints like decentralized information patterns.

Consequently, the compensator design approach considered here is
a modification of that considered in [5]. Specifically, the distributed
parameter plant P is approximated here by a sequence of finite dimensional
plants $\{P_n\}$ as just described. However, rather than designing full-
state controllers for each model P_n, the optimal <u>fixed form</u> compensator
K_n^* is designed for each P_n. That is, the desired compensator structure
is fixed initially and the free parameters that define specific com-
pensators of this form are optimized for each model in the sequence
$\{P_n\}$. Finally, the limit of the sequence of compensators $\{K_n^*\}$ will be
taken as $n \to \infty$.

More specifically, in the problem considered here, the dynamics of the distributed parameter plant P will be assumed to satisfy Eq. (2-31). The observations and control inputs will be assumed to satisfy Eqs. (2-48) and (2-46), respectively, where the influence operators B and C are compact. In addition, it will be assumed that the damping operator A_1 is "almost sufficient" to endow the system with a uniform exponential decay rate. Specifically, a finite number of unstable modes will be allowed but the asymptotic nature of the spectrum must be such that when these unstable modes are stabilized, the resulting system has a uniform exponential decay rate. Similarly, a finite number of rigid body (i.e., zero frequency) modes will be allowed. However, since this would violate the positivity assumption on A made in Chapter two, these modes must be treated as a separate finite dimensional subsystem by augmenting the plant state. Finally, to provide a basis for optimizing performance, some form of uncertainty must be included in the plant model. For deterministic problems, this will take the form of a random initial state with zero mean, Gaussian probability density and known covariance. For stochastic problems, plant driving noise and observation noise will be assumed with known statistics. Specifically, zero-mean white Gaussian plant driving noise will enter through a finite number of "equivalent disturbance actuators," of the same type as the control input actuators and zero-mean white Gaussian observation noise will be present in the outputs, arising from noise sources external to the plant.

Given this distributed parameter plant model P, the approximating plants $\{P_n\}$ will be truncated modal models similar to those employed in [2, 5, 22]. Physically, this means each approximate model P_n represents a collection of n (possibly coupled) damped harmonic oscillators.

The compensators K_n^* will be of the form of Eq. (2-67) for some fixed non-negative integer q. For q = 0, this reduces to the constant gain output feedback compensator and if no decentralization constraints are imposed on the problem, all mp elements of the gain matrix are free design parameters. For q > 0, q^2 elements of the (m+q)x(p+q) compensator matrix K may be fixed without affecting the compensator's transfer function [29] (e.g., the compensator may be put into any one of several cannonical forms [30]), reducing the number of free design parameters to mp + (m+p)q. Decentralization constraints will further reduce the number of free design parameters by requiring certain elements of K to be zero. Consequently, the feedback map F = BKC may be decomposed into a fixed part F_0 and a variable part F_1 which will be chosen to minimize a cost functional J(.).

The cost functionals J(.) considered here will be standard quadratic functionals like those considered in [5]. The cost functionals $J_n(.)$ used to define the optimal compensators K_n^* will then be taken as the projections of J(.) onto the modes defining P_n. The optimality results developed in the next section are more general, however, and will only

2-24

require that each cost functional $J_n(.)$ be continuous and that the sequence $\{J_n(.)\}$ converge to $J(.)$ in a manner described in the next section. It is, of course, not possible to assess the severity of this convergence requirement without a detailed examination of the approximate models $\{P_n\}$ even for specific cost functionals $J(.)$ since the manner in which $\{J_n(.)\}$ converges (or does not converge) depends on the manner in which $\{P_n\}$ converges. The continuity requirement on the cost functionals, however, is not restrictive since most practical parameter optimization schemes involve either gradient searches or the solution of gradient-derived necessary conditions, both of which require $J_n(.)$ to be differentiable, hence continuous.

2.8   Optimality Conditions

The compensator design approach just described raises two very important questions. First, when does the sequence $\{K_n*\}$ converge? That is, what conditions must be imposed on the plant model P, the approximating plants P_n, the compensators K_n and the cost functionals $J_n(.)$ and $J(.)$ to insure that the sequence of compensators $\{K_n*\}$ converges to a well-defined limit $K*$? Clearly, this is a difficult question to answer in general since it will depend on both the nature of the convergence of the approximation plants $\{P_n\}$ and the nature of the dependence of the optimal compensator $K*$ on the plant P_n. The results of [5] are encouraging, however, since they provide necessary and sufficient conditions for the convergence of the sequence of compensators considered there. Specifically, in [5], no constraints are imposed on the compensator structure and $J(.)$ is taken as a quadratic cost functional with positive definite, bounded, self-adjoint weighting operators on both the state and the control and examines the convergence of the resulting sequence of full-state feedback compensators. Results are presented that indicate the existence of sufficient inherent damping in the plant P to insure a uniform exponential decay rate is a necessary and sufficient condition for this sequence of compensators to converge to a compact limiting operator.

The second question raised is that of whether the limiting compensator $K*$ is optimal with respect to $J(.)$ when it exists. Specifically, if K_n* minimizes the cost functional $J_n(.)$ for the plant P_n and $K_n* \to K*$ as $n \to \infty$, what conditions are sufficient to insure that $K*$ minimizes $J(.)$ for the plant P? This section will show that if the sequence of cost functionals $\{J_n(.)\}$ converges to the limit $J(.)$ appropriately, then $K*$ does minimize $J(.)$ for the limiting plant P.

Specifically, it will be assumed that the sequence $\{K_n^*\}$ converges to K^* in the sense that $||K_n^* - K^*|| \to 0$ as $n \to \infty$. That is, given $\varepsilon > 0$, there exists N such that $||K_n^* - K^*|| < \varepsilon$ for all $n \geq N$. Here, the norm $||.||$ is defined as [8]

$$||K|| = \sup_{\underline{y} \neq 0} \frac{||K_{\underline{y}}||_2}{||\underline{y}||_1} \qquad (2-76)$$

where $\underline{y} \in R^p$, $||.||_1$ is the Euclidian norm on R^p and $||.||_2$ is the Euclidian norm on R^m. The compensators K_n^* will also be required to belong to the set Λ of compensators meeting the structure constraints described in the last section. Note that by fixing the structure of the compensator in this manner, only the free parameters depend on P_n and $J_n(.)$ so that if K^* exists, it will be of the correct form. In addition, two other constraints will be imposed on K^*. First, it must stabilize the plant P in order for the infinite time horizon problems considered here to make sense. Similarly, the optimization problem becomes meaningless if $J(K^*)$ is not finite. Thus, defining

$$S = \{K \in \Lambda \mid K \text{ stabilizes } P\} \qquad (2-77)$$

and

$$T = \{K \in \Lambda \mid J(K) < \infty \} \qquad (2-78)$$

the set Γ of admissable compensators will be defined as

$$\Gamma = (S \cap T)^\circ \qquad (2-79)$$

where Ω° indicates the interior of the set Ω. Note that Γ will generally shrink as additional constraints are imposed on the structure of the compensator, possibly reducing to the empty set if these constraints are severe enough.

Given the set Γ of admissable compensators defined by the plant P, the cost functional $J(.)$ and the compensator form constraints defining Λ, the sequence of approximating cost functionals must satisfy the

2-26

following convergence requirement. For arbitrary $K \in \Gamma$ and $\varepsilon > 0$, there must exist a positive integer N and a positive constant δ such that

$$n > N \text{ and } ||L - K|| < \delta$$

$$=> |J_n(L) - J(L)| < \varepsilon$$

Basically, this requires the sequence $\{J_n(.)\}$ to converge uniformly in some open neighborhood of every element of Γ. This insures the following results.

Lemma 2-1: If a sequence of continuous cost functionals $\{J_n(.)\}$ converges in the manner just described, the limiting cost functional $J(.)$ is continuous on Γ.

Proof:

1. Given $\varepsilon > 0$, it follows from the convergence condition on $\{J_n(.)\}$ that there exists a positive integer N and $\mu > 0$ such that $|J_N(L) - J(L)| < \varepsilon/3$ for all $L \in B_\mu(K)$ where

$$B_\mu(K) = \{L : ||L - K|| < \mu\}.$$

2. Since $J_N(.)$ is continuous, there is a positive constant ν such that $|J_N(L) - J_N(K)| < \varepsilon/3$ for all $L \in B_\nu(K)$.

3. Let $\delta = \min(\mu, \nu)$ so $L \in B_\delta(K) => L \in B_\mu(K)$ and $L \in B_\nu(K)$ so that

$$|J(L) - J(K)| \leq |J(L) - J_N(L)|$$

$$+ |J_N(L) - J_N(K)|$$

$$+ |J_N(K) - J(K)|$$

$$< \varepsilon/3 + \varepsilon/3 + \varepsilon/3 = \varepsilon.$$

4. Thus, $J(.)$ is continuous on Γ. $\square$

Lemma 2-2: If a sequence of continuous cost functionals $\{J_n(.)\}$ converges in the manner just described and if the sequence of compensators $\{K_n\}$ converges to a limit K, then

$$\lim_{n \to \infty} J_n(K_n) = J(K).$$

Proof:

1. From the convergence condition on $\{J_n(.)\}$, given $\epsilon > 0$ there exists an integer N_1 and $\nu > 0$ such that if $n \geq N_1$, then $\left| J_n(L_n) - J(L_n) \right| < \epsilon/2$ for all $L \in B_\nu(K)$.

2. Since Γ is open, if $K_n \to K$ and $K \in \Gamma$, there exists an integer N_2 such that $n \geq N_2 = > K_n \epsilon \Gamma$ so that $J(K_n)$ is a finite, physically meaningful quantity.

3. Since $K_n \to K$, there exists an integer N_3 such that $n \geq N_3 = > K_n \epsilon B_\nu(K)$.

4. Thus, let $N_4 = \max (N_1, N_2, N_3)$ so that $n \geq N_4 = > \left| J_n(K_n) - J(K_n) \right| < \epsilon/2$.

5. By lemma 2-1, there exists $\mu > 0$ such that $L \in B_\mu(K) = > \left| J(L) - J(K) \right| < \epsilon/2$.

6. Again, since $K_n \to K$, there exists an integer N_5 such that $n \geq N_5 = > K_n \epsilon B_\mu(K)$.

7. Let $N = \max(N_4, N_5)$. Then $n \geq N = >$

$$\left| J_n(K_n) - J(K) \right| \leq \left| J_n(K_n) - J(K_n) \right|$$

$$+ \left| J(K_n) - J(K) \right|$$

$$< \epsilon/2 + \epsilon/2 = \epsilon.$$

8. Consequently, $\lim_{n \to \infty} J_n(K_n) = J(K).$ $\square$

It is important to note the significance of this convergence requirement on the sequence $\{J_n(.)\}$. First, this is a stronger condition

than local convergence which only requires $J_n(K) \to J(K)$ for all $K \in \Gamma$.

In particular, local convergence does <u>not</u> guarantee the continuity of the limiting cost functional $J(.)$. Similarly, this condition is weaker than uniform convergence since given $\varepsilon > 0$, the minimum N and maximum δ for which $|J_n(L) - J(L)| < \varepsilon$ for all $L \in B_\delta(K)$ may vary with K. In particular, the convergence may become local on the boundary of the set Γ. In fact, the convergence required here is equivalent to uniform convergence of $\{J_n(.)\}$ on compact subsets of Γ, as shown in the following lemma.

Lemma 2-3: The following convergence requirements on $\{J_n(.)\}$ are equivalent:

    i)   Given $K \in \Gamma$ and $\varepsilon > 0$, there exists an integer N and a positive constant δ such that $n \geq N \Rightarrow |J_n(L) - J(L)| < \varepsilon$ for all $L \in B_\delta(K)$.

    ii)   Given a compact subset Ω of Γ, there exists N such that $n \geq N \Rightarrow |J_n(L) - J(L)| < \varepsilon$ for all $L \in \Omega$.

Proof:

    1.   To show i) $\Rightarrow$ ii), let Ω be a compact subset of Γ. Then given $K \in \Omega$ and $\varepsilon > 0$, there exists an integer N_K and a positive constant δ_K such that $n \geq N_K \Rightarrow |J_n(L) - J(L)| < \varepsilon$ for all L such that $||L - K|| < \delta_K$.

    2.   Since Ω is a compact subset of Γ, it is closed and bounded so

$$\sup_{K \in \Omega} (\min N_K) = \max_{K \in \Omega} (\min N_K) = N < \infty$$

and

$$\inf_{K \in \Omega} (\sup \delta_K) = \min_{K \in \Omega} (\sup \delta_K) = \delta > 0.$$

Clearly, $N \geq N_K$ and $\delta \leq \delta_K$ for all $K \in \Gamma$ so that $n \geq N \Rightarrow |J_n(L) - J(L)| < \varepsilon$ for all L such that $||L - K|| < \delta.$

    3.   However, K is an arbitrary element of Ω so $n \geq N \Rightarrow |J_n(L) - J(L)| < \varepsilon$ for any $L \in \Omega$, establishing ii).

4. To prove ii) = > i), select an arbitrary $K \varepsilon \Gamma$. Since Γ is open, there exists some $\delta > 0$ such that the open ball $B_{2\delta}(K)$ is contained in Γ

5. Let $\bar{B}_{2\delta}(K)$ represent the closed ball

$$\bar{B}_{2\delta}(K) = \{L : ||L - K|| \leq 2\delta\}$$

and note that $B_\delta(K) \subset \bar{B}_{2\delta}(K) \subset B_{3\delta}(K) \subset \Gamma$.

6. From ii), there exists N such that $n \geq N = >$ $|J_n(L) - J(L)| < \varepsilon$ for all $L \varepsilon \bar{B}_{2\delta}(K)$.

7. Thus, given $K \varepsilon \Gamma$, $n \geq N = > |J_n(L) - J(L)| < \varepsilon$ for all $L \varepsilon B_\delta(K)$, establishing i). $\square$

The principal result of this section is the following theorem that establishes sufficient conditions for the optimality of the limit K* of the sequence $\{K_n*\}$ of optimal compensators for the approximating plants $\{P_n\}$.

Theorem 2-1: Suppose the following conditions are met:

i) each functional $J_n(.)$ is continuous

ii) K_n* minimizes $J_n(.)$ for all n

iii) $K_n* \rightarrow K*$ for some $K* \varepsilon \Gamma$

iv) $J_n(.) \rightarrow J(.)$ in the sense of lemma 2-3.

Then,

v) $\lim_{n\to\infty} J_n(K_n*) = J(K*)$

vi) K* minimizes $J(.)$

Proof:

1. Result v) follows immediately from conditions i) and iii) by lemma 2-2.

2. To prove vi), suppose K* is not optimal. Then there exists some $\tilde{K} \varepsilon \Gamma$ such that

$$J(K^*) - J(\tilde{K}) = d > 0.$$

3. From the convergence condition on $\{J_n(.)\}$, there exist integers N_1 and N_2 such that

$$n > N_1 \Rightarrow |J_n(\tilde{K}) - J(\tilde{K})| < d/2$$

and

$$n \geq N_2 \Rightarrow |J_n(K_n^*) - J(K^*)| < d/2.$$

4. Let $N = \max(N_1, N_2)$, then

$$-d/2 < J_N(\tilde{K}) - J(\tilde{K}) < d/2$$

$$-d/2 < J_N(K_N^*) - J(K^*) < d/2$$

5. Thus,

$$
\begin{aligned}
J_N(K_N^*) &= J(K^*) - [J(K^*) - J_N(K_N^*)] \\
&= J(\tilde{K}) + d - [J(K^*) - J_N(K_N^*)] \\
&> J(\tilde{K}) + d/2 \\
&> J(\tilde{K}) + [J_N(\tilde{K}) - J(\tilde{K})] \\
&= J_N(\tilde{K})
\end{aligned}
$$

which contradicts the definition of K_N^*.

6. Consequently, K^* minimizes $J(.)$. $\square$

Finally, the following corollary is an important practical result that follows immediately from the convergence of $\{K_n^*\}$. In particular, it guarantees that compensator designs based on sufficiently accurate finite dimensional dynamic models (e.g., sufficiently large finite element models) will stabilize the distributed parameter plant and achieve approximately optimal performance.

Corollary 2-1: If conditions i) through iv) of Theorem 2-1 are met, then there exists some integer N such that

i) $n \geq N \Rightarrow K_n*$ stabilizes P

and

ii) given $\epsilon > 0$, there exists $N' \geq N$ such that

$J(K_n*) - J(K*) < \epsilon$ for all $n \geq N'$.

Proof:

1. Since Γ is open and $K* \epsilon \Gamma$, there exists $\delta > 0$ such that $B_\delta(K*) \subset \Gamma$. Thus, since $K_n* \rightarrow K*$, there exists an integer N such that $n \geq N \Rightarrow K_n* \epsilon B_\delta(K*) \Rightarrow K_n*$ stabilizes P.

2. By lemma 2-1, $J(.)$ is continuous on Γ so given $\epsilon > 0$, there exists $\mu > 0$ such that $L \epsilon B_\mu(K*) \Rightarrow |J(L) - J(K*)| = J(L) - J(K*) < \epsilon$.

3. Consequently, since $K_n* \rightarrow K*$ and $K_n* \epsilon \Gamma$ for all $n \geq N$, there exists $N' \geq N$ such that $n \geq N' \Rightarrow K_n* \epsilon \Gamma$ and $J(K_n*) - J(K*) < \epsilon$. □

2.9 Conclusions

The compensator design approach suggested in [1] has been generalized to a wider class of cost functionals and specialized to the flexible structure control problem. In addition, sufficient conditions for the optimality of the resulting compensator have been established. If these conditions can be met, this design approach has three principal advantages. First, it does yield the best compensator, relative to the cost functional $J(.)$, that meets any given set of structure constraints imposed on the control system. Consequently, the difficulty of implementing the control system may be specified a priori as a design constraint. The second advantage of this design approach is that the value of $J(K*)$ provides a quantitative measure of the performance achievable subject to the implementation constraints. Thus, if this cost is too great to meet the desired performance objectives, the optimality of K* implies that some of the structure constraints must be relaxed to achieve acceptable performance. Finally, as a practical matter, this approach allows the design of the optimal compensator K* from a sufficiently accurate finite element model, eliminating the need for exact knowledge of the distributed parameter dynamics.

Unfortunately, this design approach also has two fairly significant disadvantages. First, the finite dimensional optimal fixed form compensater problem is numerically difficult to solve. Specifically, unlike the case of the optimal full-state feedback compensator, no explicit solution is available for this problem. Only necessary conditions for optimality are known and these are difficult to solve [29].

The other major disadvantage of this approach is that it is new so several important open questions exist. First, it is not clear under what conditions the sequence $\{K_n*\}$ of approximating compensators converges to a well-defined, stabilizing compensator $K*$ with finite cost $J(K*)$. Similarly, it is not clear under what conditions the sequence $\{J_n(.)\}$ of approximating cost functionals converge in the sense required by lemma 2-3. Finally, even if these sequences do converge for a particular problem, their rate of convergence will determine how practical this design approach will be. Clearly, all of these questions depend on the nature of the distributed parameter plant P, the cost functional $J(.)$ and the approximation scheme that determines the sequences $\{P_n\}$ and $\{J_n(.)\}$. In particular, in view of the results of [3,5,22], it is likely that the answers of all of these questions will depend strongly on the nature of the damping mechanisms present.

In conclusion, the results presented here suggest the following avenues of research might yield useful results:

1. Examine the convergence of standard quadratic cost functionals for modal approximations $\{P_n\}$ of the plant P. In particular, do the corresponding approximate cost functionals $\{J_n(.)\}$ meet the convergence requirements of lemma 2-3?

2. Examine the possibility of extending Gibson's results [5,22] to the case of fixed form compensators. Specifically, is the existence of a uniform decay rate in stable open-loop plants a necessary and sufficient condition for the convergence of the sequence $\{K_n*\}$ arising from quadratic cost functionals $J(.)$ and modal approximation schemes?

3. As a specific example, examine the convergence of stochastic output feedback compensators $\{K_n*\}$ for representative plants like the Draper model number 2. Specifically, what is the relation between inherent damping and convergence rate for this problem?

4. Examine the possibility of developing numerically efficient algorithms for evaluating the optimal compensator K_n* for the finite dimensional plant P_n. In particular, is it possible to develop a recursive algorithm to compute $K_{n+1}*$ from K_n*?

References

[1]   T. L. Johnson, "Optimization of Low Order Compensators for
        Infinite Dimensional Systems," Proceedings of the 9th IFIP
        Symposium on Optimization Techniques, Warsaw, Poland, Sept. 1979.

[2]   M. J. Balas, "Modal Control of Certain Flexible Dynamic Systems,"
        SIAM J. Control and Optimization, 16, 3, 1978, pp. 450-462.

[3]   G. Chen and D. L. Russell, A Mathematical Model for Linear Elastic
        Systems with Structural Damping, MRC Technical Summary Rept.
        #2089, Wisconson University, Madison, June 1980.

[4]   D. L. Russell, "Linear Stabilization of the Linear Oscillator in
        Hilbert Space," J. Math. Anal. Appl., 25, 1969, pp. 663-675.

[5]   J. S. Gibson, "Convergence and Stability in Linear Modal Regulation
        of Flexible Structures," Second UPI & SU/AIAA Symposium on Dynamics
        and Control of Large Flexible Spacecraft, Blacksburg, Virginia,
        June 1979.

[6]   E. F. Infante and J. A. Walker, "On the Behavior of Linear
        Undamped Elastic Systems Perturbed by Follower Forces," in
        Dynamical Systems, A. R. Bednarek and L. Cesari, Eds., Academic
        Press, New York, 1977.

[7]   D. L. Russell, "Decay Rates for Weakly Damped Systems in Hilbert
        Space Obtained with Control-Theoretic Methods," J. Diff. Equations,
        19, 1975, pp. 344-370.

[8]   E. Kreysig, Introductory Functional Analysis with Applications,
        Wiley, New York, 1978.

[9]   T. K   , Perturbation Theory for Linear Operators, Springer-
        Verlag, New York, 1980.

[10]   A. W. Naylor and G. R. Sell, Linear Operator Theory in Engineering
        and Science, Holt, Rinehart and Winston, New York, 1971.

[11]   F. Treves, Basic Linear Partial Differential Equations, Academic
        Press, New York, 1975.

[12]   P. M. Morse and H. Feshbach, Methods of Theoretical Physics,
        McGraw-Hill, New York, 1953.

[13]   M. Köhne, "The Control of Vibrating Elastic Systems," Chapter 7
        of Distributed Parameter Systems: Identification, Estimation
        and Control, W. H. Ray and D. G. Lainiotis, eds., Marcel Dekker
        Inc., New York, 1978.

[14]   C. Croxton, Introductory Eigenphysics, Wiley, London, 1974.

[15]   R. F. Curtain and A. J. Pritchard, Infinite Dimensional Linear
        Systems Theory, Springer-Verlag, New York, 1978.

[16]   G. Stein and C. Greene, "Inherent Damping, Solvability Conditions
        and Solutions for Structural Control," Proceedings of the 18th
        IEEE Conference on Decision and Control, Ft. Lauderdale, Florida,
        December, 1978.

[17]   C. M. Dafermos, "Wave Equations with Weak Damping," SIAM J.
        Appl. Math., 18, 4, June, 1970, pp. 759-767.

[18]   W. G. Heller, "Feedback Stabilization of a Distributed Parameter
        System by Scanning," IFAC Symposium on the Control of Distributed
        Parameter Systems, Banff, Canada, June, 1971.

[19]   W. Rudin, Functional Analysis, McGraw-Hill, New York, 1973.

[20]   D. L. Russell, Controllability and Stabilizability Theory for Linear
        Partial Differential Equations, MRC Technical Summary Rept. No. 1700,
        Wisconson University, Madison, November, 1976.

[21]   F. M. Brasch and J. B. Pearson, "Pole Placement Using Dynamic
        Compensators, IEEE Trans. Auto. Control, 15, 1, 1970, pp. 34-43.

[22]   J. S. Gibson, "A Note on Stabilization of Infinite Dimensional
        Linear Oscillators by Compact Feedback," SIAM J. Control and
        Optimization, 18, 1, 1980, pp. 311-316.

[23]   V. Balakrishman, Applied Functional Analysis, Springer-Verlag,
        New York, 1976.

[24]   A. G. Ramm, "Perturbations Preserving Asymptotic of Spectrum,"
        J. Math. Aml. Appl., 76, 1980, pp. 10-17.

[25]   P. Sannuti and P. V. Kokotovic, "Near-Optimum Design of Linear
        Systems by a Singular Perturbation Method," IEEE Trans. Auto.
        Control, 14, 1, 1969, pp. 15-22.

[26]   M. Aoki, "Control of Large Scale Dynamic Systems by Aggregation,"
        IEEE Trans. Auto. Control, 13, 3, 1968, pp. 246-253.

[27]   M. R. Chidambara and R. B. Shainker, "Lower Order Generalized
        Aggregated Model and Suboptimal Control," IEEE Trans. Auto.
        Control, 16, 2, 1971, pp. 175-180.

[28]   J. H. Lang, "A Perturbation Analysis of Spillover in Closed-Loop
        Distributed-Parameter Systems," Proceedings of the 19th IEEE
        Conference on Decision and Control, Albuquerque, New Mexico,
        December, 1980.

[29]   C. J. Wenk, <u>Parameter Optimization for Linear Systems with
        Arbitrarily Constrained Information and Control Structure</u>,
        University of Connecticut Department of Electrical Engineering
        and Computer Science, Technical Report TR 79-4, February 1979.

[30]   C. T. Chen, <u>Introduction to Linear System Theory</u>, Holt, Rinehart
        and Winston, New York, 1970.

SECTION 3

CLOSED-LOOP STABILITY AND ROBUSTNESS CONDITIONS
FOR LARGE SPACE SYSTEMS WITH REDUCED-ORDER CONTROLLERS

3.1   Introduction

Consider the active (or passive) control of a generic large space system which may contain rigid as well as elastic modes, undamped as well as damped modes, unstable as well as stable modes. As usual, let such a large-scale distributed-parameter mechanical system be adequately represented by a finite-element model of a reasonable (high) dimension, L, as

$$M\ddot{q} + D\dot{q} + Kq = f \tag{3-1}$$

where the vector q denotes the L generalized coordinates, the vector f the L generalized forces. The matrices M, D, and K denote the mass (or inertia), the "damping", and the "stiffness", respectively, of the structure. As usual, M is real, symmetric, and positive definite; K is real, and symmetric; and D is real. Note that not even non-negative definiteness is assumed of matrices D or K, so that rigid modes, undamped modes, and even unstable modes[1], if they exist, need not be excluded from discussions. No symmetry of matrix D is assumed so that gyroscopic effects, represented by the skew-symmetric part of D, need not be excluded either. For controlling the structure, let there be m force actuators:

$$f = B_F u \tag{3-2}$$

where vector u denotes the m actuator inputs, one for each actuator, to be controlled (or manipulated); the L x m matrix B_F denotes the actuator influence coefficients. Also let there be ℓ sensors for separate or mixed measurement of displacements and velocities:

$$y = C_D q + C_V \dot{q} \tag{3-3}$$

---

[1]   For example, orbiting structures without equal moments of inertia about all three axes will contain unstable rigid modes if gravity gradient torques are not ignorable.

where the vector y denotes the ℓ sensor outputs; the ℓ x L matrices C_D and C_V denote the displacement and velocity influence coefficients. Now, consider the following general form[2] of (static) output feedback control:

$$u = -Gy \qquad (3-4)$$

where the m x ℓ matrix G denotes the time-invariant feedback gains. The gain matrix can be designed for various control objectives by many different ways. Will any design at least ensure that the resultant closed-loop system

$$M\ddot{q} + (D + B_F G C_V)\dot{q} + (K + B_F G C_D)q = 0 \qquad (3-5)$$

is asymptotically stable?[3] For realistically large space systems, the answer is generally no. First of all, the L x L additional damping matrix

$$D^* \overset{d}{=} B_F G C_V \qquad (3-6)$$

and the L x L additional stiffness matrix

$$K^* \overset{d}{=} B_F G C_D \qquad (3-7)$$

are singular matrices since the number m of actuators and the number ℓ of sensors are, realistically, much smaller than the number L of generalized coordinates. In other words, for whatever design of the output feedback controllers, the matrices D* and K* can be non-negative definite at best. An arbitrary gain matrix G, therefore, will not ensure the positive definiteness[4] of both the augmented damping matrix (D + D*) and the augmented stiffness matrix (K + K*). Hence, the asymptotic stability of

---

[2] See Subsect. 3.7.1 for examples of common special forms.

[3] See Subsect. 3.7.2 for some comments on displacement feedback, velocity feedback, and stability conditions, and Subsect. 3.7.3 for some generalized asymptotic stability conditions.

[4] Again, see Subsect. 3.7.2 for some comments on these stability conditions.

the resulting closed-loop system **does not follow unconditionally** from arbitrary design of output feedback controllers.

The common practice of using only reduced-order modal models in controller design makes it even more legitimate to question the stability of the resulting full-order closed-loop system. Like the standard case of no unstable modes, rewrite Eqs. (3-1) and (3-3) in terms of normal modes as follows.

$$\ddot{\eta} + \Delta\dot{\eta} + \Sigma\eta = \Phi^T f \tag{3-8}$$

$$y = C_D \Phi \eta + C_V \Phi \dot{\eta} \tag{3-9}$$

where Σ is a diagonal matrix of real numbers, each denoting the "stiffness" of a normal mode; depending on the specific structure concerned, the diagonal elements can be positive, zero, or even negative. Each column of matrix Φ denotes a normalized mode shape. In the standard practice of finite-element modeling and analysis (using NASTRAN, for example), damping is assumed to be absent first and an identical damping ratio (say, $\zeta_i \equiv 0.01$) is then assigned (rather arbitrarily) to all modes. Therefore, we shall follow **the common practice of assuming Δ to be diagonal** in the main part of our subsequent discussions; nevertheless, discussions will be extended to the non-diagonal case, particularly the more realistic case of **non-proportional damping**, at the end. Various practical reasons have necessitated the truncation of the high-dimensional modal model (3-8)-(3-9). As a result, reduced-order models for design of output feedback controllers take the following general form.

$$\ddot{\eta}_M + \Delta_M \dot{\eta}_M + \Sigma_M \eta_M = \Phi_M^T f \tag{3-10}$$

$$y = C_D \Phi_M \eta_M + C_V \Phi_M \dot{\eta}_M \tag{3-11}$$

where subscript M denotes the portion retained[5] in the controller design

---

[5] In general, substantially more modes can be retained for design of output feedback controllers than for design of dynamic compensators (including linear-quadratic optimal regulators combined with Luenberger observers or Kalman filters). After design, reduced-order models are also required for implementing dynamic compensators by the capability-limited onboard computers but not so at all for implementing (static) output feedback controllers.

model. The output feedback controllers are thus designed, say, to augment certain amounts of damping or stiffness to the retained modes, or to move the poles or zeros of the design model to desirable locations, or to minimize certain cost functions regarding the control of the design model. Assume that, with whatever design approach taken, asymptotic stability of the resultant reduced-order closed-loop (ROCL) system,

$$\ddot{\eta}_M + (\Delta_M + \Phi_M^T D^* \Phi_M)\dot{\eta}_M + (\Sigma_M + \Phi_M^T K^* \Phi_M)\eta_M = 0 \tag{3-12}$$

can be achieved explicitly or implicitly, where the matrices D^* and K^* are as defined by (3-6) and (3-7). Will ROCL asymptotic stability insure the asymptotic stability of the resulting full-order closed-loop (FOCL) system? If not unconditionally, under what conditions will it? Useful answers to these and other related questions are provided in this section, including an elaboration and expansion of the preliminary results summarized earlier in an interim report [1].

Subsection 3.2 addresses asymptotic stability for the general case where the systems in question may have unstable as well as stable modes. Subsections 3.3 and 3.4 address asymptotic stability and robustness, respectively, for the case of large space structures having only stable modes, rigid or elastic, damped or undamped. Subsection 3.5 addresses the more realistic case of nonproportional damping. Subsection 3.7 contains relevant appendices.

For reporting convenience, we assume, in the sequel, that there are no reasons against making the additional stiffness matrix $B_F CC_D$ symmetric and that if the additional damping matric $B_F GC_V$ is asymmetrical, then D^* is to be interpreted as the symmetric part of $B_F GC_V$.

3.2 Full-Order Closed-Loop Stability Conditions

In what follows, we shall mainly be concerned with asymptotic stability of the resulting FOCL system.

$$\ddot{\eta} + (\Delta + \Phi^T D^* \Phi)\dot{\eta} + (\Sigma + \Phi^T K^* \Phi)\eta = 0 \tag{3-13}$$

Note that both representations (3-5) and (3-13) are equivalent with respect to the following nonsingular coordinate transformation:

$$q = \Phi\eta \tag{3-14}$$

Recall that System (3-13) is asymptotically stable if both the augmented damping $(\Delta + \Phi^T D^* \Phi)$ and the augmented stiffness $(\Sigma + \Phi^T K^* \Phi)$ <u>are positive definite</u>. Since one may need to augment only damping, or only stiffness, or both together, we shall provide separate conditions for ensuring the the positive definiteness of the augmented damping matrix and that of the augmented stiffness matrix; FOCL asymptotic-stability conditions are simply these separate positive-definiteness conditions combined.

Denote by subscript U the unmodeled portion. The matrices involved in (3-13) can be partitioned into modeled (M) and unmodeled (U) parts as follows.

$$
\eta = \left[\begin{array}{c} \eta_M \\ \hline \eta_U \end{array} \right], \qquad
\Phi = \left[\begin{array}{c|c} \Phi_M & \Phi_U \end{array} \right]
$$

$$
\Delta = \left[\begin{array}{c|c} \Delta_M & 0 \\ \hline 0 & \Delta_U \end{array} \right], \qquad
\Sigma = \left[\begin{array}{c|c} \Sigma_M & 0 \\ \hline 0 & \Sigma_U \end{array} \right] \tag{3-15}
$$

In particular, the augmented damping and stiffness matrices can be explicitly written as

$$
\Delta + \Phi^T D^* \Phi \equiv \left[\begin{array}{c|c} \Delta_M + \Phi_M^T D^* \Phi_M & \Phi_M^T D^* \Phi_U \\ \hline \Phi_U^T D^* \Phi_M & \Delta_U + \Phi_U^T D^* \Phi_U \end{array} \right] \tag{3-16}
$$

$$
\Sigma + \Phi^T K^* \Phi \equiv \left[\begin{array}{c|c} \Sigma_M + \Phi_M^T K^* \Phi_M & \Phi_M^T K^* \Phi_U \\ \hline \Phi_U^T K^* \Phi_M & \Sigma_U + \Phi_U^T K^* \Phi_U \end{array} \right] \tag{3-17}
$$

3-5

It is not difficult to see from Eqs. (3-16) and (3-17) that ensuring the positive definiteness of upper left blocks of the matrices during the reduced-order design does not automatically ensure that the whole matrices are positive definite. The conditions to ensure positive definiteness are provided by the following two theorems combined.

<u>Theorem 1A (Damping Augmentation)</u>: Assume the feedback gain G is such that

(a) D^* is symmetric, and

(b) $\Delta_M + \Phi_M^T D^* \Phi_M$ is positive definite.

Then the whole augmented damping matrix $(\Delta + \Phi^T D^* \Phi)$ is positive definite if and only if the following test matrix

$$\Delta_T \overset{d}{=} \Delta_U + \Phi_U^T D^* \Phi_U - \Phi_U^T D^* \Phi_M \left(\Delta_M + \Phi_M^T D^* \Phi_M \right)^{-1} \Phi_M^T D^* \Phi_U \qquad (3\text{-}18)$$

is positive definite

<u>Theorem 1B (Stiffness Augmentation)</u>: Assume the feedback gain G is such that

(a) K^* is symmetric, and

(b) $\Sigma_M + \Phi_M^T K^* \Phi_M$ is positive definite.

Then the whole augmented stiffness matrix $(\Sigma + \Phi^T K^* \Phi)$ is positive definite if and only if the following test matrix

$$\Sigma_T \overset{d}{=} \Sigma_U + \Phi_U^T K^* \Phi_U - \Phi_U^T K^* \Phi_M \left(\Sigma_M + \Phi_M^T K^* \Phi_M \right)^{-1} \Phi_M^T K^* \Phi_U \qquad (3\text{-}19)$$

is positive definite

These two theorems are direct consequences of a general statement on positive definiteness of partitioned real symmetric matrices (see Theorem 1 of Subsect. 3.7.4) applied to the partitioned matrices (3-16) and (3-17), respectively. The following important implications are worth observing.

1. Ensuring ROCL asymptotic stability is <u>not enough</u> to ensure FOCL asymptotic stability, except when all unmodeled modes are damped stable elastic modes and have no control or observation spillover whatsoever. Positive definiteness of the unmodeled part $\Delta_U + \Phi_U^T D^* \Phi_U$ is necessary (but not sufficient) for ensuring the positive definiteness of test matrix Δ_T and hence that of the whole augmented damping matrix $\Delta + \Phi^T D^* \Phi$. Similarly, positive definiteness

of $\Sigma_U + \phi_U^T K^* \phi_U$ is necessary for the positive definiteness of test matrix Σ_T and that of the whole augmented stiffness matrix $\Sigma + \phi^T K^* \phi$.

2. Arbitrary truncation can be a problem. If unmodeled modes include a rigid mode or an unstable mode with negative stiffness, the whole augmented stiffness matrix cannot be positive definite. Similarly if unmodeled modes include an undamped mode or an unstable mode with negative damping, the whole augmented damping matrix cannot be positive definite. In either case, ROCL asymptotic stability will not ensure FOCL asymptotic stability, unless all those unmodeled rigid, undamped, or unstable modes are properly compensated by favorable spillover, which is rather accidental.

3. Spillover can be unfavorable. Control spillover combined with observation spillover can prevent the test matrices, Δ_T and Σ_T, and hence the whole augmented damping and stiffness, $(\Delta + \phi^T D^* \phi)$ and $(\Sigma + \phi^T K^* \phi)$, from being positive definite even when Δ_U and Σ_U are positive definite. In other words, even structures that are initially stable can become unstable because of spillover when the feedback loops are closed.

4. Advantages of making (or trying hard to make) D^* and K^* non-negative definite are obvious. Spillover will become favorable: the matrices $\phi_U^T D^* \phi_U$ and $\phi_U^T K^* \phi_U$ will be at least non-negative definite, making test matrices Δ_T and Σ_T more likely to be positive definite. As we shall see in the following subsection, ROCL asymptotic stability thereby can ensure FOCL asymptotic stability in case there are no unstable modes and all rigid or undamped modes are included in the design of output feedback controllers.

5. Collocation of sensors with actuators is desirable but not necessary: it does not contribute directly to ensure FOCL asymptotic stability. Sensor-actuator collocation is mathematically the easiest way for making D^* and K^* symmetric, yet these matrices can be made symmetric without such collocation. See Subsect. 3.7.5 for a general design procedure. As mentioned above, it is the non-negative definiteness of D^* and K^*, rather than their symmetry, that plays the principal role in ensuring FOCL stability.

To provide a better insight into the requirements for ensuring FOCL asymptotic stability, regroup the modes as follows. Designate as group G all those modes which have positive damping (i.e. $\Delta_{ii} > 0$) and the remainder as group LE. Similarly, designate as group G' all those which have positive stiffness (i.e., $\Sigma_{jj} > 0$), and the remainder as group L'E'. With matrices Λ, Σ, and ϕ partitioned accordingly, we have the following similar conditions for ensuring positive definiteness.

Corollary 1A (Damping Augmentation): Assume the gain G is such that

(a) D^* is symmetric, and

(b) $\Delta_{LE} + \Phi_{LE}^T D^* \Phi_{LE}$ is positive definite.

Then the whole augmented damping matrix $(\Delta + \Phi^T D^* \Phi)$ is positive definite if and only if the following matrix

$$\Delta_G + \Phi_G^T D^* \Phi_G - \Phi_G^T D^* \Phi_{LE} \left(\Delta_{LE} + \Phi_{LE}^T D^* \Phi_{LE}\right)^{-1} \Phi_{LE}^T D^* \Phi_G$$

is positive definite.

Corollary 1B (Stiffness Augmentation): Assume that the gain G is such that

(a) K* is symmetric, and

(b) $\Sigma_{L'E'} + \Phi_{L'E'}^T K^* \Phi_{L'E'}$ is positive definite.

Then the whole augmented stiffness matrix $(\Sigma + \Phi^T K^* \Phi)$ is positive definite if and only if the following test matrix

$$\Sigma_{G'} + \Phi_{G'}^T K^* \Phi_{G'} - \Phi_{G'}^T K^* \Phi_{L'E'} \left(\Sigma_{L'E'} + \Phi_{L'E'}^T K^* \Phi_{L'E'}\right)^{-1} \Phi_{L'E'}^T K^* \Phi_{G'}$$

is positive definite.

These corollaries are direct consequences of Theorems 1A and 1B when the modeled (M) part is interpreted as having only the group LE for Corollary 1A and having only the group L'E' for Corollary 1B. It follows from implication 2 of Theorems 1A and 1B that all those modes which have either non-positive damping (group LE) or non-positive stiffness (group L'E') should be included as modeled modes and be properly compensated. Very often, satisfaction of assumption (b) in Theorems 1A and 1B is difficult to ensure or to verify either because too many modes are involved or because the design method (such as the Levine-Athans optimal output feedback or the Kosut suboptimal output feedback) used does not directly guarantee it. Corollary 1A (Corollary 1B) indicates that a basic requirement is to satisfy a similar assumption with only those modes that have either zero or negative damping (either zero or negative stiffness). This is particularly attractive when velocity measurements have their own separate matrices of feedback gains (see Subsect. 3.7.1 for such special forms of output feedback). As will be seen later (Corollaries 2A and 2B), such basic (minimum) requirements are sufficient in the common case of large space structures.

3.3   Case of No Unstable Modes: FOCL Stability Conditions

Support structures for large space systems, namely, large space structures, are commonly assumed to have no unstable modes of their own. In other words, both damping and stiffness matrices Δ and Σ are assumed to have <u>only non-negative</u> diagonal elements. For such a special case, we have the following sharper FOCL stability conditions, Theorems 2A and 2B combined.

<u>Theorem 2A (Damping Augmentation)</u>:   Assume the feedback gain G is such that

(a)   D* is symmetric and non-negative definite, and

(b) $\Delta_M + \Phi_M^T D^* \Phi_M$ is positive definite.

Then the whole augmented damping matrix $(\Delta + \Phi^T D^* \Phi)$ is positive definite if Δ_U is positive definite.

<u>Proof</u>:   The additional damping matrix $\Phi^T D^* \Phi$ is non-negative definite by assumption (a).   Its sum with a non-negative definite matrix,

$$
\begin{bmatrix} \Delta_M + \Phi_M^T D^* \Phi_M & \Phi_M^T D^* \Phi_U \\ \\ \Phi_U^T D^* \Phi_M & \Phi_U^T D^* \Phi_U \end{bmatrix} \equiv \Phi^T D^* \Phi + \begin{bmatrix} \Delta_M & 0 \\ \\ 0 & 0 \end{bmatrix}
$$

is thus non-negative definite.   Assumption (b) and a general statement on non-negative definiteness of partitioned real symmetric matrix (see Theorem 2 of Subsect. 3.7.4) together then imply that

$$
\Phi_U^T D^* \Phi_U - \Phi_U^T D^* \Phi_M (\Delta_M + \Phi_M^T D^* \Phi_M)^{-1} \Phi_M^T D^* \Phi_U
$$

is non-negative definite.   Consequently, the test matrix Δ_T as defined in Theorem 1A is positive definite if Δ_U is positive definite.   This proves the theorem.

<u>Theorem 2B (Stiffness Augmentation)</u>:   Assume the feedback gain G is such that

(a)   K* is symmetric and non-negative definite, and

(b) $\Sigma_M + \Phi_M^T K^* \Phi_M$ is positive definite.

Then the whole augmented stiffness matrix $(\Sigma + \Phi^T K^* \Phi)$ is positive definite if Σ_U is positive definite.

Proof: Same as for Theorem 2A except for appropriate notational changes.

Interesting and important insights into FOCL stability can be derived from these theorems when modes are grouped according to damping or stiffness. Note that the group LE as designated at the end of last subsection now reduces to the group, specifically designated as group E, that consists of only undamped modes. Similarly, the group L'E' now reduces to the group, designated as group E', that is composed of only rigid modes. The following are derived from Theorems 2A and 2B by interpreting the modeled modes as being exactly the group E and the group E', respectively.

Corollary 2A (Damping Augmentation): Assume the feedback gain G is such that

(a)   D* is symmetric and non-negative definite, and

(b)   the additional damping matrix $\Phi_E^T D^* \Phi_E$ is positive definite.

Then the whole augmented damping matrix $(\Delta + \Phi^T D^* \Phi)$ is positive definite.

Corollary 2B (Stiffness Augmentation): Assume the feedback gain G is such that

(a)   K* is symmetric and non-negative definite, and

(b)   the additional stiffness matrix $\Phi_{E'}^T K^* \Phi_{E'}$ is positive definite.

Then the whole augmented stiffness matrix $(\Sigma + \Phi^T K^* \Phi)$ is positive definite.

These corollaries imply that any gain matrix G that makes both D^* and K^* non-negative definite (their best possible) while adding positive definite stiffness to all rigid modes and positive definite damping to all undamped modes will ensure FOCL asymptotic stability.

3.4   Case of No Unstable Modes: FOCL Stability Robustness Conditions

For large space structures having no unstable modes, adding positive definite damping and stiffness to modeled modes will also make asymptotic stability insensitive to parameter errors or variations. Let $\tilde{M}$, $\tilde{D}$, and $\tilde{K}$ denote, respectively, the actual mass matrix, the actual damping matrix, and the actual stiffness matrix, which differ from the nominal values, M, D, and K, because of parameter errors or variations. The actual modal matrix $\tilde{\Phi}$, the actual modal damping matrix $\tilde{\Delta}$, and the actual modal stiffness matrix $\tilde{\Sigma}$ will thus differ from their corresponding nominal values Φ, Δ, and Σ. The following theorems imply that, under certain reasonably weak conditions, FOCL asymptotic stability can still be ensured even when the reduced-order controllers are designed using nominal values that are different from the actual.

Theorem 3A (Damping Augmentation): Assume the feedback gain G is such that

(a) $D* \overset{d}{=} B_FGC_V$ is symmetric and non-negative definite, and

(b) $\Phi_M^T D^* \Phi_M$ is positive definite.

Assume the actual case is such that

(c) $\tilde{\Phi}_M = \Phi_M \Gamma$ for some nonsingular matrix Γ,

(d) $\tilde{\Delta}_M$ is non-negative definite, and

(e) $\tilde{\Delta}_U$ is positive definite.

Then the whole augmented damping matrix

$$(\tilde{\Delta} + \tilde{\Phi}^T D^* \tilde{\Phi})$$

for the actual case is positive definite.

Proof: This theorem is obvious from Theorem 2A, since its assumption (b) holds for the actual case, namely,

$$\tilde{\Delta}_M + \tilde{\Phi}_M^T D^* \tilde{\Phi}_M = \tilde{\Delta}_M + \Gamma^T (\Phi_M^T D^* \Phi_M) \Gamma$$

is positive definite.

Theorem 3B (Stiffness Augmentation): Assume the feedback gain G is such that

(a) $K* \overset{d}{=} B_FGC_D$ is symmetric and non-negative definite, and

(b) $\Phi_M^T K^* \Phi_M$ is positive definite.

Assume the actual case is such that

(c) $\tilde{\Phi}_M = \Phi_M \Gamma$ for some nonsingular matrix Γ,

(d) $\tilde{\Sigma}_M$ is non-negative definite, and

(e) $\tilde{\Sigma}_U$ is positive definite.

Then the whole augmented stiffness matrix

$$(\tilde{\Sigma} + \tilde{\Phi}^T K^* \tilde{\Phi})$$

for the actual case is positive definite.

3-11

Proof: This theorem is obvious from Theorem 2B, since

$$\tilde{\Sigma}_M + \tilde{\Phi}_M^T K^* \tilde{\Phi}_M = \tilde{\Sigma}_M + \Gamma^T (\Phi_M^T K^* \Phi_M) \Gamma$$

is positive definite.

Note that condition (b) of Theorem 3A requires that no more modes be used in the controller design than there are velocity sensors or there are force actuators. Similarly, condition (b) of Theorem 3B requires that the number of displacement sensors and that of force actuators be at least equal to the number of modeled modes, respectively.

The following specific interpretations (Corollaries 3A and 3B) of these two theorems provide interesting insights into the stability robustness of such reduced-order controllers. For Corollary 3A, consider only undamped modes (the nominal group E) as the modeled modes, whereas for Corollary 3B, consider only rigid modes (the nominal group E').

<u>Corollary 3A (Damping Augmentation)</u>: Assume the feedback gain G is such that

    (a) D^* is symmetric and non-negative definite, and

    (b) $\Phi_E^T D^* \Phi_E$ is positive definite.

Suppose that, under parameter variations,

    (c) the number of undamped modes does not increase, and

    (d) the undamped-mode shapes remain inside the space spanned by those of the nominal, namely, $\tilde{\Phi}_E = \Phi_E \Gamma_E$ for some non-singular matrix Γ_E.

Then the whole augmented damping matrix

$$(\tilde{\Delta} + \tilde{\Phi}^T D^* \tilde{\Phi})$$

remains positive definite despite the parameter variations.

<u>Corollary 3B (Stiffness Augmentation)</u>: Assume the feedback gain G is such that

    (a) K^* is symmetric and non-negative definite, and

    (b) $\Phi_{E'}^T K^* \Phi_{E'}$ is positive definite.

Suppose that, under parameter variations,

    (c) the number of rigid modes does not increase, and

<div align="center">3-12</div>

(d) the rigid-mode shapes remain inside the space spanned by those of the nominal, namely, $\Phi_{E'} = \Phi_E \Gamma_{E'}$ for some nonsingular matrix $\Gamma_{E'}$.

Then the whole augmented stiffness matrix

$$(\tilde{\Sigma} + \tilde{\Phi}^T K^* \tilde{\Phi})$$

remains positive definite despite the parameter variations.

Three additional insights are worth mentioning.

1. A careful examination of the assumptions in Theorems 3A and 3B will reveal that feedback controllers that may not ensure FOCL asymptotic stability for the nominal case <u>may still ensure FOCL asymptotic stability</u> for the actual case with such parameter variations or errors as described by assumptions (c) through (e). Assumptions (d) and (e) in both theorems are self evident. Assumption (c) means that the actual mode shapes of the modeled modes remains in the same space spanned by their nominal mode shapes, and are nothing but linear combinations of the nominal.

2. Examination of the proof of Theorems 3A and 3B also show that Assumptions (c) through (e) need not be satisfied for the same partition $\{M,U\}$ of the nominal modes to ensure the FOCL stability for the actual case. Specifically, Theorem 3A remains valid if its assumptions (c) and (d) are satisfied by a <u>smaller number of modeled modes</u> (i.e., with the M part and the matrix Γ replaced by M' and Γ', respectively) while its assumption (e) is satisfied by a correspondingly larger number of unmodeled modes (i.e., with the U part replaced by U') when more damped modes are actually truncated. Similarly, Theorem 3B remains valid if its assumptions are satisfied by <u>another smaller number of modeled modes</u> (i.e., with M and Γ replaced by M'' and Γ'', respectively) while its assumption (e) is satisfied by a correspondingly larger number of unmodeled modes (i.e., with U replaced by U'') when the number of rigid modes is actually smaller and more elastic modes are truncated.

3. Assumption (c) of Corollary 3A implies that if a damped mode is expected to become undamped in the actual case with parameter errors or variations, it should be treated as if it were also an undamped mode (a member of group E) and included as a nominal modeled mode in the controller design. Similarly, assumption (c) of Corollary 3B implies that if an elastic mode is anticipated to become a rigid mode subject to parameter variations or errors, it should be included in the controller design and treated as if it were also a rigid mode.

3.5 Case of Non-Proportional Damping

The damping matrix D of realistic large space systems may not be diagonalized simultaneously with the mass and stiffness matrices, M and K, since the Rayleigh <u>proportional damping</u> condition or even the general

3-13

Caughey-O'Kelly commutativity condition [5]-[7] may not be satisfied. Therefore, the modal damping matrix takes on the following general non-diagonal form.

$$\Phi^T D \Phi \overset{\mathrm{d}}{=} \Delta = \begin{bmatrix} \Delta_M & \Gamma_{MU} \\ \Gamma_{UM} & \Delta_U \end{bmatrix}$$

when partitioned with respect to modeled (M) and unmodeled (U) parts. The diagonal blocks Δ_M and Δ_U need not be diagonal matrices and the off-diagonal blocks Γ_{MU} and Γ_{UM} need not be null matrices, either. Note that the symmetry of damping matrix D implies the symmetry of Δ_M and Δ_U and the equality of Γ_{UM} to Γ_{MU}^T.

In case of non-proportional damping, the test matrix Δ_T in the conclusion of Theorem 1A, regarding the FOCL asymptotic stability, needs to include the off-diagonal blocks Γ_{MU} and Γ_{UM} and therefore be rewritten as

$$\Delta_T \overset{\mathrm{d}}{=} \Lambda_U + \Phi_U^T D^* \Phi_U - (\Gamma_{UM} + \Phi_U^T D^* \Phi_M)(\Lambda_M + \Phi_M^T D^* \Phi_M)^{-1}(\Gamma_{MU} + \Phi_M^T D^* \Phi_U) \quad (3\text{-}20)$$

This means that one should design the feedback controllers for such large space systems based on the whole modeled part Δ_M, not just its diagonal elements. Furthermore, for ensuring FOCL asymptotic stability, the off-diagonal blocks Γ_{MU} and Γ_{UM} (i.e., the coupling effects of non-proportional damping) must not be ignored, either. Of course, a stability ensuring design is less straightforward than that for the idealized case with a diagonal modal damping matrix.

The presence of non-proportional damping can degrade (or accidentally improve) the asymptotic stability and robustness of FOCL systems with reduced-order controllers based on proportional damping. It is worth mentioning, however, that when modeled modes can be appropriately selected, or the feedback gain G can be appropriately determined, such that the off-diagonal block Γ_{MU} is negligible compared to $\Phi_M^T D^* \Phi_U$, then the modal damping matrix Δ essentially has only diagonal blocks Δ_M and Δ_U. The foregoing conclusions on FOCL stability, e.g., Theorems 1A and 2A, remain applicable provided Δ_M and Δ_U thereof are no longer interpreted as only diagonal matrices. Similarly, when $\tilde{\Gamma}_{MU}$ is negligible compared to $\tilde{\Phi}_M^T D^* \tilde{\Phi}_U$ in the case of parameter variations or errors, the

foregoing conclusions on stability robustness, e.g., Theorem 3A, also remain applicable.

3.6 Conclusion

Vibration controllers for large flexible space systems must be designed using only a reduced-order (RO) model of the space system concerned because of many practical limitations, whereas asymptotic stability of the full-order closed-loop (FOCL) system is a basic requirement. Ensuring that the reduced-order model is closed-loop asymptotically stable (e.g., that the augmented damping and stiffness matrices in the reduced-order model are positive definite), however, is not enough to ensure asymptotic stability of the FOCL system. The stability conditions as given by Theorems 1-2, or Corollaries 1-2, must also be taken into account in some practical manner during the design of RO controllers. For example, include all rigid, undamped, or unstable modes in the reduced-order design model; stabilize all unstable modes separately first; constrain the feedback gain G so that the additional damping and stiffness matrices, $B_F GC_V$ and $B_F GC_D$, are nonnegative definite. According to Theorem 3 and Corollary 3, such special efforts will also help make FOCL asymptotic stability robust to parameter errors or variations.

It is worth mentioning that if only passive devices, such as dashpots and springs, are used in damping and stiffness augmentation, the resulting additional damping and stiffness matrices, $D*$ and $K*$, are naturally symmetric and nonnegative. In other words, the assumption (a) in Theorems 2 and 3 is satisfied automatically. Moreover, the design parts $\phi_M^T D* \phi_M$ and $\phi_M^T K* \phi_M$, which represent the additional damping and stiffness to the modeled modes, are at least nonnegative definite; the assumption (b) in Theorems 2A and 2B may have been satisfied already. All that remains for the designer is to ensure that no rigid modes or undamped modes are truncated. He may want to select the size, number, and location of the dashpots and springs to assure that the damping and stiffness augmented to the modeled modes are positive definite. Therefore, according to Theore   : and 3, FOCL asymptotic stability and its robustness become very easy with purely passive control. A practical and important question is how much damping and stiffness can actually be added this way. Passive control can be used to significantly alleviate stability problems with active control, however. All these theorems clearly imply that augmentation of damping and stiffness, even with a very small but positive amount, to as many unmodeled modes as possible by passive devices will positively and greatly help active control ensure the asymptotic stability and robustness of FOCL systems.

Nonproportional damping can complicate the stability and robustness of FOCL systems. The design of RO controllers for such structures should consider not only individual damping of the modeled modes but also their coupling through mutual damping; so should the stability and robustness conditions. Nevertheless, when appropriate selection of modeled modes or appropriate design of RO controllers can render damping coupling between modeled and unmodeled modes negligible, the asymptotic stability and robustness conditions become as simple as the purposefully general statement of Theorems 1-3 and Corollaries 1-3.

Positive definiteness of both the damping matrix and the stiffness matrix is a sufficient condition for asymptotic stability and has been adopted in this initial study of FOCL stability and robustness. Such a condition is strong but not unreasonable nor unrealistic. Many useful simple insights for improving or guiding the design of RO controllers have been generated. RO controllers, such as modal dashpots and modal springs to be discussed in Section 4, can be so designed that asymptotic stability and robustness of FOCL systems are actually possible.

Positive definiteness of the stiffness matrix is also necessary, whereas that of damping matrix can be relaxed to nonnegative definiteness together with a certain rank condition of the type for complete observability or complete controllability (see Subsection 3.7.3). In any case, at least non-negative definiteness of the damping matrix needs to be ensured (for FOCL neutral Liapunov stability) and conditions similar to part A of Theorems 1-3 and Corollaries 1-3 can be easily established in the same way but using only Theorem 2 of Subsection 3.7.4. The rank condition, however, involves high powers and products of the full-order mass, damping and stiffness matrices and are not easy in providing "uncomplicated" insights for guiding RO controller design. Of course, additional useful and less restrictive asymptotic stability conditions can be derived from such a rank condition, but further research on this condition including laborious expansion of the complex stack of matrix products and an in-depth analysis of its rank must be conducted first.

3.7   Appendices

3.7.1   Common Special Forms of Output Feedback Control

The following are some special forms of output feedback control commonly considered.

Form 1: $u = -G_V y_V - G_D y_D = -[G_D | G_V] \begin{bmatrix} y_D \\ \hline y_V \end{bmatrix}$

where y_D and y_V denote the separate measurements of displacements and velocities, respectively.

Form 2: $u = -\begin{bmatrix} G_D y_D \\ G_V y_V \end{bmatrix} = -\begin{bmatrix} G_D & 0 \\ \hline 0 & G_V \end{bmatrix} \begin{bmatrix} y_D \\ \hline y_V \end{bmatrix}$

where one set of actuators is strictly for feedback of displacement measurements and another is strictly for feedback of velocity measurements.

Form 3: G_D and G_V in Form 2 are diagonal matrices.

3.7.2 Displacement Feedback, Velocity Feedback, and Stability Conditions

Velocity feedback alone cannot stabilize a system that has negative stiffness; for such an unstable system, appropriate displacement feedback must be provided first. Therefore, at least non-negative definiteness of the whole augmented stiffness matrix (K + K*) is necessary for stability of the resulting closed-loop system. Similarly, displacement feedback alone cannot stabilize a system that has negative damping; for such an unstable system, appropriate velocity feedback must be provided first. Therefore, at least non-negative definiteness of the whole augmented damping matrix (D + D*) is necessary for stability of the resulting closed-loop system.

Canavin [2] initially stated (without proof) that if matrices M, D + D*, and K + K* are all positive definite, then the closed-loop system (3-5) is asymptotically stable. A simple direct proof was later provided by Lin and Lin [3]. This is a stronger result than the classical Kelvin-Tait-Chetaev theorem and Zajac's extension [4], since asymptotic stability, not just neutral Liapunov stability, can be ensured under exactly the same conditions. Moreover, the proof indicates that actually only the symmetric part of matrices D and D* needs to be considered when either is not symmetric; in over words, gyroscopic effects or any other factors that affect the symmetry of either D or D* can be ignored. Such sufficient conditions for asymptotic stability are used, as reported in this section, for providing initial "uncomplicated" answers to the FOCL stability questions and for generating useful insights to guide the design of FOCL-stability-ensuring RO controllers.

3.7.3 Generalized Asymptotic Stability Conditions

The requirements of positive definite damping for asymptotic stability can be relaxed to that of "pervasive damping". The specific concept of pervasive damping was defined by Zajac [8] following Pringle's discussion [9] on the use of Hamilton functions as testing "energy" functions for Liapunov stability of gyroscopic systems and on the use of LaSalle's extension [10,11] of Liapunov conditions in case the "power" function (i.e., the time derivative of the Hamiltonian function used) is not negative definite but only nonpositive definite. An analytical condition that a certain observability or controllability matrix be of its full rank was given by Walker and Schmitendorf [12] and Russell [13] for pervasive damping of nongyroscopic systems (with a symmetric damping matrix), and a similar one by Müller [14] and Hughes and Gardner [15] for gyroscopic systems (with a symmetric damping matrix and a skew-symmetric gyroscopic matrix). Under the assumption that the (closed-loop) system in question is already Liapunov stable, i.e., that (a) the (augmented) stiffness and mass matrices are symmetric and positive definite and (b) the symmetric part of the (augmented) damping matrix is nonnegative definite, such a condition is necessary and sufficient for asymptotic stability [12,17].

Instead of starting with the assumption of Liapunov stability as in [12-17], we have recently established a necessary and sufficient condition for asymptotic stability that further improves and generalizes the classical Kelvin-Tait-Chataev (KTC) theorem (see the foregoing Appendix 3.7.2 for an earlier improvement). Assuming only pervasive damping, or specifically that the (augmented) damping matrix is only nonnegative definite but satisfies the

above-mentioned analytical condition (slightly weakened), we have shown that positive definiteness of the (augmented) stiffness and mass matrices is necessary as well as sufficient for asymptotic stability of the (closed-loop) system. Recall that the classical KTC theorem or even Zajac's extension [4] only established the sufficiency of the stiffness and mass matrices being positive definite, and could assert only Liapunov stability even under the assumption that the (augmented) damping matrix is positive definite. The proof and applications of this theorem as well as other new results on asymptotic stability of linear systems (in first-order as well as in second-order representations) will be discussed elsewhere in greater detail.

Appendix 3.7.4   Positive and Nonnegative Definiteness of Real Symmetric Matrices

Let S denote a real symmetric matrix partitioned as follows

$$S = \begin{bmatrix} A & B \\ C & D \end{bmatrix}$$

Theorem 1 (Positive definiteness):

Assume that A is nonsingular. Then S is positive definite if and only if both A and $D - CA^{-1}B$ are positive definite.

Proof: Since A is nonsingular, we have the following identity

$$\begin{bmatrix} I & 0 \\ -CA^{-1} & I \end{bmatrix} \begin{bmatrix} A & B \\ C & D \end{bmatrix} \begin{bmatrix} I & -A^{-1}B \\ 0 & I \end{bmatrix} \equiv \begin{bmatrix} A & 0 \\ 0 & D - CA^{-1}B \end{bmatrix}$$

Consider the following coordinate transformation

$$x = Ty$$

where

$$T \overset{d}{=} \begin{bmatrix} I & -A^{-1}B \\ 0 & I \end{bmatrix} , \qquad y \overset{d}{=} \begin{bmatrix} y_1 \\ y_2 \end{bmatrix}$$

It follows from the symmetry of matrix S that

$$x^T S x = y_1^T A y_1 + y_2^T (D - CA^{-1}B) y_2$$

3-18

Now, since T is nonsingular, the quadratic form on the left-hand side is positive definite if and only if the two independent quadratic forms on the right-hand side are positive definite. The theorem thus follows from the fact that both matrices A and $D - CA^{-1}B$ are also symmetric because of matrix S.

Theorem 2 (Nonnegative definiteness):

Assume that A is nonsingular. Then S is nonnegative definite if and only if both A and $D - CA^{-1}B$ are nonnegative definite.

Proof. Same as for Theorem 1 except the term "positive definite" is replaced by "nonnegative definite" at the end.

3.7.5 A General Design of G for Symmetry and Nonnegative Definiteness of D* and Positive Definiteness of $\Delta_M + \phi_M^T D* \phi_M$

Let the feedback gain matrix G be determined as a product of three matrices

$$G = L_V S_V R_V \qquad (3-21)$$

Then the additional damping matrix is given by

$$D* \stackrel{d}{=} B_F G C_V = B_F L_V S_V R_V C_V \qquad (3-22)$$

To make D^* symmetric and hence to satisfy assumption (a) of Theorem 1A, choose the three matrices such that

$$(R_V C_V)^T = B_F L_V \qquad (3-23)$$

and

$$S_V^T = S_V \qquad (3-24)$$

Note that collocation of the sensors with the actuators is not required, although it is desirable.

To determine matrix S_V specifically, notice that the modeled portion of the additional damping matrix is given by

$$\phi_M^T D* \phi_M = \phi_M^T B_F L_V S_V R_V C_V \phi_M$$

Thus, for positive definiteness of the modeled portion, $\Delta_M + \phi_M^T D* \phi_M$, of the augmented damping matrix and hence satisfying assumption (b) of Theorem 1A,

3-19

let Δ_M^* be any symmetric positive definite matrix and solve for S_V from the following equation

$$(\phi_M^T B_V^-) \, S_V \, (R_V C_V \phi_M) \; = \; \Delta_M^* - \Delta_M \qquad (3\text{-}25)$$

where only the symmetric part of Δ_M is considered if it is not symmetric or diagonal.

If nonnegative definiteness of D^* is also desired, choose Δ_M^* to be a symmetric positive definite matrix such that the right-hand side of Eq. (3-25),

$$\Delta_M^* - \Delta_M$$

is at least nonnegative definite.

Finally, to compute a solution of Eq. (3-25), consider the following general expression

$$AXB \; = \; C \qquad (3\text{-}26)$$

where A, B, and C are given rectangular matrices and X is an unknown matrix of the appropriate dimension. Let certain row or column operations, denoted by nonsingular matrices P, Q, R, and S, be performed on the known matrices. Denote the outcomes by the following partitioned matrices

$$\begin{bmatrix} F_{11} & F_{12} \\ \hline F_{21} & F_{22} \end{bmatrix} = PAQ, \quad \begin{bmatrix} G_{11} & G_{12} \\ \hline G_{21} & G_{22} \end{bmatrix} = RBS, \quad \begin{bmatrix} H_{11} & H_{12} \\ \hline H_{21} & H_{22} \end{bmatrix} = PCS$$

where F_{11} and G_{11} are nonsingular and have the same rank as matrices A and B, respectively. Partition the nonsingular matrices of operations accordingly as

$$P \; \overset{d}{=} \; \begin{bmatrix} P_1 \\ \hline P_2 \end{bmatrix}, \quad Q \; \overset{d}{=} \; \begin{bmatrix} Q_1 & Q_2 \end{bmatrix}, \quad R \; \overset{d}{=} \; \begin{bmatrix} R_1 & R_2 \end{bmatrix}, \quad S \; \overset{d}{=} \; \begin{bmatrix} S_1 \\ \hline S_2 \end{bmatrix}$$

Then the following is the general solution to Eq. (3-26).

$$X \; = \; Q_1 F_{11}^{-1} H_{11} G_{11}^{-1} R_1$$

$$+ (Q_2 - Q_1 F_{11}^{-1} F_{12}) \, (Y_{21} G_{11} + Y_{22} G_{21}) \, G_{11}^{-1} R_1$$

$$+ Q_1 F_{11}^{-1} (F_{11} Y_{12} + F_{12} Y_{22}) \, (R_2 - G_{21} G_{11}^{-1} R_1)$$

$$+ (Q_2 - Q_1 F_{11}^{-1} F_{12}) \, Y_{22} (R_2 - G_{21} G_{11}^{-1} R_1)$$

where Y_{12}, Y_{21}, and Y_{22} are matrices of free parameters.

Other details concerning such a design procedure and solution of Eq. (3-26) will be discussed elsewhere.

LIST OF REFERENCES

1. *Active Control of Space Structures Interim Report*, CSDL Report No. R-1404, September 1980 (also Rome Air Development Center Report No. RADC-TR-80-377, January 1981), Section 6.

2. Canavin, J.R., "The Control of Spacecraft Vibrations Using Multivariable Output Feedback," Paper 78-1419, *AIAA/AAS Conference*, Los Angeles, CA, August, 1978.

3. *Actively Controlled Structures Theory Interim Technical Report — Volume 1: Theory of Design Methods*, CSDL Report No. R-1249, April 1979.

4. Zajac, E.E., "The Kelvin-Tait-Chataev Theorem and Extensions," Journal of Astronautical Sciences, Vol. 11, No. 2, pp. 46-49, Summer 1964.

5. Caughey, T.K., "Classical Normal Modes in Damped Linear Dynamic Systems," *Journal of Applied Mechanics*, Vol. 27 (*Trans. ASME*, Vol. 32, Series E), pp. 269-271 June 1960.

6. Caughey, T.K., and M.E.J. O'Kelley, "Classical Normal Modes in Damped Linear Dynamic Systems," *Journal of Applied Mechanics*, Vol. 32 (*Trans. ASME*, Vol. 87, Series E), pp. 583-588, June 1965.

7. Kwatny, H.G., et al. "Hamiltonian Representations and Averaging for Reduced Order Models," presented at *Engineering Foundation Conference on Systems Engineering for Power III: Organizational Forms for Large Scale Systems*, Pacific Grove, Calif. April 23-28, 1978.

8. Zajac, E.E., "Comments on 'Stability of Damped Mechanical System' and a Further Extension," *AIAA J.*, Vol. 3, No. 9, pp. 1749-1750, September 1965.

9. Pringle, R., Jr., "Stability of Damped Mechanical Systems," *AIAA J.*, Vol. 3, No. 2, pp. 363-364, February 1965.

10. LaSalle, J.P., "Some Extensions of Liapunov's Second Method," *IRE Trans. Circuit Theory*, Vol. CT-7, pp. 520-527, 1960.

11. LaSalle, J.P., "Asymptotic Stability Criteria," *Proc. Symposia Applied Mathematics*, Vol. 13, pp. 299-307, American Mathematical Society, Providence, RI, 1962.

12. Walker, J.A., and W.E. Schmitendorf, "A Simple Test for Asymptotic Stability in Partially Dissipative Symmetric Systems," *J. Applied Mechanics*, Vol. 40, No. 4, (*Trans. ASME*, Vol. 95, Series E), pp. 1120-1121, December, 1973.

13. Russell, D.L., "Linear Stabilization of the Linear Oscillator in Hilbert Space," *J. Mathematical Analysis and Applications*, Vol. 25, pp. 663-675, 1969.

14. Müller, P.C., *Special Problems of Gyrodynamics, Courses and Lectures* No. 63, International Center for Mechanical Sciences, Udine, Italy, Springer-Verlag, 1972.

15. Hughes, P.C., and Gardner, L. T., "Asymptotic Stability of Linear Stationary Mechanical Systems," *J. Applied Mechanics*, pp. 228-229, March 1975.

16. Hughes, P.C., and R.E. Skelton, "Stability, Controllability and Observability of Linear Matrix-Second-Order Systems," presented at *1979 Joint Automatic Control Conf.*, Denver, CO, June 17-19, 1979.

17. Miller, R.K., and A.N. Michel, "Asymptotic Stability of Systems: Results Involving the System Topology," *SIAM J. Control and Optimization*, Vol. 18, No. 2, pp. 181-190, March 1980; also *Proc. 18th IEEE Conf. Decision and Control*, Fort Lauderdale, FL, pp. 587-592, December 12-14, 1979.

SECTION 4

AUGMENTATION OF DAMPING, STIFFNESS, AND STABILITY TO
LARGE SPACE STRUCTURES BY MODAL DASHPOTS AND MODAL SPRINGS

4.1   Introduction

The notion, conceived by Canavin [1], of vibration controllers for
large space structures as "modal dashpots" is interesting: each modal
dashpot is, in principle, designed to add any specified amount of damping
to a specific mode independently, as if the modal dashpot and the correspon-
ding mode were completely isolated from any other pairs. A large space
structure is commonly modeled as a large number of rigid bodies intercon-
nected by massless elastic structural elements, and its small motions are
described by a highly coupled system of linear second-order differential
equations. As usual, transformation of the discrete coordinates into the
normal coordinates will uncouple the displacement variables, and there-
fore enable one to specify separately the amount of additional damping re-
quired for each linear harmonic oscillator represented by a vibration mode.
In practice, the additional damping, if not provided by structural material,
must be provided by feedback of velocity-sensor outputs through force
actuators. Such a transformation will, however, further couple the actuator
input variables and the sensor ouput variables, respectively. A velocity
feedback which is to provide the required damping will generally recouple
the open-loop decoupled dynamic equations. Because of the closed-loop
recoupling, the additional damping actually provided may be very far from
the specified damping. Nonetheless, it is possible to transform the actu-
ator input variables so as to let each of the transformed variables actuate
or "control" a different mode independently [1-3]. It is also possible to
transform the sensor output variables so as to let each of the transformed
output variables sense or "estimate" a different mode independently [1-2].
Now, let a transformed output variable which is to sense the velocity of a
certain mode independently, be fed back with a negative gain to the corre-
sponding transformed input variable (which will actuate that mode indepen-
dently). Then, conceptually, the harmonic oscillator represented by this
mode is attached with an exclusive linear "dashpot". Such a modal dashpot
has a damping coefficient given by the (adjustable) gain of the feedback
amplifier.

Since its conception by Canavin in 1978 [1], the modal-dashpot design
philosophy has undergone significant advancement at Draper as a result of
two initially separate research efforts [18-20]. The discouraging high-
gain problem of Canavin [1] with modal-dashpot design can now be alleviated
by a bi-objective design optimization algorithm, which exploits the existent
free parameters. Subsections 4.2 through 4.6 contain discussions of such a

bi-objective modal dashpot optimizer (for adding the largest possible damping to primary modes while requiring the smallest possible feedback gains) and many interesting numerical results on closed-loop stability and robustness of the modal-dashpot designs.

The presence of rigid-body modes was considered a difficult technical issue in stability analysis [1] or modal analysis [16], and some unnecessary separate control was suggested to eliminate them [1,16]. Numerical results [1, 15, 18] and the inherent energy dissipativeness of (passive) dashpots and member dampers have indicated that modal dashpots can ensure stability and can be robust. Neither an analytic proof of these stability and robustness properties, nor a rigorous statement of the enabling conditions, has ever been given. Subsections 4.7 through 4.9 will (1) discuss an integrated design of modal dashpots and "modal springs" which will easily and practically resolve the problem with rigid modes, (2) provide two simple but rigorous theorems on the full-order closed-loop asymptotic stability and robustness properties, and (3) contain a simple numerical demonstration with various kinds of parameter variations.

4.2 Modal-Dashpot Design Philosophy; Associated Bi-Objective Design Optimization Problem

The structural model assumed is (as in [1]) an undamped linear finite-element approximation with no gyroscopic terms.

$$M\ddot{q} + Kq = B_F u \qquad (4-1)$$

where q denotes the L physical coordinates of the model, M and K are the mass and stiffness matrices respectively; u denotes the control inputs to force (and torque) actuators, and B_F is the actuator influence matrix.

Transformation into normal coordinates, i.e.

$$q = \phi \eta \qquad (4-2)$$

yields the following modal representation

$$\ddot{\eta} + \Omega^2 \eta = \phi^T B_F u \qquad (4-3)$$

where

$\quad\quad \eta \quad$ denotes the L modal coordinates

$$\phi = [\phi_1, \ldots, \phi_L]$$

$$\phi^T M \phi = I = \text{identity matrix}$$

$$\phi^T K \phi = \Omega^2 = \text{diag} \{\omega_1^2, \ldots, \omega_L^2\}$$

ω_i and ϕ_i denote the ith natural frequency and the ith mode shape, respectively. Discarding the rigid modes as in [1] leaves a collection of undamped oscillators.

Let y_V denote the outputs from velocity sensors, i.e.

$$y_V = C_V \dot{q} \qquad (4-4)$$

where C_V is the velocity-sensor influence matrix. Consider constant-gain feedback of the form

$$u = -G_V y_V \qquad (4-5)$$

As a result, the closed-loop system takes the following form

$$M\ddot{q} + D\dot{q} + Kq = 0 \qquad (4-6)$$

where

$$D^* \overset{d}{=} B_F G_V C_V \qquad (4-7)$$

denotes the additional damping matrix.

Computation of the higher frequency modes is inaccurate, and the high dimensionality of the complete finite element model makes control computation expensive if not impossible. It is a common practice to truncate the structural model by eliminating some of the elastic modes to obtain a control design model. After a modal truncation, the damping matrix to be designed is actually defined by

$$D_M^* \overset{d}{=} \Phi_M^T B_F G_V C_V \Phi_M \qquad (4-8)$$

where Φ_M is the modeled partition of Φ (for controller design) after it has been reordered to group modeled and unmodeled modes. Canavin considered those modes which are critical to line-of-sight (LOS) performance as the modeled modes and assumed collocation of the sensors with the actuators

$$C_V = B_F^T \qquad (4-9)$$

Fundamental to the modal-dashpot design philosophy is the requirement that the additional damping preserves the classical normal modes such that

$$D_M^* = 2Z_M^* \Omega_M \qquad (4-10)$$

where Z_M^* denotes a diagonal matrix of the additional damping ratios for the modeled modes and Ω_M denotes a diagonal matrix of the modeled natural frequencies. Canavin's primitive modal-dashpot design concept has now been

4-3

generalized (and interpreted to properly reflect the true meaning of output-feedback as he intended). The output-feedback gain matrix G_V is to be determined directly from Eq. (4-10) and (4-8) combined (without transforming the actuator and sensor variables). The combined equation

$$\phi_M^T B_F G_V C_V \phi_M \;=\; 2Z_M^* \Omega_M \qquad (4\text{-}11)$$

will be referred to as the modal-dashpot constraint. Canavin's derivations and interpretations can be summarized and simplified as solving Eq. (4-11) for a gain matrix G_V using pseudo inverses of matrices $\phi_M^T B_F$ and $C_V \phi_M$ as

$$G_V \;=\; \left(\phi_M^T B_F\right)^T \left[\phi_M^T B_F \left(\phi_M^T B_F\right)^T\right]^{-1} \left(2Z_M^* \Omega_M\right) \left[\left(C_V \phi_M\right)^T C_V \phi_M\right]^{-1} \left(C_V \phi_M\right)^T$$

$$(4\text{-}12)$$

Canavin computed the feedback gains according to (4-12) in order to add 10% damping to a sample large space structure. The results, however, led him to feel that the modal-dashpots "may be of limited utility due to the high gains (mostly of the order 10^{12}) produced by this approach" [11]. An analysis, as briefly reported earlier in Section 5 of the recent interim report [4], shows that such a high-gain problem need not exist. It essentially shows that when either $\phi_M^T B_F$ or $C_V \phi_M$ is a singular matrix there are free parameters that can help minimize the magnitude of the feedback gains. Note that Eq. (4-11) is of the same general form as Eq. (3-26) in Subsection 3.7.5 and that the Y_{ij} in Eq. (3-27) represent matrices of free parameters in its general solution. Other methods may be able to utilize these free parameters better than pseudo-inversion. For example, many standard optimization methods enable one to compute matrix G_V taking the modal-dashpot equation (4-11) as a constraint instead of solving it explicitly. Furthermore, the free parameters can be used in optimizing the design of modal dashpots.

Once the existence and advantage of free parameters is recognized, an obvious question is how to choose their values to minimize feedback gains while adding as much damping as possible to primary modes (which include critical modes and other noncritical but serious modes). The underlying two performance objectives now become evident, and are formulated as a bi-objective optimization problem. Note that in the interest of improving model fidelity, we also retain in the control design model some other important modes which we call secondary modes. Active damping of secondary modes is not required, but prevention of control spillover to and observation spillover from them is desired. Both primary and secondary modes (denoted by subscripts P and S, respectively) are referred to as modeled modes and are denoted by subscript M. Therefore, the bi-objective modal-dashpot design problem is to find the feedback gains g_{jk} and the damping ratios ζ_i that

$$\text{maximize } J_1 = \sum_i w_i \zeta_i \qquad (4\text{-}13)$$

and

$$\text{maximize } J_2 = -\sum_{j,k} g_{jk}^2 \qquad (4\text{-}14)$$

subject to

$$\phi_M^T B_F G_V C_V \phi_M = 2Z_M^* \Omega_M \quad \text{(modal-dashpot constraint)} \qquad (4\text{-}11)$$

$$\zeta_i \geq \zeta_{Pmin} \quad \text{for primary modes} \qquad (4\text{-}15)$$

$$\zeta_i \geq \zeta_{Smin} \quad \text{for secondary modes} \qquad (4\text{-}16)$$

where g_{jk} denotes the (j,k)th element of gain matrix G_V, and w_i are weights
intended to allow the designer to express relative importance of the modes.
Weights could also be added to the elements of the gain matrix, but this
seems to offer little advantage if gain elements are presumed similar. Ad-
ditional constraints may be added as necessary. Observe that no computation
of the pseudo-inverses, or the free parameters is required. They are all
embedded in the equality constraint Eq. (4-11).

4.3   A Brief Review of Pareto Optimization

Zadeh [5] noted that one of the most serious weaknesses of optimal
control theory is the selection of a single criterion of optimality. Any
single criterion is likely to ignore important design features or combine
dissimilar features artificially into a single objective. Instead, Pareto
optimization is a systematic method of dealing directly with multiple ob-
jectives by imposing a useful partial order on the vector-valued performance
criterion. Stated simply, Pareto optimal solutions are solutions for which
no single objective can be improved without degrading one of the remaining
objectives. More descriptive synonyms for Pareto optimal are efficient or
non-inferior. The result of Pareto optimization is the "efficent frontier"
of the feasible region in the objective space. The efficient frontier is
a set of designs that represent the best compromises between the explicitly
stated objectives. The designer may then choose the most satisfying ef-
ficient design with confidence.

Computational methods for finding efficient solutions reduce the
multiple objective problem to a series of single objective problems. Zadeh
[5] suggested repeatedly optimizing a weighted sum of the objectives for
various weights when the feasible region in objective space is convex. This
corresponds to finding feasible points through which hyperplanes can be
passed that separate the feasible region from the superior points. Un-
fortunately the method fails if no such hyperplane can be found as for example
when the feasible region is not convex. Also, selection of appropriate
weights to obtain a useful sampling of points on the efficient frontier is
not straightforward. Beeson [6], motivated by the pattern recognition

approach to developing separating surfaces between pattern classes, sug-
gested a quadric surface as an alternative to the hyperplane. This suffers
from the complexity of determining the parameters of the quadratic aggre-
gations of objectives which depend on the frontier they are trying to
locate. Another approach for dealing with non-convexity is to optimize an
arbitrarily selected objective while parametrically constraining the remain-
ing objectives. If the constraint is equality, the method is that of Proper
Equality Constraints (PEC) [7], if the constraint is better than or equal to
the parametric constant vector, the method is Proper Inequality Constraints
(PIC) [8]. Both methods require examination of solutions to discard those
on inefficient portions of the frontier. Variation of the parametric con-
stant vector is reasonbly straightforward since it is tied directly to the
objectives. The PEC and PIC methods were incorporated in the bi-objective
optimizer described below.

4.4   A Bi-Objective Modal-Dashpot Design Optimizer

The bi-objective optimization problem given by Eq. (4-23) through
(4-17) has a computationally convenient form. Taking the sensors and
actuators as given for the problem leaves only the elements of the gain ma-
trix and the modal damping ratios as variables. Objective J_2 is a quadratic

in the problem variables. The other objective and all the constraints are
linear in the problem variables. Parametrically constraining objective J_1

converts the bi-objective problem to a quadratic programming problem, the
simplest nonlinear programming problem. For the method of proper equality
constraints [7], the associated Parametric-Equality-Constrained-Single-
Objective (PECSO) optimization problem is

Maximize
$$J_2 = -\sum_{j,k} g_{jk}^2$$

(i.e., minimize $\sum_{j,k} g_{jk}^2$)

subject to

$$\sum_i w_i \zeta_i = \alpha \qquad (4-17)$$

$$\Phi_M^T B_F G_V C_V \Phi_M = 2Z_M^* \Omega_M$$

$$\zeta_i \geq \zeta_{Pmin} \qquad \text{all primary modes}$$

$$\zeta_i \geq \zeta_{Smin} \qquad \text{all secondary modes}$$

where α denotes the parameter. For applying the method of proper inequality
constraints [8], the associated Parametric-Inequality-Constrained-Single-
Objective (PICSO) optimization problem is the same as the above PECSO problem
except the parametric equality constraint (4-17) is replaced by

$$\sum_i w_i \zeta_i \geq \alpha$$

For expediency in software development a quadratic programming algorithm was chosen. The method employed was Lemke's complementary pivot algorithm [9] since it requires a semi-definite rather than definite quadratic weighting matrix. Also Ravindran had published a FORTRAN code of the algorithm [10] and reported successful use of the algorithm on linear programs. Lemke's general form of the quadratic programming problem is

minimize $\qquad$ $J = c^T x + x^T Q x$ $\qquad$ (4-18)

subject to $\qquad$ $Ax \geq b$ $\qquad$ (4-19)

$\qquad$ $x \geq 0$ $\qquad$ (4-20)

The non-negativity constraint Eq. (4-20) is convenient for the damping ratios but awkward for the elements of the gain matrix. To accommodate it, the gain matrix is expressed as the difference of two matrices whose elements are constrained non-negative. The linear, homogenous equality constraint, Eq. (4-15), could be expressed as a pair of inequality constraints. However, because the theoretical iteration limit of the algorithm increases combinatorially with the number of constraints and variables, considerable computation is saved by eliminating it. Also, expressing an equality constraint as two inequalities results in degeneracy of the constraints which requires additional computation. Therefore, the homogenous modal-dashpot constraint equation is expressed in Kronecker product form and solved by Gaussian elimination. The parametrically constrained quadratic programming problem is then transformed to carry out the single objective optimizations in the free parameters of the homogenous solution. The computational savings is not without cost. If ζ_{Smin} of Eq. (4-17) is zero,

floating point round-off error in the transformation may sometimes give slightly negative secondary-mode damping ratios when the stability constraint is nominally satisfied by the transformed variables. To remedy this, a small positive number is substituted for the zero. The number used was 0.005, selected quite arbitrarily because it was comfortably larger than the round-off error. Incorporation of Ravindran's code in the bi-objective program required the addition of Charnes' perturbation of the problem to resolve degeneracies in the constraints. Lemke's proof of the algorithm excluded degeneracy but noted that degenerate problems could be perturbed to remove the degeneracy. Without perturbation the algorithm's success depends on the order of appearance of the constraints (Eq. (4-19)). With that modification, Lemke's algorithm performed satisfactorily on a variety of small test problems. On some of the larger problems the algorithm could fail to terminate in a short time.

The bi-objective computer program accepts as input the description of the structure and the user's desires and produces a sampling of points on the efficient frontier and the designs that map into those points. Specifically, the inputs required of the user are:

4-7

(1) The numbers of sensors, actuators, and design model modes.

(2) The natural frequencies of the modes and the Kronecker product of the modal influence matrices $\phi_M^T B_F$ and $C_V \phi_M$ of the actuators and sensors.

(3) The weights on the modal damping ratios (nonzero weight implies primary mode), the range of values of the parametrically constrained objective to be searched and the minimum and maximum number of designs to evaluate in that range.

(4) Any additional user-defined linear inequality constraints to be concatenated to the basic problem.

In (3) above, instead of specifying upper and lower limits on J_1, the user can force a default process of determining extreme values of J_1 by minimizing and maximizing J_1 without regard for J_2. These optimizations are linear programs solved by Lemke's algorithm with Q set to zero. The lower bound occurs with inequality constraints Eq. (4-16) and (4-17) active. In the absence of other user constraints there is no upper bound on J_1 with the problem statement as formulated. If the linear program produces an unbound result, then an arbitrary, practical upper limit is set, say, at 70% of critical damping for primary modes.

The outputs of the program are the gains and damping ratios for all efficient solutions and the objectives for all solutions, efficient and inefficient.

The bi-objective program will accommodate more general problems than can be solved with the quadratic programming single-objective optimizer. Some of the features described below are not exercised by the example problem. They provide a framework amenable to more complicated problems requiring only the installation of a more general single-objective subroutine. To obtain the solutions of the bi-objective program, J_1 is constrained parametrically to values within the specified limits beginning at the upper limit. (For PEC the constraint is equality; for PIC the constraint is greater than or equal to the parameter.) In the process the program makes heavy use of the Lagrange multipliers provided as a by-product of Lemke's algorithm. The first use is to adapt the step size of the parameter. Using the "shadow price" interpretation of the Lagrange multiplier, the multiplier associated with the parametric objective indicates the slope of the frontier. As the magnitude of the slope increases the step size is reduced. The second use is to save unnecessary comparisons between solutions in the PEC method by eliminating immediately any solutions that are locally inefficient, i.e., any that are associated with positive multipliers (See [11]). The third use is to trigger closer scrutiny of the frontier at the interface between regions of efficiency. When the sign of the multiplier changes while stepping the parameter down from the upper limit, a binary search is made to locate within the permitted granularity the point where the change occurred. As each locally efficient solution is found, it is chained to a linked list of globally (so far) efficient solutions.

The list is linked in increasing order in J_1 to minimize the number of comparisons necessary to establish "global" efficiency. The linked list data structure is necessary instead of a simpler array structure because the solutions are not necessarily obtained in monotonically decreasing order in J_1. A locally efficient solution is added to the global list only if it is efficient relative to those in the list. Any earlier solutions inefficient by comparison are removed from the list.

4.5 Numerical Applications to Draper Tetrahedral Model: Design

The 12-mode Draper tetrahedral model [12] was used as an example. Bi-objective Pareto optimal designs of modal dashpots and the trade-off curve were sequentially generated by the bi-objective optimization program. In the spirit of model truncation, modes 9 through 12 were considered unavailable to the designer (e.g., because their computation is too inaccurate or too expensive to proceed). Modes one, two, four, and five were critical because of their major contribution to line-of-sight error. All six collocated pairs of force actuators and velocity sensors are used. For this example, the control design model consisted of modes one through six, taking only critical modes as primary modes.

In order to apply the bi-objective optimization program, one needs to specify the weights w_i on the damping of the primary modes. A first attempt to formulate weights to express satisfaction with the additional damping achieved by a gain matrix would probably weight the critical-mode damping ratios according to the mode's importance to mission performance, if a single measure of importance is available. In our case the individual contribution to line-of-sight (LOS) error suggests itself. Weighting the damping ratios accordingly produces the efficient frontier (i.e., the Pareto optimal tradeoff curve) shown in Figure 4-1. The frontier shows no terribly flat nor terribly steep regions where nearly arbitrary improvement in one objective can be had at the expense of small degradation in the other. All the corresponding Pareto optimal designs are equally good so far as the two objectives are concerned. The corresponding pole loci are shown in Figure 4-2. The starting points of the pole loci as the magnitude of the feedback gains increases are indicated by the numbers that represent the modes. The feature of interest in this figure is not the shape of the individual pole loci; that is dictated by the constancy of their natural frequencies. Rather, it is the relative movement of the poles under efficient gain tradeoffs. The results show that the high-frequency critical modes, which have lighter LOS weights, are moved much faster to the left (i.e., attain damping much easier) than the low-frequency critical modes, which had heavier LOS weights. Indeed, mode 5 soon becomes overdamped while mode 1 obtains no higher damping ratio than the preset minimum. The net effect is that each of these designs is bi-objective Pareto optimal in the sense that the LOS-weighted-sum of critical mode damping ratios is the largest possible, while the magnitude of required feedback gains is the smallest possible.

An obvious remedy for overdamping, if one wishes to avoid it, is to clamp an upper limit on the critical mode damping ratios. For an upper bound of 0.7 the efficient frontier and corresponding pole loci are shown in Figures 4-3 and 4-4. Now, modes 1 and 2 are moved, but only after modes 4 and 5 have reached the boundary. The problem has an inherent

4-9

ordering of the modes that dominate the pole movement. The sharper knee of the frontier and the greatly increased range of the magnitude of required feedback gains hint at the order explicit in the pole movement. It essentially implies that the feedback controllers have much smaller influence on modes 1 and 2 than modes 4 and 5.

If uniform movement of the critical modes is desired, the LOS weights need to be modified to reflect such an inherent order. Keen hindsight directed at the sensor and actuator influences discloses that the modes moved most were those most easily moved, i.e., those with larger sensor and actuator influences. In search of a more or less uniform movement let us weight each critical mode damping ratio by the inverse of the sum of the squares of its actuator influences, i.e.

$$w_i = 1/(\phi_i^T B_F)(B_F^T \phi_i)$$

The sum of squared influences (instead of magnitude or root-sum-square) accounts for collocations of sensors and actuators. The results of <u>inverse-sum-of-squared-influence</u> (ISSI) weights are shown in Figures 4-5 and 4-6. The pole movements are reasonably uniform, although the upper bound constraints are still reached first by modes 4 and 5. The frontier still encompasses the higher gains (there is no free lunch) but the sharpness of the knee is gone.

Combining the ISSI weights with the LOS weights gives the efficient frontier and pole loci as shown in Figures 4-7 and 4-8, respectively. It is curious to observe that the pole movement is now more uniform than before for all critical modes except mode 4, the movement of which is stopped. Finally, it is worth mentioning that in all these Pareto optimal designs, the two secondary modes, namely modes 3 and 6, remain decoupled from all other modes and get no more damping beyond their preset minimum. All these gains are automatically directed to the four critical modes in minimizing their magnitude while maximizing the weighted sum of critical-mode damping.

4.6   Numerical Applications to Draper Tetrahedral Model: Robustness

Having explored our bi-objective design optimization of modal dashpots for the example, we now address the robustness of these designs to violations of assumptions underlying the initial notion of modal dashpots. Besides gross properties of the system, such as stability, we should examine the sensitivity of the design objectives to the violations. Of the two objectives only the damping objective is of real interest; the gains are presumably under our control. Instead of examining the weighted sum of damping ratios, it is more direct and informative to examine the individual pole loci. For robustness, we thus look for qualitatively similar pole loci resulting from the designed gains applied to truth models incorporating combinations of spillover parameter variations, and noncollocation of sensors and actuators.

ElSPACK eigenvalue subroutines were used to calculate the closed-loop "truth model" poles directly and thereby generate the pole loci for examination. The bi-objective Pareto optimal designs of modal dashpots with ISSI weights are arbitrarily selected for evaluation. As a check on the

4-10

Pareto optimization, the first truth model employed was identical with the design model. The independent results were identical with Figure 4-2. Since the loci in Figure 4-2 were indirectly generated from the damping ratios calculated in solving the bi-objective problem Eq. (4-13) through (4-16), this verified the accuracy of the bi-objective program.

4.6.1   Robustness to Spillover

For a look at the effects of spillover, the next truth model consisted of the first eight modes. The behavior of the design-model modes is shown in Figure 4-9. The diamonds represent the truth-model poles and the crosses the design-model poles as before. The other two modes (not shown) were consistently overdamped. The two low-frequency modes are severely disappointing; their motion with increasing gain is towards the imaginary axis. The (excessive) increase in damping of the truncated modes (namely modes 7 and 8) is a small consolation for the decrease in damping of critical modes 1 and 2. Nevertheless, spillover causes no instabilities. Observe that the two secondary modes (modes 3 and 6) remain unaffected.

The third truth model consisted of all twelve modes. The behavior of all the full-order truth-model modes is shown in Figure 4-10. The portion corresponding to the six-mode design model is shown in greater detail in Figure 4-11. Although the unavailable modes (9 through 12) are moved considerably, all the available modes (1 through 8) behave virtually the same way as the above case of the eight-mode truth model. In both cases, the dominant effect on the sensitivity in critical-mode damping appears to stem from the exclusion of modes 7 and 8 from the controller design model. It is worth observing that stability is robust despite such severe spillover.

4.6.2   Robustness to Parameter Variation

To examine the effect of parameter variation, the perturbed version [12] of the Draper tetrahedral model was used. As a result of doubling the mass at node 1 and increasing the cross section of the thinner elastic members by 50% and that of the thicker members by 20%, the first two frequencies are decreased, while all others are increased. The mode shapes are nearly indistinguishable from the nominal.

The fourth truth model consisted of the same modes (1 through 6) but from the perturbed model. This displays the effects of parameter errors in the control design model. The results are shown in Figure 4-12. Again, truth-model poles are diamonds, and design-model poles are crosses. Each critical mode received less damping than expected for the corresponding nominal dsign. The pole loci with parameter variations are, however, gratifyingly similar to those designed with the nominal model.

Evaluation with the full-order perturbed model, consisting of all 12 perturbed modes, produced results similar to those shown by Figures 4-10 and 4-11 for the full-order nominal model. In comparison with spillover, parameter variation has very little effect.

4.6.3 Robustness to Noncollocation of Sensors with Actuators

A design with noncollocation of sensors and actuators was evaluated. The sensors used were those on members 7, 8, 9, and 10; the actuators those on members 9, 10, 11, and 12. The design model consisted of modes 1, 2, 4, and 5. Figure 4-13 displays the joint effect of noncollocation and parameter variation, with the truth model consisting of modes 1, 2, 4, and 5 of the perturbed structural model. The effect of parameter variation is much worse than with collocated sensors and actuators, although stability is still robust. The hook in the second mode's path is especially surprising. Much more surprising, though, is the devastating effect of spillover with noncollocation. An expanded view of the twelve-mode nominal-truth-model pole loci is shown in Figure 4-14. All of the designs could cause instabilities. Only the locus of the lowest-frequency mode showed any similarity to what was designed. Apparently, for sensors and actuators, togetherness is very much desirable if the gain matrix G_V is to satisfy only Eq. (4-11) or (4-12). Closed-loop stability can still be ensured without collocating sensors with actuators if the gain matrix satisfies another condition (see Section 3, particularly Subsection 3.7.5).

4.7 Velocity and Displacement Output Feedback Control

As a separate research effort, the modal-dashpot design philosophy is extended to achieve the following: (a) increase in both the damping and frequency of selected modes for more effective control, (b) integrated control of elastic and rigid body modes, and, in particular, (c) full-order closed-loop system asymptotic stability and its robustness to modal truncation and to parameter variation. The technique encompasses "modal springs" as well as modal dashpots.

As before, assume that large space structures are approximated by Eq. (4-1). It is not unrealistic to assume that elastic modes have some positive inherent damping, finite or infinitesimal. According to a standard structural engineer's practice, Eq. (4-2), the modal form of Eq. (4-1), is therefore augmented as

$$\ddot{\eta} + 2Z\Omega\dot{\eta} + \Omega^2\eta = \phi^T B_F u \qquad (4-21)$$

where Z denotes the diagonal matrix of inherent damping ratios ζ_i, and Ω the diagonal matrix of natural frequencies ω_i.

To control all the L modes represented by Eq. (4-3) is impractical, since the number L is very large in general. The design of output feedback controllers based only on primary modes which include all of the rigid-body modes ($\omega_i = 0$) and the critical elastic modes is discussed here. In other words, the controller design model is obtained from Eq. (4-3) by truncating all but these primary modes. Denote the primary modes by P and the residual modes by R. Then the matrices involved in Eq. (4-3) can be partitioned as follows

$$2Z \, \Omega = \text{block-diag} \, \{2Z_P \Omega_P, 2Z_R \Omega_R\} \qquad (4\text{-}22)$$

$$\Omega^2 = \text{block-diag} \, \{\Omega_P^2, \Omega_R^2\} \qquad (4\text{-}23)$$

$$\Phi = [\Phi_P, \Phi_R] \qquad (4\text{-}24)$$

$$\eta^T = [\eta_P^T, \eta_R^T] \qquad (4\text{-}24)$$

Furthermore, let C denote the critical elastic modes. Then we have the following refinements

$$2Z_P \Omega_P = \text{block-diag} \, \{0, 2Z_C \Omega_C\} \qquad (4\text{-}26)$$

$$\Omega_P^2 = \text{block-diag} \, \{0, \Omega_C^2\} \qquad (4\text{-}27)$$

Consider the following velocity and displacement output feedback control

$$u_V = -G_V y_V \qquad (4\text{-}28)$$

$$u_D = -G_D y_D \qquad (4\text{-}29)$$

where y_V and y_D represent outputs from velocity sensors and displacement sensors, i.e.

$$y_V = C_V \dot{q} \qquad (4\text{-}30)$$

$$y_D = C_D q \qquad (4\text{-}31)$$

partitioning the actuator-influence matrix appropriately yields the following expression of the force applied to the structure

$$f = B_F u = [B_V \quad B_D] \begin{bmatrix} u_V \\ u_D \end{bmatrix} = B_V u_V + B_D u_D \qquad (4\text{-}32)$$

Substituting Eq. (4-28) through (4-32) in Eq. (4-21) we get

$$\ddot{\eta} + (2Z\Omega + \Phi^T D^* \Phi)\dot{\eta} + (\Omega^2 + \Phi^T K^* \Phi)\eta = 0 \qquad (4\text{-}33)$$

where

$$D^* \overset{d}{=} B_V G_V C_V \tag{4-34}$$

$$K^* \overset{d}{=} B_D G_D C_D \tag{4-35}$$

Thus, feedback of outputs from velocity and displacement sensors will result in additional "damping" and "stiffness" for the structure.

In his stability analysis of the resulting closed-loop system, Canavin [1] considered the presence of rigid modes a difficult technical issue. He thought that such modes would "have to be eliminated" by separate attitude control and station-keeping control. Another approach, which he used in order to proceed his stability analysis, was to assume the rigid modes to be ignorable coordinates, and thus displacement feedback "must be eliminated" [1]. His problem was essentially the fear that the augmented stiffness matrix $(\Omega^2 + \phi^T K^* \phi)$ "may not be positive definite for the stability tests" [1]. His problem is now resolved in what follows by proper design of the displacement output feedback control. The problem considered here is to design the gain matrices G_V and G_D based only on the primary modes but to achieve the three design objectives stated above. These will be achieved if both the augmented damping matrix $(2Z\Omega + \phi^T D^* \phi)$ and the stiffness matrix $(\Omega^2 + \phi^T K^* \phi)$ in Eq. (4-33) are positive definite. Note that matrix Ω^2 and matrix product $Z\Omega$ are nonnegative definite but singular whenever rigid modes and undamped modes are not excluded from consideration, as shown by Eq. (4-26) and (4-27). Also note that both the additional damping matrix $\phi^T D^* \phi$ and the additional stiffness matrix $\phi^T K^* \phi$ are always singular, since the dimension of realistic LSS is always greater than the number of sensors or actuators. Therefore, asymptotic stability of the full-order closed-loop system Eq. (4-33) does not follow automatically from an arbitrary design of matrices G_V and G_D. A special design technique that can make both $(2Z\Omega + \phi^T D^* \phi)$ and $(\Omega^2 + \phi^T K^* \phi)$ symmetric and positive definite is presented in the following subsection. The resulting controllers also will be robust to modal truncation and to parameter variation. This technique represents an improvement over previous work [1, 13-16].

4.8   Modal Springs and Modal Dashpots; FOCL Stability and Robustness

According to Theorems 2A and 2B in Section 3.3, desirable designs for ensuring full-order closed-loop asymptotic stability are those gain matrices G_V and G_D such that

(a)   Both D^* and K^* are symmetric and nonnegative definite.

(b)   Both $(2Z_p \Omega_p + \phi_p^T D^* \phi_p)$ and $(\Omega^2 + \phi_p^T K^* \phi_p)$ are positive definite.

Among many possible ways to design the gains G_V and G_D to satisfy these conditions, the design as modal dashpots and "modal springs" will prove to be the simplest and the most reliable in both full-order closed-loop (FOCL) asymptotic stability and its robustness. As an extension of the concept of modal dashpots which add damping to individual primary modes independently, modal springs increase stiffness of individual modes independently. In other words, through modal springs, rigid modes can become elastic modes with desirable natural frequencies and elastic primary modes can have their natural frequencies shifted towards desirable higher values. Let $\overline{\Omega}_P$ denote the diagonal matrix of desired closed-loop natural frequencies for the primary modes, and $\overline{Z}_P$ the diagonal matrix of desired closed-loop damping ratios. Then, to design the feedback controllers as modal dashpots and modal springs is to compute the feedback gains G_V and G_D such that

$$\Phi_P^T B_V G_V C_V \Phi_P = 2\overline{Z}_P\overline{\Omega}_P - 2Z_P\Omega_P \qquad (4\text{-}36)$$

$$\Phi_P^T B_D G_D C_D \Phi_P = \overline{\Omega}_P^2 - \Omega_P^2 \qquad (4\text{-}37)$$

are satisfied respectively. The following two theorems we have recently established will provide concrete theoretical foundations for the attractive stability and robustness properties modal dashpots and modal springs possess.

Theorem 1 (FOCL Asymptotic Stability): Assume that

(a) each sensor is collocated with a force actuator: $C_V = B_V^T$, $C_D = B_D^T$

(b) the ranks of $\Phi_P^T B_V$ and $\Phi_P^T B_D$ are all equal to the number of primary modes, and

(c) the primary modes include all rigid modes and all undamped modes.

Let p denote the number of primary modes. Then the full-order closed-loop system Eq. (4-33) is asymptotically stable if the gain matrices G_V and G_D are computed as follows

$$G_V = (\Phi_P^T B_V)^T [\Phi_P^T B_V (\Phi_P^T B_V)^T]^{-1} \Delta_P^* [(C_V\Phi_P)^T C_V\Phi_P]^{-1}(C_D\Phi_P)^T$$

$$(4\text{-}38)$$

$$G_D = (\Phi_P^T B_D)^T [\Phi_P^T B_D (\Phi_P^T B_D)^T]^{-1} \Sigma_P^* [(C_D\Phi_P)^T C_D\Phi_P]^{-1}(C_D\Phi_P)^T$$

$$(4\text{-}39)$$

where Δ_P^* and Σ_P^* are two arbitrary p x p positive definite diagonal matrices representing additional damping and stiffness, respectively, desirable for the primary modes.

4-15

<u>Proof</u>: First of all, because of assumptions (a) and (b), $\Phi_P^T B_V$ and $\Phi_P^T B_D$ have right inverses and $C_V \Phi_P$ and $C_D \Phi_P$ have left inverses. Hence the right sides of Eq. (4-38) and (4-39) are well defined by pseudo-inverses. Now observe that G_V and G_D thus defined are symmetric and nonnegative definite by assumptions. Consequently D^* and K^* as defined by Eq. (4-34), (4-35), (4-38), and (4-39) are symmetric and nonnegative definite. Furthermore, the matrix sums

$$2Z_P \Omega_P + \Phi_P^T D^* \Phi_P = 2Z_P \Omega_P + \Delta_P^*$$

$$\Omega_P^2 + \Phi_P^T K^* \Phi_P = \Omega_P^2 + \Sigma_P^*$$

are all positive definite. Finally, because of assumption (c), it follows from Theorems 2A and 2B in Subsection 3.3 that the full-order closed-loop system Eq. (4-33) is asymptotically stable.

Since feedback controllers as defined by Eq. (4-38) and (4-39) are based primary modes only, the asymptotic stability of full-order closed-loop system implies that such a design is robust to modal truncation so far as full-order closed-loop (FOCL) asymptotic stability is concerned.

Under some reasonably weak conditions, such a controller design is also robust in FOCL asymptotic stability to parameter variations or errors in mass, damping, or stiffness matrices. Useful basic conclusions can be obtained by interpreting the Corollaries 3A and 3B in Subsection 3.4. Recall that the group of nominal modes which are considered undamped modes is denoted by subscript E while the group which are considered rigid modes is denoted by subscript E'.

<u>Theorem 2 (Robustness of FOCL Asymptotic Stability)</u>: Assume that the gain matrices G_V and G_D are defined by Eq. (4-38) and (4-39) respectively, and that assumptions (a) through (c) of Theorem 1 are satisfied. Then the FOCL system Eq. (4-33) remains asymptotically stable in the presence of parameter variations or errors if

(a) the number of undamped modes does not increase,

(b) the number of rigid modes does not increase,

(c) the undamped-mode shapes remain in the space spanned by those of the nominal model, i.e.

$$\tilde{\Phi}_E = \Phi_E \Gamma_E$$

for some nonsingular matrix Γ_E, and

(d) the rigid-mode shapes remain in the space spanned by those of the nominal mode, i.e.

$$\widetilde{\Phi}_{E'} = \Phi_{E'} \Gamma_{E'}$$

for some nonsingular matrix $\Gamma_{E'}$, where Φ_E denotes the E-portion of the nominal modal matrix Φ, and $\widetilde{\Phi}_E$ the corresponding E-portion of the modal matrix $\widetilde{\Phi}$ (having parameter variations or errors); $\Phi_{E'}$ and $\widetilde{\Phi}_{E'}$ denote the E'-portion of Φ and $\widetilde{\Phi}$, respectively.

A couple of numerical examples have clearly indicated the possibility of such attractive stability and robustness properties (see Refs. 1, 14, 15, and Subsection 4.6 of this report), but neither analytical proof nor clear formulation of enabling conditions has been given before. Even in his stability analysis, Canavin [1] stopped short of proving that the specific gain matrix as defined by Eq. (4-38) for modal dashpots could satisfy the stability criteria he developed; he only mentioned that the stability criteria involved a check for nonnegative definiteness of a certain (rather ambiguous) reduced matrix. These Theorems 1 and 2, though very simple and intuitively apparent (as the properties of modal dashpots have been demonstrated by various numerical examples), are the first such concrete statements (with a simple but rigorous proof) concerning the original Canavin's form of modal dashpots and our direct extension to modal springs. For FOCL asymptotic stability and robustness properties of general-form reduced-order output feedback control (including modal dashpots and modal springs in their general forms), the reader is referred to Section 3 of this report and Subsection 6.2 of Ref. 4. Note, in particular, that collocation of sensors with actuators is very desirable but not necessary for FOCL asymptotic stability and its robustness (see Subsection 3.7.5 of this report).

4.9   A Numerical Example

To demonstrate that the proposed design technique can achieve the three objectives stated in the beginning of Subsection 4.7, consider a free-free beam [17]. The open-loop 5-mode representation for a beam 10 meters long with a constant mass distribution of 15 kilograms/meter, and a constant structural rigidity of 11,820 kilogram-meter^3/second^3 is given by

$$\ddot{\eta}_i + 2\zeta_i \omega_i \dot{\eta}_i + \omega_i^2 \eta_i = \phi_i^T B_F u \quad , \qquad i = 1,\ldots,5 \tag{4-40}$$

where

$$\omega_1 = \omega_2 = 0, \quad \omega_3 = 6.28 \text{ rad/s}, \quad \omega_4 = 17.13 \text{ rad/s}$$

$$\omega_5 = 33.94 \text{ rad/s}$$

$$\zeta_1 = \zeta_2 = 0$$

and it is assumed that

$$\zeta_3 = \zeta_4 = \zeta_5 = 0.005$$

There is one force actuator collocated with a sensor providing both velocity and displacement data at points 1, 4, 8 and 9 meters from the left end of the beam. The corresponding control influence matrix $\Phi^T B_F$ is

$$\begin{bmatrix} 0.0211 & 0.0211 & 0.0211 & 0.0211 \\ -0.0292 & -0.0073 & 0.0219 & 0.0212 \\ 0.0227 & -0.0219 & 0.0041 & 0.0227 \\ 0.0096 & -0.0204 & 0.0168 & -0.0096 \\ -0.0022 & 0.0138 & -0.0271 & -0.0022 \end{bmatrix}$$

The transpose of this matrix is also the velocity and displacement measurement matrices, $C_V \Phi$ and $C_D \Phi$.

Assume that rigid-body modes η_1, η_2, and the first bending mode η_3 are to be controlled with these four pairs of sensors and actuators. Therefore η_1, η_2, and η_3 represent primary modes with η_4 and η_5 being residual modes. Also assume that the desired frequencies for the primary modes are 0.1, 0.5, and 8.28 radians/second, respectively, and their damping ratios are all 0.707. Then let the matrices Λ_P^* and Σ_P^* of (4-38) and (4-39) be given by

$$\Lambda_P^* = \text{diag } \{0.1414, 0.707, 11.645\} \quad , \quad \Sigma_P^* = \text{diag } \{0.01, 0.25, 29.12\}$$

Computing the velocity and displacement feedback gain matrices according to Eq. (4-38) and (4-39), we have

$$G_V = \begin{bmatrix} 2.348E+3 & -3.281E+3 & -5.631E+2 & 1.564E+3 \\ -3.281E+3 & 5.271E+3 & 7.604E+2 & -2.620E+3 \\ -5.631E+2 & 7.604E+2 & 1.783E+2 & -2.994E+2 \\ 1.564E+3 & -2.620E+3 & -2.994E+2 & 1.399E+3 \end{bmatrix}$$

$$G_D = \begin{bmatrix} 5.450E+3 & -8.359E+3 & -1.240E+3 & 4.154E+3 \\ -8.359E+3 & 1.303E+4 & 1.872E+3 & -6.536E+3 \\ -1.240E+3 & 1.872E+3 & 2.902E+2 & -9.167E+2 \\ 4.154E+3 & -6.536E+3 & -9.167E+2 & 3.301E+3 \end{bmatrix}$$

With these feedback gains, closed-loop poles of the nominal free-free beam are given as Case 1 in Table 4-1. For the controller design model consisting of only the three primary modes, the desired frequencies and damping ratios are achieved precisely. In the evaluation model Eq. (4-40) consisting of primary and residual modes, the rigid-body modes remain controlled as desired whereas the first bending mode is shifted from the design frequency and damping ratio by no more than 4%. All modes are asymptotically stable, indicating that the control design is robust to modal truncation.

Case 1. Nominal

Open-loop frequencies: 0, 0, 6.28, 17.31, 33.94

Closed-loop poles --- Design Model

No.	Real	Imaginary	ω	ζ
1,2	-7.07E-2	+7.07E-2	0.1	0.707
3,4	-3.54E-1	∓3.54E-1	0.5	0.707
5,6	-5.86	∓5.86	8.28	0.707

Closed-loop poles --- Evaluation Model

No.	Real	Imaginary	ω	ζ
1,2	-7.07E-2	+7.07E-2	0.1	0.707
3,4	-3.54E-1	∓3.54E-1	0.5	0.707
5,6	-6.19	∓5.96	8.59	0.720
7,8	-7.76E-1	∓1.68E+1	16.8	0.046
9,10	-5.52E-1	∓3.38E+1	33.8	0.016

Case 2. Sensor/Actuator Location Shift

Open-loop frequencies: 0, 0, 6.28, 17.31, 33.94

Closed-loop poles --- Design Model

No.	Real	Imaginary	ω	ζ
1,2	-7.07E-2	+7.07E-2	0.1	0.707
3,4	-3.00E-1	∓5.55E-1	0.63	0.475
5,6	-3.35	∓6.63	7.43	0.451

Closed-loop poles --- Evaluation Model

No.	Real	Imaginary	ω	ζ
1,2	-7.07E-2	+7.07E-2	0.1	0.707
3,4	-3.00E-1	∓5.54E-1	0.63	0.476
5,6	-3.37	∓6.71	7.51	0.449
7,8	-1.64E-1	∓1.73E+1	17.3	0.0095
9,10	-2.26	+3.36E+1	33.68	0.067

Case 3. Mass Reduction

Open-loop frequencies: 0, 0, 7.02, 19.35, 37.95

Open-loop poles --- Design Model

No.	Real	Imaginary	ω	ζ
1,2	-1.10E-1	+5.85E-2	0.125	0.883
3,4	-5.52E-1	∓2.93E-1	0.625	0.883
5,6	-9.13	∓3.37	9.73	0.938

Closed-loop poles --- Evaluation Model

No.	Real	Imaginary	ω	ζ
1,2	-1.11E-1	+5.85E-2	0.125	0.885
3,4	-5.52E-1	∓2.93E-1	0.625	0.883
5,6	-1.01E+1	∓2.13	10.32	0.979
7,8	-8.32E-1	∓1.85E+1	18.52	0.045
9,10	-7.14E-1	∓3.77E+1	37.7	0.019

Case 4. Rigidity Reduction

Open-loop frequencies: 0, 0, 4.44, 12.24, 24.0

Closed-loop poles --- Design Model

No.	Real	Imaginary	ω	ζ
1,2	-7.07E-2	+7.07E-2	0.1	0.707
3,4	-3.54E-1	∓3.54E-1	0.5	0.707
5,6	-5.85	∓3.83	6.99	0.837

Closed-loop poles --- Evaluation Model

No.	Real	Imaginary	ω	ζ
1,2	-7.07E-2	+7.07E-2	0.1	0.707
3,4	-3.54E-1	∓3.54E-1	0.5	0.707
5,6	-6.40	∓3.73	7.4	0.864
7,8	-5.61E-1	∓1.17E+1	11.7	0.048
9,10	-4.65E-1	∓2.38E+1	23.8	0.020

Case 5. Beam Length Reduction

Open-loop frequencies: 0, 0, 7.58, 20.90, 40.99

Closed-loop poles --- Design Model

No.	Real	Imaginary	ω	ζ
1,2	-8.66	+5.06	10.3	0.8634
3	-7.09E-2			
4	-3.54E-1			
5	-3.46E+1			
6	-2.12E+2			

Closed-loop poles --- Evaluation Model

No.	Real	Imaginary	ω	ζ
1,2	-4.63E-1	+9.73	9.74	0.048
3,4	-1.09E-1	∓2.09E+1	20.9	0.005
5	-7.09E-2			
6	-3.54E-1			
7	-4.11			
8	-3.44E+1			
9	-2.12E+2			
10	-6.80E+2			

The other cases reported in Table 4-1 indicate that the proposed design technique is also robust to parameter errors or variations, namely, that the closed-loop system with the same feedback gains remains asymptotically stable under four different types of system perturbations, as briefly discussed below.

Case 2. The first sensor/actuator pair is relocated from 1 meter to 2 meters measured from the left end of the beam while feedback gains remain unchanged. The effect of this type of perturbation appears in the first column $\Phi^T B_F$. Note that the fourth mode (a residual mode) becomes less damped.

Case 3. The mass per unit length is reduced to 80% of its original value. Therefore all open-loop bending frequencies increase and matrix $\Phi^T B_F$ is perturbed. Note that closed-loop frequencies and the primary-mode damping ratios are all increased.

Case 4. The structural rigidity is reduced to 50% of the original value. As a result, open-loop bending frequencies decrease whereas matrix $\Phi^T B_F$ remains unchanged. In this case, the closed-loop poles of rigid-body modes are not perturbed at all, as expected. The damping ratios for all bending modes are increased.

Case 5. A length of 0.9 meter is cut off from the right end of the beam. This results in an increase of all open-loop pending frequencies and drastic changes in all elements of $\Phi^T B_F$. Note that the damping of all closed-loop modes is increased due to large increases in either frequency or damping ratio.

4.10   Conclusion

4.10.1   Bi-Objective Pareto Optimization of Modal-Dashpot Design

Two practical objectives underlie the modal-dashpot design of vibration controllers for large flexible space structures: to provide as much primary-mode damping as possible, but to require feedback gains as small as possible. From this brief review of an initial attempt to refine Canavin's modal-dashpot controllers using Pareto optimization, we conclude that multi-objective optimization (e.g., by the methods of PEC or PIC) is a promising design tool. In particular, a weighted sum of damping ratios is a useful expression for additional multiple pole-movement objectives provided that the critical-mode damping ratios are pre-weighted to offset sensor and actuator influences, and the upper bounds are imposed to prevent artificial inflation of the objective by overdamped modes. The ISSI weights are reasonable for the case of collocated sensors and actuators.

Comparison with Canavin's computational method is a little unfair. For instance, the computation of the feedback gain matrix, unlike Canavin's design technique, does not require the complication of pseudo-inversion of singular matrices: it is automatic and systematic in the optimization program. The free parameters associated with the singular matrices are automatically used

to optimize the design. Each gain matrix computed is Pareto optimal with respect to the two objectives considered. Efficient trade-off curves and pole loci are generated for making systematic tradeoff between Pareto-optimal designs.

A 12-mode tetrahedral model of large space structure was used as an example. Pareto optimal designs of modal dashpots were sequentially generated by the bi-objective optimizer. The resulting designs were then examined for their robustness to model parameter variation and spillover. For all designs with velocity sensors collocated with force actuators, robustness of stability to parameter variation and to spillover was clearly demonstrated. The damping performance is relatively insensitive to parameter variation and to spillover; however, the sensitivity rapidly increases as the desired level of critical-mode damping increases. In other words, modal dashpots can theoretically be designed to provide any desired level of damping to the critical vibration modes. In practice, however, only low designed levels of modal damping can be closely achieved due to such sensitivity to parameter variation and spillover.

When the sensors and actuators are not all collocated, stability and damping performance are also relatively insensitive to parameter variation. However, spillover causes all the corresponding designs to destabilize the originally stable structure; at least half of the resultant closed-loop poles have positive real parts. Destabilization by modal dashpots, which were also referred to as "robust controllers", has not been demonstrated before. Consequently, collocation of sensors with actuators is very much desirable for the robustness of modal dashpots when used as vibration dampers for realistic large space structures, unless an additional condition is imposed on the design.

4.10.2 Modal Dashpots and Modal Springs, Closed-Loop Asymptotic Stability and Robustness

The modal dashpot design philosophy has been extended to form the similar modal-spring design concept. An integrated use of modal dashpots and modal springs can achieve (a) increases in both the damping and the frequency of selected modes (including rigid-body modes) for effective control, (b) integrated control of elastic and rigid-body modes, and (c) asymptotic stability and robustness of the resulting full-order closed-loop system.

The asymptotic stability and robustness properties of modal dashpots and modal springs, which have been separately demonstrated numerically by several researchers at Draper and elsewhere, have now been proved rigorously and analytically with the enabling conditions precisely stated. Such intuitively "trivial" and appealing results, namely, the Theorems 1 and 2 in Subsection 4.9 also apply to modal dashpots alone and therefore provide concrete theoretical foundations to Canavin's original concept of modal dashpots, as well.

A 5-mode model of a free-free beam was used to demonstrate numerically the design and integrated use of modal dashpots and modal springs. Four different kinds of parameter variations were also simulated. The full-order closed-loop asymptotic stability and robustness properties were convincingly demonstrated.

4-21

4.10.3 Concluding Remarks

Research results reported here were obtained from two separate initial efforts, which can be synergistic when they are combined. The concrete theoretical results justify and encourage continued pursuit for improved computational methods for designing modal dashpots and modal springs. On the other hand, the bi-objective modal-dashpot design optimization algorithm can be easily extended to optimize the design of modal springs. In fact, in a similar manner, multi-objective optimization methods can be applied to optimize the joint design of modal dashpots and modal springs, taking more than two pressing design objectives into account, if necessary.
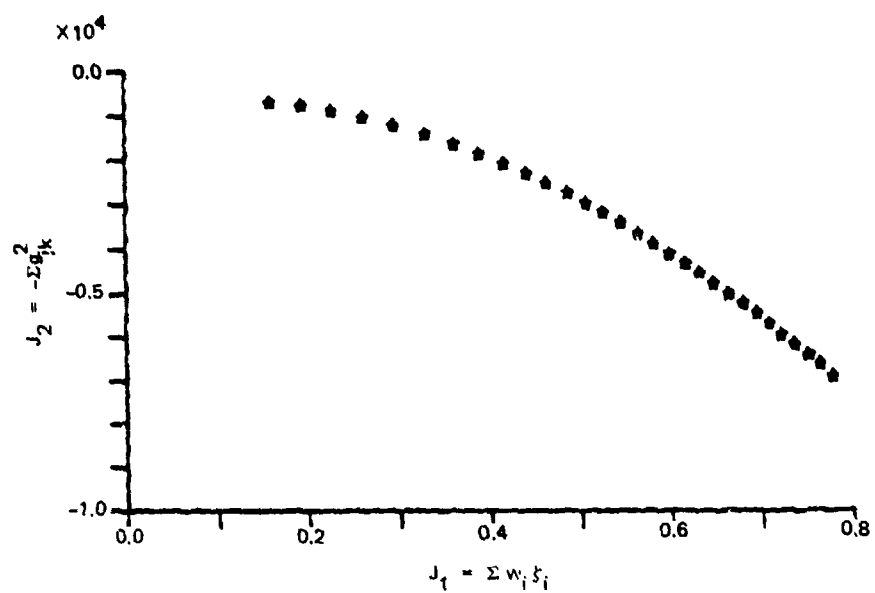
Figure 4-1. LOS weight: efficient frontier.
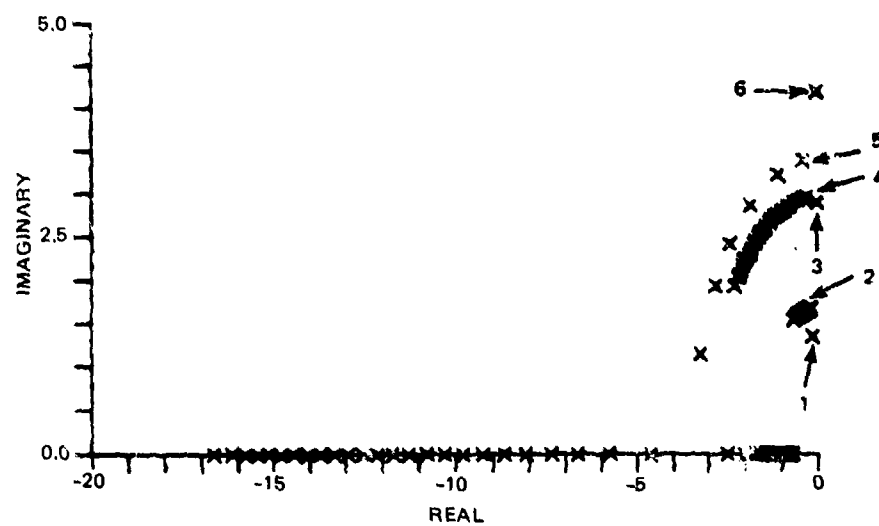
Figure 4-2. LOS weight: pole loci.

4-23
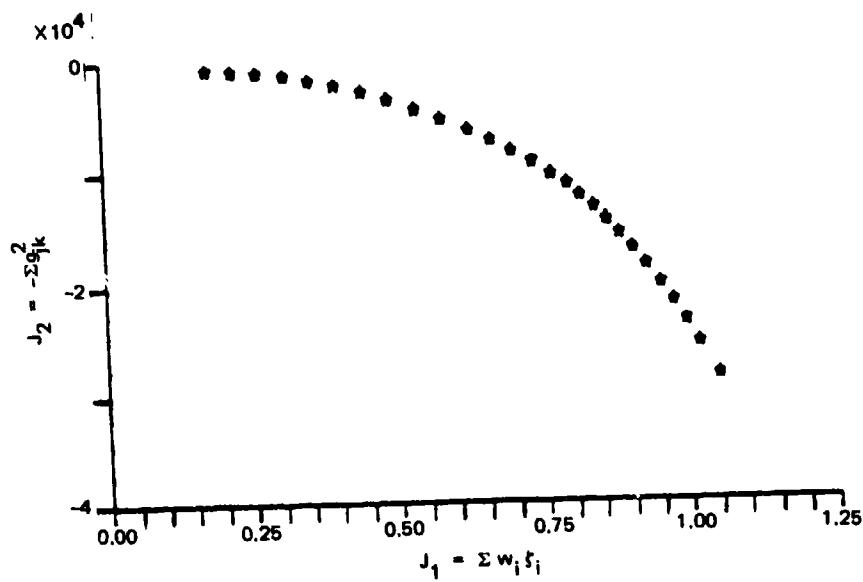
Figure 4-3. LOS weight with limits: efficient frontier.
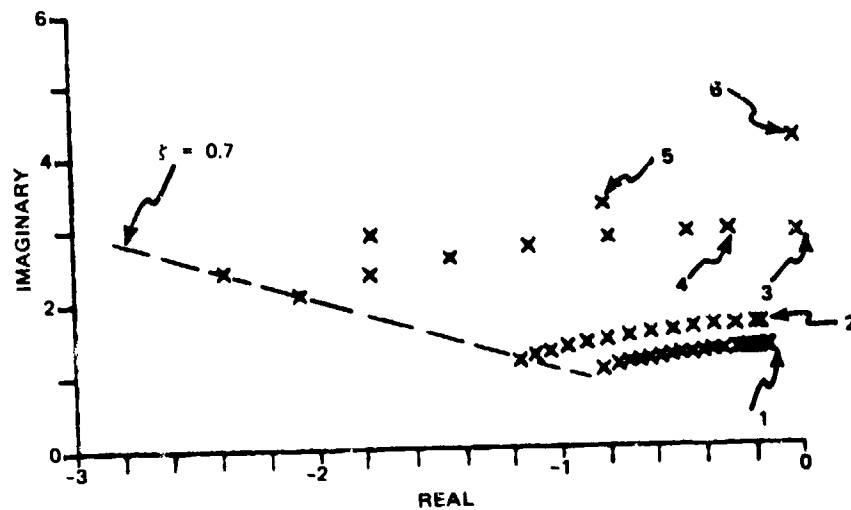
Figure 4-4. LOS weight with limits: pole loci.

4-24
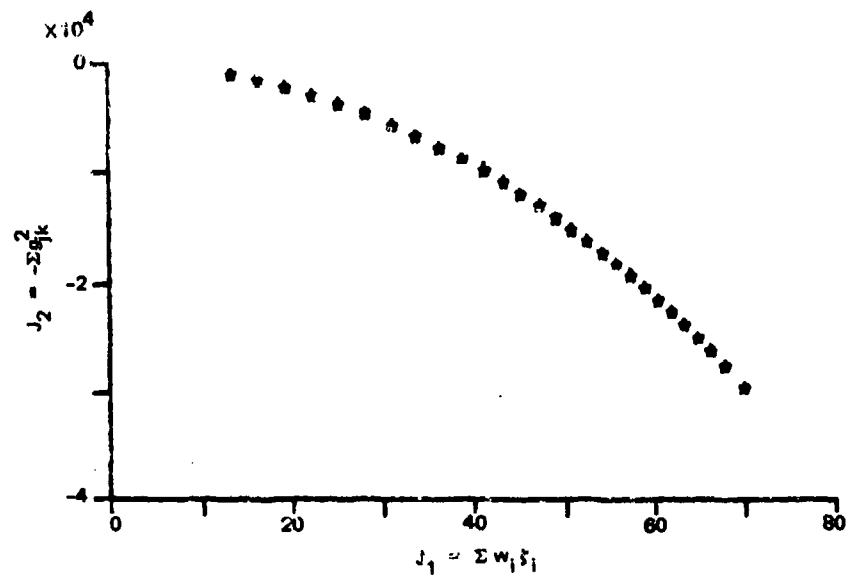
Figure 4-5.   ISSI weight: efficient frontier.
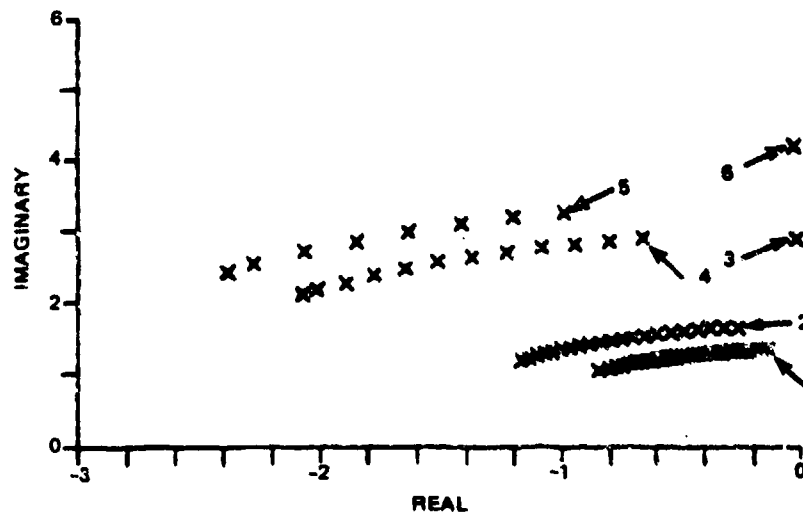
Figure 4-6.   ISSI weight: pole loci.
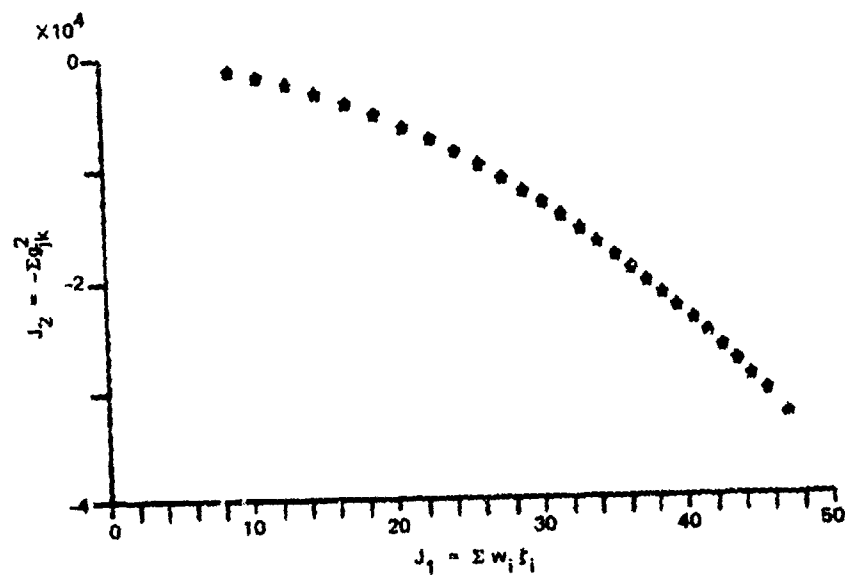
Figure 4-7.   ISSI·LOS weight: efficient frontier.
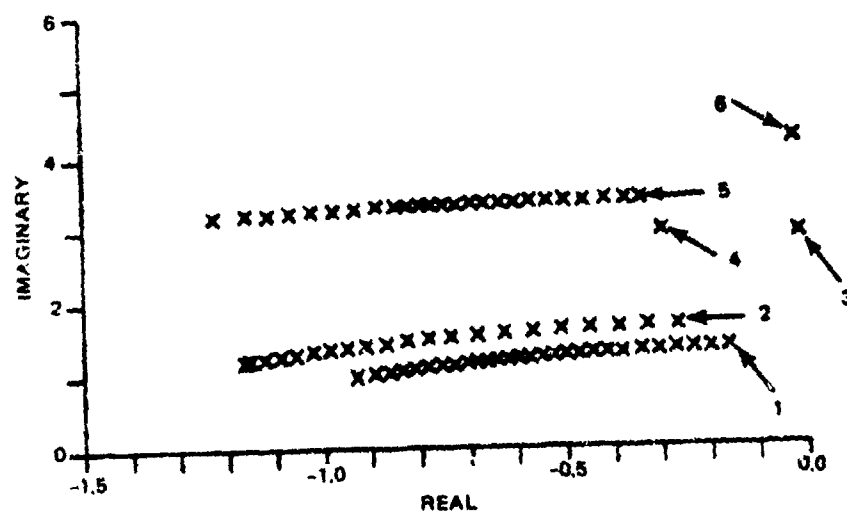
Figure 4-8.   ISSI·LOS weight: pole loci.

4-26
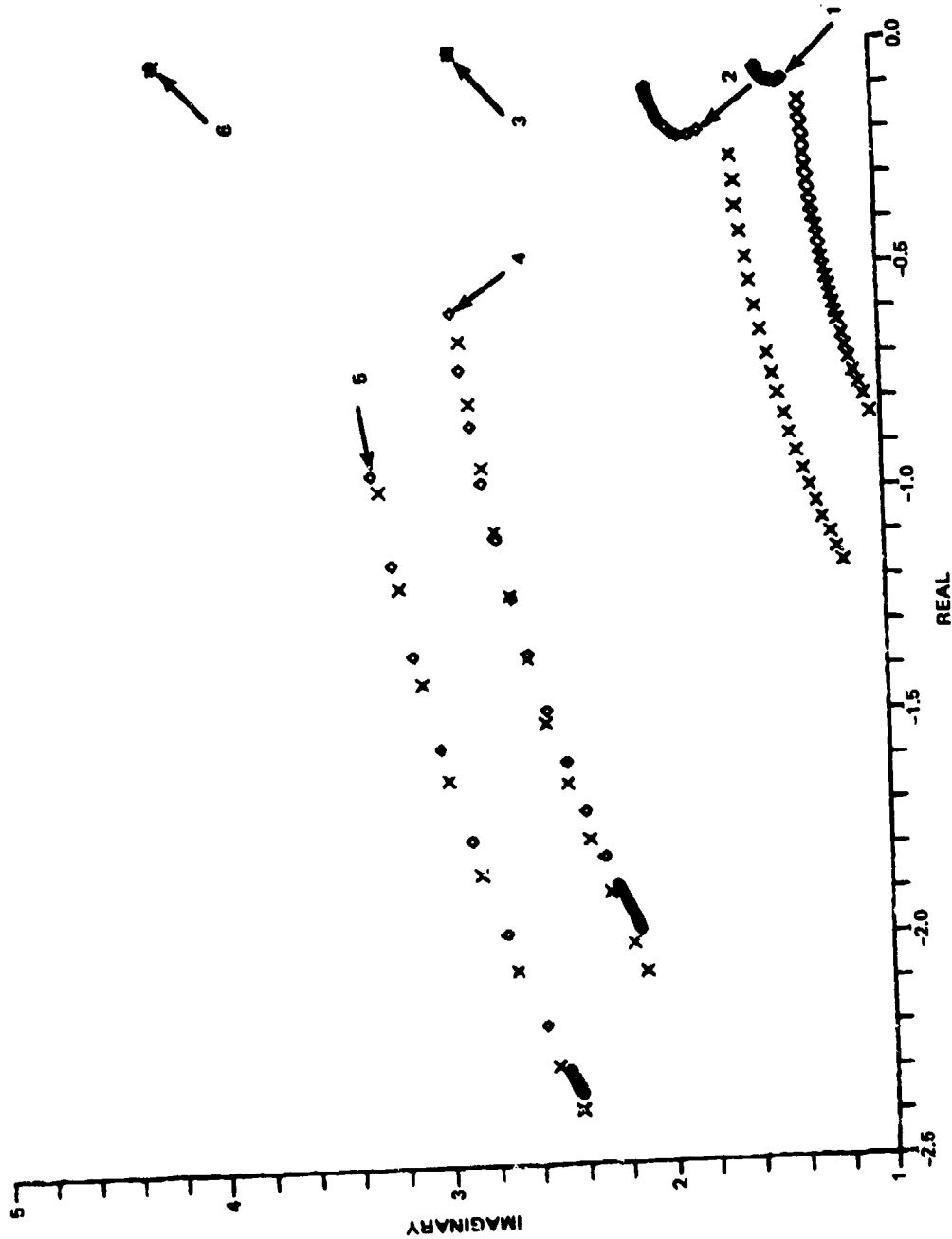
Figure 4-9. Pole loci of eight-mode truth model.
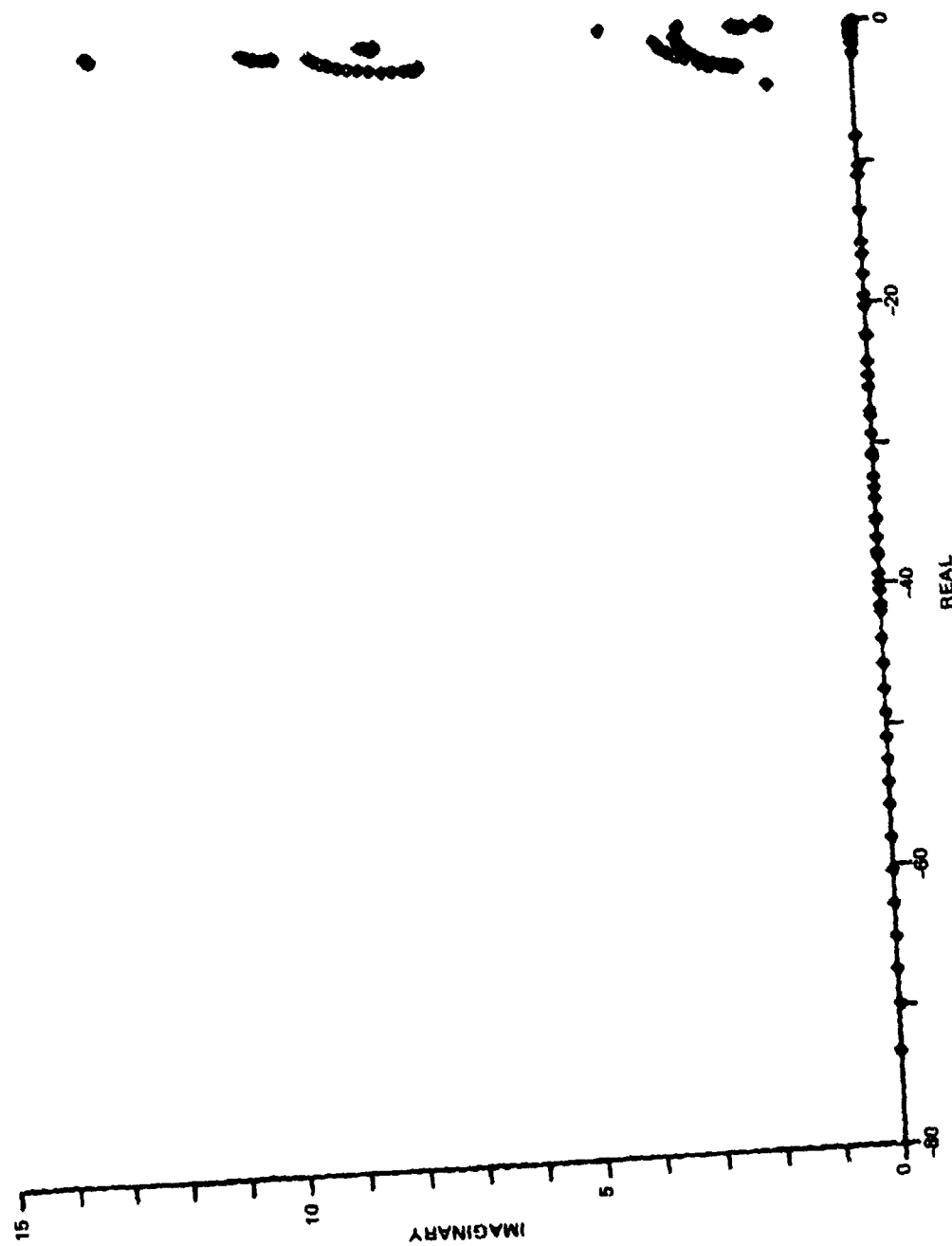
Figure 4-10. Pole loci of 12-mode (full order) truth model.
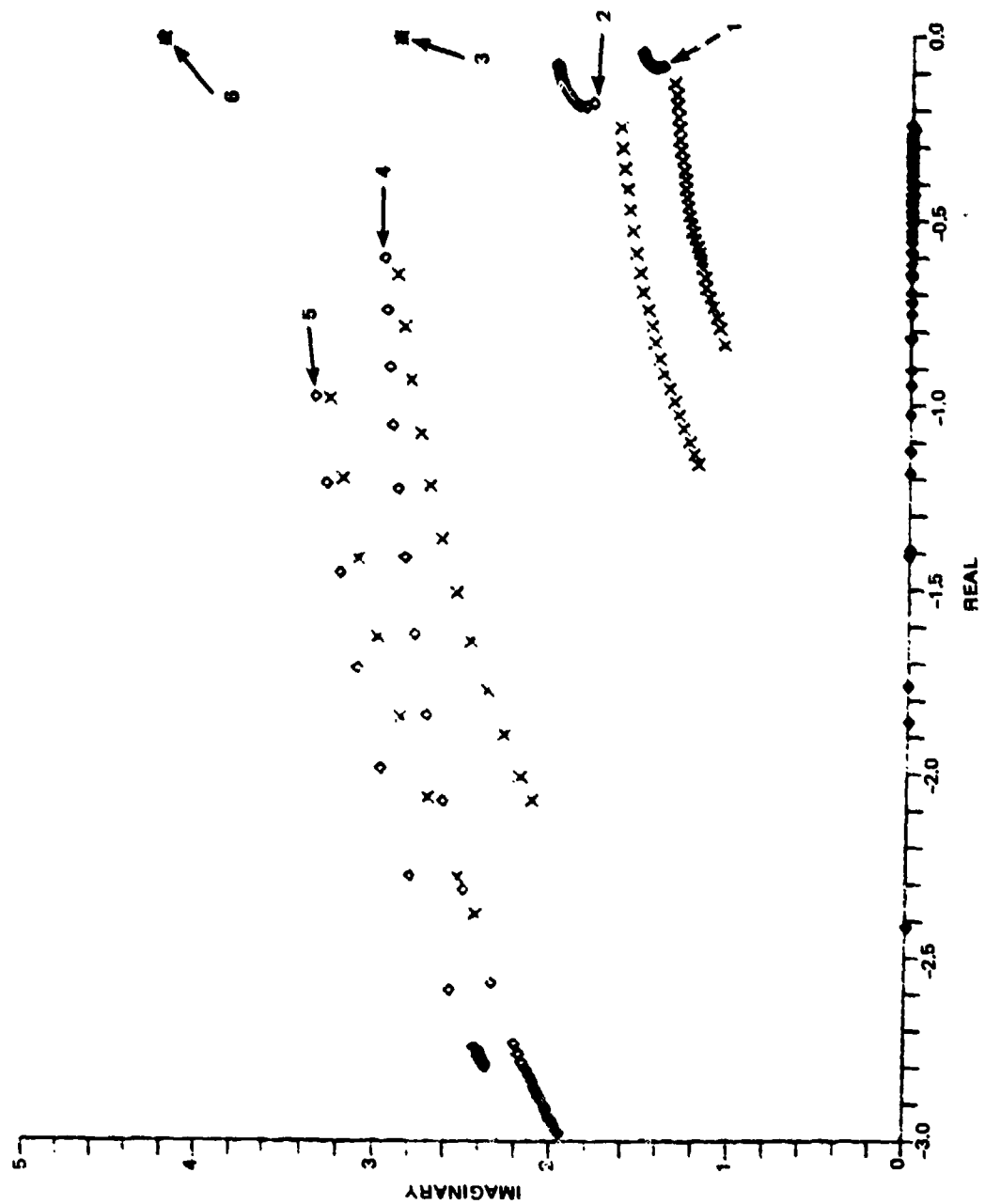
Figure 4-11. Pole loci of 12-mode truth model (expanded).
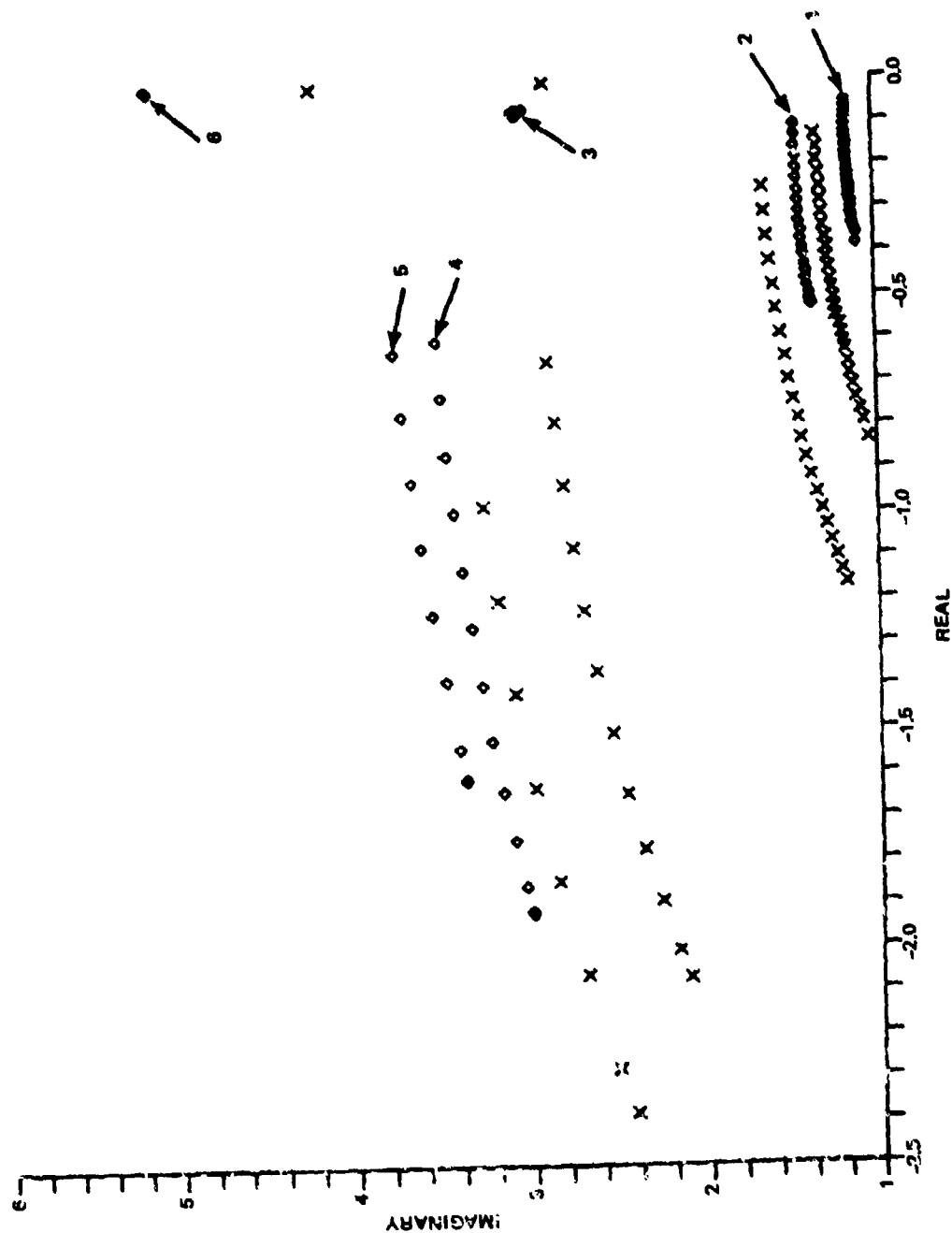
Figure 4-12. Pole loci of six-mode nominal (X) and perturbed (•) truth model.
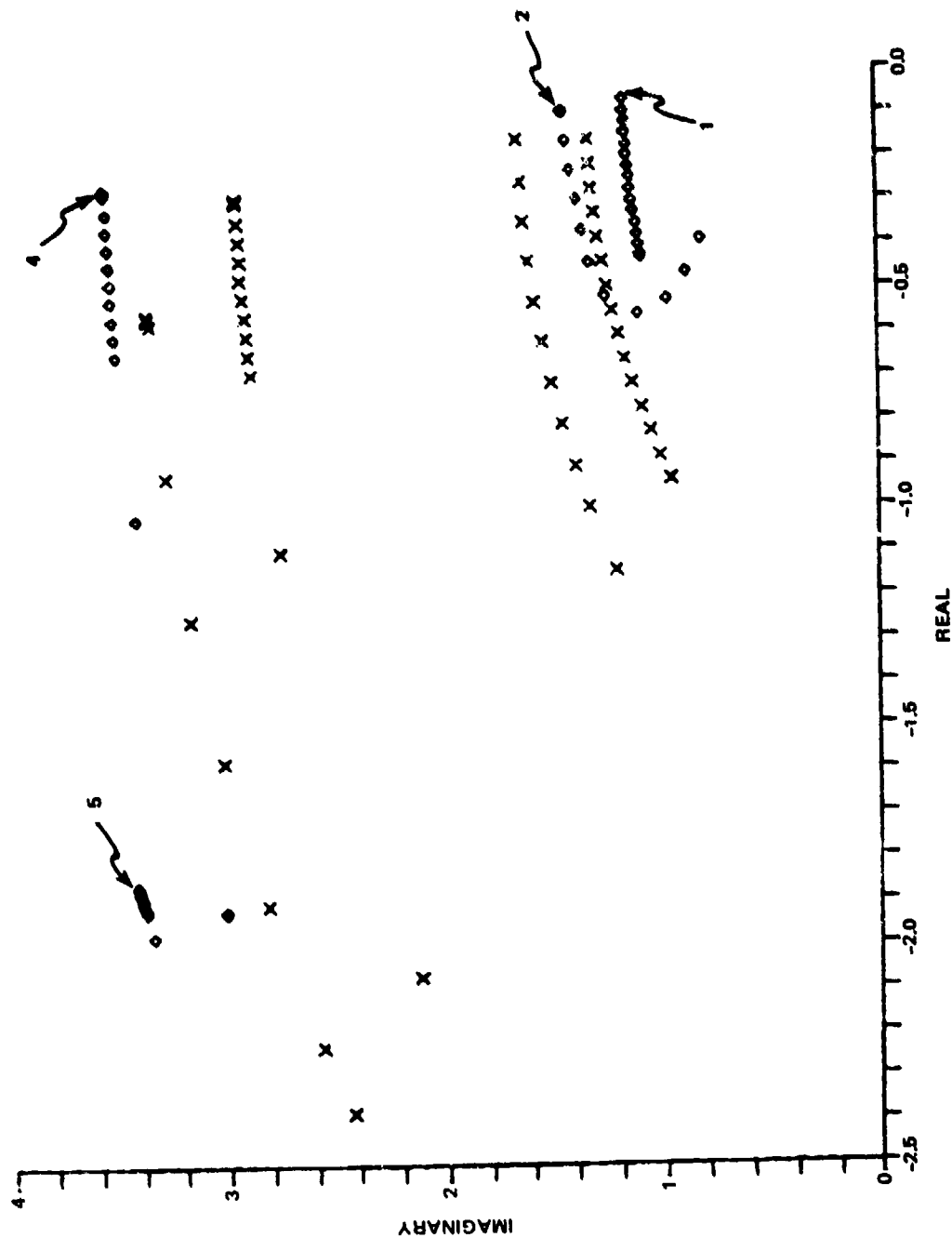
Figure 4-13. Pole loci of four-mode design model (X) and perturbed (●) truth model. Actuators and sensors are not all collocated.

4-31
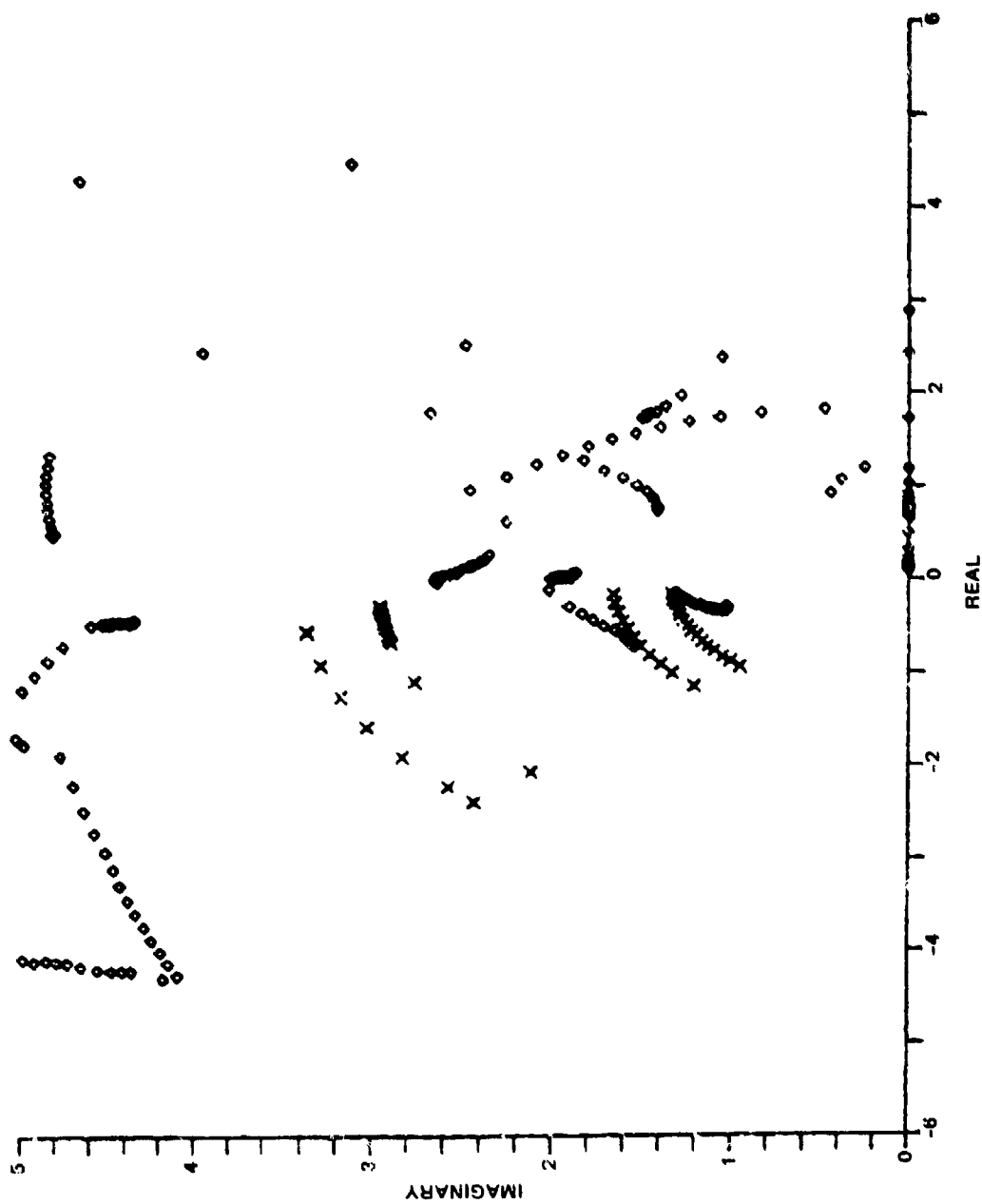
Figure 4-14. Pole loci of 12-mode truth model with noncollocation (expanded).

LIST OF REFERENCES

1. Canavin, J.R., "The Control of Spacecraft Vibrations Using Multivariable Output Feedback," Paper 78-1419, AIAA/AAS Conference, Los Angeles, CA, August 1978, also Passive and Active Suppression of Vibration Response in Precision Structures, State-of-the-Art Assessment Vol. 2 Technical Analysis, Report No. R-1138 CSDL, Feb 1978, Section 3.

2. Quartararo, R., "Modal Control of Flexible Spacecraft," Adv. Tech. Lab. Prog. for Large Space Structures, I, App. B, Rockwell International SD-76-SA-0010, November 1976.

3. Meirovitch, L., VanLandingham, H.F., and Oz, H. "Control of Spinning Flexible Spacecraft by Modal Synthesis," Acta Astronautica, Vol. 4, pp. 985-1010, 1977.

4. Active Control of Space Structures Interim Report, Report No. R-1404, CSDL, September 1980 (also Rome Air Development Center Report No. RADC-TR-60-377, January, 1981), Sections 5 and 6.

5. Zadeh, L.A., "Optimality and Non-scalar-Valued Performance Criteria", IEEE Transactions on Automatic Control, January 1963, pp. 59-60.

6. Beeson, R.M., "Optimization with Respect to Multiple Criteria," Ph.D. Thesis, Department of Electrical Engineering, University of Southern California, 1971.

7. Lin, J.G., "Multiple Objective Problems: Pareto-Optimal Solutions by Method of Proper Equality Constraints," IEEE Trans. of Automatic Control, AC-21, No. 5, October 1976, pp. 641-650.

8. Lin, J.G., "Proper Inequality Constraints and Maximization of Index Vectors," J.O.T.A., Vol. 21, No. 4, April 1977, pp. 505-521.

9. Lemke, C.E., "Bimatrix Equilibrium Points and Mathematical Programming," Management Science, Vol. 11, No. 7, pp. 681-689, May 1965.

10. Ravindran, A., "Algorithm 431, A Computer Routine for Quadratic and Linear Programming Problems," CACM, Vol. 15, No. 9, September 1972, pp. 818-820.

11. Lin, J.G., "Multiple Objective Optimization by a Multiplier Method of Proper Equality Constraints - Part I: Theory," IEEE Trans. on Automatic Control, AC-24, No. 4, August, 1979, pp. 567-573.

12. Actively Controlled Structures Theory Final Report, Report No.
     R-1338, CSDL, December 1979, Appendix A.

13. Balas, M.J. "Direct Velocity Feedback Control of LSS," J. Guidance
     and Control, March-April, 1979, pp. 252-253.

14. Lin, J.G., Hegg, D.R., Lin, Y.H., and Keat, J.E., "Output Feedback
     Control of Large Space Structures: An Investigation of Four Design
     Methods," Proceedings of Second Symposium on Dynamics and Control of
     Large Flexible Spacecraft, Blacksburg, Virginia, June 1979.

15. Elliott, L.E., Mingori, D.L., and Iwens, R.P., "Performance of Robust
     Output Feedback Controller for Flexible Spacecraft," Proceedings of
     Second Symposium on Dynamics and Control of Large Flexible Space-
     craft, Blacksburg, Virginia, June 1979.

16. Meirovitch, L., and Oz, H., "Computational Aspects of the Control of
     Large Flexible Structures," 18th IEEE CDC, Fort Lauderdale, FL,
     December 1979.

17. Ginter, S.D., Attitude Control of Large Flexible Spacecraft, MIT M.S.
     Thesis, September, 1978.

18. Preston, R.B. and Lin, J.G., "Pareto Optimal Vibration Damping of
     Large Space Structures with Modal Dashpots," Proceedings of 1980
     Joint Automatic Control Conference, August 1980, Paper FP1-C.

19. Preston, R.B. and Lin, J.G., "An Application of Pareto Optimization
     Methods to Vibration Damping of Large Space Sructures," presented at
     19th IEEE Conference on Decision and Control, Albuquerque, NM,
     December 1980.

20. Lin, Y.H. and Lin, J.G., "An Improved Output Feedback Control of
     Flexible Large Space Sructures," Proceedings of 19th IEEE Conference
     on Decision and Control, Albuquerque, NM, December 1980, pp. 1248-1250.

SECTION 5

SPILLOVER PREVENTION VIA
PROPER SYNTHESIS/PLACEMENT OF
ACTUATORS AND SENSORS

5.1 Introduction

Control spillover and observation spillover can occur in the control of large space structures when low-dimensional reduced-order mathematical models are used as the design basis for determining control inputs. Such a controller presumes that only the state of the reduced-order model is controlled and that only the state is sensed. However, when the controller is implemented on the large space structure, it will excite and observe the unmodeled dynamics of the structure as well. Many researchers have demonstrated with various examples that the structure can be destabilized by such a controller, contrary to the original design objective, because of control spillover and observation spillover.

The control actuators (sensors) can be synthesized through proper amplifications and combinations of their influences so that spillover will not exist for most influential uncontrolled modes of vibration. The necessary steps in synthesizing the actuator (sensor) influences (finding the interconnecting gains) have been implemented on a computer program which is explained in this section. The underlying principle of synthesis, finding vectors in the nullspace of matrices, is extended to answer the question of how actuators (sensors) should be placed on large space structures to prevent spillover to (from) all uncontrolled modes. Proper placement of actuators and sensors and proper synthesis of their influences so as to prevent spillover regardless of how a control is designed are the main objectives in this study.

Numerical results from various applications of the synthesis program on two representative models of large space structures are reported here.

5.2 The Nature of Spillover

Flexible space structures are obviously continuous systems which have an infinite number of modes of vibration. When these modes are excited by some external or internal disturbance they will have to be quickly damped for the space structure to execute its stringent mission. Because the damping in these structures is inherently very light, active control of vibrations is generally considered necessary.

The frequencies and modes of vibration of a large space structure are studied by modeling the structure with the finite-element method.

5-1

In the model the structure has a finite number of degrees of freedom, and for the particular numerical models in this study, the mass of the structure is lumped at the degrees of freedom yielding a diagonal mass matrix.

The finite element modal representation is already a reduced-order model of the infinite-dimensional structure, yet one cannot reasonably expect to actively control even all of the modes calculated because of the limited computer capability on board space structures and many other practical reasons. Thus the designer is forced to choose from the computed modes a small subset which has the greatest impact on the structure's performance, including those elastic modes which are critical to line-of-sight accuracy, and then design a controller to adequately damp these modes. The vibration modes selected for control will be labeled primary (P) modes, while the remaining modes in the finite-element model will be designated residual (R) modes, as usual.

Mathematically, this means that the standard finite element modal representation has been divided into a primary and a residual part.

$$\ddot{\eta}_P + 2Z_P\Omega_P\dot{\eta}_P + \Omega_P^2\eta_P = \phi_P^T B_F u \qquad (5\text{-}1)$$

$$\ddot{\eta}_R + 2Z_R\Omega_R\dot{\eta}_R + \Omega_R^2\eta_R = \phi_R^T B_F u \qquad (5\text{-}2)$$

$$y = C_D\Phi_P\eta_P + C_V\Phi_P\dot{\eta}_P + C_D\Phi_R\eta_R + C_V\Phi_R\dot{\eta}_R \qquad (5\text{-}3)$$

The control input u is designed with only the primary modes taken into account whose dynamics represent a reduced-order model. Observe, however, that the control u acts also as an input to the residual modes through the $\phi_R^T B_F u$ term in Eq. (5-2) to which the name control spillover has been attached. This term means that control energy intended for the primary modes spills over and excites the residual modes. Observation spillover, a dual effect to control spillover, can be identified in the observation Eq. (5-3) through the terms $C_D\Phi_R\eta_R$ and $C_V\Phi_R\dot{\eta}_R$. They represent contamination of the observations of primary modes by the residual modes. The combination of the control and observation spillover has been shown to cause closed-loop instability in the control of a structure. Now the designer is confronted not only with the task of controlling primary modes but also with the requirements that either the control inputs not force the residual modes or the sensors not observe the residual dynamics. The discussion that follows will explore methods by which control and observation spillover can be prevented for all control inputs and observation outputs. Because observation is the dual

5-2

of control, the focus of the methods in this report will be on the prevention of control spillover. These techniques can be dualized for the prevention of observation spillover.

5.3 Prevention of Spillover via Synthesis of Actuator Influences

When actuators have been placed on a flexible structure for vibration control, some means will be needed to make all of the terms of the spillover influence matrix, $\Phi_R^T B_F$, as close to zero as possible. One way to effect the desired change in $\Phi_R^T B_F$ is to introduce a matrix Γ such that

$$\Phi_R^T B_F \Gamma = 0 \qquad (5\text{-}4)$$

Γ is an m x m' matrix whose columns obviously must be in the nullspace of $\Phi_R^T B_F$. Physically this means that each of the m' control inputs will direct the m existent actuators through gains corresponding to the values in the appropriate column of Γ. In other words, from the m physical actuators, we form m' synthetic actuators whose influences B_F' are given by

$$B_F' = B_F \Gamma \qquad (5\text{-}5)$$

The matrix Γ is to be found so that spillover is prevented to as many non-primary modes as possible if not all of them.

5.3.1 A Practical Consequence of Synthesis

Recall that the dimension of the nullspace of r x m matrix $\Phi_R^T B_F$ is

$$\text{null} \left(\Phi_R^T B_F \right) = m - \text{rank} \left(\Phi_R^T B_F \right) \qquad (5\text{-}6)$$

Generally r >> m so the rank of $\Phi_R^T B_F$ is virtually always m, which implies that the dimension of the nullity is virtually always zero. To get around this impasse, the designer should select from the residual modes a subset to which spillover is particularly important to prevent, and designate those modes as secondary (S) modes. The selection of secondary modes is a challenging problem, and one that will not be addressed here.

5-3

The modal equation for the secondary modes is of course

$$\ddot{\eta}_S + 2z_S\Omega_S\dot{\eta}_S + \Omega_S^2\eta_S = \phi_S^T B_F u \tag{5-7}$$

The nonprimary modes which are of interest but are not selected as secondary modes will be called tertiary (T) modes.

5.3.2 Synthesis Equations

The designer can now focus on the primary and secondary parts of the model which are of some reasonable size and attempt to calculate a synthesizer Γ such that:

$$\phi_S^T B_F \Gamma = 0 \tag{5-8}$$

for spillover prevention and

$$\phi_P^T B_F \Gamma \neq 0 \tag{5-9}$$

for adequate control.

Theorem 4 of Reference 1 (or Subsection 2 of Reference 2) provides a method for finding a Γ to alleviate spillover. If

$$\rho \overset{d}{=} \text{rank } (\phi_S^T B_F) \leq m - 1 \tag{5-10}$$

then

$$\Gamma = (-Q_1 W_{11}^{-1} W_{12} + Q_2) \hat{\Gamma} \tag{5-11}$$

where

$$\begin{bmatrix} W_{11} & W_{12} \\ \\ W_{21} & W_{22} \end{bmatrix} = P (\phi_S^T B_F) Q \tag{5-12}$$

with P, Q, and W_{11} being nonsingular matrices, and W_{11} having rank ρ, and $\hat{\Gamma}$ being arbitrary. Consequently

$$\Phi_P^T B_F \Gamma = (-V_1 W_{11}^{-1} W_{12} + V_2)\hat{\Gamma} \qquad (5\text{-}13)$$

is nonzero for nonzero $\hat{\Gamma}$, where

$$[V_1, V_2] \overset{d}{=} \Phi_P^T B_F Q \qquad (5\text{-}14)$$

5.3.3 Mathematical Concept Used for Finding Synthesizers

The essential manipulations to arrive at the terms in Eqs. (5-10) through (5-14) have been translated into FORTRAN source code for numerical applications to large space structures. The fundamental mathematical concept used in the computer program is Gaussian elimination with complete pivoting for which the following holds

$$\left(\Phi_S^T B_F\right)_{\text{eliminated}} = P \left(\Phi_S^T B_F\right) Q$$

where P, a permutation matrix, is the product of appropriate elementary matrices that perform row exchanges on $\Phi_S^T B_F$, and Q is the product of elementary matrices that either perform column exchanges or multiply one column by a constant and add it to another column.

The desirable form of the eliminated matrix is lower triangular with ones on the main diagonal. This form insures that W_{12} will be identically zero and Eqs. (5-11) and (5-13) will be greatly simplified. The number of ones on the diagonal will indicate the rank[*] of $\Phi_S^T B_F$.

When W_{12} is identically zero, the synthesizer becomes

$$\Gamma = Q_2 \hat{\Gamma} \qquad (5\text{-}15)$$

---

[*] Note that the rank ρ is a by-product of the Gaussian elimination process. The synthesis procedure does not require that the rank be calculated as the first step or that it be determined with great precision (see Subsection 5.5).

and the control influence matrix is simply

$$\Phi_P^T B_F \Gamma \;=\; V_2 \hat{\Gamma} \tag{5-16}$$

Some desirable values or properties for $\Phi_P^T B_F \Gamma$ may aid in the final selection of elements for $\hat{\Gamma}$. The problem of obtaining a proper control influence matrix, $\Phi_P^T B_F \Gamma$, will not be pursued in this report.

5.4   A Computer Program to implement Synthesis via Gaussian Elimination

The computer software designed for synthesis requires that the portion of the control influence matrix $\Phi^T B_F$ that is of interest be partitioned and rearranged as follows

$$\begin{bmatrix} \Phi_S^T B_F \\ \hline \Phi_P^T B_F \\ \hline \Phi_T^T B_F \end{bmatrix}$$

The program then proceeds to perform various manipulations (Subsection 5.4.1) on this matrix and on the P_P, P_S and Q matrices which are initially set to be identity matrices of appropriate dimension such that

$$\begin{bmatrix} \Phi_S^T B_F \\ \hline \Phi_P^T B_F \\ \hline \Phi_T^T B_F \end{bmatrix}_{\text{eliminated}} = \begin{bmatrix} P_S\left(\Phi_S^T B_F\right) \\ \hline P_P\left(\Phi_P^T B_F\right) \\ \hline \Phi_T^T B_F \end{bmatrix} Q \tag{5-17}$$

5.4.1 The Elimination Procedure

The program begins Gaussian elimination with complete pivoting in the secondary (S) partition, where only terms in this upper partition are examined for potential pivots. The row exchange required to bring a row with a pivot to the proper position is repeated in the P_S matrix. The possible column exchange to put the pivot in its final position and the ensuing column multiplications/additions necessary for elimination apply to the entire matrix, and are repeated in the Q matrix.

The elimination will continue until it reaches either the last column of the matrix, or the bottom of the primary (P) partition, or the point in the primary partition where every potential pivot is below a preset tolerance. The elimination is forbidden to proceed into the tertiary (T) partition.

If while eliminating in the secondary partition, the largest possible pivot in that partition is smaller than the preset tolerance, the algorithm will jump to the primary partition and resume the elimination process in the same column where it had stopped in the secondary partition. During elimination in the primary partition, pivots come exclusively from that partition and row exchanges are represented by the primary permutation matrix, P_P.

5.4.2 Features of the Elimination Algorithm

Originally, the elimination process was to have used partial pivoting (as in Section 2 of Reference 2) to arrive at the terms in the synthesis equations. If while using partial pivoting, a row was encountered all of whose potential pivots were smaller than the tolerance, that row would be transferred to the bottom of its partition and the elimination would resume with the next available row. This process would insure that the search for independent rows could continue throughout the entire matrix of interest; otherwise, the elimination process would halt whenever a row with very small terms was encountered without regard to later rows which could possibly be eliminated. Complete pivoting, on the other hand, brings the largest possible element to the pivot position by row and column exchanges which are simple to implement in a program and will produce the same results as the more complicated partial pivoting scheme described above.

The computer program developed for handling high-dimensional numerical models of the large space structures stores all matrices as one-dimensional double precision arrays. The use of one-dimensional arrays as opposed to the more natural two-dimensional arrays will save greatly on storage; however, that savings may be offset by both the added calculations needed to determine the position of an element in its matrix, and the extra challenges the use of one-dimensional arrays pose to the software designer.

The program will output all the matrices of Eq. (5-17) with the user providing only the matrix to be eliminated (properly partitioned and rearranged), the number of rows and columns in the matrix, and the number of rows in the secondary and primary partitions as input.

The algorithm has been successfully applied to matrices as small as 12 x 4 and as large as 84 x 85. The only work involved in adapting the algorithm to matrices of various dimensions involves the time consuming task of I/O alterations. Converting the software to a language that would allow more flexibility in I/O would be helpful.

5.5 Application of Synthesis Concept to Numerical Models of Large Space Structures

Once the program has produced its results in the form of the eliminated matrix, the P_S matrix, the P_P matrix, and the Q matrix, the designer then has the means to check if the rank condition of Eq. (5-10) is satisfied, and then either proceed to find a synthesizer, Γ, or try another group of secondary modes that will satisfy the rank condition.

The synthesis concept will be demonstrated on two representative large space structure models, Draper Models 1 and 2.

5.5.1 Draper (Tetrahedral) Model 1

Synthesis will first be demonstrated on the Draper tetrahedral model which is described in Appendix A of Reference 2. In Section 2 of Reference 2 we learn that the minimum number of physical actuators needed for complete controllability of the primary modes as well as the alleviation of control spillover to the secondary modes is:

$$m \geq \text{rank}(\Phi_S^T B_F) + \max\{\text{multiplicity of } \omega_{Pi}\} \qquad (5\text{-}18)$$

where m is the number of actuators placed on the structure. For the tetrahedron the maximum multiplicity of the primary natural frequencies is 1 so: $m \geq \rho + 1$ where ρ is the rank of $\Phi_S^T B_F$. Because synthesis presumes the m actuators have already been placed on the structure, the equation is more meaningful for our purpose when written with the unknown on the left

$$\rho \leq m - 1 \qquad (5\text{-}19)$$

Therefore, the same rank condition, (5-10), applies. Condition (5-19) implies that the placement of more actuators on the structure would allow prevention of spillover to more secondary modes.

The 12-degree-of-freedom tetrahedral model has eight known modes; four (numbers 1, 2, 4, and 5) are chosen as primary modes and the remaining four are designated secondary modes as in Section 2 of Reference 2. Figure 1 (at the end of this section) shows the Gaussian eliminated matrix $\phi^T B_F$ partitioned into secondary and primary parts. Clearly the rank condition is satisfied ($\rho = 4 < 5$). The results indicate that six actuators can be controlled as one or two independent synthetic actuators without spillover to the four secondary modes. For completing the synthesis (i.e., computing the matrices $\hat{\Gamma}$ and Γ) see Section 2 of Reference 2 for illustration.

5.5.2 Draper Model 2

The algorithm has also been applied to the 432-degree-of-freedom Draper Model 2 which is described in Section 9 of Reference 3. This large space structure model has 84 degrees of freedom with mass or rotational inertia and 19 control actuators.

For a first synthesis example, the lowest 44 elastic modes of vibration are used, and 17 of them are considered primary modes. While all the primary natural frequencies are unique, a primary mode and a nonprimary mode (modes 12 and 13) have nearly identical natural frequencies. So, according to Appendix B of Reference 4, the maximum multiplicity of the primary natural frequencies should be considered two in condition (5-18). Thus with m being 19 for Model 2, the rank condition for both controllability and spillover prevention is

$$\rho \leq 17 \tag{5-20}$$

For demonstration, all 27 nonprimary elastic modes have been chosen as secondary modes, and the elimination result is shown in Figure 2. The rank of spillover influence matrix, $\phi_S^T B_F$, is clearly 19, and even the rank condition (5-10) is not satisfied. Notice that rows 21, 22, 26, and 27 of the eliminated matrix are extremely small (they fall below the tolerance for the pivots) and are essentially zero. Consider repartitioning $\phi^T B_F$ so that the secondary partition would include the original rows that formed the first 17 rows of the previous eliminated matrix plus these four rows that were noted to be very small after the previous elimination. The tertiary partition would include the six remaining modes. The algorithm would then show the new 21 x 19 matrix $\phi_S^T B_F$ to have a rank of 17; even the rank condition (5-20) would then be satisfied and spillover to 21 modes could be prevented with two independent synthetic actuators for complete control of the primary modes.

A second synthesis example has the elastic part of the control influence matrix partitioned into 17 primary modes as before, 17 secondary modes (selected because of high "degree of modal controllability"), and

5-9

ten tertiary modes (not selected as secondary modes because of low "degree of modal controllability"). The Gaussian elimination result is shown in Figure 3. Observe that all of the potential pivots in the last row of the eliminated matrix $\phi_S^T B_F$ were below the tolerance, so the elimination resumed in the appropriate column of the primary partition. The rank of the upper (secondary) partition is 16, so one could successfully calculate a 17 x 1 synthesizer Γ to prevent spillover to the 17 secondary modes, with negligibly small spillover to the 10 tertiary modes.

5.6   Extension of Synthesis Techniques to the Prevention of Spillover by Proper Placement of Actuators

While discussing the principle of synthesis in Section 5.3, one may have wondered why an actuator influence matrix B_F was not chosen initially so that

$$\phi_R^T B_F = 0 \tag{5-21}$$

for all nonprimary modes. These last sections will examine the possibilities of placing actuators on a structure to yield an influence matrix so that all spillover is prevented.

Specifically, Theorems 1, 2, and 4 of Reference 1 will be reformulated to account for the practical difficulties in placing actuators on structures to prevent spillover. These placement reformulations will then be demonstrated on Models 1 and 2.

5.6.1   Use of the Synthesis Algorithm for Realizing Ideal Placement

Hopefully one could find physically realizable positions at nodes or along structural members for actuators to control primary modes without any control spillover. One approach to finding an influence matrix to prevent all spillover is that of Theorem 1 of Reference 1

$$B_F = M\phi_P \hat{B} \tag{5-22}$$

What this ideal placement requires are vectors (to form columns of matrix $\hat{B}$) each of which is in the nullspace of those L-3 rows (or L-6 rows when the actuator is between two nodes) of $M\phi_P$ which correspond to the nodes not in contact with the specific actuator to be placed, where L denotes the total number of modes. One can now begin to realize how the algorithm described earlier can be used for this actuator placement problem. Those rows of

$M\Phi_P$ corresponding to the degrees of freedom not to be influenced directly by an actuator will be lumped together to form the "secondary" partition of $M\Phi_P$, while the "primary" partition refers to the degrees of freedom directly influenced by the actuator, hence

$$\begin{bmatrix} (M\Phi_P)_S \\ \text{------} \\ (M\Phi_P)_P \end{bmatrix}$$

Once again a rank condition

$$\text{rank}[(M\Phi_P)_S] < \text{ number of columns in } (M\Phi_P)_S$$

must be satisfied.

The algorithm was first applied to the properly arranged and partitioned 12 x 4 matrix $M\Phi_P$ of Model 1 (i.e., the tetrahedral model) in an attempt to place an actuator at node 4. The rank of the 9 x 4 secondary partition of $M\Phi_P$ was found to be four as shown in Figure 4. This same procedure was repeated in an attempt to place an actuator at node 1, node 2, and node 3, respectively. The result was always the same: the rank of the 9 x 4 $(M\Phi_P)_S$ was four each time, and such placement could not prevent spillover. Further, attempts to place an actuator connecting a pair of nodes to prevent spillover failed, no matter what pair was chosen, because the rank of the 6 x 4 secondary partition of $M\Phi_P$ was again always four

These results imply that all spillover can be prevented only when an actuator influences at least three nodes, and not just one node or a pair of nodes as was structurally desired. One way of physically interpreting this new kind of placement is to think of an actuator appropriately placed at each of three nodes, yet all are controlled simultaneously by the same input. This type of actuator will be called a superactuator.

5.6.2 Superactuators and a Reformulation of the Placement Problem

The problem of having to place actuators at substantially more than L-3 (or L-6) degrees of freedom has led to a convenient mathematical formulation for the superactuator according to Theorems 1, 2, or 4 of Reference 1. Indeed, Theorem 2 of Reference 1 presents a necessary and sufficient condition for the actuator influence matrix, B_F, so the results of using Theorems 1 and 4 should agree with those using Theorem 2 by at least some linear transformation.

The main idea is to consider each superactuator as some combination of "elementary actuators" placed at a sufficient number of nodes, where an elementary actuator refers to any actuator that influences only one degree of freedom. In other words

$$B_F = EF \qquad (5\text{-}23)$$

where B_F denotes the influence matrix computed for the superactuators, E is an L x J matrix indicating which degrees of freedom will be influenced, and F denotes the combination coefficients to be determined, where J denotes the number of degrees of freedom that will have nonzero influences. The only nonzero term in each column of the matrix E is a "1" corresponding to a degree of freedom to be influenced by an actuator.

5.6.2.1 Theorem 1 and Model 1

The ideal actuator placement, expressed by Eq. (5-22) according to Theorem 1, can be re-expressed as

$$M\Phi_p \hat{B} = EF \qquad (5\text{-}24)$$

using Eq. (5-23), and hence

$$\left[M\Phi_p, \ -E \right] \begin{bmatrix} \hat{B} \\ F \end{bmatrix} = 0 \qquad (5\text{-}25)$$

Once again the algorithm for solving Eq. (5-4) can be used to solve this problem. The matrices $\hat{B}$ and F can be determined like Eq. (5-15) as

$$\begin{bmatrix} \hat{B} \\ \hline F \end{bmatrix} = \begin{bmatrix} Q_{2\hat{B}} \\ \hline Q_{2F} \end{bmatrix} \hat{\Gamma} \qquad (5\text{-}26)$$

where $Q_{2\hat{B}}$ and Q_{2F} denote the appropriate parts of the matrix Q_2 resulting from applying the Gaussian elimination algorithm on the augmented matrix $[M\Phi_p, \ -E]$.

If need be, the number of columns E can be increased to insure that the rank condition is satisfied, which physically means that the number of degrees of freedom to be influenced by actuators is increased.

For Model 1, the augmented matrix is shown in Figure 5(a). The nine 1's of the E matrix indicate that nine degrees of freedom will be influenced by actuators. The matrix after the Gaussian elimination is shown in Figure 5(b). The resulting Q_2 matrix used in Eq. (5-26) is shown in Figure 6.

5-12

Later, the Q_{2F} partition as shown in Figure 6 will be compared with similar results from the Theorem-2 and Theorem-4 superactuator approaches.

5.6.2.2   Theorem 2 and Model 1

The formulation of the superactuator placement problem according to Theorem 2 of Reference 1 proceeds as follows with all residual modes considered secondary modes. Perform Gaussian elimination on matrix ϕ_R^T first

$$[W_1, \ 0] \ = \ \phi_R^T Q \qquad (5\text{-}27)$$

partition the resulting matrix Q correspondingly

$$Q \ = \ [Q_1, \ Q_2] \qquad (5\text{-}28)$$

then represent the superactuator influence matrix R_F as

$$B_F \ = \ Q_2 \hat{B} \qquad (5\text{-}29)$$

Combining with Eq. (5-23), it is rewritten as

$$Q_2 \hat{B} \ = \ EF \qquad (5\text{-}30)$$

or equivalently

$$[Q_2, \ -E] \ \begin{bmatrix} \hat{B} \\ F \end{bmatrix} \ = \ 0 \qquad (5\text{-}31)$$

Observe that Eq. (5-31) is similar to (5-25). Thus the computation of $\hat{B}$ and F from Eq. (5-31) follows the same procedure as described before.
Notice the same notation Q_2 has a different meaning in a different context, because the same general algorithm is used to solve different problems of the same form as Eq. (5-8).

5-13

For Model 1 with the same E matrix as before, the resulting matrix Q_2 and its partitions Q_{2B} and Q_{2F} are shown in Figure 7. Observe that Q_{2F} in Figure 6 with the Theorem-1 approach can be postmultiplied by 1.283 to yield the Q_{2F} in Figure 7 with the Theorem-2 approach.

5.6.2.3 Theorem 4 and Model 1

Theorem 4 is of course the synthesis procedure described in Section 5.3, with all residual modes considered as secondary modes. For the placement application, the actuator influence matrix that is presumed is simply the E matrix used previously. In other words, letting all residual modes be secondary modes we have

$$\Phi_S^T B_F = \Phi_R^T E \tag{5-32}$$

where the goal is to find a matrix F such that

$$\Phi_R^T E \, F = 0 \tag{5-33}$$

as in Eq. (5-8). After performing Gaussian elimination on $\Phi_R^T E$, the solution F can be computed from the resulting Q_2 matrix as follows

$$F = Q_2 \, \hat{\Gamma} \tag{5-34}$$

This Q_2 matrix for Model 1 is shown in Figure 8, and is seen to be exactly the Q_{2F} obtained using the Theorem-2 approach.

To summarize, results for Model 1 from the three superactuator formulations (Theorems 1, 2 and 4) confirm that control spillover can be prevented to all the nonprimary modes of the tetrahedral model if the nine elementary actuators at three nodes (nine degrees of freedom) are simultaneously controlled by the same input.

5.6.2.4 Superactuator Placement Problem and Model 2

The superactuator placement schemes discussed in Sections 5.6.2.1 through 5.6.2.3 and represented by the E matrix are convenient for application to higher-dimensional large space structures. In this subsection, applications to Model 2 are demonstrated. This model is represented by an 84 x 84 modal matrix, corresponding to the 84 degrees of freedom with nonzero mass or inertia. The numerical model has 17 primary elastic modes and 67 nonprimary modes which include the six rigid body modes.

The E matrix, which is 84 x 68, represents unit actuators influencing 68 degrees of freedom. The specific degrees of freedom selected are listed in Figure 9.

The formulations with respect to Theorems 1, 2, and 4 can now be applied separately to Model 2 just as they were to Model 1. The resulting Q_2 matrices are shown in Figures 10, 11, and 12. The Q_{2F} resulting from the Theorem-1 approach and that from the Theorem-2 approach and the Q_2 from the Theorem-4 approach are all 68 x 4 matrices of rank 4 and are found to be related by nonsingular transformations. Figure 13 shows the transformation T_{12} relating the Q_{2F} from the Theorem-1 approach to the Q_{2F} of the Theorem-2 approach, and the transformation T_{42} relating the Q_2 of the Theorem-4 approach to the Q_{2F} of the Theorem-2 approach.

These results, obtained from different approaches, all indicate that four independent superactuators, each being a proper combination and interconnection of 68 elementary actuators, can control the 17 primary elastic modes with no spillover to any of the remaining 61 elastic modes and the six rigid-body modes.

Because all these approaches yield equivalent results, one must question their relative complexity. A comparison of the cpu times required for Model 2 (Figure 14) indicates that the Theorem-4 approach is the most efficient. Each approach first requires the extraction of an appropriate matrix from the computed 432 x 84 modal matrix. Specifically, only those terms in the mode shapes that correspond to degrees of freedom with nonzero mass or inertia are extracted, and in fact for the Theorem-4 approach only a subset of the mass degrees of freedom are extracted. These correspond to the degrees of freedom where actuators are placed. The Theorem-2 approach requires elimination to be done on the transposed residual matrix and then the resulting Q_2 matrix is augmented by the -E matrix as in Eq. (5-31). Similarly, for Theorem 1, the primary modal matrix is multiplied by the diagonal mass matrix and augmented with the -E matrix. All three approaches require a final elimination to arrive at the required answer. The control system designer must be aware that the mode shapes become less accurate with higher natural frequency, and should keep this in mind when trying to judge which approach is best for a particular application.

5.7   Conclusion

This study has demonstrated two methods of preventing control spillover on two representative numerical models of large space structures. The prevention of spillover to a significant number of nonprimary vibration modes was shown to be possible by proper synthesis of the influences of actuators existing on a structure. The synthesis procedure was programmed in FORTRAN, and successfully demonstrated on Model 1 (the tetrahedral model) and Model 2. For Model 1, six actuators were properly combined into two synthetic actuators for independent control of four selected primary modes and simultaneous prevention of spillover to four secondary modes.

For Model 2, synthesis of the 19 member actuators was found to prevent spillover to between 17 and 21 secondary modes, depending on the particular group of nonprimary modes selected as secondary modes; at least two independent synthetic actuators were available for control of the primary modes.

The synthesis progam, because of its mathematical generality, was found to be useful in reducing the number of structural nodes at which actuators must be placed for prevention of spillover to all nonprimary modes. However, the alleviation of all spillover in Model 1 by only the placement of one actuator at one node, or by the placement of an actuator between two nodes was found to be impossible. For Model 1, at least nine elementary actuators, each of which is placed to influence one degree of freedom but all of which are controlled simultaneously by a single input, were required for total spillover prevention. This superactuator scheme using common inputs for all elementary actuators was also implemented on Model 2 where 68 elementary actuators controlled independently by as many as four common inputs (i.e., four superactuators) was found to inhibit any spillover.

Three approaches to finding a superactuator for a given structure, each based on a different theorem of spillover prevention, were formulated. When tested on Models 1 and 2, all approaches produced equivalent results.

$$
\left.
\begin{array}{cccccc}
1.00000000 & 0.0 & 0.0 & 0.0 & 0.0 & 0.0 \\
-0.810840011 & 1.00000000 & 0.0 & 0.0 & 0.0 & 0.0 \\
-0.782113850 & 0.862970829 & 1.00000000 & 0.0 & 0.0 & 0.0 \\
0.735501230 & -0.253100084 & -0.539032459 & 1.00000000 & 0.0 & 0.0 \\
0.131436200 & 0.181745350 & -0.203383965 & 0.525876045 & 1.00000000 & 0.0 \\
0.161354959 & -0.385415435 & -0.446513951 & -0.000236826 & -0.973122716 & 1.00000000 \\
0.045311652 & 0.155920386 & -0.174574077 & 0.323387765 & -0.094534814 & -0.000119091 \\
0.181734383 & -0.056084499 & -0.064984620 & -0.000029064 & -0.141694665 & 0.145593882
\end{array}
\right\}
$$

$\left. \right\} \Phi_S^T B_F$

$\left. \right\} \Phi_P^T B_F$

Figure 5-1. The secondary and primary partitions of $\Phi^T B_F$ (of Model 1) after Gaussian Elimination.

5-16

$\phi_S^T B_F$

$\phi_P^T B_F$

Figure 5-2. The secondary and primary partitions of the matrix $\phi^T B_F$

(of Model 2 with 27 secondary modes) after Gaussian
Elimination. Columns 1-10.

$\phi_S^T F_B$

$\phi_P^T F_B$

Figure 5-2. The secondary and primary partitions fo the matrix $\phi^T F_B$ after Gaussian Elimination. Columns 11-19. (Continued).

Figure 5-3. The secondary, primary, and tertiary partitions of the matrix $\phi^T B_F$ (of Model 2 with 17 secondary modes) after Gaussian Elimination. Columns 1-10.

$\phi_S^T B_F$

$\phi_P^T B_F$

$\phi_T^T B_F$

Figure 5-3. The secondary, primary, and tertiary partitions of the matrix $\Phi^T B_F$ (of Model 2 with 17 secondary modes) after Gaussian Elimination. Columns 11-19. (Continued).

The partitions are labeled: $\Phi_S^T B_F$, $\Phi_P^T B_F$, $\Phi_T^T B_F$.

	11	12	13	14	15	16	17	18	19
1	0.0	0.0	0.0	0.0	0.0	0.0	0.0	0.0	0.0
2	0.0	0.0	0.0	0.0	0.0	0.0	0.0	0.0	0.0
3	0.0	0.0	0.0	0.0	0.0	0.0	0.0	0.0	0.0
4	0.0	0.0	0.0	0.0	0.0	0.0	0.0	0.0	0.0
5	0.0	0.0	0.0	0.0	0.0	0.0	0.0	0.0	0.0
6	0.0	0.0	0.0	0.0	0.0	0.0	0.0	0.0	0.0
7	0.0	0.0	0.0	0.0	0.0	0.0	0.0	0.0	0.0
8	0.0	0.0	0.0	0.0	0.0	0.0	0.0	0.0	0.0
9	0.0	0.0	0.0	0.0	0.0	0.0	0.0	0.0	0.0
10	-0.1000D+01	0.0	0.0	0.0	0.0	0.0	0.0	0.0	0.0
11	-0.2097D+00	0.1000D+01	0.0	0.0	0.0	0.0	0.0	0.0	0.0
12	-0.1372D+00	0.9022D-01	0.1000D+01	0.0	0.0	0.0	0.0	0.0	0.0
13	-0.9022D+00	0.9919D+00	-0.1551D-01	0.1000D+01	0.0	0.0	0.0	0.0	0.0
14	-0.6675D-02	0.2964D-02	0.1655D-01	-0.3364D-01	0.1000D+01	0.0	0.0	0.0	0.0
15	-0.4954D-02	0.3403D-02	0.4774D-02	-0.7499D-01	0.9587D+00	0.1000D+01	0.0	0.0	0.0
16	0.7345D-01	-0.8097D-01	0.1933D-04	-0.4090D+00	-0.2603D-03	0.5720D-03	-0.8503D-09	-0.6651D-08	0.4930D-08
17	0.1742D+02	-0.3472D+01	0.4073D+01	0.1403D+03	-0.2103D+04	-0.1745D+04	0.1000D+01	0.0	0.0
18	-0.2255D+01	-0.3395D+01	0.5141D+01	0.4033D+03	-0.6750D+03	-0.3774D+03	-0.3372D+00	0.1000D+01	0.1000D+01
19	-0.3916D+01	-0.6105D+00	0.5111D+01	0.8570D+02	0.1203D+04	0.1030D+04	-0.2351D+00	0.3756D+00	-0.3632D-01
20	-0.9151D+00	0.2530D+00	-0.1265D-01	-0.9465D+01	0.2126D+03	-0.1293D+03	0.1735D-02	-0.1074D-01	0.715D-03
21	0.6357D-02	-0.7000D+02	0.3263D-01	-0.1425D+01	-0.1002D+00	-0.2455D-01	-0.2845D-03	-0.1299D-05	0.2269D-02
22	0.5476D-01	-0.1537D-01	0.8420D-01	0.6182D+00	-0.1347D+02	0.7703D+01	-0.6740D-04	0.6665D-03	-0.2038D-03
23	-0.1651D+02	0.1815D+02	-0.9671D-02	0.4412D+00	-0.1600D-01	0.4207D+00	0.1237D-03	-0.5336D-05	0.1652D-01
24	0.1449D+01	-0.4850D+00	-0.4082D+01	-0.3343D+02	0.4134D+03	0.1539D+04	0.6013D-01	0.2661D-01	0.5191D-03
25	0.2895D+02	-0.3183D+02	0.9137D-01	-0.5708D+01	0.4284D+00	-0.3221D+00	-0.4236D-03	0.2237D-04	-0.6560D-02
26	-0.2457D+01	0.2200D+01	0.6173D+01	-0.4089D+03	0.9756D+01	0.3295D+02	0.4601D-02	-0.1506D-02	0.2306D+00
27	-0.5901D+01	-0.1679D+01	0.3605D+01	-0.2521D+01	-0.4099D+03	-0.1114D+04	-0.3204D-01	0.3470D-01	-0.3509D-01
28	-0.4002D+00	0.1722D+00	-0.4925D-01	-0.1326D+02	-0.1058D+02	-0.1450D+02	-0.4774D-01	-0.6371D-02	-0.3309D-01
29	0.4929D+01	-0.2264D+01	-0.3155D+00	0.1870D+03	0.31800D+03	0.9535D+02	0.6737D+00	0.9459D-01	0.467D+00
30	-0.4373D+00	0.4765D+00	0.7561D-02	-0.5039D+00	-0.2722D-01	-0.6791D+00	-0.9571D-04	-0.5205D-05	-0.1290D-12
31	0.7095D+01	-0.1454D+01	0.9504D+01	-0.1519D+03	-0.1406D+04	-0.5274D+03	0.4329D+00	-0.5380D+00	-0.9100D+00
32	-0.3744D+02	0.4115D+02	-0.1876D-01	0.8200D+01	0.9691D-01	0.8568D+00	0.1331D-03	0.5352D-05	-0.4171D-03
33	0.5784D+00	-0.1789D-02	0.4375D-02	0.4941D-01	-0.1211D+01	0.8095D+00	-0.1207D-04	0.5937D-04	0.1699D-03
34	0.3626D-01	-0.3544D-01	0.8441D-03	0.5301D-01	0.2305D-01	0.7111D-01	0.1006D-04	0.5694D-06	-0.6380D-04
35	-0.4556D-01	0.2729D-01	0.1323D+00	-0.1793D+00	0.4424D-01	-0.1712D+00	0.1003D-00	-0.5323D-04	-0.1790D-05
36	0.3410D+00	-0.3752D+00	0.1720D-02	-0.6976D-01	-0.1024D-01	-0.8477D-01	-0.1297D-04	-0.3006D-06	0.4016D-04
37	-0.1258D-07	-0.1335D-07	-0.5935D-11	0.2771D-09	-0.1165D-10	0.3096D-09	0.4799D-13	0.4629D-14	-0.1290D-12
38	0.3616D-01	-0.1450D-01	-0.2873D-01	0.2660D+00	-0.5153D-01	0.6704D-01	-0.8032D-04	0.6272D-03	0.2142D-02
39	-0.9113D-08	0.1002D-07	-0.5143D-11	0.2354D-09	0.2928D-12	0.2341D-09	0.7678D-13	-0.3701D-14	-0.1104D-12
40	0.2883D-09	-0.3163D-09	0.4916D-12	-0.1660D-10	-0.1863D-10	-0.7343D-10	-0.1015D-13	-0.4345D-15	-0.2929D-14
41	0.3214D+00	-0.3544D+00	-0.123D-01	0.8399D+00	-0.3486D-01	-0.2461D+00	-0.3845D-06	0.4249D-05	0.5957D-04
42	0.3371D-02	0.576D-03	-0.3705D-02	-0.2430D+00	0.8217D-01	0.1737D-01	0.2936D-03	-0.3453D-03	-0.7438D-03
43	0.1083D-11	0.3349D-11	-0.1771D-11	-0.3088D-11	0.4247D-09	0.5090D-09	0.1345D-12	-0.5986D-12	-0.1774D-12

5-20

```
0.100000000D+01      0.0                0.0                  0.0
-0.577471170D+00     0.100000000D+01    0.0                  0.0
0.0                  0.134771359D+00    0.100000000D+01      0.0
0.109278695D+00      0.101737733D-01    -0.176987308D+00     0.100000000D+01
0.901832383D-01      0.616704946D-01    -0.237035043D+00     0.891413784D+00
0.0                  -0.274865085D+00   0.834931335D+00      -0.242532736D-03
-0.851624861D-01     0.188492422D+00    -0.401653287D+00     -0.703030417D+00
-0.520941810D-01     0.197023457D+00    -0.410625461D+00     -0.515097333D+00
0.106964908D+00      -0.139254967D+00   0.196240198D+00      -0.230181259D+00
-0.520855462D-01     0.148143870D+00    -0.354234276D+00     -0.515027485D+00
0.128367446D+00      0.469686682D-01    -0.259182345D+00     0.110848050D+01
-0.106946464D+00     -0.466262829D-01   0.196221325D+00      0.230037133D+00
```

$(M\Phi_P)_S$

$(M\Phi_P)_P$

Figure 5-4. The secondary and primary partitions of $M\Phi_P$
(of Model 1) after Gaussian Elimination.
Ideal placement at Node 4 is considered.

```
-0.63884  1.03577  0.11452 -0.27357  0.0      0.0      0.0      0.0      0.0      0.0      0.0      0.0      0.0
 1.19265  0.60702 -0.19330 -0.15011  0.0      0.0      0.0      0.0      0.0      0.0      0.0      0.0      0.0
 0.0     -0.39796 -0.00029 -0.68527  0.0      0.0      0.0      0.0      0.0      0.0      0.0      0.0      0.0
-0.06214  0.25260 -0.35192  0.32415 -1.00000  0.0      0.0      0.0      0.0      0.0      0.0      0.0      0.0
 0.10750  0.14594  0.60916  0.13712  0.0     -1.00000  0.0      0.0      0.0      0.0      0.0      0.0      0.0
 0.0      0.19513 -0.00014 -0.99375  0.0      0.0     -1.00000  0.0      0.0      0.0      0.0      0.0      0.0
-0.10159  0.21951 -0.47756  0.32402  0.0      0.0      0.0     -1.00000  0.0      0.0      0.0      0.0      0.0
 0.13035  0.03325  0.68175  0.14618  0.0      0.0      0.0      0.0     -1.00000  0.0      0.0      0.0      0.0
 0.12759 -0.13455 -0.18315 -0.15142  0.0      0.0      0.0      0.0      0.0     -1.00000  0.0      0.0      0.0
-0.06213  0.18183 -0.35189  0.28574  0.0      0.0      0.0      0.0      0.0      0.0     -1.00000  0.0      0.0
 0.15312  0.14849  0.75428  0.20737  0.0      0.0      0.0      0.0      0.0      0.0      0.0     -1.00000  0.0
-0.12757 -0.13457  0.18293 -0.15141  0.0      0.0      0.0      0.0      0.0      0.0      0.0      0.0     -1.00000
           MΦ_p                                                    -E
```

Figure 5-5(a). Augumented matrix $[M\Phi_p, -E]$ of Model 1.

```
 1.00000  0.0      0.0      0.0      0.0      0.0      0.0      0.0      0.0      0.0      0.0      0.0      0.0
-0.57747  1.00000  0.0      0.0      0.0      0.0      0.0      0.0      0.0      0.0      0.0      0.0      0.0
-0.05209  0.19702  1.00000  0.0      0.0      0.0      0.0      0.0      0.0      0.0      0.0      0.0      0.0
 0.09018  0.06167  0.0      1.00000  0.0      0.0      0.0      0.0      0.0      0.0      0.0      0.0      0.0
 0.0      0.13477  0.0      0.0      1.00000  0.0      0.0      0.0      0.0      0.0      0.0      0.0      0.0
-0.08516  0.18849  0.0      0.0      0.0      1.00000  0.0      0.0      0.0      0.0      0.0      0.0      0.0
 0.10928  0.01017  0.0      0.0      0.0      0.0      1.00000  0.0      0.0      0.0      0.0      0.0      0.0
 0.10696 -0.13925  0.0      0.0      0.0      0.0      0.0      1.00000  0.0      0.0      0.0      0.0      0.0
-0.05209  0.14814  0.0      0.0      0.0      0.0      0.0      0.0      1.00000  0.0      0.0      0.0      0.0
 0.12837  0.04697  0.0      0.0      0.0      0.0      0.0      0.0      0.0      1.00000  0.0      0.0      0.0
-0.10695 -0.04663  0.0      0.0      0.0      0.0      0.0      0.0      0.0      0.0      1.00000  0.0      0.0
 0.0     -0.27487  0.0      0.0      0.0      0.0      0.0      0.0      0.0      0.0      0.0      1.00000  0.0
```

Figure 5-5(b). Augumented matrix $[M\Phi_p, -E]$ of Model 1
after Gaussian Elimination.

Figure 5-6. The resulting matrix Q_2 and its partitions Q_{2B} and Q_{2F} from Theorem-1 approach.

Figure 5-7. The resulting matrix Q_2 and its partitions $Q_{2\hat{B}}$ and Q_{2F} of Model 1 from Theorem-2 approach.

$Q_{2\hat{B}}$

Q_{2F}

Q_2

Q_1

0.0	0.0	0.0	0.0	0.0	0.0	1.00000	0.0	0.0
0.90214	-0.02954	0.0	0.05603	0.0	0.0	-0.03986	0.06808	0.90215
0.0	0.0	0.0	1.00000	0.0	0.0	0.0	1.19778	0.00026
0.0	1.00000	-1.00000	-0.53107	0.0	0.0	0.29043	0.0	0.0
0.0	0.0	0.0	-0.02861	-1.00000	0.0	0.02775	-0.63610	-0.46481
0.0	0.0	0.0	0.0	0.0	-1.00000	0.29457	-0.03427	0.80417
0.0	0.0	0.0	0.0	0.0	0.0	-0.03986	1.19778	0.00026
0.0	0.0	0.0	0.0	0.0	0.0	-0.14870	-0.67799	-0.63438
0.0	0.0	0.0	0.0	0.0	0.0	0.23394	0.06808	0.90215
0.0	0.0	0.0	0.0	0.0	-1.00000	0.0	0.17059	-0.20762
0.0	0.0	0.0	0.0	0.0	0.0	0.0	-0.56854	-0.46475
0.0	0.0	0.0	0.0	0.0	0.0	0.0	0.0	1.00000
0.0	0.0	0.0	0.0	0.0	-1.00000	0.0	0.29946	0.20759

```
0.0       0.0       0.0       0.0       0.0       0.0      -1.53139  1.27350 -0.46483
0.0       0.0       0.0       0.0       0.0       2.04493 -1.09697  0.11049  0.80417
0.0       0.0       0.0       0.0      -1.69799  0.29445 -0.12072 -0.71617  0.00026
0.0       0.0       0.0       0.0       0.0       0.0      0.0       1.20196 -0.63439
0.0       0.0       0.0      -1.65164   0.92474  1.24694 -0.79235 -0.11034  0.90215
2.05200  -1.06430   0.20800  -0.08293  -0.13043 -0.12303 -0.13210  0.21349 -0.20762
0.0       0.0       2.44948  -1.43034   0.00090 -0.69105 -0.50226  1.08656 -0.46475
0.0       0.0       0.0       0.0       0.0       0.0      0.0       0.0      1.00000
0.0      -1.06466   0.03478  -0.17301  -0.07990  0.32041 -0.21442 -0.02828  0.20759
```

$\underbrace{\hspace{8cm}}_{Q_1}$ $\underbrace{\hspace{1.5cm}}_{Q_2}$

Figure 5-8. The resulting Q_2 matrix of Model
1 from Theorem-4 approach.

5-25

25 nodes (grid points) with nonzero mass

Node	Direction
9 - 12	x, y, z
14	x
15 - 19	x, y
27 - 30	
32 - 35	
44	
48	
50	x, y, z
52, 53	
55	
57	

Figure 5-9. 68 DOF of Model 2 selected for placement of 68 elementary actuators at 25 nodes (grid points) with nonzero mass.

1	0.74580-06	0.40690-05	0.28390-01	0.61040-05
2	-0.6373D-01	0.23430-01	-0.11080-01	-0.11190-01
3	-0.30670-07	-0.81460-04	-0.16950-02	-0.77720-04
4	-0.44840-02	0.11130-01	-0.56430-02	-0.81730-02
5	-0.69980-06	-0.90720-04	-0.42510-03	-0.13820-03
6	-0.13090+00	-0.26290-01	0.13130-01	0.13380-01
7	-0.38290-07	-0.25020-04	-0.12970-04	-0.39360-04
8	-0.32280-03	-0.22250-01	-0.22920-01	0.55790-01
9	0.15080-06	0.42930-03	0.20010-03	0.33870-03
10	0.19120-04	0.44420-01	0.11550-01	0.41680-01
11	0.13350-03	0.12940+00	-0.71610-01	0.15590+00
12	-0.70340-01	-0.28720-01	0.14390-01	0.12740-01
13	0.49100-02	-0.22440-01	0.25350-01	-0.14860-02
14	-0.85710-04	0.12190+00	-0.78230-01	0.14030+00
15	-0.49340-03	0.11150-01	-0.14460-01	0.95040-03
16	-0.37860-04	0.91190-02	0.22610-01	-0.39780-01
17	0.19870-04	0.15780-01	0.74420-02	0.19210-01

$$Q_{2\hat{B}}$$

18	-0.65850-02	0.21440+00	-0.99760-01	0.15510+00
19	-0.28010-03	0.14200-01	-0.37440+00	-0.31210-01
20	0.49490-02	-0.32270+00	0.30340+00	-0.10930+01
21	-0.92890-02	-0.31600-01	0.49330-02	0.19820+00
22	-0.10140-03	-0.31010+00	-0.13410+00	-0.39270+00
23	-0.50680-02	-0.66150+00	0.28330+00	-0.52760+00
24	-0.65560-02	-0.74430-01	0.70930-02	-0.17730+00
25	0.14680-03	-0.63560-01	-0.28660+00	-0.19430-01
26	-0.41740-02	-0.75360+00	-0.23000+00	0.50290-01
27	-0.92920-02	-0.22990+00	0.13120+00	-0.42040-01
28	-0.64660-04	-0.39280+00	-0.13180+00	-0.40530+00
29	0.34430-02	-0.30880+00	0.10930+00	-0.65510+00
30	0.92690-04	0.13080+00	-0.86080-01	0.13700+00
31	0.94870-03	0.26350+00	-0.15810+00	0.22400+00
32	-0.38090-03	0.42260-02	-0.11040-01	0.31810-01
33	-0.67770-03	0.33810+00	-0.84780+00	0.39470+00
34	-0.41590-03	0.20240-01	-0.23810-01	0.43060-01
35	0.90290-03	-0.29380+00	0.26800+00	-0.44490+00
36	0.38150-03	0.22310-01	0.10950-01	-0.87580-02
37	-0.89440-03	-0.28590+00	0.61140-01	-0.31790+00
38	0.40510-03	0.31920-01	0.13010-02	0.10560-01
39	0.42820-04	-0.11030+00	0.76320-01	-0.16460+00
40	-0.32070-04	0.15640-01	-0.19860-01	0.17770-01
41	0.33100-02	-0.71600-01	0.12170+00	-0.15280+00
42	-0.28470-02	0.93740-01	-0.11210-01	0.27640-01
43	-0.20450-02	0.20360+00	-0.28390+00	0.36100+00
44	0.51910-02	0.11320+00	-0.14330+00	0.23360+00
45	-0.24350-02	0.68030-02	0.13200+00	-0.86330-01
46	-0.49880-03	0.79190+00	-0.37420+00	0.87670+00
47	0.30340-02	-0.39520+00	0.26930+00	-0.64710+00
48	0.35790-02	0.14620+00	-0.87580-01	0.26250+00
49	0.17170-02	0.21930+00	0.89160-02	0.94500-01
50	0.40240-02	0.77690-01	0.50460-01	0.88460-01
51	0.20230-02	-0.26890-01	-0.37490-01	0.64170-01
52	0.14690-02	0.62990+00	-0.15060+00	0.80330+00
53	0.39890-02	0.12230+00	-0.21880+00	0.49360+00
54	-0.47000-02	0.14750+00	0.57040-01	-0.87880-01
55	0.0	0.0	0.0	0.10000+01
56	0.22520-02	0.56270-01	-0.10490+00	0.20970+00
57	0.43170-02	0.16100+00	-0.86530-01	0.36220+00
58	0.0	0.10000+01	0.0	0.0
59	0.14640-02	0.86750-01	-0.75010-02	-0.69140-01
60	-0.13960-02	0.88270-01	0.34010-01	0.62650-01
61	0.61880-02	-0.36710+00	0.21500+00	-0.47020+00
62	0.49940-03	0.11140+00	-0.93610-03	-0.11670+00
63	0.18100-02	0.57170-01	-0.41260-01	0.14800+00
64	-0.66050-02	-0.43900+00	0.75650-31	-0.41060+00
65	0.61430-02	-0.80320-03	-0.15740-02	-0.65320-03
66	0.0	0.0	0.10000+01	0.0
67	0.13820-05	0.29930-02	-0.44200-01	0.34030-02
68	0.15820-03	-0.18740-04	-0.39090-04	-0.22300-04
69	-0.45330-02	0.23010-02	-0.28600-01	-0.90950-03
70	0.44610+00	-0.58400-01	0.28800-01	0.27720-01
71	0.31620-03	-0.38160-04	-0.78700-04	-0.42560-04
72	0.78570-02	-0.45740-02	0.12010-01	0.16950-02
73	-0.10000+01	-0.18330-03	-0.14340-02	-0.18130-03
74	0.15800-03	-0.20110-04	-0.40110-04	-0.16330-04
75	0.76260-03	-0.16100-03	0.23760-01	0.22170-02
76	0.69290+00	0.30080+00	-0.14100+00	-0.14140+00
77	0.15800-03	-0.20110-04	-0.40110-04	-0.18330-04
78	-0.76220-03	0.16910-02	0.24480-01	-0.50950-03
79	-0.69290+00	-0.30000+00	0.13920+00	0.14210+00
80	0.31620-03	-0.38160-04	-0.78700-04	-0.42560-04
81	-0.78650-02	0.42330-02	0.71930-02	-0.20240-02
82	0.10000+01	0.0	0.0	0.0
83	0.15820-03	-0.18740-04	-0.39090-04	-0.22300-04
84	0.45350-02	-0.22350-02	-0.26390-01	0.10510-02
85	-0.44610+00	0.58440-01	-0.26490-01	-0.27670-01

$$Q_{2F}$$

Figure 5-10. The resulting Q_2 matrix and its partitions $Q_{2\hat{B}}$ and Q_{2F} of Model 2 from Theorem-1 approach.

5-27

$Q_{2\hat{B}}$

1	0.1000D+01	0.0	0.0	0.0
2	0.0	0.0	0.0	0.1000D+01
3	0.0	0.0	0.0	0.0
4	-0.23?2D+00	0.5090D-01	-0.7542D+00	0.4389D-02
5	0.0	0.1000D+01	0.0	0.0
6	0.3934D+00	-0.1093D+0?	-0.3269D+00	-0.4964D-02
7	0.0	0.0	0.0	0.0
8	0.1401D+00	0.1416D+0?	-0.3003D+00	0.6928D+00
9	0.0	0.0	0.0	0.0
10	-0.3729D+00	0.8744D+00	0.7915D+00	0.1270D-03
11	0.2620D+00	-0.5258D+00	-0.6312D+00	0.5409D-02
12	-0.1502D+00	0.8029D+00	0.6318D+00	-0.2037D-0?
13	0.0	0.0	0.0	0.0
14	0.0	0.0	0.1000D+01	0.0
15	0.7525D-01	-0.4095D+00	-0.4389D+00	0.6144D-02
16	0.1092D+00	-0.6889D+00	-0.3117D+00	-0.2881D-02
17	-0.2140D-11	0.5445D-13	0.8240D-14	-0.4395D-14

$Q_{2\hat{B}}$

18	-0.9949D-01	0.1546D+00	0.2141D+00	0.6469D-02
19	-0.3743D+00	-0.3117D-01	0.1379D-01	0.2943D-03
20	0.3934D+00	-0.1093D+01	-0.3269D+00	-0.4964D-02
21	0.4930D-02	0.1954D+00	-0.3104D-01	0.9178D-02
22	-0.1344D+00	-0.3921D+00	-0.3099D+00	0.2043D-03
23	0.2820D+00	-0.5258D+00	-0.6312D+00	0.5409D-02
24	0.7002D-01	-0.1730D+00	-0.7433D-01	0.6899D-02
25	-0.2865D+00	-0.1934D-01	-0.6342D-01	-0.1747D-03
26	-0.2308D+00	0.5090D-01	-0.7542D+00	0.4389D-02
27	0.1309D+00	-0.4147D-01	-0.2290D+00	0.9293D-02
28	-0.1320D+00	-0.4851D+00	-0.3929D+00	0.8239D-03
29	0.1092D+00	-0.6889D+00	-0.3117D+00	-0.2881D-02
30	-0.6589D-01	0.1365D+00	0.1306D+00	-0.1433D-03
31	-0.1578D+00	0.2233D+00	0.2683D+00	-0.1093D-02
32	-0.1104D-01	0.3152D-01	0.4181D-02	0.3973D-03
33	-0.2472D+00	0.3937D+00	0.3348D+00	0.8744D-03
34	-0.2379D-01	0.4304D-01	0.2017D-01	0.4180D-03
35	0.2643D+00	-0.4443D+00	-0.2936D+00	-0.8314D-03
36	0.1096D-01	-0.6749D-02	0.2233D-01	-0.3825D-03
37	0.6092D-01	-0.3176D+00	-0.2666D+00	0.1111D-02
38	0.1286D-02	0.1057D-01	0.3201D-01	-0.4148D-03
39	0.7617D-01	-0.1684D+00	-0.1303D+00	0.3790D-04
40	-0.1983D-01	0.1772D-01	0.1557D-01	0.3566D-04
41	0.1214D+00	-0.1523D+00	-0.7112D-01	-0.3262D-02
42	-0.1114D-01	0.2748D-01	0.9350D-01	0.2661D-02
43	-0.2858D+00	0.3613D+00	0.2033D+00	0.2043D-02
44	-0.1433D+00	0.2356D+00	0.1133D+00	-0.5234D-02
45	0.1319D+00	-0.8635D-01	0.6898D-02	0.2444D-02
46	-0.3729D+00	0.8744D+00	0.7915D+00	0.1270D-03
47	0.2686D+00	-0.6446D+00	-0.3949D+00	-0.2811D-02
48	-0.8747D-01	0.2625D+00	0.1464D+00	-0.3644D-02
49	0.9067D-02	0.9422D-01	0.2197D+00	-0.1616D-02
50	0.5069D-01	0.8839D-01	0.7309D-01	-0.4092D-02
51	-0.3744D-01	0.6409D-01	-0.2715D-01	-0.1982D-02
52	-0.1502D+00	0.8029D+00	0.6318D+00	-0.2037D-02
53	-0.2184D+00	0.4931D+00	0.1221D+00	-0.4098D-02
54	0.5711D-01	-0.8812D-01	0.1473D+00	0.4710D-02
55	0.0	0.1000D+01	0.0	0.0
56	-0.1066D+00	0.2095D+00	0.5612D-01	-0.2294D-02
57	-0.6643D-01	0.3622D+00	0.1614D+00	-0.4411D-02
58	0.0	0.0	0.1000D+01	0.0
59	-0.7438D-02	-0.6931D-01	0.8661D-01	-0.1458D-02
60	0.3410D-01	0.6244D-01	0.8040D-01	0.1362D-02
61	0.2149D+00	-0.4706D+00	-0.3670D+00	-0.6124D-02
62	-0.8545D-03	-0.1165D+00	0.1112D+00	-0.4920D-03
63	-0.4121D-01	0.1481D+00	0.5736D-01	-0.1853D-02
64	0.7525D-01	-0.4095D+00	-0.4389D+00	0.6166D-01
65	-0.1650D-02	-0.5500D-03	-0.7754D-03	-0.6204D-02
66	0.1000D+01	0.0	0.0	0.0
67	-0.4432D-01	0.3602D-02	0.2816D-02	0.9130D-03
68	-0.4106D-04	-0.1959D-04	-0.1806D-04	-0.1597D-03
69	-0.2859D-01	-0.9746D-03	0.2296D-02	0.4536D-02
70	0.2816D-01	0.2755D-01	-0.5857D-01	-0.4460D+00
71	-0.8254D-04	-0.3726D-04	-0.3676D-04	-0.3193D-03
72	0.1200D-01	0.1708D-02	-0.4569D-02	-0.7859D-02
73	0.0	0.0	0.0	0.1000D+01
74	-0.4207D-04	-0.1562D-04	-0.1935D-04	-0.1595D-03
75	0.2376D-01	0.2217D-02	-0.1636D-03	-0.7636D-03
76	-0.1420D+00	-0.1409D+00	0.3010D+00	-0.6928D+00
77	-0.4207D-04	-0.1562D-04	-0.1935D-04	-0.1595D-03
78	0.2447D-01	-0.5085D-03	0.1895D-02	0.7628D-03
79	0.1401D+00	0.1416D+00	-0.3003D+00	0.6928D+00
80	-0.8254D-04	-0.3726D-04	-0.3676D-04	-0.3193D-03
81	0.7204D-02	-0.2025D-02	0.4229D-02	0.7859D-02
82	-0.1445D-02	-0.1589D-03	-0.2005D-03	-0.1000D+01
83	-0.4106D-04	-0.1959D-04	-0.1806D-04	-0.1597D-03
84	-0.2640D-01	0.1050D-02	0.2228D-02	-0.4531D-02
85	-0.2585D-01	-0.2749D-01	0.5861D-01	0.4460D+00

Q_{2F}

Figure 5-11. The resulting Q_2 matrix and its partitions $Q_{2\hat{B}}$ and Q_{2F} of Model 2 from Theorem-2 approach.

1	-0.4386D-01	0.1678D+03	0.5761D-02	-0.1415D+00
2	-0.3855D+00	0.2341D-01	0.4354D-03	0.2862D-01
3	0.0	0.0	0.0	0.1000D+01
4	0.7521D-01	-0.8986D-01	0.8296D-02	-0.1788D+00
5	-0.2754D+00	-0.1924D+00	0.1985D-02	0.3588D+00
6	0.9311D-01	-0.4936D+00	0.7795D-02	0.4809D+00
7	0.8589D-02	-0.2247D-01	0.7384D-02	0.1583D+00
8	-0.2935D+00	-0.7770D-01	-0.8539D-04	0.1772D-01
9	-0.2118D+00	-0.7693D+00	0.4130D-02	-0.4602D-01
10	0.1159D+00	-0.2168D+00	0.9481D-02	0.3006D-01
11	-0.2778D+00	-0.2709D+00	0.2062D-02	0.3705D+00
12	-0.1384D+00	-0.1038D+00	0.2399D-03	0.6296D+03
13	-0.3673D-01	0.8977D-01	-0.7635D-03	-0.1251D+00
14	-0.7739D-01	0.1984D+00	-0.2107D-02	-0.2045D+00
15	0.3033D-03	-0.5244D-02	0.2542D-03	-0.2882D-01
16	-0.1056D+00	0.2166D+00	-0.1213D-02	-0.3604D+00
17	-0.0298D-02	0.7304D-02	0.2225D-03	-0.3938D-01
18	0.1047D+00	-0.1605D+00	0.1184D-02	0.4065D+00
19	0.7798D-02	0.2494D-01	-0.3426D-03	0.8022D-02
20	-0.3333D-01	-0.1910D+00	0.1552D-02	0.2907D+00
21	0.5088D-02	0.2881D-01	-0.4027D-03	-0.9683D-02
22	0.1560D-01	-0.7936D-01	0.8019D-03	0.1541D+00
23	-0.1345D-01	0.1030D-01	-0.4495D-04	-0.1624D-01
24	0.6661D-01	-0.2559D-01	-0.2596D-02	0.1394D+00
25	-0.1260D-02	0.8538D-01	0.2736D-02	-0.2522D-01
26	-0.1559D+00	0.9509D-01	0.4051D-03	-0.3299D+00
27	-0.5858D-01	0.4268D-01	-0.6302D-02	-0.2154D+00
28	0.1008D+00	0.3479D-01	0.2833D-02	0.7879D-01
29	-0.5824D-01	0.5294D+00	-0.3847D-02	-0.8007D+00
30	0.3620D-01	-0.2014D+00	0.1249D-03	0.5912D+00
31	0.6939D-02	0.6758D-01	-0.4833D-02	-0.2400D+00
32	0.4293D-01	0.1912D+00	-0.2244D-02	-0.8629D-01
33	0.8249D-01	0.5150D-01	-0.4493D-02	-0.8102D-01
34	-0.1440D-01	-0.4631D-01	-0.2272D-02	-0.5856D-01
35	0.1386D+00	0.3903D+00	-0.5681D-02	-0.7347D+00
36	-0.4101D-01	-0.2561D-01	-0.6337D-02	-0.4511D+00
37	0.2542D-01	0.1737D+00	0.5108D-02	0.8041D-01
38	0.3597D+00	-0.2998D+00	-0.4542D-02	-0.9149D+00
39	-0.3139D-01	-0.6658D-02	-0.3246D-02	-0.1916D+00
40	0.4186D-01	0.5269D-01	-0.6054D-02	-0.3313D+00
41	0.0	0.1000D+01	0.0	0.0
42	-0.3273D-01	0.1074D+00	-0.1146D-02	0.6335D-01
43	0.5657D-01	0.6958D-01	0.1077D-02	-0.5726D-01
44	0.4567D-01	-0.2261D+00	-0.3987D-02	0.4304D+00
45	-0.4291D-01	0.1463D+00	0.3350D-04	0.1069D+00
46	0.1204D-01	0.1285D-01	-0.2524D-02	-0.1354D+00
47	-0.7208D-01	-0.3162D+00	0.8028D-02	0.3750D+00
48	-0.1849D-02	-0.6107D-03	-0.6199D-02	0.5014D-03
49	0.1000D+01	0.0	0.0	0.0
50	-0.4303D-01	0.1736D-02	0.1750D-03	-0.3296D-02
51	-0.4811D-04	-0.1218D-04	-0.1597D-03	0.1792D-04
52	-0.2894D-01	0.2592D-02	0.4542D-02	0.8932D-03
53	0.3806D-01	-0.6684D-01	-0.4461D+00	-0.2325D-01
54	-0.9598D-04	-0.2565D-04	-0.3192D-03	0.3398D-04
55	0.1261D-01	-0.5082D-02	-0.7866D-02	-0.1567D-02
56	0.0	0.0	0.1000D+01	0.0
57	-0.4769D-04	-0.1472D-04	-0.1595D-03	0.1429D-04
58	0.2456D-01	-0.8260D-03	-0.7740D-03	-0.2028D-02
59	-0.1926D+00	0.3433D+00	-0.6920D+00	0.1292D+00
60	-0.4769D-04	-0.1472D-04	-0.1595D-03	0.1429D-04
61	0.2427D-01	0.2070D-02	0.7654D-03	0.5396D-03
62	0.1910D+00	-0.3428D+00	0.6920D+00	-0.1298D+00
63	-0.9598D-04	-0.2565D-04	-0.3192D-03	0.3398D-04
64	0.6475D-02	0.4838D-02	0.7872D-02	0.1857D-02
65	-0.1502D-02	-0.1527D-03	-0.1000D+01	0.1453D-03
66	-0.4811D-04	-0.1210D-04	-0.1597D-03	0.1792D-04
67	-0.2603D-01	-0.2543D-02	-0.4537D-02	-0.9618D-03
68	-0.3573D-01	0.6687D-01	0.4461D+00	0.2520D-01

Figure 5-12. The resulting Q_2 matrix of Model 2
from Theorem-4 approach.

5-29

$$T_{12} = \begin{bmatrix} -.1445\text{x}10^{-2} & -.1589\text{x}10^{-3} & -.2005\text{x}10^{-3} & -\text{?} \\ 0 & 0 & 1 & 0 \\ 1 & 0 & 0 & 0 \\ 0 & 1 & 0 & 0 \end{bmatrix}$$

$$T_{42} = \begin{bmatrix} 1 & 0 & 0 & 0 \\ 0 & 0 & 1 & 0 \\ 0 & 0 & 0 & 1 \\ .3934 & -.1093\text{x}10^{1} & -.3269 & -.4964\text{x}10^{-2} \end{bmatrix}$$

$$Q_{2F}(\text{Theorem 2}) = Q_{2F}(\text{Theorem 1})T_{12}$$

$$Q_{2F}(\text{Theorem 2}) = Q_{2}(\text{Theorem 4})T_{42}$$

Figure 5-13. T_{12} and T_{42} transformations.

Theorem - 1 Approach

	cpu time (sec)
extract Φ_P	1.46
form $[M\Phi_P, -E]$	1.53
perform elimination	5.39
total	8.38

Theorem - 2 Approach

	cpu time (sec)
extract Φ_R^T	2.13
compute Q_2 from $\Phi_R^T Q$	3.36
form $[Q_2, -E]$	1.33
perform elimination	5.52
total	12.34

Theorem - 4 Approach

	cpu time (sec)
extract $\Phi_R^T E$	1.89
perform elimination	4.12
total	6.01

Figure 5-14. CPU comparisons.

LIST OF REFERENCES

1.   Lin, J.G., "Three Steps to Alleviate Control and Observation
     Spillover Problems of Large Space Structures," Proceedings of
     19th IEEE Conference on Decision and Control, Albuquerque, NM,
     December 1980, pp. 438-444.

2.   Actively Controlled Structures Theory-Final Report, Report No.
     R-1338, CSDL, December 1979.

3.   Active Control of Space Structures - Interim Report, Report No.
     R-1404, CSDL, September 1980.

4.   Actively Controlled Structures Theory - Interim Technical Report,
     Vol. 1, Theory of Design Methods, Report No. R-1249, CSDL,
     April 1979.

FEEDBACK CONTROL OF ELASTIC SYSTEMS
USING DAMPING AND STIFFNESS AUGMENTATION

6.1   Introduction

A number of methods have been proposed for design of controllers for elastic structures. In many cases the methods are particularly simple if certain special assumptions are made, e.g., if all sensors and actuators are collocated. Even though the methodology may be applicable without such assumptions, this fact is often not strongly emphasized. Consequently, the generality of the methods (and thereby the flexibility allowed in application) is not always clear.

Here we focus on one particularly simple method: namely, the augmentation of system damping using velocity feedback and the augmentation of system stiffness using displacement feedback. Although some specialized assumptions are made, our objective is to emphasize ways in which the method can be expanded to make it more flexible in applications. We are not able to characterize the maximum attainable flexibility, but we do indicate how flexibility in the design process can arise. Finally, some possible implications of this flexibility are mentioned. The results presented here are not new, but they are viewed from a somewhat uncommon perspective.

6.2   Basic Equations

Consider the second order vector equation for an elastic system

$$\ddot{\eta} + D\dot{\eta} + \Omega^2\eta = \Phi^T Bu \qquad (6\text{-}1)$$

where $\eta = (\eta_1,\ldots,\eta_n)$ are modal coordinates, Ω^2 is an $n \times n$ positive definite, diagonal modal stiffness matrix of squares of the natural frequencies, D is an $n \times n$ symmetric, nonnegative definite modal damping matrix, B is an $n \times m$ actuator influence matrix, Φ is an $n \times n$ nonsingular matrix whose columns are the elastic mode shapes; and the control input is $u = (u_1,\ldots,u_m)$. Such models arise from application of finite element methods to distributed elastic structures or from lumped elastic systems.

We consider control of the elastic modes by using a feedback controller of the form

$$u = -G_p y_p - G_v y_v \qquad (6\text{-}2)$$

where G_p and G_v are constant gain matrices and the modal displacement vector and modal velocity vector are given by

$$y_p = C_p \Phi \eta$$

$$y_v = C_v \Phi \dot{\eta}$$

<div align="right">(6-3)</div>

where C_v is a velocity sensor influence matrix and C_p is a displacement sensor influence matrix. Thus the closed loop system is described by

$$\ddot{\eta} + \left(D + \Phi^T BG_v C_v \Phi \right) \dot{\eta} + \left(\Omega^2 + \Phi^T BG_p C_p \Phi \right) \eta = 0 \qquad (6-4)$$

Our fundamental objective is to choose the gain matrices G_v and G_p so that the closed loop system described by (6-4) is asymptotically stable. Moreover, the closed loop eigenvalues of (6-4) are of interest in characterizing the response properties of (6-4).

6.3 Controller Design

An early approach, due to Canavin [1,3], was to require that only velocity feedback be used, $G_p = 0$, and the G_v be chosen to satisfy the equation

$$D + \Phi^T BG_v C_v \Phi = \Delta \qquad (6-5)$$

where Δ is a diagonal matrix of desired positive damping coefficients. In addition, Canavin assumed that the actuators and velocity sensors are collocated, that is, that the matrices B and C_v^T are related by a scalar factor.

Various extensions of Canavin's idea have been proposed; in particular, any desired modal damping matrix Δ which is symmetric and positive definite can be chosen, with $G_p = 0$. The resulting closed loop system (6-4) is consequently asymptotically stable [8].

In any event, the gain matrix G_v is determined by finding a solution, if one exists, of the linear matrix equation (6-5).

The approach suggested here is similar to that suggested by Canavin, except that both displacement and velocity feedback are used as expressed in (6-2). In particular, a desired modal damping matrix Δ and a desired modal stiffness matrix K are selected; then the velocity and displacement feedback gain matrices G_v and G_p are chosen to satisfy the equations

$$D + \Phi^T BG_v C_v \Phi = \Delta \qquad (6\text{-}6)$$

$$\Omega^2 + \Phi^T BG_p C_p \Phi = K \qquad (6\text{-}7)$$

so that the corresponding closed loop system is

$$\ddot{\eta} + \Delta\dot{\eta} + K\eta = 0 \qquad (6\text{-}8)$$

The most important issue is the proper selection of the matrices Δ and K so that: (a) the closed loop system (6-8) is asymptotically stable, and (b) solutions do exist for the linear equations (6-6) and (6-7).

We refer to Δ as the desired modal damping matrix and to K as the desired modal stiffness matrix, <u>although there is no a priori reason to assume that Δ and K are either symmetric or nonnegative definite.</u>

We would like to make the weakest possible requirement on Δ and K which guarantees asymptotic stability of (6-8). The following result is clear.

Theorem 6-1. The matrices K and Δ are such that all zeros of the characteristic polynomial

$$\det \, [s^2 I + \Delta s + K]$$

have negative real part if and only if the solutions of (6-8) are asymptotically stable.

This result is not particulary suitable for purposes of design in that individual conditions on K and Δ are not easily discerned. A more suitable result, for purposes of choosing Δ and K, is the following sufficient condition for asymptotic stability of (6-8).

Theorem 6-2. [2, 6] Assume K is symmetric and positive definite and Δ is nonnecessarily definite (but not necessarily symmetric). Then the solutions of (6-8) are asymptotically stable if and only if the associated system:

$$\ddot{x} + \Delta_{ss}\dot{x} + Kx = 0$$
$$y = \Delta_s \dot{x} \qquad (6\text{-}9)$$

is completely observable, where Δ_s and Δ_{ss} are symmetric and skew symmetric matrices, respectively, such that $\Delta = \Delta_s + \Delta_{ss}$.

Proof: Using the Liapunov function

$$V = \frac{1}{2} \dot{\eta}^T \dot{\eta} + \frac{1}{2} \eta^T K \eta$$

we obtain

$$\frac{dV}{dt} = - \dot{\eta}^T \Delta_s \dot{\eta}$$

For asymptotic stability we require that any solution of (6-8) satisfy the following:

$$\text{if } \dot{\eta}^T \Delta_s \dot{\eta} \equiv 0, \text{ then } \eta \equiv 0$$

But this condition is guaranteed if and only if the stated observability assumption is made. ∎

There are a number of possible special cases of this general result. Only the following are stated.

Corollary 6-2.1 Assume K is symmetric and positive definite and Δ_s is positive definite (but Δ is not necessarily symmetric). Then the solutions of (6-8) are asymptotically stable.

Corollary 6-2.2 [2, 4] Assume K is symmetric and positive definite and Δ is symmetric and nonnegative definite. Then the solutions of (6-8) are asymptotically stable if and only if the matrix pair (K, Δ) is completely observable, i.e.,

$$\text{rank } [\Delta | K\Delta | \ldots | K^{n-1}\Delta] = n$$

Corollary 6-2.2 has often formed the basis for extensions of Canavin's method; however it seems desirable to use the more general result in Theorem 6-2 as basis for an extension. Namely, the modal damping matrix Δ and the modal stiffness matrix K should be selected to meet the following requirements:

Δ is nonnegative definite (not necessarily symmetric);

6-4

K is symmetric and positive definite;

the system (6-9) is completely observable; and

equations (6-6), (6-7) have solutions.

Then it is guaranteed that gain matrices G_v and G_p exist for which the solutions of (6-4) are asymptotically stable.

In using active feedback control of the form (6-2), it should be recognized that the desired modal damping matrix need not be symmetric. This is to be contrasted with the case where any inherent structural damping (such as results from dashpots) is represented by a "symmetric damping matrix", while gyroscopic effects (such as due to spinning wheels or rotors) result in a "skew symmetric damping matrix". In the case of active control, this physical interpretation of the symmetric and skew symmetric parts of the damping matrix need not be valid. In using active feedback control, the desired modal stiffness matrix is required to be symmetric, not because inherent structural stiffness has that characteristic, but due to the fact that asymptotic stability of (6-8), as developed using the particular Liapunov function in Theorem 6-2, cannot be guaranteed otherwise. Although extra flexibility could be obtained by allowing the desired modal stiffness matrix to be nonsymmetric, there are no available stability conditions for this case, where the conditions are in a "nice form" for choosing K and Δ as in Theorem 6-2. This avenue for extension of design flexibility remains unexplored.

6.4   Closed Loop Eigenvalues

Since the eigenvalues of the closed loop system determine the closed loop stability properties and the response properties, it is sui   to relate the choice of the desired modal damping matrix Δ and th   a   red modal stiffness matrix K to the closed loop eigenvalues. We first point out that different choices of the modal damping matrix and modal stiffness matrix may lead to closed loop systems with identical spectrum.

characteristic equation of (6-8) is given by

$$\det [s^2 I + s\Delta + K] = 0,$$

whose zeros are the closed loop eigenvalues.

We now consider conditions under which the choice of damping matrix $\overline{\Delta}$ and stiffness matrix $\overline{K}$, corresponding to

$$\ddot{\eta} + \overline{\Delta}\dot{\eta} + \overline{K}\eta = 0 \tag{6-10}$$

6-5

result in identical spectrum as that of (6-8). Although general results for such a problem have been developed in [5], we prefer to use a different parametric characterization using similarity concepts.

__Theorem 6-3.__ Assume the eigenvalues of (6-8) are distinct. Then (6-10) has identical spectrum with (6-8) if and only if there is a nonsingular $2n \times 2n$ matrix

$$\begin{bmatrix} P_{11} & P_{12} \\ P_{21} & P_{22} \end{bmatrix}$$

such that

$$-P_{12}\overline{K} = P_{21}$$

$$P_{11} - P_{12}\overline{\Delta} = P_{22}$$

$$-P_{22}\overline{K} = -KP_{11} - \Delta P_{21} \qquad (6-11)$$

$$P_{21} - P_{22}\overline{\Delta} = -KP_{12} - \Delta P_{22}.$$

__Proof:__ Verify that

$$\begin{bmatrix} P_{11} & P_{12} \\ P_{21} & P_{22} \end{bmatrix} \begin{bmatrix} 0 & I \\ -\overline{K} & -\overline{\Delta} \end{bmatrix} = \begin{bmatrix} 0 & I \\ -K & -\Delta \end{bmatrix} \begin{bmatrix} P_{11} & P_{12} \\ P_{21} & P_{22} \end{bmatrix}$$

so that the $2n \times 2n$ matrices

$$\begin{bmatrix} 0 & I \\ -\overline{K} & -\overline{\Delta} \end{bmatrix} \quad \text{and} \quad \begin{bmatrix} 0 & I \\ -K & -\Delta \end{bmatrix}$$

are similar; hence

$$\det [s^2 I + \Delta s + K] = \det [s^2 I + \overline{\Delta}s + \overline{K}].$$

6-6

The arguments are easily reversed, since the eigenvalues are assumed to
be distinct. ■

It should be recognized, consistent with the discussion in the
previous section, that the matrices Δ, $\bar{\Delta}$, K, and $\bar{K}$ need be neither
symmetric nor nonnegative definite. Further, even if Δ and K are
symmetric and nonnegative definite a particular choice of P_{11}, P_{12}, P_{21},
P_{22} does not imply that $\bar{\Delta}$ and $\bar{K}$ are symmetric and nonnegative definite.

An interesting special case of the above result is obtained by
selecting P_{11} = P_{22} = P and P_{12} = P_{21} = 0.

Corollary 6-3.1. The spectrum of (6-8) and the spectrum of (6-10) are
identical if there is nonsingular n×n matrix P such that

$$\bar{\Delta} = P^{-1}\Delta P$$

$$\bar{K} = P^{-1}KP.$$

Corollary 6-3.1 has the interesting interpretation that a necessary
condition, but not generally a sufficient one, that (6-8) and (6-10)
have identical spectrum is that matrices Δ and $\bar{\Delta}$ have identical spectrum
and that K and $\bar{K}$ have identical spectrum.

The linear algebraic equations (6-6), (6-7), with G_v and G_p viewed
as unknowns, may have no solutions or many solutions. We do not examine
existence questions, but we are interested in the case of multiple
solutions of (6-6), (6-7). It has often been assumed that the matrices
$\Phi^T B$, $C_v\Phi$, and $C_p\Phi$ are full rank, but this need not be the case; if these
matrices are rank deficient then there are many solutions of (6-6),
(6-7); that is, there are many choices of gain matrices G_v and G_p which
lead to identical modal damping and modal stiffness matrices Δ and K.

Theorem 6-4. Suppose that G_v and G_p satisfy equations (6-6), (6-7). Then
$\bar{G}_v$ and $\bar{G}_p$ also satisfy equations (6-6), (6-7) if and only if

$$\bar{G}_v = G_v + L_v + R_v$$

$$\bar{G}_p = G_p + L_p + R_p$$

where matrices L_v, L_p, R_v, and R_p satisfy the homogeneous equations

$$(\Phi^T B) R_v \; = \; 0$$

$$(\Phi^T B) R_p \; = \; 0$$

$$L_v (C_v \Phi) \; = \; 0$$

$$(6\text{-}12)$$

$$L_p (C_p \Phi) \; = \; 0.$$

Finally, we combine the results of Theorem 6-3 and Theorem 6-4 to obtain conditions for which different choices of gain matrices G_v, G_p and $\overline{G}_v$, $\overline{G}_p$ lead to identical closed loop spectrum.

<u>Theorem 6-5.</u> Suppose that

$$\Phi^T B G_v C_v \Phi \; = \; \Delta - D$$

$$\Phi^T B G_p C_p \Phi \; = \; K - \Omega^2$$

and

$$\Phi^T B \overline{G}_v C_v \Phi \; = \; \overline{\Delta} - D$$

$$\Phi^T B \overline{G}_p C_p \Phi \; = \; \overline{K} - \Omega^2.$$

Assume the eigenvalues of (6-8) are distinct. Then (6-8) and (6-10) have identical spectrum if and only if

$$\overline{G}_v \; = \; G_v + L_v + R_v$$

$$\overline{G}_p \; = \; G_p + L_p + R_p$$

for some nonsingular matrix

$$\begin{bmatrix} P_{11} & P_{12} \\ P_{21} & P_{22} \end{bmatrix}$$

6-8

such that Δ, $\overline{\Delta}$, K, $\overline{K}$ satisfy (6-11) and L_v, R_v, L_p, R_p satisfy (6-12).

Thus, it is seen that: (a) many different choices of modal damping and modal stiffness matrices may lead to identical closed loop spectrum, and (b) even for fixed modal damping and fixed modal stiffness matrices, there may be many possible choices of feedback gain matrices. This substantial flexibility in determining feedback gain matrices with fixed closed loop spectrum should be recognized and exploited.

6.5   Example.

The previous ideas have been expressed in rather general terms, so that it seems useful to examine a simple example which illustrates in concrete terms those general ideas.

Consider two identical uncoupled mass-spring systems as described by the two second order differential equations

$$\ddot{\eta}_1 + \omega^2 \eta_1 = u_1$$

$$\ddot{\eta}_2 + \omega^2 \eta_2 = u_2$$

where u_1, u_2 are forces applied to the respective masses. For purpose of discussion, the controller is assumed to be of the fixed form given by

$$u_1 = -g_1(\dot{\eta}_1 - \dot{\eta}_2) - g_2 \dot{\eta}_2 - g_3 \dot{\eta}_1$$

$$u_2 = -g_1(\dot{\eta}_2 - \dot{\eta}_1) + g_2 \dot{\eta}_1 - g_3 \dot{\eta}_2$$

where the gain constants g_1, g_2, g_3 are to be determined to stabilize the resulting closed loop system.

The closed loop system is described by:

$$\begin{bmatrix} \ddot{\eta}_1 \\ \ddot{\eta}_2 \end{bmatrix} + \begin{bmatrix} g_1 + g_3 & -g_1 + g_2 \\ -g_1 - g_2 & g_1 + g_3 \end{bmatrix} \begin{bmatrix} \dot{\eta}_1 \\ \dot{\eta}_2 \end{bmatrix} + \begin{bmatrix} \omega^2 & 0 \\ 0 & \omega^2 \end{bmatrix} \begin{bmatrix} \eta_1 \\ \eta_2 \end{bmatrix} = \begin{bmatrix} 0 \\ 0 \end{bmatrix}$$

6-9

We see that the closed loop system is asymptotically stable, as a consequence of Corollary 6-2.1, if the symmetric part of the modal damping matrix is positive definite, i.e., if

$$g_1 > 0, \quad g_3 > 0, \quad \text{(arbitrary } g_2\text{)}$$

But suppose that, a priori, we require that $g_3 = 0$; then the symmetric part of the modal damping matrix is always singular. If now we require that the modal damping matrix be symmetric, i.e., $g_2 = 0$, there is no possible choice of g_1 which can stabilize the closed loop system [4]. However, if we examine the flexibility obtained by not imposing the symmetry requirement on the damping matrix, we obtain that the closed loop system is asymptotically stable if

$$g_1 > 0, \quad g_2 \neq 0, \quad (g_3 = 0),$$

using Theorem 6-2. In summary, we have shown that (with $g_3 = 0$) the closed loop system cannot be stabilized if the modal damping matrix is required to be symmetric; but it can be stabilized if that symmetry requirement is eliminated.

Next, we consider the flexibility resulting from choosing the gain constants g_1, g_2, g_3 so that the closed loop system has fixed spectrum. Note that for any desired modal damping matrix Δ (with equal diagonal entries) the equation

$$\begin{bmatrix} g_1 + g_3 & -g_1 + g_2 \\ -g_1 - g_2 & g_1 + g_3 \end{bmatrix} = \Delta$$

has a unique solution. However, applying the results of Corollary 6-3.1, recognizing that the particular matrix K in this case commutes with any 2×2 matrix P, it follows that the closed loop spectrum is unchanged if g_1, g_2, g_3 are determined from

$$\begin{bmatrix} g_1 + g_3 & -g_1 + g_2 \\ -g_1 - g_2 & g_1 + g_3 \end{bmatrix} = P^{-1} \Delta P$$

for any nonsingular 2×2 matrix P. This flexibility is easily exhibited by making the special choice that

$$\Delta = \begin{bmatrix} 2 & -1 \\ -1 & 2 \end{bmatrix}$$

with eigenvalues 1 and 3. With this choice the closed loop system is asymptotically stable. And any gains satisfying the above condition for some P will correspond to a closed loop system with identical closed loop spectrum. Using the result of Corollary 6-3.1 stated in terms of the characteristic polynomial for Δ we obtain the more transparent condition that

$$(s - g_1 - g_3)^2 - (-g_1 - g_2)(-g_1 + g_2) = (s - 1)(s - 3)$$

which is satisfied if

$$2(g_1 + g_3) = 4$$

$$2g_1 g_3 + g_3^2 + g_2^2 = 3.$$

In summary, we have shown that for any gain constants g_1, g_2, g_3 satisfying the above conditions, of which there are an infinite number of possibilities, the closed loop system is asymptotically stable, with fixed spectrum given by the zeros of

$$\det \begin{bmatrix} s^2 + 2s + \omega^2 & -s \\ -s & s^2 + 2s + \omega^2 \end{bmatrix}$$

6.6   Conclusions

We have pointed out that in augmenting the system damping and stiffness through velocity and displacement feedback there is no need to require that the desired modal damping matrix (or even the desired modal stiffness matrix) be either symmetric or nonnegative definite. In fact, as illustrated by the simple example, addition of a skew-symmetric part of a damping matrix may be sufficient to stabilize the closed loop system. This extra flexibility in choosing the modal damping and modal stiffness matrix in extending Canavin's design approach should be exploited.

In addition, we have pointed out that (typically) there may be many choices of feedback gain matrices which have identical closed loop spectrum. This flexibility may occur with different sets of damping and stiffness matrices. Such flexibility may also arise due to rank deficiencies in certain system matrices. In all such cases, there are many closed loop feedback gains leading to identical closed loop spectrum.

It is not clear how this design flexibility can be exploited to practical advantage in the design process. But several possibilities can be mentioned. A more flexible choice of desired damping and stiffness matrices may allow "easier" choice of a stabilizing feedback controller or may result in smaller feedback gains. A more flexible choice of particular feedback gains may also allow choice based on reduction of the magnitude of feedback gains [7]. Moreover, the approach suggested here in no way requires that sensors and actuators be collocated. In addition, the flexibility might allow a choice based on reduction of control or observation spillover (for any ignored modes) [8].

The objective of this section has been to emphasize the existence of design flexibility in augmenting system damping and stiffness using velocity and position feedback. We have pointed out that, apparently, a great deal of flexibility does exist. We have not completely characterized that flexibility, nor have we determined how that flexibility can be meaningfully used. Such issues require additional research.

References

1. J. R. Canavin, "The Control of Spacecraft Vibrations Using Multivariable Output Feedback," Paper 78-1419, AIAA/AAS Astrodynamics Conference, Palo Alto, California, August 7-9, 1978.

2. P. C. Hughes and R. E. Skelton, "Stability, Controllability and Observability of Linear Matrix-Second-Order Systems," Proc. 1979 Joint Automatic Control Conference, Denver, Colorado, June 17-20, 1979.

3. Y. H. Lin, "Output Feedback Control Via Canavin Method of Modal Decoupling," in Interim Report, Actively Controlled Structures Theory, Volume 1, Charles Stark Draper Laboratory Report R-1249, April 1979.

4. R. K. Miller and A. N. Michel, "Asymptotic Stability of Systems: Results Involving the System Topology," SIAM J. Control and Optimization, Vol. 18, No. 2, March 1980, pp. 181-190.

5. B. C. Moore, "On the Flexibility Offered by State Feedback in Multi-variable Systems Beyond Closed Loop Eigenvalue Assignment," IEEE Trans. Automatic Control, Vol. AC-21, No. 5, October 1976, pp. 689-692.

6. R. E. Skelton, "Control Design of Flexible Spacecraft," submitted for publication.

7. J. G. Lin, "Pareto-Optimal Control," in <u>Interim Report, Active Control</u> <u>of Space Structures</u>, Charles Stark Draper Laboratory Report R-1404, September 1980.

8. J. G. Lin, "General Requirements for Stabilization," in <u>Interim Report</u>, <u>Active Control of Space Structures</u>, Charles Stark Draper Laboratory Report R-1404, September 1980.

SECTION 7

OUTPUT FEEDBACK STABILIZABILITY

7.1   Introduction

7.1.1 Motivation

A closed-loop control system incorporating only static output feed-
back operates under two significant constraints. First, information about the
system at any instant is obtained from current measurements of only those
state variables that can be physically measured. In particular, no process-
ing of the available information to estimate unmeasurable state variables is
done. Current measurements of measurable states are not stored for future
use, and the inevitable delay in their processing is not accounted for in the
mathematical model of the system. State (i.e., full-state) feedback is evi-
dently a special case of output (i.e., incomplete-state) feedback. Second,
the feedback path contains no (modeled) dynamic elements as compensators.
Static feedback may be viewed as dynamic feedback of zero order. These con-
straints are severe. The lack of information associated with incomplete-
state measurements is potentially destabilizing, and the unavailability of
dynamic feedback compensation limits the available performance.

However, in spite of the severe implications of these constraints,
their essential nature makes output feedback attractive for many potential
applications. For one thing, measurement of the full state may not be phys-
ically possible. Even if it is possible, the cost in measurement hardware and
processing software of obtaining full-state information may not be worth the
benefits. Output feedback allows the selection of a proper subset of the full
state for measurement, and explicitly incorporates such a constraint in the
mathematical model of the system. In addition, dynamic elements in the feed-
back path require actuating hardware and processing software for implementa-
tion, which introduces delay that can be destabilizing; they may also magnify
unmodeled disturbances entering the system. For large-scale decentralized
systems in particular, output feedback controllers are attractive from the
viewpoint of implementation. These facts have motivated recent research on,
and comparison of, several design methods for output feedback controllers for
large space structures [1-4]. It remains to establish their feasibility.

The key elements of feasibility are economy of construction and opera-
tion, stabilizability, and performance. In this section, attention is focused
on stabilizability for control systems relying solely on output feedback.
Moreover, only linear time-invariant systems are treated. Stabilizability is
an _existence_ statement. The system with state and output equations

$$\dot{x}(t) = Ax(t) + Bu(t) \quad , \quad t \geq 0 \qquad\qquad (7\text{-}1)$$

$$y(t) = Cx(t) \quad , \quad t \geq 0 \qquad\qquad (7\text{-}2)$$

where x, u, and y are vectors representing the state, input, and output, respec-
tively (with generally distinct dimensions), and A, B, and C are matrices of

compatible order, is <u>stabilizable</u> by output feedback if there exists a matrix K such that the closed-loop system

$$\dot{x}(t) = (A + BKC)x(t) , \quad t \geq 0 \qquad (7-3)$$

is asymptotically stable in the sense of Liapunov [5]. The bare assertion of stabilizability sheds no light in general on how to find a stabilizing output feedback matrix K; this is a separate question. The reverse assertion (i.e., nonstabilizability), if true, displays the fundamental role of this concept, for it suggests either that the mathematical model is inadequate, or that in fact the actual system cannot be stabilized with only output feedback. Design approaches for output feedback controllers recognize the stabilizability question in various ways; some make provision to ensure it [6], others explicitly assume it [7], while others make no guarantee but implicitly assume it [8].

Although much work has been done in this direction, a simple characterization of output feedback stabilizability has not been found. Nandi and Herzog [9] have shown that stability of the uncontrollable and unobservable eigenvalues of the open-loop system matrix A is a necessary condition for output feedback stabilizability. Li [10] and Denham [11] have shown that stability of those eigenvalues of A associated with certain subspaces derived from the matrices A, B, C is sufficient for output feedback stabilizability. In order to use these conditions, a spectral analysis of the open-loop system must be made and then associated with certain geometric constructions. Johnson [12] discusses the surprising difficulty of the stabilizability problem, and gives solutions for certain special cases. Anderson et al. [13,14] show that the question of output feedback stabilizability (as well as the construction of a stabilizing controller, if one exists) can be answered in principle by performing a finite number of rational operations associated with making decisions regarding the solution of a set of multivariable polynomial inequalities. In this approach, the computational burden is excessive and the structure of the underlying problem is lost. Some approaches to the stabilizability question [15,16] are essentially experimental and can never really answer it. The purpose of the work reported in this section is to develop an explicit algebraic characterization of output feedback stabilizability.

The approach taken toward the stabilizability question rests on the notion of suboptimality and has been influenced by several factors. First, recent study of the Kosut design method [8], and in particular, extensions which render it more attractive for large space structure application [3], highlight the simplicity associated with that suboptimal method. Interest has also been expressed in using the Kosut method in adaptive control algorithms. Second, a simple expression for the cost penalty in using suboptimal controllers [17] lends itself quite naturally to this approach. It is hoped that the general results obtained for the output feedback stabilizability problem will shed some light on the stability of controllers designed using the Kosut suboptimal output feedback method, a question that has eluded solution to date.

Before the stabilizability approach is presented, it is appropriate to review briefly some basic information from stability theory.

7.1.2 Some Facts from Stability Theory

7.1.2.1 Stability in the Sense of Liapunov

The Liapunov theory of stability has had a profound influence on the study of dynamical systems since its appearance in 1893 in a Russian mathematical journal [5]. Numerous papers and books have been devoted to an exposition of this theory [18-22]. A key to its importance lies in the fact that it gives information about the stability (or instability) of dynamical systems without requiring explicit solutions to the system equations.

Two of the Liapunov notions of stability are used in this section. They are most easily described in terms of the solution function of the dynamical system. Only time-invariant systems are considered here; i.e.

$$\dot{x}(t) = f(x(t)) \quad , \quad x(0) = x_0 \tag{7-4}$$

Denote by

$$x_0 \mapsto \phi(\cdot; x_0) \tag{7-5}$$

the real-valued mapping which assigns to each n-vector x_0 (initial state) a solution $\phi(t; x_0)$, $t \geq 0$ to the system equations (7-4). Liapunov stability notions are defined in terms of equilibrium states x_E of dynamic systems, which have the special property that $\phi(t; x_E) = x_E$ for all $t \geq 0$. An equilibrium state x_E is said to be stable if the solution function [Eq. (7-5)], viewed as a mapping of the initial values, is continuous at x_E. Note that this definition does not preclude large transients (in the engineering sense) or undamped oscillations of the solution. Further, an equilibrium state x_E is said to be asymptotically stable if it is stable, and if

$$\phi(t; x_0) \to x_E \quad \text{as} \quad t \to +\infty$$

for all x_0 in some open set containing x_E. Note that initially-large oscillations of the solution (as a function of time) are still possible.

The key concept that provides stability information apart from explicit solutions of the system equations is that of a Liapunov function [20]. Any real-valued function

$$x \mapsto V(x)$$

which is defined on the state space and is continuously differentiable in an open set Ω about the origin, satisfying $V(0) = 0$; $V(x) > 0$, $x \neq 0$; and $\dot{V}(x) \equiv [\text{grad } V(x)]^T f(x) < 0$ for all states in Ω is called a Liapunov function. This definition assumes (without loss of generality) that the equilibrium state

to be tested for stability is the origin. The principal results of Liapunov pertinent to this section are as follows:

Theorem 7-1 (Stability) [20]. If there exists a Liapunov function in some open set Ω containing the origin, then the origin is stable.

Theorem 7-2 (Asymptotic Stability) [20]. If, in addition, $\dot{V}(x) < 0$ for all nonzero states in Ω, then the origin is asymptotically stable.

7.1.2.2 The Liapunov Matrix Equation

Matrix equations of the form

$$A^{T}P + PA = -Q \qquad (7-6)$$

occur frequently in linear system theory [23]. However, the chief interest in such an equation arises from its connection with Liapunov stability theory for time-invariant differential systems. Consider the homogeneous system associated with Eq. (7-1)

$$\dot{x}(t) = Ax(t) \quad , \quad t \geq 0 \qquad (7-7)$$

for which the origin is an equilibrium state. The central result is:

Theorem 7-3 [18]. With respect to Eq. (7-7), the origin is asymptotically stable if and only if, for each symmetric positive-definite matrix Q (denoted $Q > 0$) there exists a unique symmetric matrix $P > 0$ satisfying Eq. (7-6).

The connection is essentially that, when such pairs of matrices exist, the function

$$x \mapsto V(x) \triangleq x^{T}Px$$

is a Liapunov function for the system of Eq. (7-7) and $\dot{V}(x) = -x^{T}Qx$. More generally, it can be stated that the question of existence and properties of solutions to Eq. (7-6) has immediate relevance to the stability of the system of Eq. (7-7). This fact has motivated extensive research into the theory of, and solution methods for, Eq. (7-6). Before proceeding, it should be noted that the Liapunov matrix equation that corresponds to Eq. (7-6) for the difference equation

$$x(t_{n+1}) = Cx(t_n) \quad , \quad n = 0,1,\ldots \qquad (7-8)$$

has the form [24]

$$C^{T}PC - P = -R \qquad (7-9)$$

where the matrices A and C are related by the linear fractional transformation

$$A \mapsto C \triangleq (I + A)(I - A)^{-1} \qquad (7-10)$$

7-4

Consequently, stability results connected with solutions of Eq. (7-6) are also applicable to difference equations (7-8).

An important key to understanding Eq. (7-6) lies in the spectral properties of the slightly more general Sylvester [25] mapping

$$P \rightarrow A^T P + PB \qquad (7-11)$$

Bellman [26] shows that the eigenvalues of this operator are the sums $\lambda + \mu$, where λ (resp. μ) is an eigenvalue of A (resp. B). It follows that solutions to the Sylvester equation

$$A^T P + PB = -Q \qquad (7-12)$$

exist and are unique whenever none of the sums $\lambda + \mu$ vanishes. The integral

$$P = -\int_0^{+\infty} e^{At} Q \, e^{Bt} \, dt$$

is an explicit representation for the solution of Eq. (7-11) under the assumption that all the eigenvalues of A and B have negative real parts [27]. (See [28] for a complete analysis of the Liapunov mapping associated with Eq. (7-11); i.e., $B = A^T$.)

The discussion up to this point has not treated the following more subtle situations regarding Eq. (7-6): (a) conditions for existence of solutions when Q is only positive semidefinite (denoted $Q \geq 0$); (b) general conditions for existence of positive definite solutions; and (c) existence and properties of solutions when the Liapunov operator $P \rightarrow A^T P + PA$ has eigenvalues with zero real part. Full answers to these questions are provided in clear geometric terms by Snyders and Zakai [29].

Much has been written regarding explicit algebraic representations for solutions to Eq. (7-6) [30-34]. Motivation for such work has been in part to facilitate numerical computation of solutions. One obvious (and brute force) approach to computation of solutions has been to rewrite Eq. (7-6) as an equation of the form

$$\tilde{A} \, \tilde{p} = \tilde{q}$$

for a vector $\tilde{p}$ obtained by unraveling the rows of the matrix P, and then to use standard numerical solution methods for such vector equations. This approach is very inefficient and not feasible for large order equations [35,36]. The most effective numerical methods for solving Eq. (7-6) are based upon the recognition that the equation is invariant in form under similarity transformations. The most attractive algorithms developed to date appear to be the Bartels-Stewart algorithm [37] and several extensions [38,39]. (See [40,41] for brief evaluations.)

7.1.2.3 Absolute Stability and Hyperstability

In actual dynamic systems, it is important to be able to **guarantee** stability (or asymptotic stability) in the sense of Liap.nov not only for a specific system, but also for an <u>entire class of systems</u>. For example, important parameters in a system may only be known to within a certain range of values; it would be desirable to have a guarantee of system stability for all parameter values in that range. The class of systems to be considered are of the general form shown in Figure 7-1.
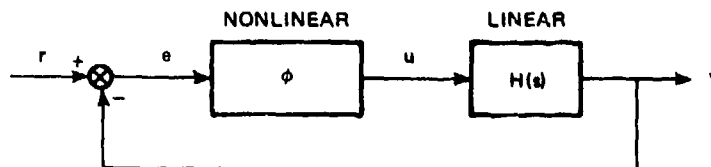

Figure 7-1. A class of nonlinear feedback control systems.

where $H(s)$ is the transfer matrix of a linear subsystem, and ϕ is the characteristic of a nonlinear subsystem. In order to be concise and yet complete, in what follows statements pertaining to asymptotic stability, in contrast to stability alone, are placed in parentheses.

The problem of (asymptotic) <u>absolute stability</u> is that of determining a characterization of (asymptotic) stability for the system of Figure 7-1 where the nonlinear characteristic can be any function ϕ satisfying the sector condition

$$\phi(e)e \;>\; 0, \quad e \neq 0 \tag{7-13}$$

Aizerman and Gantmacher [42] discuss the origin of, and the results pertaining to, this problem. A weaker (integral) form of the sector constraint Eq. (7-13)

$$\int_{0}^{t} \phi(e(\tau))\; e(\tau)\; d\tau \;\geq\; 0 \tag{7-14}$$

defines a larger class of systems. The stability problem corresponding to absolute stability for the constraint Eq. (7-14) has been termed (asymptotic) <u>hyperstability</u> by Popov [43,44].

The principal results to be used subsequently in this section are stated in terms of (strictly) positive real matrices. The mapping

$$s \;\mapsto\; H(s)$$

of the complex plane into a square matrix of complex numbers is <u>(strictly) positive real</u> [45,46] if: (a) the elements of H are analytic functions on the the open (closed) right-half plane, (b) H preserves complex conjugation

7-6

(i.e., $H(\overline{s}) = \overline{H(s)}$), and (c) the Hermitian part of $H(\triangleq \frac{1}{2}(H + H^*))$ is positive
semidefinite (definite) on the open (closed) right-half plane. The superscript
* denotes complex-conjugate transpose. The matrix form of the famous Kalman-
Yakubovich-Popov lemma gives an algebraic characterization of (strictly) posi-
tive real matrices:

Lemma 7-4 [45,47]. Assume that $H(s)$ is the transfer matrix of a linear system
with $H(\infty) = 0$ and having poles only in the left-half plane. Let (A,B,C) be
matrices such that Eq. (7-1) and (7-2) are a minimal state-space realization
of H. Then H is (strictly) positive real if and only if there exist matrices
$Q \geq 0$ $(Q > 0)$, $P > 0$, such that

$$A^*P + PA = -Q \qquad (7-15)$$

and

$$B^TP = C \qquad (7-16)$$

Note that Eq. (7-15) is a Liapunov matrix equation which is outside the scope
of Theorem 7-3 when Q is only semidefinite. Several other forms of this lemma
may be stated when H does not satisfy the assumptions stated here. Finally,
a result of Popov connects the notion of positive realness to hyperstability.

Theorem 7-5 [43,44,46]. The system of Figure 7-1 is (asymptotically) hyper-
stable if the transfer matrix H is (strictly) positive real.

7.2   Technical Approach

The relation between Liapunov stability theory as discussed in
Section 7.1.2.1 and the quadratic cost functional (cf. Section 7.1.2.2) im-
plies that it suffices to establish finiteness of such a cost functional
(under appropriate assumptions on the weighting matrices, such as those fol-
lowing Eq. (7-18)) in order to guarantee stability. We shall thus consider
the difference between the quadratic cost functional associated with a sub-
optimal control, in particular output feedback, and the minimal cost possible
using state feedback.

The performance criterion considered is given by

$$J(x_0, u(\cdot), t_f, t_0) = \int_{t_0}^{t_f} (||x(t)||_Q^2 + ||u(t)||_R^2)\, dt \qquad (7-17)$$

where $x(t)$ is the state vector and $u(t)$ is the input vector, i.e.,

$$\dot{x}(t) = Ax(t) + Bu(t) \quad , \quad x(t_0) = x_0 \qquad (7-18)$$

$$Q = Q^T \geq 0, \quad R = R^T > 0,$$

$$(Q^{1/2}, A) \quad \text{completely observable}$$

7-7

and

$$\|x\|_Q^2 \triangleq x^T Q \, x$$

Thus the quality of a control policy $u(\cdot)$ is evaluated via the penalty

$$J_{pen}(x_0, u(\cdot), t_f, t_0) = J(x_0, u(\cdot), t_f, t_0) - J(x_0, u^*(\cdot), t_f, t_0)$$
(7-19)

where

$$\min J(x_0, u(\cdot), t_f, t_0) = J(x_0, u^*(\cdot), t_f, t_0) \qquad (7-20)$$

Noting that, by the principle of optimality, $\{u^*(\tau), t \leq \tau \leq t_f\}$ depends only on $x(t)$ (and is independent of $x(\tau)$, $\tau < t$), we shall denote by $u^*(x(t))$ the optimal control function.

Analysis of the expression for $J_{pen}(\cdot)$ under the linearity assumption in Eq. (7-18) yields [17]

$$J_{pen}(x_0, u(\cdot), t_f, t_0) = \int_{t_0}^{t_f} \|u(t) - u^*(x(t))\|_R^2 \, dt \qquad (7-21)$$

where $\{u(t), t_0 \leq t \leq t_f\}$ is any control policy and $x(t)$ is the solution of Eq. (7-18) given $\{u(\cdot), t_0 \leq \tau \leq t\}$.

The remarkable expression in Eq. (7-21) is the key to the subsequent analysis.

Remarks

(1) $u^*(x(t))$ mentioned above is actually given by

$$u^*(x(t)) = K^*(t) \cdot x(t)$$

where $K^*(t)$ is the standard optimal state feedback gain.

(2)   The expression in Eq. (7-21) is valid for Q, R, A, B, being time vary-ing as well as for the time-invariant case. For the sake of the present discussion it suffices to consider the time-invariant infinite case (i.e., $t_0 = 0$, $t_f = +\infty$). Then $K^*(t) \equiv K^*$ is constant for all $t \geq 0$.

Turning attention to the stability problem with output feedback, consider

$$u(t) = G \cdot y(t) \qquad (7-22)$$

7-8

where

$$y(t) = C x(t) \qquad (7-23)$$

Combining Eqs. (7-21) to (7-23) under the assumptions noted in Remark 2, yields

$$J_{pen}(x_0, G \cdot y(\cdot)) = \int_0^{+\infty} ||(K^* - GC)x(t)||_R^2 \, dt \qquad (7-24)$$

where

$$\dot{x}(t) = Ax(t) + BGy(t) \qquad (7-25)$$

$$= (A + BGC)x(t) \quad ; \quad x(0) = x_0$$

Note that the dependence of $J_{pen}(\cdot)$ on (t_0, t_f) has been suppressed due to Remark 2.

Thus, to assess the stability of Eq. (7-25), $J_{pen}(\cdot)$ as in Eq. (7-24) must be evaluated. A convenient interpretation of Eq. (7-24) and (7-25) is obtained by rewriting Eq. (7-25) as

$$\dot{x}(t) = (A + BK^*)x(t) + B\overline{u}(t) \qquad (7-25a)$$

$$\overline{y}(t) = (K^* - GC)x(t) \qquad (7-25b)$$

$$\overline{u}(t) = -\overline{y}(t) \qquad (7-25c)$$

and thus the performance penalty is given by

$$J_{pen}(x_0, G \cdot y(\cdot)) = \int_0^{+\infty} ||\overline{y}(t)||_R^2 \, dt \qquad (7-24a)$$

This interpretation is illustrated in Figure 7-2, where the notation

$$A^* \triangleq A + BK^* \qquad (7-25d)$$

has been used. Since the system (7-18) incorporating output feedback (7-22) is asymptotically stable if $J_{pen}(\cdot)$ in Eq. (7-24) is finite, establishing the asymptotic output stability of the system in Eq. (7-25) yields the desired stability result.
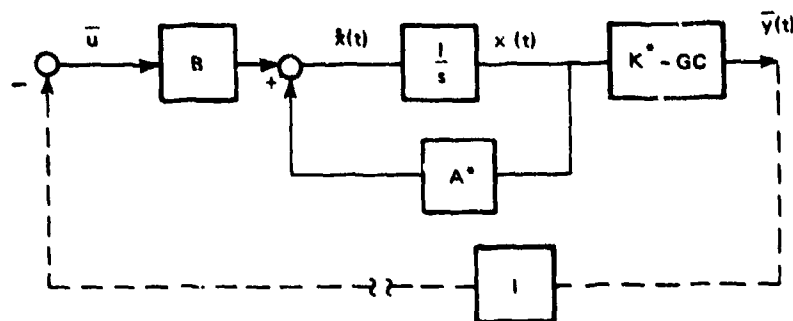
Figure 7-2. Block diagram representation of Eqs. (7-25a) to (7-25d).

To establish the asymptotic stability of the output feedback system
(7-25), i.e., to show that $J_{pen}(x_0, G \cdot y(\cdot)) < \infty$, <u>asymptotic output stability</u>
of the unity feedback configuration of Figure 7-2 must be established.

Since the feedback block (I) satisfies the Popov integral inequality
(Eq. (7-14))

$$\int_{t_1}^{t_2} -\bar{u}^T(t)\bar{y}(t) \, dt \geq 0, \quad -\infty < t_1 \leq t_2 < +\infty \qquad (7-26)$$

hyperstability theory (cf. Section 7.1.2.3) may be employed to assess the
asymptotic output stability of Eqs. (7-25a) to (7-25d).

7.3   Results

A necessary and sufficient condition for a system to be (asymptotically)
hyperstable is that the forward loop is (strictly) positive real (cf. Theorem
7-5). Thus, employing the Kalman-Yakubovich-Popov Lemma (Lemma 7-4) we have:

<u>Theorem 7-6.</u> The control law in Eqs. (7-22) to (7-23) (output feedback) is
asymptotically stable if there exists a symmetric positive-semidefinite
matrix P ($P = P^T \geq 0$) such that

$$(A^*)^T P + P(A^*) \leq 0 \qquad (7-27)$$

$$K^* - GC = B^T P \qquad (7-28)$$

Before proving Theorem 7-6, it merits some discussion.

<u>Remark 3.</u> Theorem 7-6 can be generalized by allowing the identity in the feed-
back loop of Figure 7-2 to be realized in the form I = XYZ, where X, Y, Z are
matrices of appropriate dimensions. Then Eq. (7-28) can be replaced by

$$Z(K^* - GC) = (BX)^T P$$

provided that Y satisfies the Popov inequality (7-26) (e.g., take $Y \geq 0$).

Remark 4. The conditions in Theorem 7-6 are a relaxed version of the Kalman-Yakubovich-Popov Lemma (Lemma 7-4) where strict inequality in Eq. (7-27) may be required and where P has to be positive definite (rather than semi-definite).

Corollary 7-7. Consider the system represented by the triplet (A, B, C) (cf. Eqs. (7-18) and (7-23)). A sufficient condition for (A, B, C) to be output stabilizable is that Eq. (7-27) is a consistent set of equations, where

$$K^* = -R^{-1}B^T P^*$$

$$A^T P^* + P^* A + LL^T - P^* BR^{-1}B^T P^* = 0$$

L is chosen so that (L, A) is a completely observable pair, and $R = R^T > 0$.

Remark 5. The authors believe that the statement in Corollary 7-7 should read "...A necessary and sufficient...", however, a general proof of this conjecture has not yet been established.

Proof of Theorem 7-6

The theorem statement with strict inequality follows trivially from the Kalman-Yakubovich-Popov Lemma. However, considering the case $GC = K^*$, which allows P to be singular in Eq. (7-27), implies that one can relax the strict inequality conditions. To prove the theorem, consider the "Liapunov function"

$$V(x) \triangleq x^T P x$$

where P satisfies Eq. (7-27). Note that $V(x)$ is not a standard Liapunov function since we allow P to be semidefinite (or even $P = 0$). Differentiating $V(x(t))$ subject to Eq. (7-25) and (7-27) yields

$$\dot{V}(x(t)) = x(t)^T[(A^*)^T P + PA^*]x(t) - 2x(t)^T PBB^T P\, x(t)$$

Since we have weak inequalities in the theorem statement, we have $V(x(t)) \geq 0$ and $\dot{V}(x(t)) \leq 0$. Note, however, that if there exists a $\bar{t}$ such that $V(x(\bar{t})) = 0$, the conditions $V \geq 0$ and $\dot{V} \leq 0$ imply that $V(x(t)) \equiv 0$ for all $t \geq \bar{t}$. Furthermore, $V(x(t)) = 0$ only if $Px(t) = 0$ which implies

$$\bar{y}(t) = (K^* - GC)x(t) = B^T P\, x(t) = 0$$

and thus asymptotic output stability of Eq. (7-27) has been established.

Remark 6. Note that the proof relies on an unconventional use of Liapunov stability theory. It might suggest an approach to the extension of this theory.

7.4   Conclusions

An initial step has been taken toward the development of an explicit algebraic characterization of output feedback stabilizability. The principal result is a sufficient condition. The chief open problem is to determine how this condition can be weakened so as to become also a necessary condition. The condition is a set of Kalman-Yakubovich-Popov relations in a special form dictated by the output feedback constraints. Part of this set is a Liapunov matrix equation for which the theory of solution and solution methods are well-known (cf. Section 7.1.2.2). Another open problem is to extend such results so as to apply to the full Kalman-Yakubovich-Popov set. Success in tackling these two open problems would yield a powerful tool for the stability analysis of general output feedback control systems.

Such an explicit characterization of stabilizability can be a very practical tool in controller design. Since the sensor and actuator matrices appear in the Kalman-Yakubovich-Popov equations, the conditions provide a simple means to evaluate alternative sensor and actuator locations from the standpoint of stabilizability. The present results can already be used for this purpose, although the outcome will be conservative.

LIST OF REFERENCES

1. Lin, J.G., Y.H. Lin, D.R. Hegg, T.L. Johnson, and J.E. Keat, "Theory of Design Methods," Interim Technical Report, Actively Controlled Structures Theory, Vol. 1, Charles Stark Draper Laboratory, Cambridge, Mass., Report R-1249, April 1979.

2. Lin, J.G., D.R. Hegg, Y.H. Lin, and J.E. Keat, "Output Feedback Control of Large Space Structures: An Investigation of Four Design Methods," Proceedings of the Second VPI&SU/AIAA Symposium on Dynamics and Control of Large Flexible Spacecraft, Blacksburg, Va., 21-23 June 1979, pp. 1-18.

3. Hegg, D.R., "Extensions of Suboptimal Output Feedback Control with Application to Large Space Structures," Proceedings of the 1980 AIAA Guidance and Control Conference, Danvers, Mass., 11-13 August 1980, pp. 147-153.

4. Lin, Y.H., and J.G. Lin, "An Improved Output Feedback Control of Flexible Large Space Structures," Proceedings of the 19th IEEE Conference on Decision and Control, Albuquerque, NM, 10-12 December 1980, pp. 1248-1250.

5. Liapunov, A.M., "The General Problem of the Stability of Motion," (French translation of the 1893 Russian original), Ann. Fac. Sci. Toulouse, Vol. 9, 1907, pp. 203-474. [Reprinted as Ann. Math. Stud. No. 17, Princeton University Press, New Jersey, 1947.]

6. Canavin, J.R., "The Control of Spacecraft Vibration Using Multivariable Output Feedback," Paper 78-1419, AIAA/AAS Astrodynamics Conference, Palo Alto, CA, 7-9 August 1978.

7. Levine, W.S., and M. Athans, "On the Determination of the Optimal Constant Output Feedback Gains for Linear Multivariable Systems," IEEE Trans. Automatic Control, Vol. AC-15, February 1970, pp. 44-48.

8. Kosut, R.L., "Suboptimal Control of Linear Time-Invariant Systems Subject to Control Structure Constraints," IEEE Trans. Automatic Control, Vol. AC-15, October 1970, pp. 557-563.

9. Nandi, A.K., and J.H. Herzog, "Comments on 'Design of a Single-Input System for Specified Roots Using Output Feedback'," IEEE Trans. Automatic Control, Vol. AC-16, August 1971, pp. 384-385.

10. Li, M.T., "On Output Feedback Stabilizability of Linear Systems," IEEE Trans. Automatic Control, Vol. AC-17, June 1972, pp. 408-410.

11.   Denham, M.J., "Stabilization of Linear Multivariable Systems by Output Feedback," IEEE Trans. Automatic Control, Vol. AC-18, February 1973, pp. 62-63.

12.   Johnson, C.D., "Stabilization of Linear Dynamical Systems with Output Feedback," Paper 29.3, Proceedings of the Fifth IFAC World Congress, Paris, France, 15-17 June 1972.

13.   Anderson, B.D.O, N.K. Bose, and E.I Jury, "Output Feedback Stabilization and Related Problems—Solution via Decision Methods," IEEE Trans. Automatic Control, Vol. AC-20, February 1975, pp. 53-66.

14.   Anderson, B.D.O., and R.W. Scott, "Output Feedback Stabilization—Solution by Algebraic Geometry Methods," Proc. IEEE, Vol. 65, June 1977, pp. 849-861.

15.   Kresselmeier, G., "Stabilization of Linear Systems by Constant Output Feedback Using the Riccati Equation," IEEE Trans. Automatic Control, Vol. AC-20, August 1975, pp. 556-557.

16.   Luus, R., "Solution of Output Feedback Stabilization and Related Problems by Stochastic Optimization," IEEE Trans. Automatic Control, Vol. AC-20, December 1975, pp. 820-821.

17.   Fogel, E., and K. McGill, "Spectral Analysis of Previewing Controllers," IEEE Trans. Automatic Control, Vol. AC-25, October 1980, pp. 959-967.

18.   Kalman, R.E. and J.E. Bertram, "Control System Analysis and Design via the 'Second Method' of Liapunov: I. Continuous-Time Systems," J. Basic Engineering, Vol. 82, June 1960, pp. 371-393.

19.   Kalman, R.E., and J.E. Bertram, "Control System Analysis and Design via the 'Second Method' of Liapunov: II. Discrete-Time Systems," J. Basic Engineering, Vol. 82, June 1960, pp. 394-400.

20.   LaSalle, J. and S. Lefschetz, Stability by Liapunov's Direct Method With Applications, Academic Press, New York, 1961.

21.   Hahn, W., Theory and Application of Liapunov's Direct Method, Prentice-Hall, Englewood Cliffs, New Jersey, 1963.
       [English translation of the 1959 German original].

22.   Lefschetz, S., Stability of Nonlinear Control Systems, Academic Press, New York, 1965.

23.   Barnett, S. and C. Storey, "Some Applications of the Liapunov Matrix Equation," J. Inst. Math. Applications, Vol. 4, March 1968, pp. 33-42.

24.   Taussky, O., "Matrices C with $C^n \to 0$," J. Algebra, Vol. 1, April 1964, pp. 5-10.

25. Sylvester, J.J., "Sur la solution du cas le plus général des équations lineaires en quantités binaires, c'est-a-dire en quaternions ou en matrices du second ordre," C.R. Acad. Sci. Paris, Vol. 22, 1884, pp. 117-118.

26. Bellman, R., "Kronecker Products and the Second Method of Liapunov," Math. Nachr., Vol. 20, May 1959, pp. 17-19.

27. Bellman, R., "Notes on Matrix Theory-X: A Problem in Control," Quart. Appl. Math., Vol. 14, January 1957, pp. 417-419.

28. Givens, W., "Elementary Divisors and Some Properties of the Liapunov Mapping $X \to AX + XA*$," Argonne National Laboratory, Argonne, Ill., Report ANL-6456, November 1961.

29. Snyders, J. and M. Zakai, "On Nonnegative Solutions of the Equation $AD + DA' = -C$," SIAM J. Appl. Math., Vol. 18, May 1970, pp. 704-714.

30. Smith, R.A., "Matrix Calculations for Liapunov Quadratic Forms," J. Differential Equations, Vol. 2, April 1966, pp. 208-217.

31. Ma, E.C., "A Finite Series Solution of the Matrix Equation $AX + XB = C$," SIAM J. Appl. Math., Vol. 14, May 1966, pp. 490-495.

32. Müller, P.C., "Solution of the Matrix Equations $AX + XB = -Q$ and $S^T X + XS = -Q$," SIAM J. Appl. Math. Vol. 18, May 1970, pp. 682-687.

33. Lancaster, P., "Explicit Solutions of Linear Matrix Equations," SIAM Review, Vol. 12, October 1970, pp. 544-566.

34. Hartwig, R.E., "Resultants and the Solution of $AX - XB = -C$," SIAM J. Appl. Math, Vol. 23, July 1972, pp. 104-117.

35. Hagander, P., "Numerical Solution of $A^T S + SA + Q = 0$," Info. Sci., Vol. 4, 1972, pp. 35-50.

36. Pace, I.S., and S. Barnett, "Comparison of Numerical Methods for Solving Liapunov Matrix Equations," Int. J. Control, Vol. 15, May 1972, pp. 907-915.

37. Bartels, R.H. and G.W. Stewart, "Solution of the Matrix Equation $AX + XB = C$," Comm. ACM, Vol. 15, September 1972, pp. 820-826.

38. Klienman, D.L. and P.K. Rao, "Extensions to the Bartels-Stewart Algorithm for Linear Matrix Equations," IEEE Trans. Automatic Control, Vol. AC-23, February 1978, pp. 85-87.

39. Golub, G.H., S. Nash, and C. VanLoan, "A Hessenberg-Schur Method for the Problem $AX + XB = C$," IEEE Trans. Automatic Control, Vol. AC-24, December 1979, pp. 909-913.

40. Belanger, P.R., and T.P. McGillivray, "Computational Experience with the Solution of the Matrix Liapunov Equation," _IEEE Trans. Automatic Control_, Vol. AC-21, October 1976, pp. 799-800.

41. Laub, A.J., "Survey of Computational Methods in Control Theory," in A.M. Erisman et al. (eds.), _Electric Power Problems: The Mathematical Challenge_, SIAM, Philadelphia, 1980, pp. 231-260.

42. Aizerman, M.A., and F.R. Gantmacher, _Absolute Stability of Regulator Systems_, Holden-Day, San Francisco, 1964.

43. Popov, V.M., "The Solution of a New Stability Problem for Controlled Systems," _Automat. Remote Control_, Vol. 24, September 1963, pp. 1-23.

44. Popov, V.M., "Hyperstability and Optimality of Automatic Systems with Several Control Functions," _Rev. Roumaine Sci. Techn. ser. Electrotechn. et Energ._, Vol. 9, No. 4, 1964, pp. 629-690.

45. Anderson, B.D.O., "A System Theory Criterion for Positive Real Matrices," _SIAM J. Control_, Vol. 5, May 1967, pp. 171-182.

46. Anderson, B.D.O., "A Simplified Viewpoint of Hyperstability," _IEEE Trans. Automatic Control_, Vol. AC-13, June 1968, pp. 292-294.

47. Landau, Y.D., _Adaptive Control: The Model Reference Approach_, Dekker, New York, 1979.

SECTION 8

OPTIMAL DISTRIBUTED CONTROL OF A FLEXIBLE
SPACECRAFT DURING A LARGE-ANGLE ROTATIONAL MANEUVER

8.1 Introduction

A problem of current interest is the rotational and configuration control of flexible spacecraft. In particular, we consider here the problem of optimal large-angle single-axis maneuvers with simultaneous vibration suppression when a distributed control system is employed.

The control system being considered is distributed in the sense that control is applied at several either rigid or flexible points on the vehicle's structure.

The motion of the class of vehicles being considered is described by a system of hybrid coordinates. The coordinates are referred to as hybrid, because the vehicle's equations of motion consist of both ordinary and partial differential equations. In the hybrid coordinate formulation, the ordinary differential equations describe discrete coordinates for modeling the rotations and translations of rigid bodies, and the partial differential equations describe distributed or modal coordinates for modeling the deformations of elastic bodies.

The procedure used for analyzing these hybrid systems is a spatial discretization, whereby the partial differential equations are converted into infinite sets of ordinary differential equations. Then, based on some arbitrary combination of control and computational considerations, these infinite sets of ordinary differential equations are truncated for the control law design and subsequent modeling simulations.

At the present time, there are many unresolved issues regarding how the truncation procedure should be carried out. Though interesting as these issues are, they are not considered further in this report.

Mathematically, the spatial discretization procedure [1] is carried out by replacing the deformations of the continuous elastic members by a finite series of known (admissible) space-dependent functions multiplied by time-dependent (to-be-determined) generalized coordinates.

The problem of large-angle maneuvers for both rigid and flexible spacecraft has recently been treated by a number of investigators. In the case of rigid vehicles, Turner and Junkins [2] presented the nonsingular necessary conditions for large-angle three-dimensional maneuvers of asymmetric vehicles. In particular, Turner and Junkins [2] obtained the nonlinear solution by introducing a boundary condition continuation or homotopy method, which reliably solves the resulting two-point boundary-value problem (TPBVP). When flexible vehicles restricted to single-axis maneuvers are considered, a number of investigators working independently have obtained essentially equivalent results for the time-invariant case. For example, Swigert [3] assumed a specialized Fourier series for the unknown control torque, where the coefficients in the

8-1

series are determined by requiring that the following two conditions be satisfied. First, that the integral of the square of the control torque be minimized; and second, that the maneuver satisfy the prescribed terminal boundary conditions for the problem. Markley [4] considered the effects of selecting different performance indices for the problem of controlling a flexible body modeled with a single flexible mode. Breakwell [5] addressed the problem of controlling several flexible modes and presented results for a feedback control system, as well as reporting on experimental verification of the resulting control law formulation. Alfriend, Longman, and Bercaw [6] considered a frequency response interpretation of optimal slewing maneuvers. Turner and Junkins [7] presented results for controlling several flexible modes for both linear and nonlinear formulations of the equations of motion. In particular, Turner and Junkins [7] introduced a differential equation continuation or homotopy method for reliably solving the resulting nonlinear TPBVP. As a further development of References [2,7], the authors present herein the necessary extensions when a distributed control system is employed in the flexible body case.

The specific model considered (see Figure 8-1) consists of a rigid hub with four identical elastic appendages attached symmetrically about the central hub. We consider only the case of a single-axis maneuver with the flexible members restricted to displacements in the plane normal to the axis of rotation. Furthermore, we make the assumption that the body (as a whole) experiences only antisymmetric deformation modes (see Figure 8-2). The control system for the vehicle is taken to consist of a single controller in the rigid part of the structure; in addition each elastic appendage is assumed to have one controller located half way along its span*. The extension to the case of multiple controllers along each appendage is straightforward; however, only the single appendage controller case is presented in this report.

The necessary conditions for the optimal single-axis maneuver are presented in two parts. The first part (Sections 8-2 through 8-4) consists of the formulation and solution of the linearized equations. The second part (Section 8-5) consists of presenting the nonlinear equations where the to-be-specified nonlinearity is both kinematic and structural in nature. In Section 8-6 a differential equation continuation method is presented for solving the nonlinear TPBVP, which makes efficient use of the initial costates determined in Section 8-4. In Section 8-7 we provide numerical results which support the validity and utility of the formulations described herein.

8.2   Equations of Motion

For the vehicle being considered, the equations of motion can be obtained from Hamilton's extended principle [8].

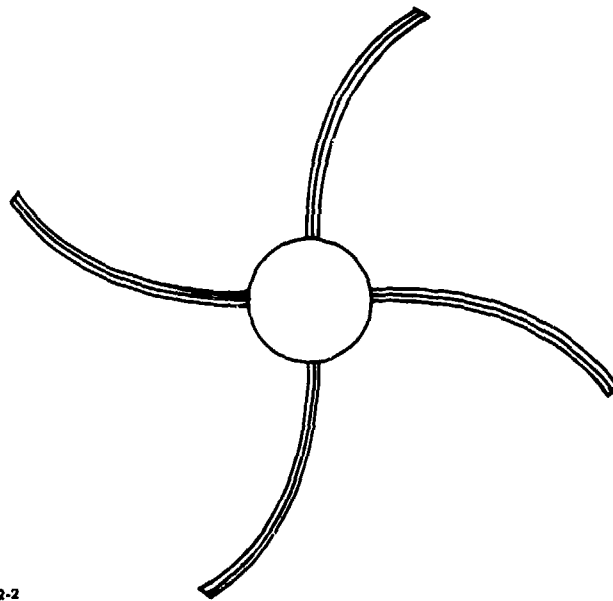$$\int_{t_1}^{t_2} (\delta L + \delta w) \, dt = 0 \qquad (8-1)$$

---

* For any real system application an optimization should be performed in order to locate the appendage control subject to enhancing the vehicle's controlled performance.
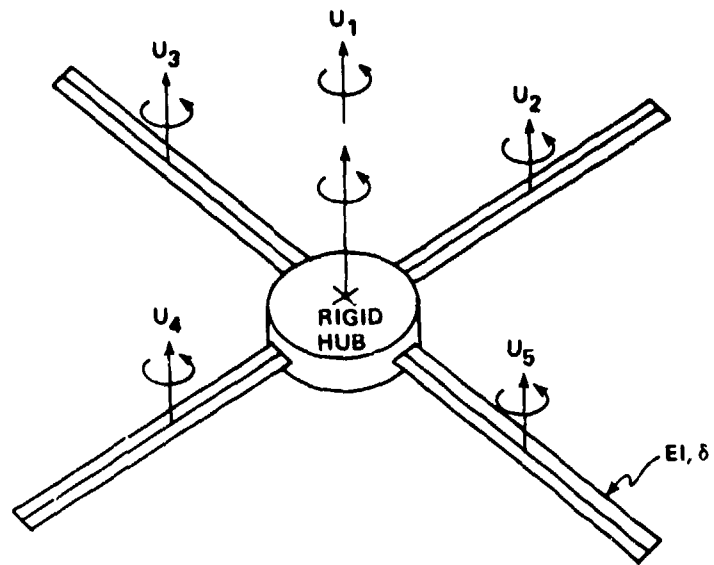
$\{U_1, U_2, \ldots, U_5\} \equiv$ **SET OF DISTRIBUTED CONTROL TORQUES**

Figure 8-1.   Undeformed structure.

8104M232-2

Figure 8-2.   Antisymmetric deformation.

subject to

$$\delta\theta = \delta u = 0 \text{ at } t_1, t_2$$

where $L = T - V$ is the system Lagrangian, δw represents the virtual work, $\delta\theta$ represents a virtual rotation and δu represents a virtual elastic displacement.

The kinetic and potential energy expressions for the vehicle can be shown to be

$$T = \frac{1}{2}\dot{\theta}^2\left[\hat{I} + 4\int_r^{r+L}(u^2 - P^2)\,dm\right] + 2\int_r^{r+L}\dot{u}^2\,dm + 4\dot{\theta}\int_r^{r+L}x\dot{u}\,dm \qquad (8-2)$$

$$P^2 = \frac{1}{2}\left[(r + L)^2 - r^2 - x^2\right]\left(\frac{\partial u}{\partial x}\right)^2$$

$$V = 2\int_r^{r+L}EI\left[\frac{\partial^2 u}{\partial x^2}\right]^2\,dx \qquad (8-3)$$

where $\hat{I}$ denotes the moment of inertia of the undeformed vehicle about the axis of rotation, r denotes the radius of the rigid hub, L denotes the undeformed length of the elastic appendages, P^2 denotes a first order correction for arc length along an appendage, and EI denotes the flexural rigidity of each of the appendages.

The virtual work in this example can be shown to be

$$\delta w = \sum_{k=1}^{n^*} Q_k \delta q_k \quad (n^* = \text{number of generalized coordinates}) \qquad (8-4)$$

where

$$Q_k = \underline{f} \cdot \frac{\partial \dot{\underline{R}}}{\partial \dot{q}_k} + \frac{\partial \underline{\omega}}{\partial \dot{q}_k} \cdot \left[\int_v \underline{r} \times d\underline{f} + \int_v \underline{u} \times d\underline{f}\right] + \int_v \frac{\partial \dot{\underline{u}}}{\partial \dot{q}_k} \cdot d\underline{f} \qquad (8-5)$$

and Q_k denotes the kth generalized force; q_k denotes the kth generalized coordinate, $\underline{R}$ denotes the vector locating the mass center of the vehicle relative to inertial space; $\underline{\omega}$ denotes the inertial angular velocity of the vehicle, $\underline{r}$ denotes the vector locating differential mass elements in the undeformed vehicle; $\underline{u}$ denotes an elastic deflection, v denotes that the integration is taken over the entire vehicle; a dot over the vector $\underline{R}$ or a scalar q_k denotes

differentiation with respect to time in the inertial frame; an open dot over a vector $\underline{u}$ denotes differentiation with respect to time in the frame fixed in the rigid hub; $d\underline{f}$ denotes the differential resultant force acting at some point in the vehicle, and $\underline{f}$ is given by

$$\underline{f} = \int_V d\underline{f} \tag{8-6}$$

Before applying Hamilton's extended principle, we express (by the assumed modes method [1]) the elastic displacements as the following series:

$$\underline{u} = \begin{Bmatrix} 0 \\ u \\ 0 \end{Bmatrix} \quad , \quad u = \sum_{k=1}^{n} \eta_k(t) \, \phi_k(x-r) \tag{8-7}$$

where $\eta_k(t)$ represents the kth time-varying amplitude, $\phi_k(x-r)$ represents the kth assumed admissable mode shape (in this instance a comparison function), and n represents the number of terms used in the approximation.

On introducing Eq. (8-7) into (8-2) and (8-3), we obtain for the system Lagrangian

$$L = \frac{\hat{I}}{2} \dot{\theta}^2 + \frac{1}{2} \underline{\dot{\eta}}^T M_{\eta\eta} \underline{\dot{\eta}} + \dot{\theta} \underline{\dot{\eta}}^T \underline{M}_{\theta\eta}$$

$$- \frac{1}{2} \dot{\theta}^2 \underline{\eta}^T \Big[M - M_{\eta\eta} \Big] \underline{\eta} - \frac{1}{2} \underline{\eta}^T K_{\eta\eta} \underline{\eta} \tag{8-8}$$

where

$$\underline{\eta} = [\eta_1, \eta_2, \ldots, \eta_n]^T$$

$$[M_{\eta\eta}]_{kp} = 4 \int_r^{r+L} \phi_k(x-r) \, \phi_p(x-r) \, dm \qquad (n \times n)$$

$$[\underline{M}_{\theta\eta}]_k = 4 \int_r^{r+L} x\phi_k(x-r) \, dm \qquad (n \times 1)$$

$$[M]_{kp} = 4 \int_r^{r+L} \frac{1}{2} \left[(r+L)^2 - r^2 - x^2 \right] \phi_k'(x-r) \, \phi_p'(x-r) \, dm$$

$$(n \times n)$$

8-5

$$[K_{nn}]_{kp} = 4 \int_r^{r+L} EI\phi_k''(x-r)\,\phi_p''(x-r)\,dx \qquad (n \times n)$$

$$(\ )' \equiv \frac{d}{dx}(\ ), \quad (\ )'' \equiv \frac{d^2}{dx^2}(\ )$$

On introducing Eq. (8-7) into Eq. (8-5), we find for Q_k

$$Q_1 = u_1 \quad \text{(Rigid Body Torque)} \qquad (8-9)$$

$$Q_{k+1} = 4\phi_k'(x_p - r)u_2 \quad \text{(Elastic Appendage Torque)} \qquad (8-10)$$

where x_p is the coordinate locating the point of application of the control torque on the elastic appendage. Equation (8-10) is obtained in the following way: first, the control torque acting on an elastic appendage is replaced by an equivalent couple*; and second, a limiting process is carried out** which leads directly to Eq. (8-10).

Substituting Eq. (8-8, 8-9, and 8-10) into Eq. (8-1) yields Lagrange's equations

$$\frac{d}{dt}\left(\frac{\partial L}{\partial \dot{\theta}}\right) - \frac{\partial L}{\partial \theta} = u_1 \qquad (8-11)$$

$$\frac{d}{dt}\left(\frac{\partial L}{\partial \underline{\dot{n}}}\right) - \frac{\partial L}{\partial \underline{n}} = \underline{F}u_2 \qquad (8-12)$$

---

* Two forces $\underline{F}$ and $-\underline{F}$, having the same magnitude, parallel lines of action, and opposite sense are said to form a couple.

** The limiting process is carried out by requiring the lever arms and forces of the couple to assume values such that

$$u_2 = \underset{\substack{|\underline{r}| \to 0 \\ |\underline{F}| \to \infty}}{\text{limit}} |\underline{r} \times \underline{F} + (-\underline{r}) \times (-\underline{F})|$$

where $\underline{r}$ is the vector connecting the couple forces, $\underline{F}$, to the point of application of control and $|\ |$ is the standard vector norm. In particular $\underline{F}$ is taken to be

$$\underline{F} = F\delta(\underline{x} - \underline{x}_p - \underline{r}), \quad -\underline{F} = -F\delta(\underline{x} - \underline{x}_p + \underline{r})$$

where F is the magnitude of the force and $\delta(\underline{x} - \underline{x}_p + \underline{r})$ is a three-dimensional Delta function.

where

$$\underline{F} = 4[\phi_1'(x_p - r) \; \phi_2'(x_p - r) \; \dots \; \phi_n'(x_p - r)]^T$$

From which the equations of motion follows as

$$(\hat{I} - \underline{n}^T M^* \underline{n})\ddot{\theta} + \underline{M}_{\theta n}^T \ddot{\underline{n}} - 2\dot{\theta}\dot{\underline{n}}^T M^* \underline{n} = u_1 \tag{8-13}$$

$$\underline{M}_{\theta n}\ddot{\theta} + M_{nn}\ddot{\underline{n}} + [K_{nn} + \dot{\theta}^2 M^*]\underline{n} = \underline{F}u_2 \tag{8-14}$$

where

$$M^* = M - M_{\eta\eta}$$

8.3 State Space Formulation

The state space form of Eq. (8-13) and (8-14) is obtained by carrying out the following steps: first, we recall the small deflection assumption which permits the quadratic deflection terms in Eq. (8-13) to be dropped. Second, we ignore (for the moment) the $\dot{\theta}^2$ term in Eq. (8-14) yielding linear time-invariant equations. Then Eq. (8-13) and (8-14) can be cast in the linear matrix form

$$M\ddot{\underline{\zeta}} + K\underline{\zeta} = Pu \tag{8-15}$$

where

$$\underline{\zeta} = \left\{ \frac{\theta}{\underline{n}} \right\} \quad M = \begin{bmatrix} \hat{I} & M_{\theta n}^T \\ \underline{M}_{\theta n} & M_{nn} \end{bmatrix} \quad K = \begin{bmatrix} 0 & \underline{0}^T \\ \underline{0} & K_{nn} \end{bmatrix}$$

$$P = \begin{bmatrix} 1 & 0 \\ \underline{0} & \underline{F} \end{bmatrix} \quad \underline{u} = [u_1 u_2]^T$$

and $M = M^T$ (positive definite), $K = K^T$ (positive semidefinite).

Equation (8-15) can be written in uncoupled form by introducing the coordinate transformation

$$\underline{\zeta} = E\underline{z} \tag{8-16}$$

8-7

where E is the matrix of normalized* eigenvectors for the generalized eigen-value problem

$$\lambda_r^2 M \underline{e}_r \;=\; K \underline{e}_r \quad (\lambda_r^2 = \text{eigenvalue},$$

$$\underline{e}_r = \text{eigenvector}) \tag{8-17}$$

On introducing Eq. (8-16) into (8-15) and premultiplying the resulting equation by E^T and recalling the normalization for E, the equation of motion becomes

$$\ddot{\underline{t}} + \Delta \underline{t} \;=\; V \underline{u} \quad , \quad V = E^T P \tag{8-18}$$

Defining the state variable subsets

$$\underline{s}_1 = \underline{t} \qquad \underline{s}_2 = \dot{\underline{t}} \tag{8-19}$$

leads to the first-order differential equations

$$\dot{\underline{s}}_1 = \underline{s}_2 \qquad \dot{\underline{s}}_2 = -\Delta \underline{s}_1 + V \underline{u} \tag{8-20}$$

Letting $\underline{s} = [\underline{s}_1^T \; \underline{s}_2^T]^T$, the state space equation becomes

$$\dot{\underline{s}} \;=\; A \underline{s} + Bu \tag{8-21}$$

where

$$A \;=\; \begin{bmatrix} 0 & I \\ -\Delta & 0 \end{bmatrix} \qquad B \;=\; \begin{bmatrix} 0 \\ V \end{bmatrix}$$

8.4   Optimal Control Problem

8.4.1   Statement of Problem

We consider here the rotational dynamics of a flexible space vehicle restricted to a single-axis large-angle maneuver, where the system dynamics is governed by Eq. (8-20). In particular, we seek a solution of Eq. (8-20) satisfying the prescribed terminal states

---

* The matrix of eigenvectors, E, is normalized as follows:

$$E^T M E \;=\; I$$

leading to

$$E^T K E \;=\; \Lambda \;=\; \text{diag} \,(\lambda_1^2, \, \ldots, \, \lambda_N^2), \; (N = n + 1)$$

$$\underline{\zeta}_0 = \left[\theta_0 \underline{n}^T(t_0)\right]^T \qquad \underline{\dot{\zeta}}_0 = \left[\dot{\theta}_0 \underline{n}^T(t_0)\right]^T \qquad (8\text{-}22a)$$

and

$$\underline{\zeta}_f = \left[\theta_f \underline{n}^T(t_f)\right]^T \qquad \underline{\dot{\zeta}}_f = \left[\dot{\theta}_f \underline{n}^T(t_f)\right]^T \qquad (8\text{-}22b)$$

where we impose the requirements that $\underline{n}(t_f) \equiv \underline{\dot{n}}(t_f) = \underline{o}$ on the right side of Eq. (8-22b) at the final time. Moreover, we seek torque history $\underline{u}(t)$ generating an optimal solution of Eq. (8-20) initiating at Eq. (8-22a) and terminating at Eq. (8-22b) which minimizes the performance index

$$J = \frac{1}{2} \int_{t_0}^{t_f} \left[\underline{u}^T W_{uu}\underline{u} + \underline{s}^T W_{ss}\underline{s}\right] dt \qquad (8\text{-}23)$$

where W_{uu} is a weight matrix on the control and W_{ss} is a weight matrix for the state variables. In particular, if W_{ss} and W_{uu} are selected to have a block diagonal structure, then Eq. (8-23) can be interpreted as seeking a solution which is proportional to the problem of minimum control effort, minimum kinetic energy, and minimum elastic potential energy. The selection of Eq. (8-23) has been made for convenience, though it is recognized that many other reasonable performance indices are possible (e.g., see References [9-13]). Moreover, it is recognized that the particular performance index selected can significantly effect the computational effort required and the resulting maneuvers. In fact, we have found that the numerical values selected for W_{uu} and W_{ss} in Eq. (8-23) must be adjusted according to how many elastic modes are retained in Eq. (8-20), in order for satisfactory solutions to be obtained. The particular weighting scheme used is discussed in Section 8-7.

8.4.2 Derivation of Necessary Conditions from Pontryagin's Principle

In preparing to make use of Pontryagin's necessary conditions, we introduce the Hamiltonian functional

$$H = \frac{1}{2}(\underline{u}^T W_{uu}\underline{u} + \underline{s}^T W_{ss}\underline{s}) + \underline{\lambda}^T(A\underline{s} + B\underline{u}) \qquad (8\text{-}24)$$

where the λ's are Lagrange multipliers (also known as costate or adjoint variables). Pontryagin's principle requires as necessary conditions that the λ's satisfy costate differential equations derivable from

$$\underline{\dot{\lambda}} = -\frac{\partial H}{\partial \underline{s}} = -W_{ss}\underline{s} - A^T\underline{\lambda} \qquad (8\text{-}25)$$

and that the control torque $\underline{u}$ must be chosen at every instant so that the Hamiltonian of Eq. (8-25) is minimized; that is, for $\underline{u}$ continuous we require

$$\frac{\partial H}{\partial \underline{u}} = \underline{0} = W_{uu}\underline{u} + B^T\underline{\lambda} \tag{8-26}$$

from which the optimal torque is determined as a function of the costate variables as

$$\underline{u} = -W_{uu}^{-1}B^T\underline{\lambda} \tag{8-27}$$

The state and costate differential equations are summarized as:

State Equations (from introducing Eq. (8-27) into (8-21))

$$\underline{\dot{s}} = A\underline{s} - BW_{uu}^{-1}B^T\underline{\lambda} \tag{8-28a}$$

Costate Equations (from Eq. (8-25))

$$\underline{\dot{\lambda}} = -W_{ss}\underline{s} - A^T\underline{\lambda} \tag{8-28b}$$

8.4.3 Solution for the Initial Costates

We observe in Eq. (8-28) that the boundary conditions for $\underline{s}$ are known both initially and finally, whereas all boundary conditions for $\underline{\lambda}$ are unknown. Thus, application of Pontryagin's principle has led, as usual, to a TPBVP. In order to obtain the solution for Eq. (8-28) we first write the merged state vector

$$\underline{X} = [\underline{s}^T \; \underline{\lambda}^T]^T \tag{8-29}$$

so that Eq. (8-28) becomes

$$\underline{\dot{X}} = \Omega\underline{X} \tag{8-30}$$

where

$$\Omega = \begin{bmatrix} A & -BW_{uu}^{-1}B^T \\ \\ -W_{ss} & -A^T \end{bmatrix} = \text{constant coefficient matrix}$$

Since Ω is constant, it is well known that Eq. (8-30) possesses the solution

$$\underline{X}(t) = e^{\Omega(t-t_o)}\underline{X}(t_o) \tag{8-31}$$

where $e^{\Omega t}$ is the 4N by 4N exponential matrix.

8-10

The solution for $e^{\Omega t}$ is conveniently obtained by a variety of methods (cf e.g., Moler and Loan [14] and Ward [15]). For the application at hand we select either eigenvector methods or special series approximations (e.g., diagonal Pade approximations) which are used in conjunction with the identity

$$e^{\Omega t} = \left(e^{\Omega t/2^n}\right)^{2^{n*}}$$ (8-32)

leading to computationally efficient algorithms. On setting $e^{\Omega t} = \phi(t, t_o)$ and writing out Eq. (8-31) in partitioned form, we obtain

$$\begin{Bmatrix} \underline{s}(t_f) \\ \underline{\lambda}(t_f) \end{Bmatrix} = \begin{bmatrix} \phi_{ss} & \phi_{s\lambda} \\ \phi_{\lambda s} & \phi_{\lambda\lambda} \end{bmatrix} \begin{Bmatrix} \underline{s}(0) \\ \underline{\lambda}(0) \end{Bmatrix}$$ (8-33)

and upon carrying out the partitioned matrix multiplication, we find for $\underline{s}(t_f)$

$$\underline{s}(t_f) = \phi_{ss}\underline{s}(0) + \phi_{s\lambda}\underline{\lambda}(0)$$ (8-34)

which can be solved for $\underline{\lambda}(0)$ as

$$\phi_{s\lambda}\underline{\lambda}(0) = \underline{s}(t_f) - \phi_{ss}\underline{s}(0)$$ (8-35)

Equation (8-35) is in the standard form for the linear algebraic equation $A\underline{x} = \underline{b}$, which can be solved via Gaussian elimination for $\underline{x}$ (thereby avoiding the computation of the explicit inverse of $\phi_{s\lambda}$).

Equations (8-35) and (8-31) comprise the complete solution of Eq. (8-28). If some of the elements of $e^{\Omega t}$ become so large that numerical precision is lost in the solution for $\lambda(0)$, then the solution process outlined above will fail. The reason numerical difficulties can arise in the solution for $\lambda(0)$ can be traced to the fact that the TPBVP defined by the differential equation in Eq. (8-31) is stiff; in the sense, that some solutions increase and others decrease rapidly as the independent variable changes. If the solution for $\lambda(0)$ fails, there are two courses of action one can take. First, the time interval for the maneuver can be shortened; thus, decreasing the growth in the elements of $e^{\Omega t}$. Second, one can elect to convert the TPBVP into a multipoint boundary-value problem by introducing several intermediate times

$$t_o < t_1 < t_2 < \ldots < t_m < t_f$$ (8-36)

The motivation for introducing these intermediate times t_k ($k = 1, \ldots, m$),

---

* n is the smallest integer such that max $||\Omega t||/2^n < 1$, where $||\Omega t||$ is a suitable matrix norm.

is to limit the growth in the elements of $e^{\Omega(t_k - t_{k-1})}$ in the kth time interval. Then assuming that some scheme can be provided for specifying the initial boundary conditions at the intermediate times, the idea is to patch all the solutions together, thereby obtaining the solution over the time interval of interest. Since the mechanics of how the scheme outlined above would work deviates from the main topic of this report, this subject will not be considered further. Instead, it is assumed in the remainder of this report that the manuevers of interest can be obtained by decreasing the overall maneuver time interval $(t - t_o)$, should computational difficulties be encountered.

We are now interested in solving a problem of the same structure, but including the previously neglected kinematic nonlinearity. The idea is to use the solution to Eq. (8-35) as starting iteratives for a continuation or homotopy chain method, which will solve this related nonlinear problem.

8.5   Optimal Control Problem Including Kinematic Nonlinearities

Due to the similarity in structure with the presentation in Section 8.4, only key equations are given.

The uncoupled equation of motion (corresponding to Eq. (8-18)) is

$$\ddot{\underline{t}} + \Lambda\underline{t} = V\underline{u} - \alpha(\underline{V}^T\dot{\underline{t}})^2 L\underline{t} \tag{8-37}$$

where

$$\dot{\omega} = \underline{V}^T\dot{\underline{t}} \qquad L = E^T \begin{bmatrix} 0 & \underline{0}^T \\ \underline{0} & M^* \end{bmatrix} E$$

$$V = E^T[1 \ \underline{0}^T]^T = [E_{11}E_{12} \ \cdots \ E_{1N}]^T \qquad (N = n + 1)$$

and α is the continuation or homotopy chain parameter. Defining the state vector as in Eq. (8-20) leads to the nonlinear state equation

$$\dot{\underline{s}} = A(\underline{s})\underline{s} + B\underline{u} \tag{8-38}$$

$$A(\underline{s}) = \begin{bmatrix} 0 & 1 \\ A_{21}(s) & 0 \end{bmatrix} \quad , \quad A_{21}(\underline{s}) = -\Lambda - \alpha(\underline{V}^T\underline{s}_2)^2 L$$

Defining the optimal control problem as in Section 8.4.1 leads to state and costate differential equations which are summarized as:

State equations

$$\dot{\underline{s}} = A(\underline{s})\underline{s} - BW_{uu}^{-1}B^T\underline{\lambda} \qquad (8\text{-}39a)$$

Costate equations

$$\dot{\underline{\lambda}} = -W_{ss}\underline{s} - C(\underline{s})\underline{\lambda} \qquad (8\text{-}39b)$$

where

$$C(\underline{s}) = \begin{bmatrix} 0 & A_{21}^T(\underline{s}) \\ I & -2\alpha(\underline{V}^T\underline{s}_2)\underline{Vs}_1^T L^T \end{bmatrix}$$

8.6 Continuation Method for the Solution of the Nonlinear TPBVP

The motivation for introducing the parameter α in Eq. (8-37) comes about from a simple observation. That is, if it is very difficult to obtain a solution for the operator equation

$$\underline{f}(\underline{x}) = \underline{0} \qquad (8\text{-}40)$$

directly, then the numerical solution of Eq. (8-40) can frequency be directly obtained by solving the family of problems

$$\underline{F}(\underline{x}, \alpha) = \underline{0} \qquad (8\text{-}41)$$

where α is a parameter which varies from 0 to 1.

The family $\underline{F}(\underline{x}, \alpha)$ is chosen so that (i) $\underline{F}(\underline{x}, 1) \equiv \underline{f}(\underline{x})$, (ii) $\underline{x}_0$ is an easily calculated (unique) soluton of $\underline{F}(\underline{x}, 0) = \underline{0}$, and (iii) $\underline{F}(\underline{x}, \alpha)$ is a continuous function of α. The solution process proceeds as follows. We introduce the sequence of parameter values

$$0 = \alpha_o < \alpha_1 < \alpha_2 < \ldots < \alpha_p = 1 \qquad (8\text{-}42)$$

where the value of p is either pre-set or determined during the iterative process as discussed in Schmidt [16] and Deuflhard, Pesch and Rentrap[17]. The solution $\underline{x}_{i+1}$ of

$$\underline{F}(\underline{x}, \alpha_{i+1}) = 0 \qquad (8\text{-}43)$$

is obtained by an iterative method (e.g., Quasi-Newton methods as described in Dennis and Schnabel [18], Greenstadt [19], and Golafarb [20]) since $\underline{F}$ is, in general, nonlinear. The starting estimates for $\underline{x}_{i+1}$ are obtained in one of the

two following ways. First, we could use the previous converged value of $\underline{x}_j$; or second, we could use an extrapolated value for $\underline{x}_{i+1}$ based on the converged $\underline{x}_i$ behavior for back α values. Based on our own numerical experiments, we have found that using the second method above accelerates convergence in the solution for $\underline{x}_{i+1}$, and the method works both efficiently and reliably.

On making the identification for $\underline{F}$ in Eq. (8-39) and (8-41), we find

$$\underline{F}(\underline{s}, \underline{\lambda}, \alpha) = \begin{Bmatrix} \underline{\dot{s}} - A(\underline{s})\underline{s} + BW_{uu}^{-1}B^T\underline{\lambda} \\ \underline{\dot{\lambda}} + W_{ss}\underline{s} + C(\underline{s})\underline{\lambda} \\ \underline{s}_f - \underline{s}(\underline{s}(0), \underline{\lambda}(0), t_f) \end{Bmatrix} = \begin{Bmatrix} \underline{0} \\ \underline{0} \\ \underline{0} \end{Bmatrix} \qquad (8-44)$$

In addition we recall that $\underline{s}(0)$ is given and $\underline{\lambda}(0)$ is provided by Eq. (8-35) for $\alpha = 0$. Hence, in Eq. (8-44) the operator equation to be satisfied consists of the state and costate differential equations, as well as terminal constraints on the final values of the state. These observations thus motivate the following successive approximation strategy for solving the nonlinear TPBVP, for homotopy chain parameters $\alpha_k (k = 1, \dots p)$.

Letting the approximate initial costates be denoted by

$$\hat{\underline{\lambda}}_o = \underline{\lambda}(t_o) \qquad (8-45)$$

the differential correction strategy is to seek the correction vector $\Delta\underline{\lambda}$ subject to the terminal constraint

$$\underline{s}_f - \underline{s}(\hat{\underline{\lambda}}_o + \Delta\underline{\lambda}, t_f) = \underline{0} \qquad (8-46)$$

where $\underline{s}_f$ denotes the vector of desired terminal boundary conditions for the variable $\underline{s}$.

On linearizing Eq. (8-46), we obtain

$$\underline{s}_f - \hat{\underline{s}} - A_{s\lambda}\Delta\underline{\lambda} = \underline{0} \qquad (8-47)$$

where $\hat{\underline{s}}$ denotes the numerically integrated solution of Eq. (8-39a), using as initial conditions $\underline{s}(t_o)$ and the approximate costate $\hat{\underline{\lambda}}_o$, and

$$A_{s\lambda} = \left[\frac{\partial \underline{s}^T}{\partial \underline{\lambda}_o} \Big|_{t_f} \right]^T = \phi_{s\lambda} \qquad (8-48)$$

where $\phi_{s\lambda}$ denotes the block of state transition matrix for the variables $\underline{s}$ and $\underline{\lambda}$. Next, defining

$$\Delta\underline{s}_f = \underline{s}_f - \hat{\underline{s}} \qquad (8\text{-}49)$$

and introducing Eq. (8-49) into (8-47) yields

$$\Delta\underline{s}_f = \phi_{s\lambda}\Delta\underline{\lambda} \qquad (8\text{-}50)$$

The solution for Eq. (8-50) is easily obtained by using a standard linear equation solver. As in the solution for Eq. (8-35) we wish to avoid algorithms requiring the explicit inverse of $\phi_{s\lambda}$. The calculation of the required partial derivatives for the nonlinear problem is a separate issue, dealt with in Appendix A.

The previous discussion can all be summarized as the differential correction algorithm in Figure 8-3 for refining given approximate initial co-states $\hat{\underline{\lambda}}_0$; by these means, a precise solution for the TPBVP can be obtained (provided the starting estimates are "sufficiently good").

The only significant assumption en route to the algorithm is the local linearization of Eq. (8-46) to obtain (8-47). The only open question remaining about the algorithm is: How to choose the sequence of α values? Clearly, this process could be made adaptive; however, in the example maneuvers the first author has previously considered, the following pre-set sequence has proven successful

$$\alpha_1 = 0.001 \quad \alpha_2 = 0.01 \quad \alpha_3 = 0.5 \quad \alpha_4 = 0.75 \quad \alpha_5 = 1.0$$

$$(8\text{-}51)$$

Using the sequence of α values given in Eq. (8-51), the algorithm in Figure 8-3 for each α_k, is integrated using converged costate extrapolations as starting estimates.

Locally singular situations and bifurcations appear possible, where the solution for $\Delta\underline{s}$ in Eq. (8-50) would fail due to a rank deficiency in $\phi_{s\lambda}$. In the numerical tests performed to date, no singularities have been encountered in the antisymmetric class of maneuvers. A more troublesome issue is the expense associated with the calculation of the required state transition matrix. Numerical integration of Eq. (A-8) is reliable and required for the nonlinear problem, but expensive. The solution obtained for $\phi(t,to)$, using eigenvalue-vector or series approximations is much less expensive, though limited to the time-invariant case presented in Section 8.4.

8.7   Applications to Example Maneuvers

Several example maneuvers have been determined using the above formulations. For all cases, we have assumed the geometry of Figure 8-1 with the following configuration parameters: the inertia of the undeformed structure
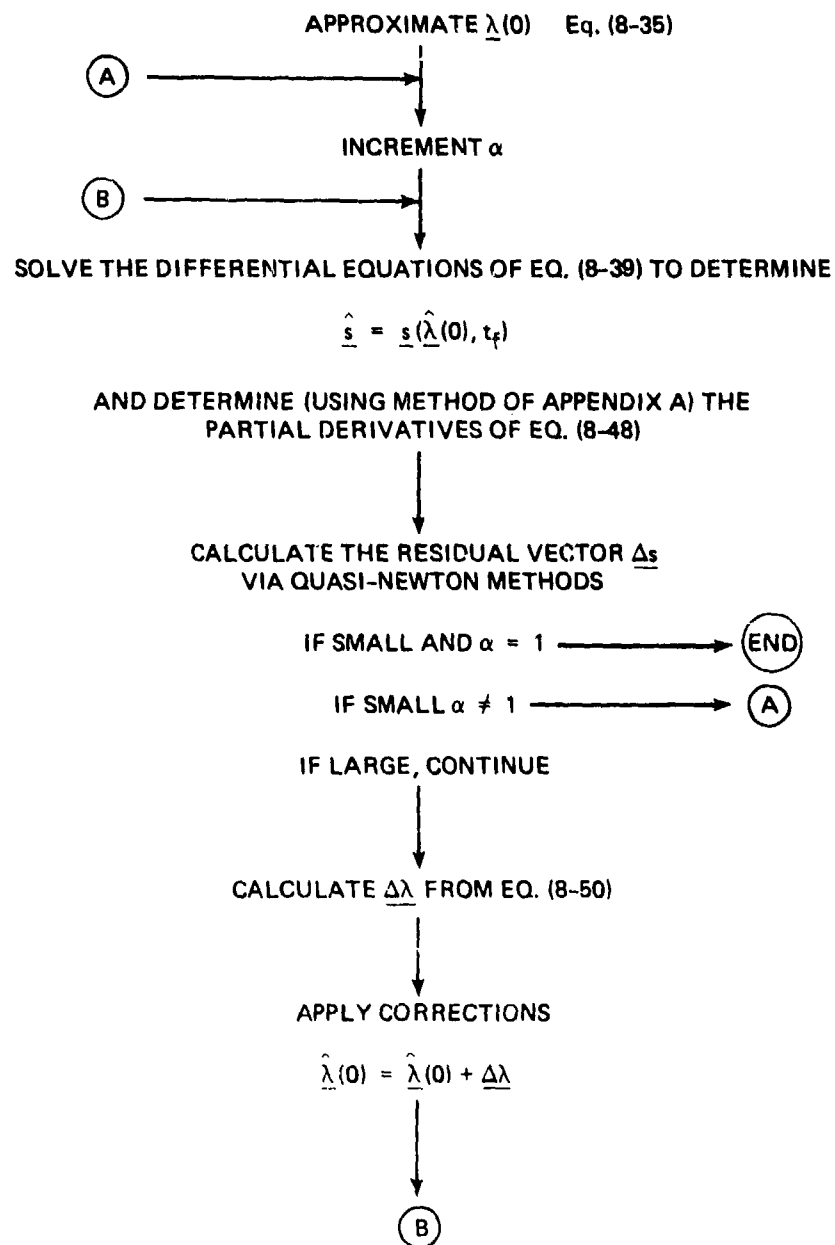
GIVEN: $\underline{s}(0)$, $\underline{s}(t_f)$

APPROXIMATE $\underline{\lambda}(0)$ Eq. (8-35)

(A) ⟶

INCREMENT α

(B) ⟶

SOLVE THE DIFFERENTIAL EQUATIONS OF EQ. (8-39) TO DETERMINE

$$\hat{\underline{s}} = \underline{s}(\hat{\underline{\lambda}}(0), t_f)$$

AND DETERMINE (USING METHOD OF APPENDIX A) THE
PARTIAL DERIVATIVES OF EQ. (8-48)

CALCULATE THE RESIDUAL VECTOR $\underline{\Delta s}$
VIA QUASI-NEWTON METHODS

IF SMALL AND $\alpha = 1$ ⟶ (END)

IF SMALL $\alpha \neq 1$ ⟶ (A)

IF LARGE, CONTINUE

CALCULATE $\underline{\Delta \lambda}$ FROM EQ. (8-50)

APPLY CORRECTIONS

$$\hat{\underline{\lambda}}(0) = \hat{\underline{\lambda}}(0) + \underline{\Delta \lambda}$$

(B)

Figure 8-3.   Differential correction algorithm for the single-axis problem.

$\hat{I}$, is 7000 kg-m^2; the mass/unit length of the four identical elastic appendages, ρ, is 0.004 kg/m; the length of each cantilevered appendage, L, is 150m; the flexural rigidity of the cantilevered appendages, EI, is 1500 kg-m^3/s^2 for cases 2-4 (Table 8-1); and the radius of the rigid hub, r, is 1m. In the integrations over the mass stiffness distributions, the radius of the hub is not neglected in comparison to the appendage length. In Eq. (8-8) we have adopted as assumed modes the comparison functions

$$\phi_p(x - r) = 1 - \cos \frac{p\pi(x - r)}{L} + \frac{1}{2}(-1)^{p+1} \left(\frac{p\pi(x - r)}{L}\right)^2 \quad (p = 1, 2, \ldots, \infty)$$

(8-52)

which satisfy the geometric and physical boundary condtions

$$\phi_p\bigg|_{x=r} = \phi_p'\bigg|_{x=r} = \phi_p''\bigg|_{x=r+L} = \phi_p'''\bigg|_{x=r+L} = 0 \qquad (8\text{-}53)$$

of a clamped-free appendage.

With reference to Table 8-1 and Figures 8-4 through 8-11, we consider qualitatively the graphical summaries of the state and control time histories.

Case 1 (Figure 8-4) corresponds to the rigid body control case, which is presented for comparison with the flexible body examples run.

For Case 2 (Figure 8-5), the required torque is antisymmetric about the time axis. The antisymmetric torque profile is observed because the maneuver time is set equal to the period of the first bending mode. Moreover, we can see that the resulting torque oscillates about the straight line rigid body torque of Figure 8-4.

The boundary conditions for Cases 3 and 4 (Figure 8-6 and 8-7) are identical; the difference between the two cases is that the diagonal matrix W_{ss} of Case 3 is mapped into modal coordinates (i.e., $W_{ss} \rightarrow E^T W_{ii} E$ for i = 1, 2), for Case 4. We observe that the torque histories for the two cases are very different. The maximum torque and modal amplitudes of Case 3 are much larger than those of Case 4, where the peak torques and modal amplitudes were found to have 4 to 1 and 6.7 to 1 ratios, respectively.

Comparing Case 4 with Case 5 (Figure 8-8), we find that the rigid body torque profile is smoothed out by the addition of one controller on each appendage. The maximum torque required for the appendage control is much less than that required for the hub control. We also find that the hub angular velocity and appendage vibration amplitudes of the five control cases are slightly lower than those for the one control case. In a similar case (not shown here) with nine controls (two on each appendage), we find that the additional appendage controls have negligible effect on the torque histories and the system response.

Table 8-1. Description of test case maneuvers.

Case No.	Qualitative Description	No. of Modes N	θ_o, rad	$\dot{\theta}_o$, rad/s	θ_f rad	$\dot{\theta}_f$ rad/s	No. of Controls	W_{uu}	W_{ss}
1	Rigid Appendages Rest-to-Rest Maneuver $t_f = 17.83$ s	0	0	0	0.1	0	1	1	$[0]$
2	Linear Kinematics Rest-to-Rest Maneuver $t_f = 2\pi/\omega_1 = 17.83$ s	1	0	0	0.1	0	1	1	$[\hat{I}]+$
3	Linear Kinematics Rest-to-Rest Maneuver $t = 60$ s	2	0	0	π	0	1	1	$[\hat{I}]*$
4	Linear Kinematics Rest-to-Rest Maneuver $t_f = 60$ s	2	0	0	π	0	1	1	$[\hat{I}]$
5	Linear Kinematics Rest-to-Rest Maneuver $t_f = 60$ s	2	0	0	π	0	5	$[I]$	$10^{-2}[\hat{I}]$
6	Linear Kinematics Rest-to-Rest Maneuver $t_f = 60$ s	2	0	0	π	0	5	$10^{-2}[I]$	$10^{-2}[\hat{I}]$

* Except for Case 3, all the W_{ss} matrices are set to diagonal matrices in physical space, and then mapped into modal space, via the equation $W_{ss} \rightarrow E^T W_{ii} E$ for $i = 1, 2$.

+ $[\hat{I}]$ is an identity matrix with the first element set to 10^{-2}. This sets a lower weight on the maneuver angle.

Table 8-1. Description of test case maneuvers. (Cont.)

Case No.	Qualitative Description	No. of Modes N	θ_o, rad	$\dot{\theta}_o$, rad/s	θ_f rad	$\dot{\theta}_f$ rad/s	No. of Controls	W_{uu}	W_{ss}
7	Linear/Nonlinear Kinematics* Rest-to-Rest Maneuver t_f = 60 s	4	0	0	π	0	5	[I]	$10^{-5}[\hat{I}]$
8	Linear Kinematics Spinup Maneuver t_f = 60 s	3	0	0	2π	0.5	5	[I]	$10^{-5}[\hat{I}]$
9	Nonlinear Kinematics Spinup Maneuver t_f = 60 s	3	0	0	2π	0.5	5	[I]	$10^{-5}[\hat{I}]$
10	Linear Kinematics Spin Reversal Maneuver t_f = 60 s	3	0	-0.5	2π	0.5	5	[I]	$10^{-4}[\hat{I}]$
11	Nonlinear Kinematics Spin Reversal Maneuver t_f = 60 s	3	0	-0.5	2π	0.5	5	[I]	$10^{-4}[\hat{I}]$
12	Linear Kinematics Rest-to-Rest t_f = 5 s	10	0	0	$\dfrac{\pi}{18}$	0	5	[I]	$10^{-6}[\hat{I}]$

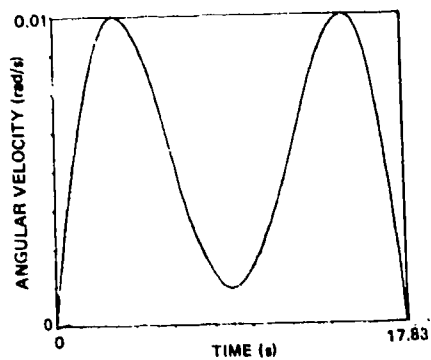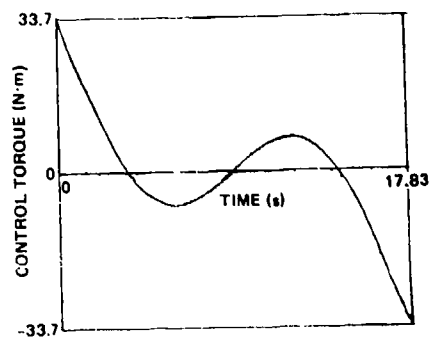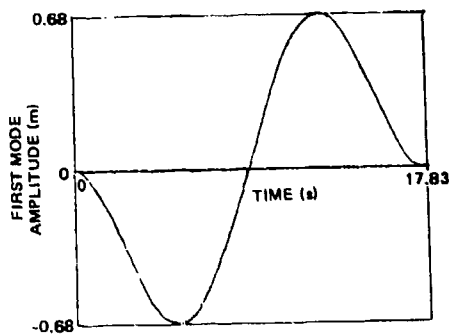* The numerical results to plotting accuracy were identical for the rest-to-rest considered.
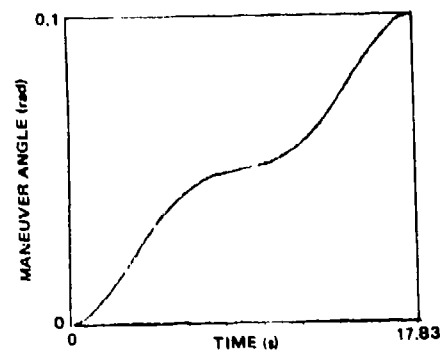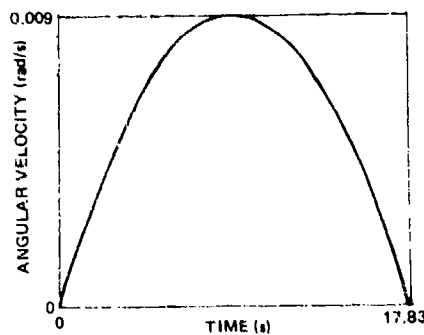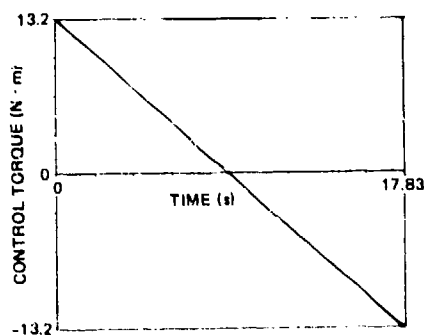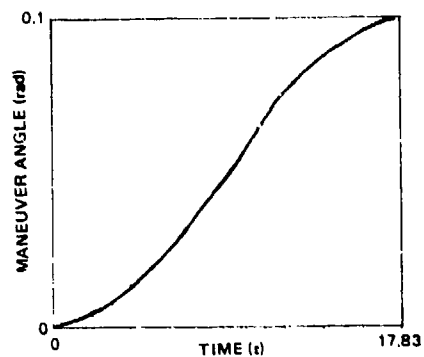
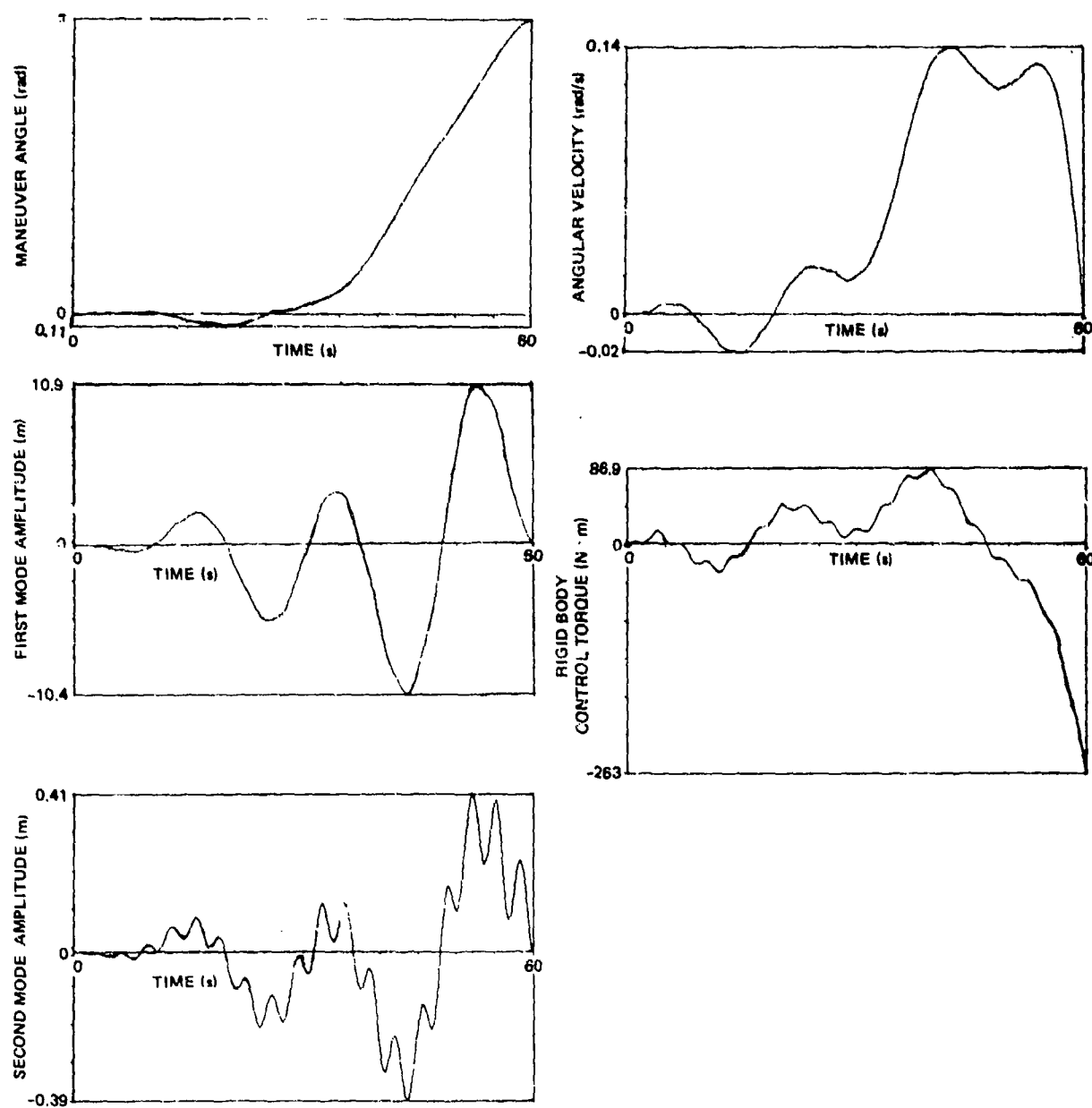Figure 8-4. Case 1, rigid appendages. Figure 8-5. Case 2, flexible appendages. Rest-to-rest maneuver. Rest-to-rest maneuver.
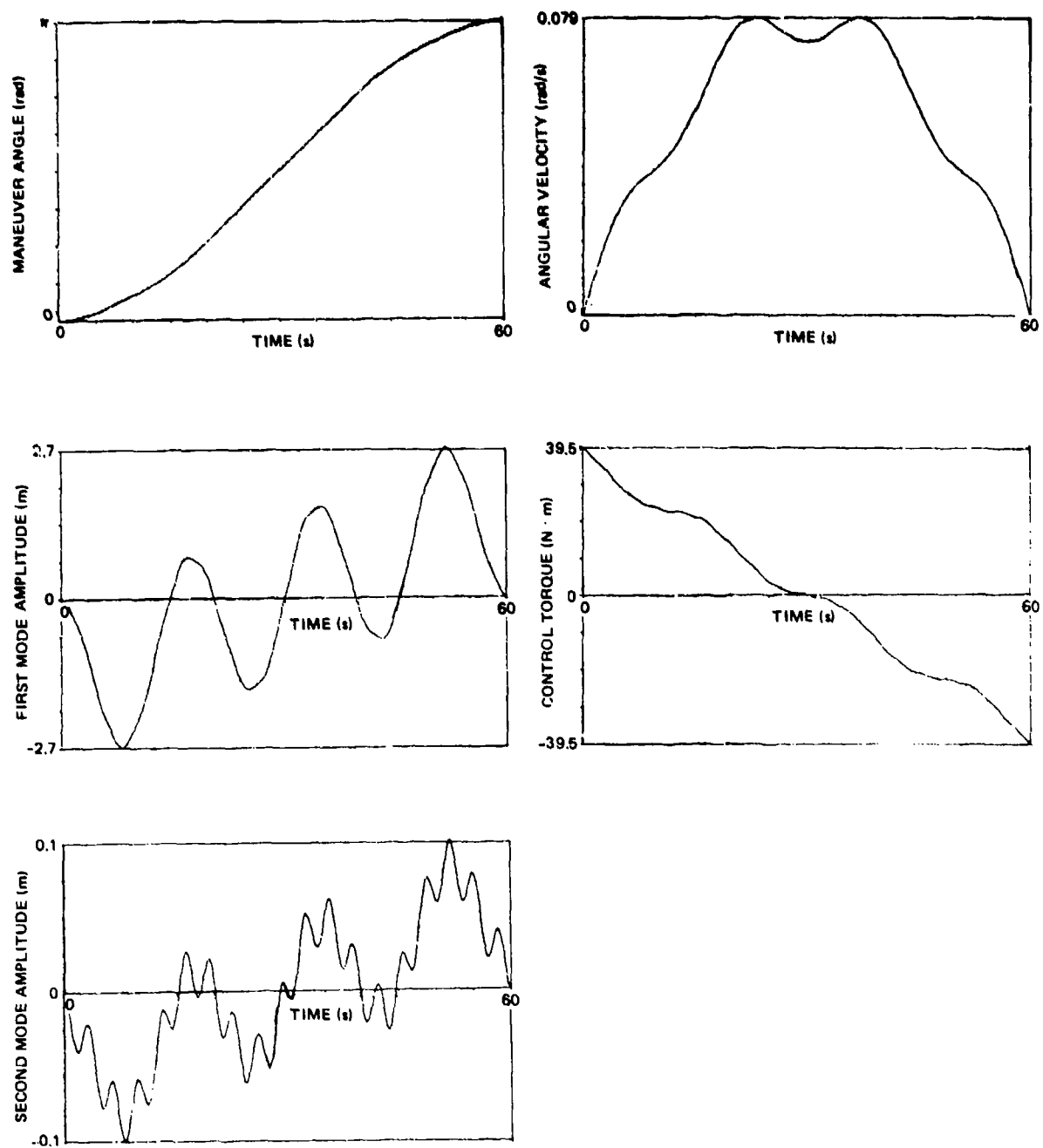
Figure 8-6. Case 3, rest-to-rest maneuver.

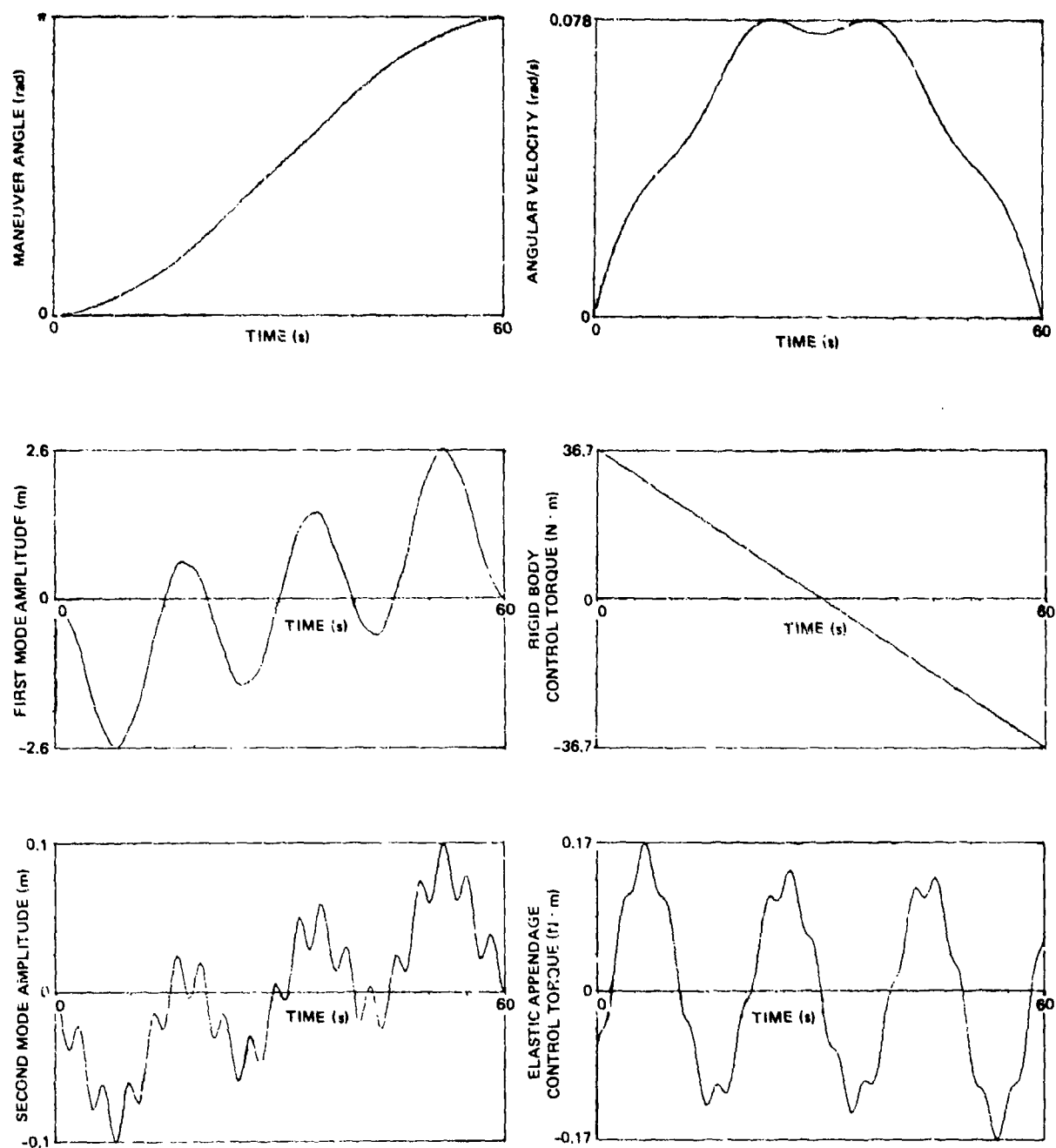Figure 8-7. Case 4, rest-to-rest maneuver.

Figure 8-8. Case 5, rest-to-rest maneuver with 5 controls.

8-23

The maneuver in Case 1 (Figure 8-9) is the same as in Case 5 except that the weighting matrix W_{lu} is set to be two orders of magnitude smaller. Note that the peak modal amplitudes decreased in a ratio of 3 to 1, even though the peak torque required remained essentially unchanged.

Referring to Case 7 (Figure 8-10), we find that the modal amplitudes, torque histories, and the vehicle angular velocities are identical to plotting accuracy for the linear and nonlinear cases. However when we compare the results of Cases 5 and 7, we do observe that the higher modes have little effect on the overall system response. This result indicates, to a considerable degree, that low order models can be used to adequately model the vehicle during slewing maneuvers.

Case 8 (Figure 8-11) is an interesting spin-up maneuver. In particular, notice that a torque reversal is required to match the final boundary conditions. In addition, the hub torque profile is nearly linear (as in previous cases) because of the presence of appendage controls. It should be pointed out that the torque reversal phenomenon is a result of solving a fixed time or fixed final angle maneuver. However, if the final angle in Case 8 is determined as part of the solution (the results are not shown), we observe the following improvements in the resulting maneuver: (1) the peak modal amplitudes decrease in a ratio of 4.5 to 10; (2) the peak torques decrease in a ratio of 7 to 16; and (3) the torque reversal disappears. The conclusion is that for either spin-up or despin maneuvers, we obtain improved controlled vehicle performance if we allow the final angle to be determined in the solution process.

Case 9 (Figure 8-12) is the nonlinear version of the maneuver run in Case 8. On comparing the results of Cases 8 and 9 we reach the following conclusions. First, the gyroscopic stiffening effect of the kinematic nonlinearity has decreased the participation of the first mode at the expense of slightly exciting the higher modes. Second, the required rigid body torque has remained unchanged while the appendage control torques have decreased. Since the observed differences between the linear and nonlinear solutions are not dramatic, it can be anticipated that if slow maneuvers are carried out a linear solution will be adequate.

Case 10 (Figure 8-13) is a spin reversal maneuver which requires the vehicle's angular velocity to reverse its algebraic sign. As in the previous cases, the rigid body control torque is nearly linear due to the presence of the appendage control torques. On comparing the results with Case 8, we find that the spin reversal maneuvers induce greater flexural deformations in the structure. In fact, as in Case 8, if the final angle is permitted to go free, the overall system response can be improved as measured by peak flexural deformations and peak torque requirements.

Case 11 (Figure 8-14) is the nonlinear version of Case 10. As in Case 9, the first mode participation decreases while the higher modes are excited somewhat more. In addition, the peak appendage control torques decrease. Moreover, the resulting time histories are somewhat smoother than in Case 10.
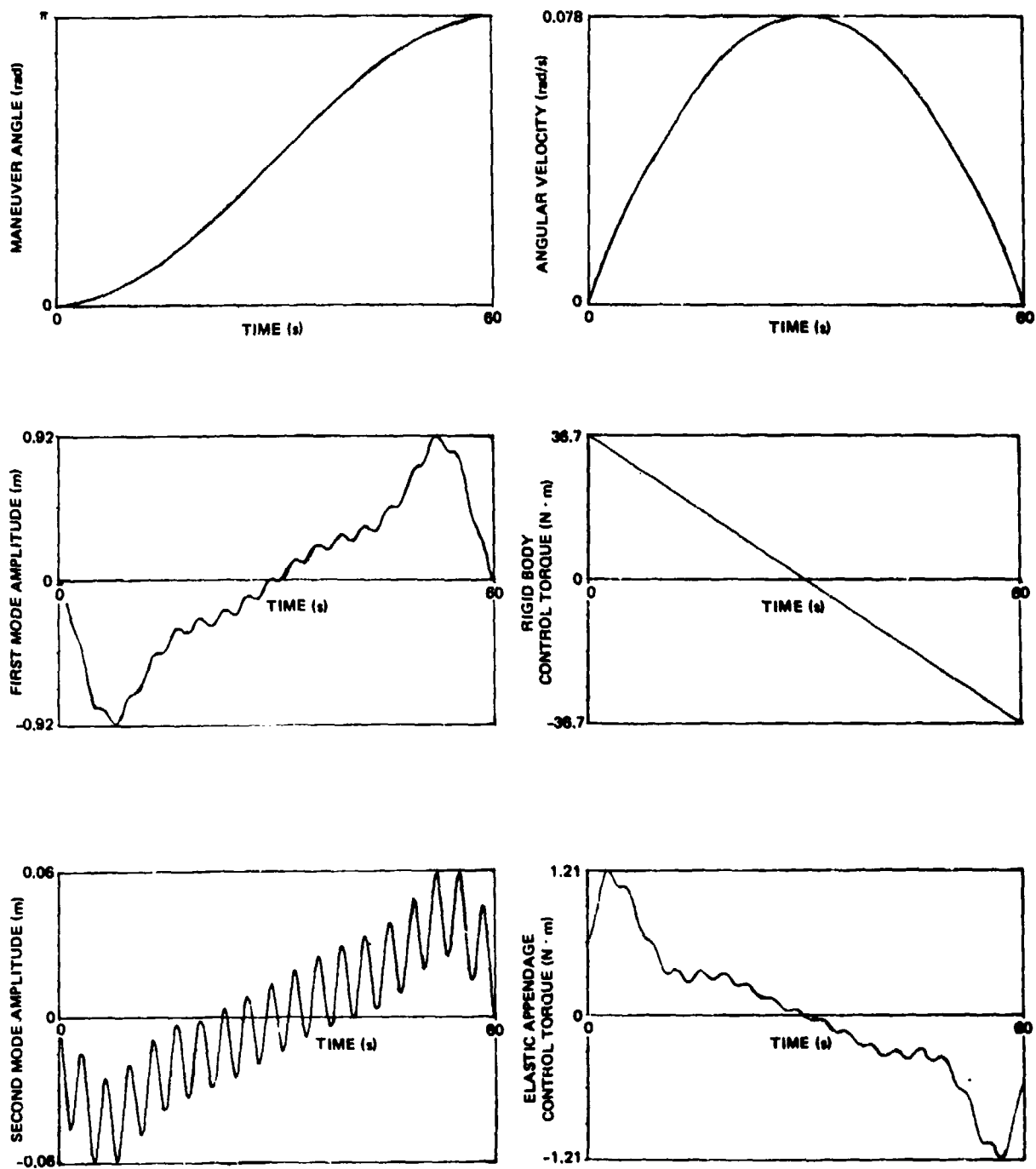
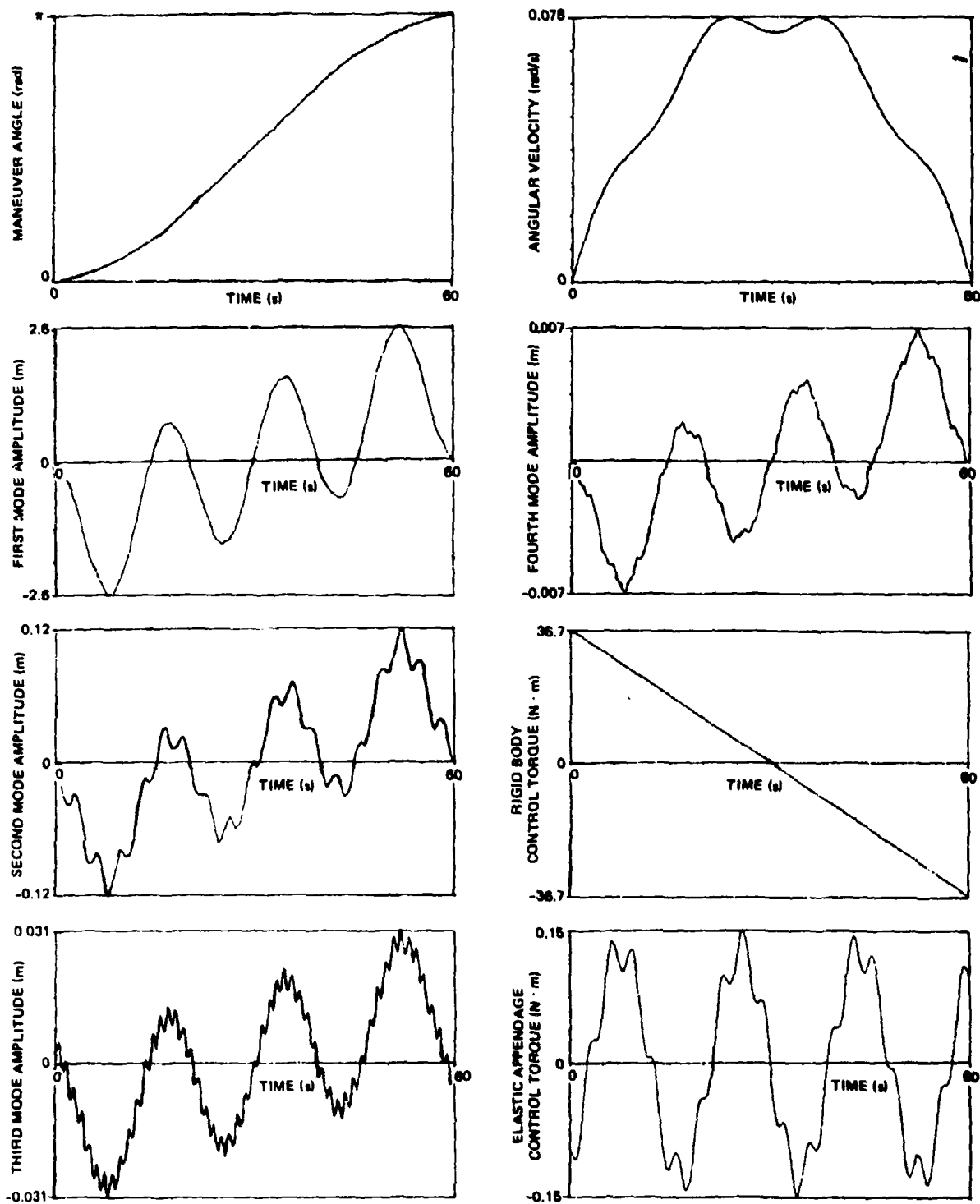Figure 8-9. Case 6, rest-to-test maneuver, $W_{uu} = 10^{-2}[I]$.

Figure 8-10. Case 7, rest-to-rest maneuver, 4 modes, 5 controls.

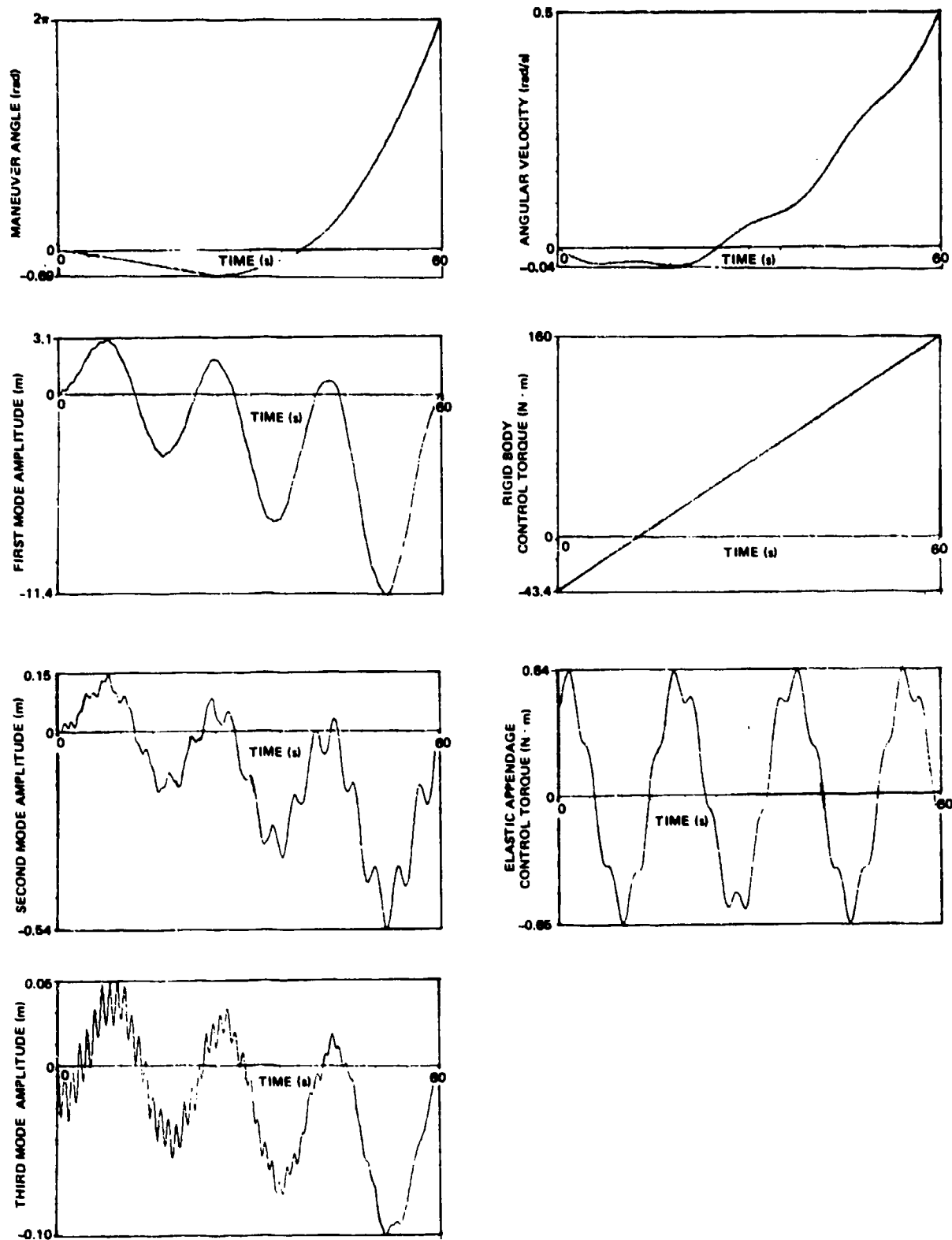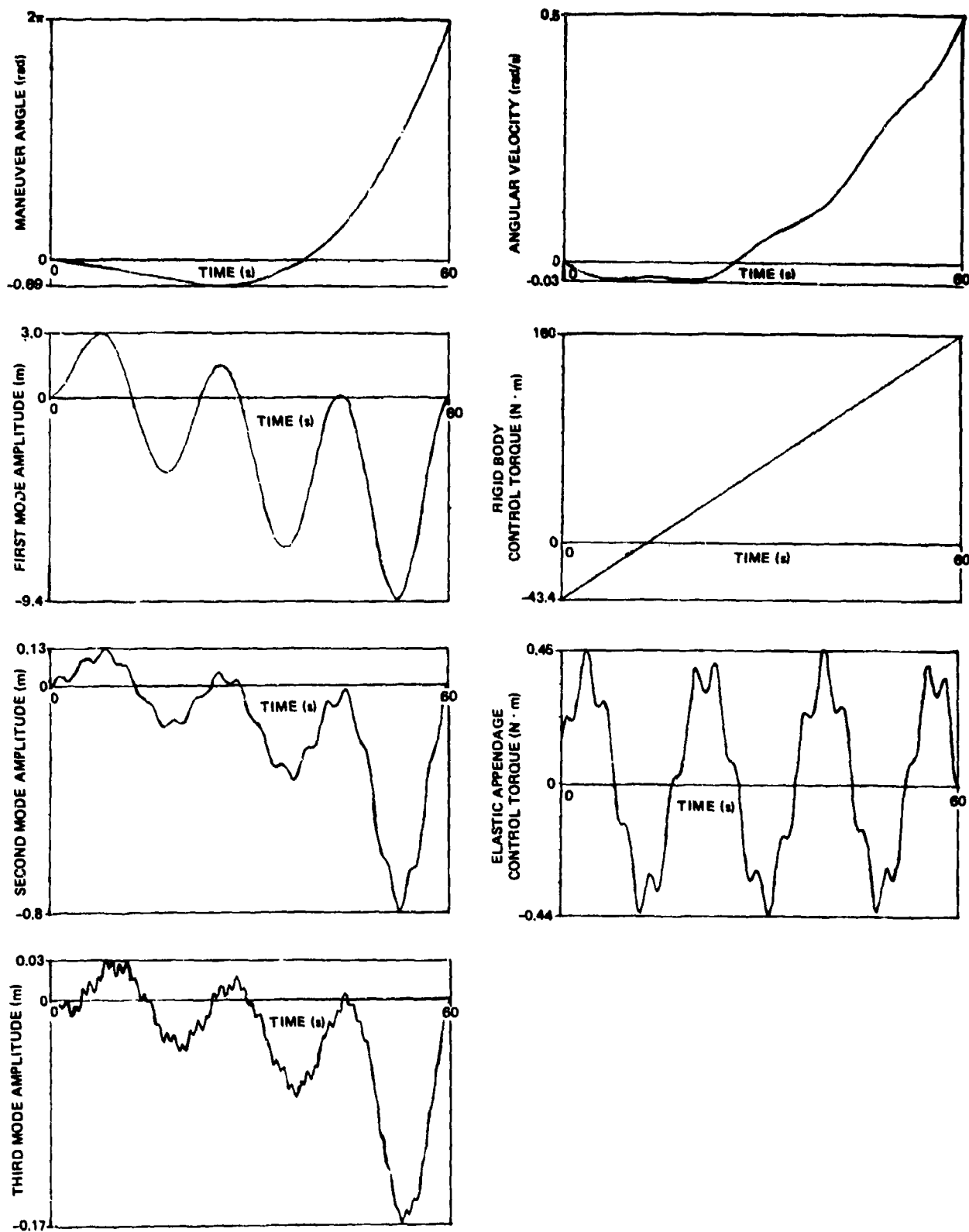Figure 8-11. Case 8, spin-up maneuver, linear kinematics.

8-27

Figure 8-12. Case 9, spin-up maneuver, nonlinear kinematics.
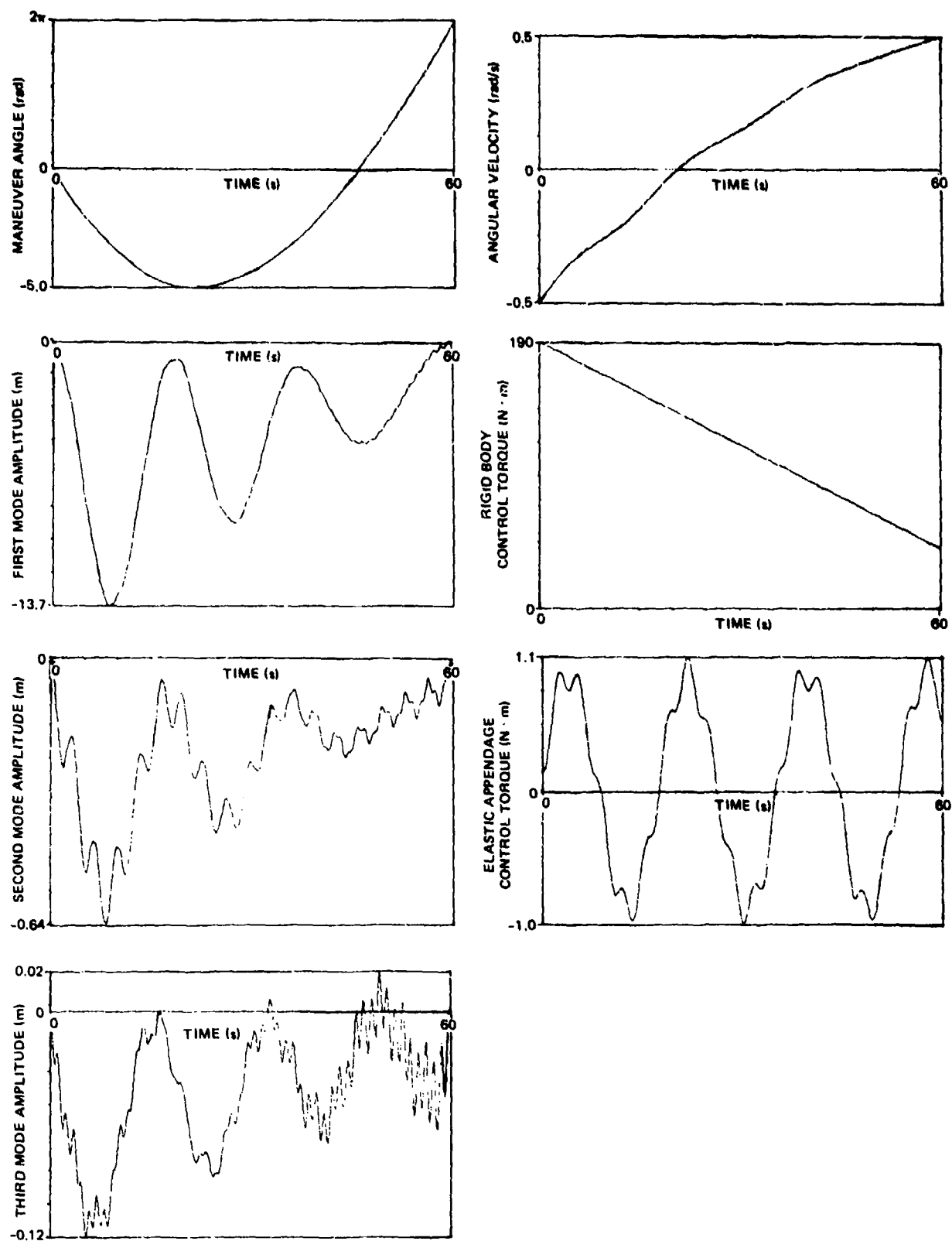
8-28

Figure 8-13. Case 10, rotation reversal, linear kinematics.
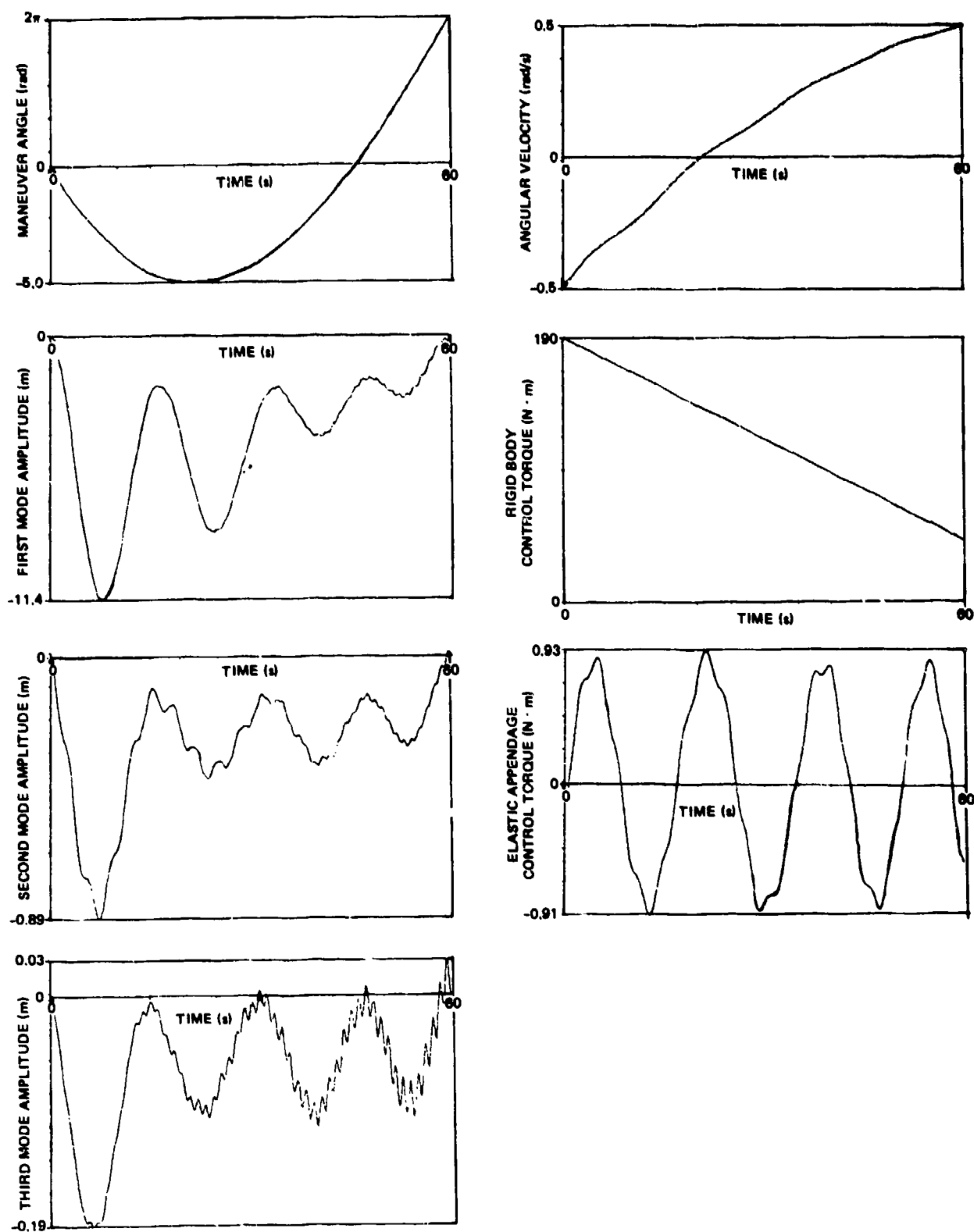
Figure 8-14. Case 11, rotation reversal, nonlinear kinematics.

Case 12 (Figure 8-15) represents a simple linear rest-to-rest maneuver where ten elastic modes of the structure are controlled. As in Case 7, we have further confirmation of the observation that only the first few elastic modes participate in the system response during a slewing maneuver.

In general, we have found that a change in the magnitude of the space weight matrix W_{ss} has little or no effect on the torque histories for the single controller cases. However, when control torques are applied to the appendages, a change in the magnitude of the W_{uu} matrix can significantly affect the appendage torque and modal amplitude time histories.

If required, many additional modes can be run in the simulations. In all example cases run, the linear solution obtained from Eq. (8-35) has been iteratively refined using Eq. (8-50), by replacing $\phi_{s\lambda}$ for the nonlinear problem with the $\phi_{s\lambda}$ used in Eq. (8-35).

8.8   Concluding Remarks

The results of this section provide a basis for systematic solution for optimal large-angle single-axis spacecraft rotational maneuvers, when a distributed control system is employed. In addition, a continuation method is presented and example nonlinear TPBVP's provided which demonstrate the utility of the formulation described herein. Moreover, we have found that unless very high angular rates are achieved during the maneuver, the linear and nonlinear solutions differ very slightly.

Figure 8-15.   Case 12, 10-mode case, rest-to-rest maneuver.

8-32
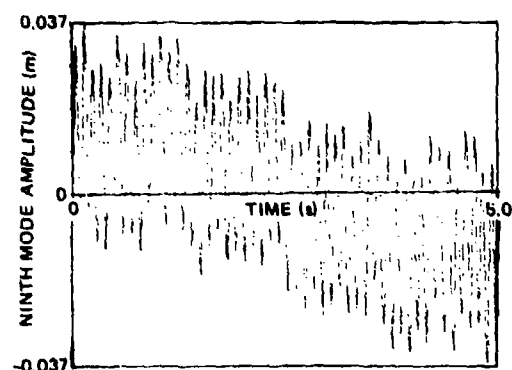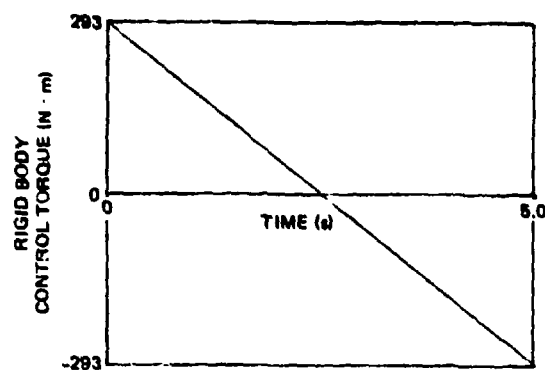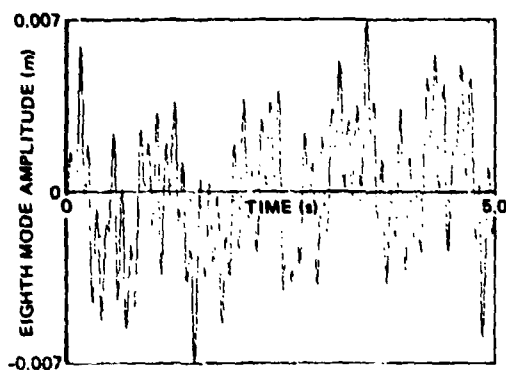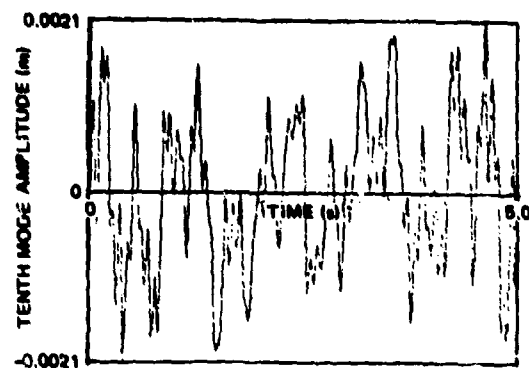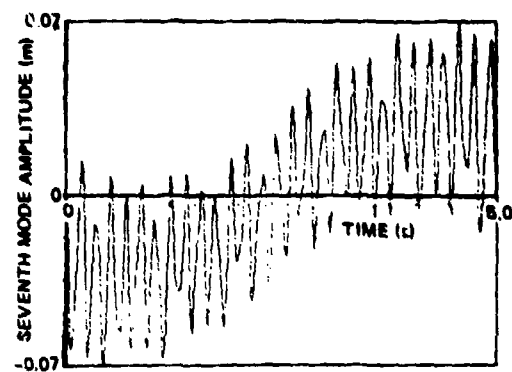
Figure 8-15. Case 12, 10-mode case, rest-to-rest maneuver. (Cont.)

REFERENCES
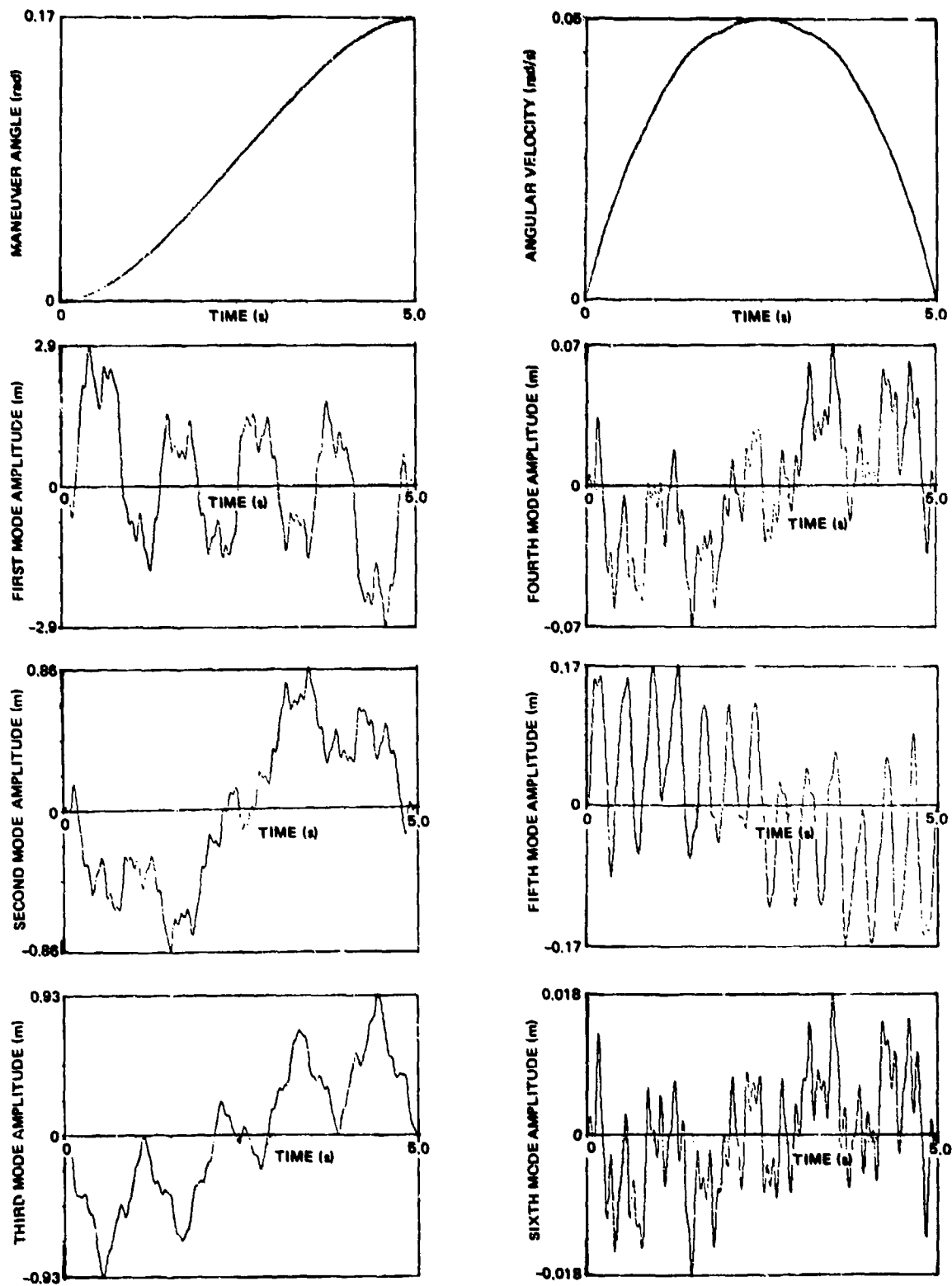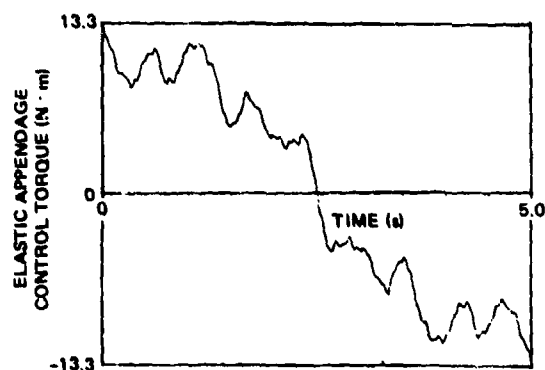
1. Meirovitch, L., "A Stationary Principle for the Eigenvalue Problem for Rotating Structures," AIAA Journal, Vol. 14, Oct. 1976, pp. 1387-1394.

2. Junkins, J. L. and J. D. Turner, "Optimal Continuous Torque Attitude Maneuvers," Paper 78-1400, presented at the AIAA/AAS Astrodynamics Conference, Palo Alto, Calif., Aug. 1978.

3. Swigert, C. J., "Shaped Torque Technique," Paper 78-1692, presented at the AIAA Conference on Large Space Platforms Future Needs and Capabilities, Los Angeles, Calif., Sept. 27-29, 1978.

4. Markley, F. L., "Large Angle Maneuver Strategy for Flexible Spacecraft," Paper 79-156, presented at the AAS/AIAA Astrodynamics Specialist Conference, Provincetown, MA, June 25-27, 1979.

5. Breakwell, J. A., "Optimal Feedback Maneuvering of a Flexible Spacecraft," AAS Preprint 79-157, presented at the AAS/AIAA Astrodynamics Conference, June 1979.

6. Alfriend, K. T., R. W. Bercaw, and W. S. Longman, "On Frequency Response Interpretations of Optimal Slewing Maneuvers," Proceedings of the Second VPI&SU/AIAA Symposium on Dynamics and Control of Large Flexible Spacecraft, Blacksburg, VA, June 21-23, 1979.

7. Turner, J. D., "Optimal Large-Angle Spacecraft Rotational Maneuvers," Ph.D. Dissertation, Virginia Polytechnic Institute and State University, Blacksburg, VA, 1980.

8. Meirovitch, L., Methods of Analytical Dynamics, McGraw-Hill Book Co., New York, 1970, p. 68.

9. Bryson, A. E., and Y. C. Ho., Applied Optimal Control, John Wiley & Sons, Inc., New York, 1975, Chapters 2 and 5.

10. Young, Y. C., Calculus of Variations and Optimal Control Theory, W. B. Saunders, Co., Philadelphia, PA, pp. 308-321.

11. Leitmann, G., Optimization Techniques with Applications to Aerospace Systems, Academic Press, New York, 1962, Chapter 7, (R. E. Kopp's contribution).

12. Pontryagin, L. S., et al., The Mathematical Theory of Optimal Processes, Interscience, London, 1962.

13. Kirk, D. E., Optimal Control Theory. An Introduction, Prentice Hall, New Jersey, 1970.

14. Moler, C., and C. V. Loan, "Nineteen Dubious Ways to Compute the Exponential of a Matrix," _SIAM Review_, Vol. 20, No. 4, Oct. 1978.

15. Ward, R. C., "Numerical Computation of the Matrix Exponential with Accuracy Estimate," _SIAM J. Numer. Anal._, Vol. 14, No. 4, Sept. 1977.

16. Schmidt, W. F., "Adaptive Step Size Selection for Use with the Continuation Method," _International Journal for Numerical Method in Engineering_, Vol. 12, pp. 677-694, 1978.

17. Deuflhard, P., H. J. Resch, and P. Rentrap, "A Modified Continuation Method for the Numerical Solution of Nonlinear Two-Point Boundary-Value Problems by Shooting Techniques," _Numer. Math._, Vol 26, pp. 327-343, 1976.

18. Dennis, J. E., Jr., and R. B. Schnabel, "Least Change Secant Updates for Quasi-Newton Methods," _SIAM Review_, Vol. 21, No. 4, pp. 443-459, Oct. 1979.

19. Greenstadt, J., "Variations on Variable-Metric Methods," _Mathematics of Computation_, Vol. 24, No. 109, pp. 1-22, Jan. 1970.

20. Goldfarb, D., "A Family of Variable-Metric Methods Derived by Variational Means," _Mathematics of Computation_, Vol. 24, No. 109, pp. 23-26, Jan. 1970.

APPENDIX A

COMPUTATION OF STATE AND COSTATE PARTIAL DERIVATIVES

Referring to Eq. (8-38) and subsequent developments in the text of this report, we need the four partial derivative matrices

$$\phi_{s_i \lambda_j} = \left[\frac{\partial s_i^T}{\partial \underline{\lambda}_{jo}} \Bigg|_{t_f} \right]^T \qquad (i, j = 1, 2)$$

To determine these partial derivatives, we first consider the state vector $\underline{s}^*$ defined by

$$\underline{s}^* = [\underline{s}_1^T(t) \quad \underline{s}_2^T(t) \quad \underline{\lambda}_1^T(t) \quad \underline{\lambda}_2^T(t)] \qquad (A-1)$$

Next, assuming that the time derivative of $\underline{s}^*$ is known to be

$$\underline{\dot{s}}^* = F(\underline{s}^*, t) \qquad (A-2)$$

we are lead to the formal solution for $\underline{s}^*$:

$$\underline{\dot{s}}^*(t) = \underline{s}^*(t_o) + \int_{t_o}^{t} \underline{F}(\underline{s}^*(\tau), \tau) d\tau \qquad (A-3)$$

Taking the partial derivatives of Eq. (A-3) with respect to $\underline{s}^*(t_o)$ we obtain

$$\left[\frac{\partial \underline{s}^*(t)}{\partial \underline{s}^*(t_o)} \right] = [I] + \int_{t_o}^{t} \left[\frac{\partial F(\underline{s}^*(\tau), \tau)}{\partial \underline{s}^*(\tau)} \right] \left[\frac{\partial \underline{s}^*(\tau)}{\partial \underline{s}^*(t_o)} \right] d\tau \qquad (A-4)$$

From Eq. (A-4), we conclude that the initial conditions for $\partial \underline{s}(t)/\partial \underline{s}(t_o)$ are given by

$$\left[\frac{\partial \underline{s}^*(t)}{\partial \underline{s}^*(t_o)} \Bigg|_{t=t_o} \right] = [I] \qquad (A-5)$$

A-1

On taking the time derivative of Eq. (A-4), we obtain

$$\frac{d}{dt}\left[\frac{\partial \underline{s}^*(t)}{\partial \underline{s}^*(t_o)}\right] = \left[\frac{\partial F(\underline{s}^*(t),t)}{\partial \underline{s}^*(t)}\right]\left[\frac{\partial \underline{s}^*(t)}{\partial \underline{s}^*(t_o)}\right] \qquad (A-6)$$

or defining

$$\phi(t,t_o) = \left[\frac{\partial \underline{s}^*(t)}{\partial \underline{s}^*(t_o)}\right] \qquad \text{(the state transition matrix)} \qquad (A-7)$$

Equation (A-6) becomes

$$\dot{\phi} = F\phi \qquad F = \left[\frac{\partial F(\underline{s}^*(t),t)}{\partial \underline{s}^*(t)}\right] \qquad (A-8)$$

On referring to Eq. (8-48) and comparing the derivation leading to Eq. (A-8), it is clear that only one partition of ϕ is required. To take advantage of this observation we express ϕ and F in the partitioned form

$$\phi = \begin{bmatrix} \phi_{ss} & \phi_{s\lambda} \\ \phi_{\lambda s} & \phi_{\lambda\lambda} \end{bmatrix} \qquad F = \begin{bmatrix} F_{ss} & F_{s\lambda} \\ F_{\lambda s} & F_{\lambda\lambda} \end{bmatrix} \qquad (A-9)$$

where

$$\phi_{s\lambda} = \left[\frac{\partial \underline{s}^T}{\partial \underline{\lambda}_o}\bigg|_{t_f}\right]^T$$

On introducing Eq. (A-9) into Eq. (A-8), we obtain the following differential equations for the matrix partitions of ϕ

$$\dot{\phi}_{ss} = F_{ss}\phi_{ss} + F_{s\lambda}\phi_{\lambda s} = G_1(\phi_{ss},\phi_{\lambda s}) \qquad (A-11)$$

$$\dot{\phi}_{s\lambda} = F_{ss}\phi_{s\lambda} + F_{s\lambda}\phi_{\lambda\lambda} = G_2(\phi_{s\lambda},\phi_{\lambda\lambda}) \qquad (A-12)$$

$$\dot{\phi}_{\lambda s} = F_{\lambda s}\phi_{ss} + F_{\lambda\lambda}\phi_{\lambda s} = G_3(\phi_{ss},\phi_{\lambda s}) \qquad (A-13)$$

$$\dot{\phi}_{\lambda\lambda} = F_{\lambda s}\phi_{s\lambda} + F_{\lambda\lambda}\phi_{\lambda\lambda} = G_4(\phi_{s\lambda},\phi_{\lambda\lambda}) \qquad (A-14)$$

From Eq. (A-12), we see that $\dot{\phi}_{s\lambda}$ is a function of $\phi_{s\lambda}$ and $\phi_{\lambda\lambda}$. From Eq. (A-14), we see that $\dot{\phi}_{\lambda\lambda}$ is a function of $\phi_{s\lambda}$ and $\phi_{\lambda\lambda}$. Hence we conclude that in order to produce $\phi_{s\lambda}\Big|_{t_f}$ (as required by Eq. (8-48)), we only need to integrate the matrix partitions for $\phi_{s\lambda}$ and $\phi_{\lambda\lambda}$; thus decreasing by half the number of equations to be integrated. In addition, if we take advantage of the sparse structure of F_{ss}, $F_{s\lambda}$, $F_{\lambda s}$, and $F_{\lambda\lambda}$ the computational effort required to produce $\phi_{s\lambda}$ can be further reduced by another factor of one half.

To obtain the complete solution for $\phi_{s\lambda}$, we integrate simultaneously Eq. (A-2), (A-12), and (A-14) from $t = t_o$ to $t = t_f$, where $\phi_{s\lambda}\Big|_{t_o} = 0$ and $\phi_{\lambda\lambda}\Big|_{t_o} = I$.

Richard W. Carman   5
RADC/OCSE

RADC/TSLD   1
GRIFFISS AFB NY 13441

RADC/DAP   2
GRIFFISS AFB NY 13441

ADMINISTRATOR   12
DEF TECH INF CTR
ATTN: DTIC-DDA
CAMERON STA BG 5
ALEXANDRIA VA 22314

Charles Stark Draper Lab   5
555 Technology Square
Cambridge,MA 02139

Charles Stark Draper Labs   5
555 Technology Square
Cambridge, MA 02139

Charles Stark Draper Lab   1
Attn: Dr. Keto Soosar
555 Technology Square
M.S. -95
Cambridge, MA 02139

Charles Stark Draper Lab   1
Attn: Dr. J.B. Linn
555 Technology Square
Cambridge, MA 02139

Charles Stark Draper Lab   1
Attn: Mr. R. Strunce
555 Technology Square
M.S.-60
Cambridge, MA 02139

Charles Stark Draper Lab   1
Attn: Dr. Daniel R. Hegg
555 Technology Square
M.S. -60
Cambridge, MA 02139

ARPA/MIS   1
1400 Wilson Blvd
Arlington, VA 22209

ARPA/STO   1
Attn: Lt Col A. Herzberg
1400 Wilson Blvd
Arlington, VA 22209

ARPA/STO   1
Attn: Mr. J. Larson
1400 Wilson Blvd
Arlington, VA 22209

ARPA/STO   1
Attn: Maj E. Dietz
1400 Wilson Blvd
Arlington, VA 22209

Riverside Research Institute   3
Attn: Dr. R. Kapoesser
Attn: Mr. A. DeVilliers
1701 N. Ft. Myer Drive Suite 711
Arlington, VA 22209

Riverside Research   1
Attn: HALO Library, Mr. Bob Passut
1701 N.Ft. Myer Drive
Arlington, VA 22209

Itek Corp   1
Optical Systems Division
10 Maguire Rd.
Lexington, MA 02173

Perkin Elmer Corp   1
Attn: Mr. H. Levenstein
Electro Optical Division
Main Avenue
Norwalk, CT 06856

Hughes Aircraft Company   1
Attn: Mr. George Speak
M.S. B_156
Culver City, CA 09230

Hughes Aircraft Company   1
Attn: Mr. Ken Beale
Centinela Teale Sts
Culver City, CA 90230

Air Force Flight Dynamics Lab   1
Attn+ Dr. Lynn Rogers
Wright Patterson AFB, OH 45433

AFWL/FIBG   1
Attn: Mr. Jerome Pearson
Wright Patterson AFB, OH 45433

Air Force Wright Aero Lab. FIEE   1
Attn: Capt Paul Wren
Wright Patterson AFB, OH 45433

Air Force Institute of Technology   1
Attn: Prof. R. Calico/ENY
Wright Patterson AFB, OH 45433

Aerospace Corp.   2
Attn: Dr. G.T. Tseng
2350 E. El Segundo Blvd
El Segundo, CA 90245

Aerospace Corp.
Attn: Mr. J. Mosich
2350 E. El Segundo Blvd
El Segundo, CA 90245   1

Aerospace Corp/Bldg 125/1054
Attn: Mr. Steve Burrin   1
Advanced Systems Tech Div.
2400 E El Segundo Blvd
El Segundo, CA 90245

SD/YCD
Attn: Lt Col T. May   1
P.O. Box 92960
Worldway Postal Center
Los Angeles CA 90009

SD/YCD
Attn: YCPT/Capt Gajewski   1
P.O. Box 92960
Worldway Postal Center
Los Angelel, CA 90009

Grumman Aerospace Corp
Attn: Dr. A. Mendelson   1
South Oyster Bay Road
Bethpage, NY 11714

Grumman Aerospace Corp
Attn: Mr. Art Rertapelle   1
Plant 25
Betnpge, NY 11714

Jet Propulsion Laboratory
Attn: Mr. D.B. Schaecnter   2
4800 Oak Grove Drive
Pasadena, CA 91103

MIT/Lincoln Laboratory
Attn: S. Wright   1
P.O. Box 73
Lexington, MA 02173

MIT/Lincoln Laboratory   11
Attn: Dr. D. Hyland
P.O. Box 73
Lexington, MA 02173

MIT/Lincoln Laboratory   11
Attn: Dr. N. Smith
P.O. Box 73
Lexington, MA 02173

Control Dynamics Co.   1
Attn: Dr. Sherman Seltzer
221 East Side Square, Suite 1B
Huntsville, Al 35801

Lockheed Space Missile Corp.   2
Attn: A. Woods, Bldg 130 Organ 62-E6
3460 Hillview Ave
Palo Alto, CA 94304

Lockheed Missiles Space Co.   1
Attn: Mr. Paul Williamson
3251 Hanover St.
Palo Alto, CA 94304

General Dynamics   1
Attn: Ray Halstenberg
Convair Division
5001 Keary Villa Rd
San Diego, CA 92123

STI   1
Attn: Mr. R.C. Stroud
20065 Stevens Creek Blvd.
Cupertiono, CA 95014

NASA Langley Research Ctr   2
Attn: Dr. G. Horner
Attn: Dr. Card
Langley Station Bldg 1293B M/s 230
Hampton, VA 23665

NASA Johnson Space Center   1
Attn: Robert Piland
Ms. EA
Houston, TX 77058

McDonald Douglas Corp   1
Attn: Mr. Read Johnson
Douglas Missile Space Systems Div
5301 Bulsa Ave
Huntington Beach, CA 92607

Integrated Systems Inc.   1
Attn: Dr. Narendra Gupta
151 University Ave.
Suite 400
Palo Alto, CA 94301

Boeing Aerospace Company   1
Attn: Mr. Leo Cline
P.O. Box 3999
Seattle, WA 98124
MS 8 W-23

TRW Defense Space Sys Group Inc.   1
Attn: Ralph Iwens
Bldg 82/2054
One Space Park
Redondo Beach, CA 90278

TRW   1
Attn: Mr. Len Pincus
Bldg R-5, Room 2031
Redondo Beach, CA 90278

Department of the navy   1
Attn: Dr. K.T. Alfriend
Naval Research Laboratory
Code 7920
Washington, DC 20375

Airesearch Manuf. Co. of Calif.   1
Attn: Mr. Oscar Buchmann
2525 West 190th St.
Torrance, CA 90509

Analytic Decisions, Inc.   1
Attn: Mr. Gary Glaser
1401 Wilson Blv.
Arlington, VA 22209

Analytic Decisions, Inc.   1
Attn: Mr. Richard mollicone
5336 West Rosecrans Ave
Suite 203
Lawndale, CA 22209

Center for Analysis   1
Attn: Mr. jim Justice
13 Corporate Plaza
Newport Beach, CA 92660

General Research Crop.   1
Attn: Mr. G. R. Curry
P.O. Box 3587
Santa Barbara, CA 93105

General Research Corp   1
Attn: Mr. Thomas Zakrzewski
7655 Old Springhouse Road
McLean, VA 22101

Institute of Defense Analysis   1
Attn: Dr. Hans Wolfhard
400 Army Navy Drive
Arlington, VA 22202

Karman Sciences Corp.   1
Attn: Dr. Walter E. Ware
1500 Garden of the Gods Road
P.O. Box 7463
Colorado Springs, CO 80933

MRJ, Inc.   1
10400 Eaton Place
Suite 300
Fairfax, VA 22030

Photon Research Associates   1
Attn: mr. Jim Myer
P.O. Box 1318
La Jolla, CA 92038

Rockwell International   1
Attn: Russell Loftman (Space Systems Group)
(Mail Code - SL56)
12214 Lakewood Blvd.
Downey, CA 90241

Science Applications, Inc.   1
Attn: Mr. Richard Ryan
3 Preston Court
Bedford, MA 01730

U.S. Army Missile Command   1
Attn: DRSMI-RAS/Mr. Fred Haak
Redstone Arsenal, AL

Naval Electronic Systems Command   1
Attn: Mr. Charles Good
PME_106-4
National Center I
Washington, DC 20360

Naval Research Laboratory   1
Attn: Dr. John McCallum
EOTPO
4555 Overlook Ave., SW
Washington, DC 20375

U.S. Army/DARCOM   1
Attn: Mr. Bernie Chasnov
AMC Bldg
5001 Eisenhower Ave
Alexandria, VA 22333

Honeywell Inc.   2
Attn: Dr. Thomas B. Cunningham
Attn: Dr. Michael F. Barrett
2600 Ridgway Parkway MN 17-2375
Minneapolis, MN 55413